THE UNIVERSITY OF QUEENSLAND

AUSTRALIA

Regulation of MDA-MB-231 breast cancer cell death by plasma membrane calcium ATPase isoforms and the mitochondrial calcium uniporter

Merril Carmel Curry

Bachelor of Science (Honours)

A thesis submitted for the degree of Doctor of Philosophy at

The University of Queensland in 2016

School of Pharmacy

Abstract

Plasma membrane calcium (Ca^{2+}) ATPase isoforms (PMCA1-4) extrude cytoplasmic free calcium ($[Ca^{2+}]_{CYT}$) and maintain low intracellular Ca^{2+} levels. Because $[Ca^{2+}]_{CYT}$ increases can trigger cell death, inhibition of PMCA-mediated Ca^{2+} efflux has been proposed as a therapeutic strategy to kill breast cancer cells. The principal aim of this thesis was to characterise, by silencing techniques, PMCA isoforms and their effects on $[Ca^{2+}]_{CYT}$ signals and cell death responses in the MDA-MB-231 breast cancer cell line. These studies were performed in human MDA-MB-231 breast cancer cells, a widely studied model of basal-like breast cancer subtypes, that express the PMCA isoforms PMCA1, PMCA4 and PMCA2.

For the measurement of cell death, changes in nuclear morphology (Hoechst 33342 fluorescence) and plasma membrane integrity (propidium iodide fluorescence) were assessed in MDA-MB-231 cells using ionomycin (Ca^{2+} ionophore), and ABT-263 (B-cell lymphoma-2 (Bcl-2) inhibitor) to activate caspase-independent and caspase-dependent cell death pathways, respectively. The consequences of PMCA1 or PMCA4 silencing on cell death, along with their effects on $[Ca^{2+}]_{CYT}$ and nuclear factor kappa-B (NFκB) nuclear translocation were evaluated. Initial studies demonstrated that in the absence of a stimulus neither PMCA1 nor PMCA4 silencing altered cell viability. PMCA1 knockdown, however, potentiated ionomycin (caspase-independent)-induced cell death and augmented global $[Ca^{2+}]_{CYT}$ signals generated with various Ca^{2+} mobilising agents. On the contrary, PMCA4 silencing promoted ABT-263 (caspase-dependent)-induced cell death, independent of global $[Ca^{2+}]_{CYT}$ signalling. Assessment of NFκB nuclear translocation showed that PMCA4 knockdown, but not PMCA1 silencing, attenuated transcription factor activity. The ability for the NFκB inhibitor IMD-0354 to phenocopy the effect of PMCA4 siRNA on the promotion of ABT-263 cell death was also demonstrated. This data support diversity amongst PMCA isoforms expressed in the same cell, identifying differential roles for PMCA1 and PMCA4 in the regulation of Ca^{2+} signals and cell death responses in the MDA-MB-231 breast cancer cell line.

Additional experiments examined in more detail, PMCA1-mediated regulation of global $[Ca^{2+}]_{CYT}$ generated by different GPCR activators and the potential for SERCA (sarco/endoplasmic reticulum Ca^{2+} ATPase) activity to compensate for PMCA1 knockdown. These experiments showed that PMCA1 siRNA has distinct effects on ATP, compared with trypsin-induced Ca^{2+} responses. As a potential mechanism to explain why trypsin-mediated Ca^{2+} responses, compared with those of ATP are not altered by PMCA1 silencing, the potential contribution of SERCA activity was assessed using the SERCA inhibitor cyclopiazonic acid (CPA). PMCA4 silencing or CPA alone did not alter the shape of trypsin or ATP Ca^{2+} responses. In combination, PMCA1 siRNA and CPA delayed trypsin-

mediated Ca^{2+} clearance. These results indicate that the calcium pumps, PMCA1 and SERCA, expressed in the same cell, can differentially contribute to Ca^{2+} clearance depending on the identity of the GPCR activated.

PMCA2 overexpression in some breast cancers, and a report that recombinant PMCA2 overexpression protects T47D breast cancer cells from Ca^{2+}-induced (ionomycin) cell death suggests that this particular PMCA isoform may be a therapeutic target for the treatment of some breast cancers. To examine PMCA2 inhibition as a therapeutic strategy, the consequences of PMCA2 siRNA on global $[Ca^{2+}]_{CYT}$ signals and cell death responses were characterised in MDA-MB-231 cells. $[Ca^{2+}]_{CYT}$ signals generated with various agents demonstrated that endogenously expressed PMCA2 does not play a major role in global Ca^{2+} signalling. PMCA2 silencing alone produced no change in cell viability. The effect of PMCA2 siRNA on cell death was then measured in response to ionomycin or ABT-263. PMCA2 silencing did not significantly alter ionomycin-induced cell death, but potentiated ABT-263-induced apoptosis. These studies provide evidence that PMCA2 inhibition may sensitise some breast cancer subtypes to apoptosis initiated through Bcl-2 inhibition.

Another calcium transporter that may be critical in regulating MDA-MB-231 cell death is the mitochondrial Ca^{2+} uniporter (MCU), which facilitates mitochondrial Ca^{2+} uptake. Molecular identification of MCU made it possible to extend these thesis studies and examine MCU distribution in clinical breast cancers. MCU levels were elevated in the oestrogen receptor-negative and basal-like subtypes of breast cancer. The significance of this elevation was addressed by down-regulating MCU expression in MDA-MB-231 cells and assessing the functional consequence on proliferation, cell death and $[Ca^{2+}]_{CYT}$ signals. MCU siRNA produced no change in proliferation and had no effect on cell viability. Cell death initiated with ABT-263 was not altered by MCU silencing. MCU down-regulation, however, acted as a sensitiser of cell death triggered by ionomycin. Assessment of $[Ca^{2+}]_{CYT}$ signals indicates that MCU siRNA-mediated regulation of ionomycin-mediated cell death, in contrast with the PMCA1 silencing studies, occurs without effects on global $[Ca^{2+}]_{CYT}$ signals.

In summary, breast cancer death responses are modulated by isoform-specific PMCA or MCU knockdown. Inhibitors of PMCA1 or MCU may sensitise some breast tumors to cancer therapies that activate caspase-independent cell death. Alternatively, specific inhibitors of PMCA4 or PMCA2 may have therapeutic potential in sensitising some aggressive breast tumors, to cancer therapies that work through caspase-dependent apoptosis via the Bcl-2 cell survival pathway.

Declaration by author

This thesis *is composed of my original work, and contains* no material previously published or written by another person except where due reference has been made in the text. I have clearly stated the contribution by others to jointly-authored works that I have included in my thesis.

I have clearly stated the contribution of others to my thesis as a whole, including statistical assistance, survey design, data analysis, significant technical procedures, professional editorial advice, and any other original research work used or reported in my thesis. The content of my thesis is the result of work I have carried out since the commencement of my research higher degree candidature and does not include a substantial part of work that has been submitted *to qualify for the award of any* other degree or diploma in any university or other tertiary institution. I have clearly stated which parts of my thesis, if any, have been submitted to qualify for another award.

I acknowledge that an electronic copy of my thesis must be lodged with the University Library and, subject to the policy and procedures of The University of Queensland, the thesis be made available for research and study in accordance with the Copyright Act 1968 unless a period of embargo has been approved by the Dean of the Graduate School.

I acknowledge that copyright of all material contained in my thesis resides with the copyright holder(s) of that material. Where appropriate I have obtained copyright permission from the copyright holder to reproduce material in this thesis.

Publications during candidature

Peer-review publications incorporated into this thesis:

M.C. Curry, N.A. Luk, P.A. Kenny, S.J. Roberts-Thomson, G.R. Monteith, Distinct regulation of cytoplasmic calcium signals and cell death pathways by different plasma membrane calcium ATPase isoforms in MDA-MB-231 breast cancer cells, J Biol Chem 287 (2012) 28598-28608.

M.C. Curry, A.A. Peters, P.A. Kenny, S.J. Roberts-Thomson, G.R. Monteith, Mitochondrial calcium uniporter silencing potentiates caspase-independent cell death in MDA-MB-231 breast cancer cells, Biochem Biophys Res Commun, 434 (2013) 695-700.

Peer-review publications not incorporated into this thesis:

A.A. Peters, M.J. Milevskiy, W.C. Lee, **M.C. Curry**, C.E. Smart, J.M. Saunus, L. Reid, L. da Silva, D.L. Marcial, E. Dray, M.A. Brown, S.R. Lakhani, S.J. Roberts-Thomson, G.R. Monteith, The calcium pump plasma membrane Ca(2+)-ATPase 2 (PMCA2) regulates breast cancer cell proliferation and sensitivity to doxorubicin, Sci Rep, 6 (2016) 25505.

M.C. Curry, S.J. Roberts-Thomson, G.R. Monteith, Plasma membrane calcium ATPases and cancer, Biofactors 37 (2011) 132-138.

S.J. Roberts-Thomson, **M.C. Curry**, G.R. Monteith, Plasma membrane calcium pumps and their emerging roles in cancer, World J Biol Chem 1 (2010) 248-253.

Conference abstracts – oral presentations:

Curry MC, Luk NA, Roberts-Thomson SJ & Monteith GR. The role of Plasma Membrane Calcium ATPase Isoforms on Caspase-dependent and Independent Cell Death Mechanisms in MDA-MB-231 breast cancer cells. The 1st Australian Workshop on Cell Death – Death on the Reef, 2011, Whitsunday Islands, Australia.

Roberts-Thomson SJ, Grice DM, Aung CS, **Curry MC**, Kenny PA & Monteith GM. Remodeling of Calcium Signaling in Tumorigenesis. New Horizons in Calcium Signaling, 2010, Beijing, China.

Conference abstracts – poster presentations:

Roberts-Thomson SJ, **Curry MC**, Luk NA & Monteith GR. Inhibition of PMCA4 as a Strategy to Increase the Effectiveness of Bcl-2 Inhibitor-mediated Cell Death in Breast Cancer Cells. Molecular Targets and Cancer Therapeutics, 2011, San Francisco, USA.

Curry MC, Roberts-Thomson SJ & Monteith GR. Consequences of Plasma Membrane Calcium ATPase isoforms 1 and 4 Silencing on Ionomycin-induced Cell Death in MDA- MB-231 Breast Cancer Cells. The 17th International Symposium on Calcium-Binding Proteins and Calcium Function in Health and Disease (CaBP17), 2011, Beijing, China.

Curry MC, Roberts-Thomson SJ & Monteith GR. Regulation of Ca2+ signals by inhibition of PMCA isoforms and consequences for caspase-independent and dependent cell death in MDA- MB-231 breast cancer cells. Gordon Research Conference, Calcium Signalling, 2011, Maine, USA.

Curry MC, Roberts-Thomson SJ & Monteith GR. The impact of Plasma Membrane Calcium ATPase isoforms 1 and 4 during GPCR-linked Ca2+ mobilization in MDA-MB- 231 breast cancer cells. Gordon Research Seminar, Calcium Signalling, 2011, Maine, USA.

Curry MC, Roberts-Thomson SJ & Monteith GR. Assessment of Plasma Membrane Calcium ATPase 1 siRNA-Mediated Inhibition in MDA-MB-231 Breast Cancer Cells. Australasian Society of Clinical and Experimental Pharmacologists and Toxicologists (ASCEPT) Annual Scientific Meeting, 2010, Melbourne, Australia.

Publications included in this thesis

M.C. Curry, N.A. Luk, P.A. Kenny, S.J. Roberts-Thomson, G.R. Monteith, Distinct regulation of cytoplasmic calcium signals and cell death pathways by different plasma membrane calcium ATPase isoforms in MDA-MB-231 breast cancer cells, J Biol Chem 287 (2012) 28598-28608.

This manuscript has been incorporated as chapter two of this thesis:

Contributor	Statement of contribution
Merril C. Curry (Candidate)	Conceived the project (10%) Designed (50%), performed (90%) and analysed majority of experiments (90%) presented in the manuscript Wrote the paper (90%)
Nicole A. Luk	Designed (5%), performed (5%) and analysed (5%) experiments presented in Figure 2-8A and B Wrote (5%) and edited (10%) the paper, providing feedback on content
Paraic A. Kenny	Designed (5%), performed (5%) and analysed (5%) the experiments presented in Figure 2-9A-D. Wrote (5%) and edited (10%) the paper, providing feedback on content.
Sarah J. Roberts-Thomson	Conceived the project (45%) Designed experiments (20%) Provided guidance on experimental design (50%) Edited the paper and provided feedback on content (20%)
Gregory R. Monteith	Conceived the project (45%) Designed experiments (20%) Provided guidance on experimental design (50%) Edited the paper and provided feedback on content (60%)

M.C. Curry, N.A. Luk, P.A. Kenny, S.J. Roberts-Thomson, G.R. Monteith, Distinct regulation of cytoplasmic calcium signals and cell death pathways by different plasma membrane calcium ATPase isoforms in MDA-MB-231 breast cancer cells, J Biol Chem 287 (2012) 28598-28608.

This manuscript has been incorporated as chapter four of this thesis:

Contributor	Statement of contribution
Merril C. Curry (Candidate)	Conceived the project (50%) Designed (50%), performed (90%) and analysed majority of experiments (90%) presented in the manuscript Wrote the paper (90%)
Amelia A. Peters	Designed (5%), performed (5%) and analysed (5%) experiments presented in Figure 4-2C and D Wrote (5%) and edited (10%) the paper, providing feedback on content
Paraic A. Kenny	Designed (5%), performed (5%) and analysed (5%) the experiments presented in Figure 4-1A and B. Wrote (5%) and edited (10%) the paper, providing feedback on content.
Sarah J. Roberts-Thomson	Designed experiments (20%) Provided guidance on experimental design (50%) Edited the paper and provided feedback on content (20%)
Gregory R. Monteith	Conceived the project (50%) Designed experiments (20%) Provided guidance on experimental design (50%) Edited the paper and provided feedback on content (60%)

Contributions by others to the thesis

This PhD research was conceived, designed and performed by me under the supervision of my advisory team: Professor Gregory Monteith and Professor Sarah Roberts-Thomson. The contributions to jointly authored manuscripts are listed in the previous section and again in the introduction to each chapter.

Statement of parts of the thesis submitted to qualify for the award of another degree

None

Acknowledgements

My PhD reflects a collaboration between myself and my supervisors, Professors Gregory R Monteith and Sarah J Roberts-Thomson, but also a collaboration between myself and my friends, family, fellow laboratory members, the School of Pharmacy and the University of Queensland. You all deserve my gratitude, because if not for these supportive relationships, I would not be able to say that I have completed my PhD.

To begin, I would like to thank both Professors Gregory R Monteith and Sarah J Roberts-Thomson for the privilege of completing my doctorate in their laboratory. Under their guidance, I have acquired a wide-variety of skills that not only shape me as scientist, but also as person. They have gone above and beyond their duties, steering me towards the completion of a high quality PhD, despite its ups and downs. I would especially like to thank Greg for generously sharing his time and passion for calcium research with me. You are truly an inspiring person, and words don't convey how fortunate I am to have studied under your constant encouragement.

Another significant person deserving of acknowledgement is my sister. Although you are not here to see this milestone completed, I want to thank you for leading me to this path. Growing up as your little sister, I always admired you, looked up to you, and wanted to be just like you! Your achievements at university certainly paved the way for me to complete my own post-graduate education. Thank you to each and every one of your five children, Jonah, Callum, Harrison, Alandra and Isobel for being resilient and for placing their trust in me during a very difficult time. Also thank you to Jason, Milkirrie and Amanda for showing me, after my sister died, that life can and does continue.

A big thank you for the laboratory members who worked alongside me on a daily basis during the experimental phase of my PhD, particularly Nicole and her husband Joel, Amelia, Jane, Yusrina, Aisyah, Felicity, Diana and her husband Ben, and Teneale. I would also like to express thanks to the School of Pharmacy for providing me with access to research facilities and for the financial support to present my research findings overseas.

Last but not least, a special thankyou to my two cats, Leo and Tulip. Especially Tulip who assisted with writing this PhD thesis by running across the keyboard repeatedly. Meow!

Keywords

Calcium, plasma membrane calcium ATPase, mitochondrial calcium uniporter, breast cancer, cell death, Bcl-2, ionomycin, G-protein coupled receptors, caspase-dependent cell death, signal transduction.

Australian and New Zealand Standard Research Classifications (ANZSRC)

ANZSRC code: 111599, Pharmacology and Pharmaceutical Sciences not elsewhere classified, 35%

ANZSRC code: 060111, Signal Transduction, 35%

ANZSRC code: 111207, Molecular Targets, 30%

Fields of Research (FoR) Classification

FoR code: 1115 Pharmacology and Pharmaceutical Sciences, 35%

FoR code: 0601 Biochemistry and Cell Biology, 35%

FoR code: 1112 Oncology and Carcinogenesis, 30%

In memory of my sister,
who died of cancer during this thesis work.
Chantelle Nichole (Walker) Bucki
29 November 1973 - 7th August 2014

Table of Contents

List of Figures

List of Abbreviations

°C	Degrees Celsius
µM	Micromolar
A	Alanine
ADP	Adenosine diphosphate
ANOVA	Analysis of variance
ATP	Adenosine-5'-triphosphate
AUC	Area under the curve
BAPTA	1,2-bis(o-aminophenoxylethane)-N,N,N',N'-tetraacetic acid.
Bcl-2	B-cell lymphoma-2
C	Cysteine
Ca^{2+}	Calcium ion
$[Ca^{2+}]_{CYT}$	Cytoplasmic Ca^{2+} levels
$[Ca^{2+}]_{ER}$	Endoplasmic reticulum Ca^{2+} levels
$[Ca^{2+}]_{MIT}$	Mitochondria Ca^{2+} levels

cDNA	Complementary DNA
D	Aspartate
DAG	Diacylglycerol
DAPI	4’,6-Diamidino-2-phenylindole dihydrochloride
DlgA	Drosophila disc large tumor suppressor
DMEM	Dulbecco’s Modified Eagle’s Medium
DMSO	Dimethyl sulfoxide
DNA	Deoxyribonucleic acid
E	Glutamate
ER	Endoplasmic reticulum
F	Phenylalanine
FAK	Focal adhesion kinase
FBS	Fetal bovine serum
FLIPR	Fluorometric imaging plate reader
G	Glycine

GPCR	G-protein coupled receptors
h	Hour
H	Histidine
HRP	Horse radish peroxidase
IF	Immunofluorescence
IF	Isoleucine
IP_3	Inositol (1,4,5) triphosphate
IP_3R	Inositol (1,4,5) triphosphate receptor
K	Lysine
kDa	Kilodalton
L	Liter
L	Leucine
M	Molar
M	Methionine
MAGUK	Membrane-associated guanylate kinase
MCU	Mitochondrial calcium uniporter

min	Minute
mM	Millimolar
mRNA	Messenger RNA
N	Asparagine
Na^+	Sodium ion
NCX	Sodium (Na^+)-Ca^{2+} exchanger
NFAT	Nuclear factor of activated T-cells
NFκB	Nuclear factor kappa-B
nM	Nanomolar
nNOS-1	Neuronal nitric oxide synthase-1
NO	Nitric oxide
P	Proline
P2Y	Metabotropic P2 receptor
PAR	Protease-activated receptor
PBS	Phosphate buffered saline
PBST	Phosphate buffered saline with Tween-20

PCR	Polymerase chain reaction
PDZ	Post synaptic density protein (PSD95), Drosophila disc large tumor suppressor (DlgA), and Zonula occludens-1 protein (zo-1)
PI	Propidium iodide
PIP_2	Phosphatidylinositol 4,5-bisphosphate
PIP_2	Phosphatidylinositol 4,5-bisphosphate
PKA	Protein kinase A
PKC	Protein kinase C
PLC	Phospholipase C
PMCA	Plasma membrane Ca^{2+} ATPase
PSD95	Post synaptic density protein
PSS	Physiological salt solution
Q	Glutamine
R	Arginine
RNA	Ribonucleic acid

ROCE	Receptor operated calcium entry
rRNA	Ribosomal RNA
RT	Reverse transcription
S	Serine
s	Second
SD	Standard deviation
SERCA	Sarcoplasmic-endoplasmic reticulum Ca^{2+} ATPase
siMCU	MCU small interfering RNA
siNT	Non-targeting small interfering RNA
siPMCA1	PMCA1 small interfering RNA
siPMCA2	PMCA2 small interfering RNA
siPMCA4	PMCA4 small interfering RNA
siRNA	Small interfering RNA
SOCE	Store operated calcium entry
STIM	Stromal interaction molecule

T	Threonine
t	Time
TRPM8	Transient receptor potential melastatin 8
UQ	The University of Queensland
V	Valine
VGCC	Vascular smooth muscle cell
W	Tryptophan
Y	Tyrosine
zo-1	Zonula occludens-1 protein

1.1 Calcium Homeostasis

1.1.1 Introduction

Free ionised calcium (Ca^{2+}) is present in every eukaryotic cell and has an essential second messenger function. Many stimuli including membrane depolarisation, stretch, noxious agents, and hormones transiently increase cytoplasmic Ca^{2+} levels ($[Ca^{2+}]_{CYT}$) [1, 2]. This increase in $[Ca^{2+}]_{CYT}$ acts as a signal, decoded by the cell into a myriad of events [1, 2] ranging from synaptic transmission [3] through to the regulation of life and death [4]. Regulating such a plethora of physiological processes, however, is conditional on the shape of a Ca^{2+} signal [1, 2] including parameters such as the duration and amplitude. The distribution of Ca^{2+} between cell compartments such as the mitochondria and endoplasmic reticulum [1, 2] is also significant. High magnitude Ca^{2+} levels, for example, is characteristic of the endoplasmic reticulum Ca^{2+} store [5], whereas high magnitude Ca^{2+} increases can trigger cell death in the cytoplasm [6].

"Ca^{2+} signalling toolkit" [2] is a term coined by Berridge et al., which describes the wide variety of Ca^{2+} signalling proteins utilised by cells to process Ca^{2+} transients into specific shapes and sizes. Calcium transport proteins such as ion channels, pumps and exchangers are important components of the "Ca^{2+} signalling toolkit", and coordinate Ca^{2+} signals by controlling Ca^{2+} flux across lipid membranes [1, 2]. Calcium transport proteins are heterogeneously expressed, and thus divide the Ca^{2+} signal into distinct compartments including the cytoplasm, endoplasmic reticulum, mitochondria and the Golgi apparatus [1, 2]. Figure 1-1 illustrates some Ca^{2+} transporters located at the cell surface and on the membrane encasing the endoplasmic reticulum [7]. Described herein are some of the key Ca^{2+} transport proteins, and their role in shaping Ca^{2+} signals.

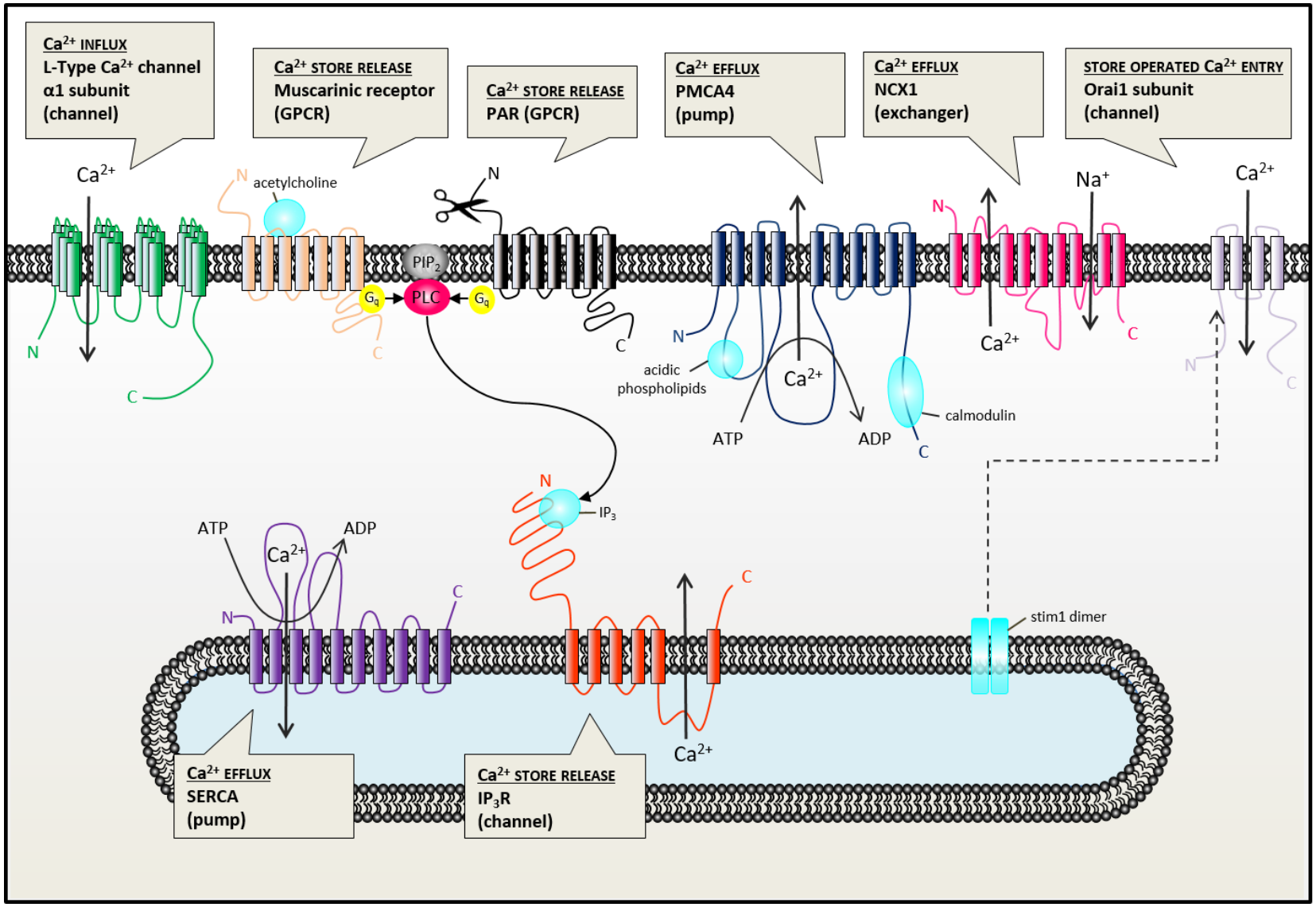
Ca2+ INFLUX
L-Type Ca2+ channel
α1 subunit
(channel)
Ca2+ STORE RELEASE
Muscarinic receptor
(GPCR)
Ca2+ STORE RELEASE
PAR (GPCR)
Ca2+ EFFLUX
PMCA4
(pump)
Ca2+ EFFLUX
NCX1
(exchanger)
STORE OPERATED Ca2+ ENTRY
Orai1 subunit
(channel)
Ca2+
acetylcholine
N
C
PIP2
PLC
Gq
IP3
acidic
phospholipids
ATP
ADP
calmodulin
Na+
stim1 dimer
Ca2+ EFFLUX
SERCA
(pump)
Ca2+ STORE RELEASE
IP3R
(channel)

Figure 1-1: Integral Ca^{2+} transport proteins found on the ER and plasma membranes.

Solid arrows indicate the direction of Ca^{2+} flux. Light blue shapes represent examples of endogenous activators for the specific Ca^{2+} transport proteins. This figure does not provide an accurate interpretation of ion stoichiometry or of the exact domains for the example Ca^{2+} transport proteins shown. Plasma membrane ion channels permeable to Ca^{2+} allow Ca^{2+} influx [1, 2]. The example is a voltage-gated Ca^{2+} channel subunit α1, which mediates L-Type Ca^{2+} currents as a functional multimer in response to membrane depolarisation [8]. Store release of Ca^{2+} requires receptor activation at the plasma membrane [1, 2]. The muscarinic receptor shown, is a GPCR protein linked to the PLC transduction pathway [9]. Acetylcholine binds to the extracellular face of the muscarinic receptor and mobilises cytosolic IP_3, which engages the ligand-gated Ca^{2+} channel, IP_3R (in multimeric form) to release the Ca^{2+} store within the ER [1, 2, 9]. PAR is another GPCR protein linked to the PLC transduction pathway [10, 11]. Proteolytic cleavage of the extracellular N terminus activates PAR [10, 11]. Depicted as scissors, an example protease that activates PAR is trypsin [10, 11]. Pumps and exchangers mediate Ca^{2+} efflux [1, 2]. The exchanger, NCX1 removes Ca^{2+} from the cell in exchange for Na^{+} influx [12]. SERCA is another Ca^{2+} efflux pump, but its position on the ER refills the intracellular Ca^{2+} store [1, 2]. PMCA4 is also a Ca^{2+} efflux pump [1, 2] that is activated by acidic phospholipids and calmodulin [13]. Store-operated Ca^{2+} entry is the response to depletion of stored Ca^{2+} inside the ER [14]. The broken arrow indicates the translocation path of STIM1 dimers [15, 16] to regions adjacent the ER and Orai [17, 18]. STIM1 dimers activate the flux of Ca^{2+} through Orai channels, which are functional as tetramers and specifically replenish ER Ca^{2+} [19, 20]. Figure adapted from a review article [21].

1.1.2 Cytoplasmic calcium levels ($[Ca^{2+}]_{CYT}$)

In an unstimulated cell, $[Ca^{2+}]_{CYT}$ is maintained at a low concentration of approximately 100 nM [1, 2]. To initiate a signalling event, free ionic Ca^{2+} must cross impermeable cell membranes, and rapidly accumulate in the cytoplasm to concentrations of up to 1 µM, before the signal is terminated by Ca^{2+} efflux mechanisms [1, 2]. Figure 1-2A is an example Ca^{2+} transient typical of the cytoplasm. The extracellular medium and the endoplasmic reticulum, because they contain high Ca^{2+} concentrations are Ca^{2+} reservoirs to increase $[Ca^{2+}]_{CYT}$ [1, 2]. Although thermodynamically favoured by the electrochemical gradient, Ca^{2+} entry depends on the activation of Ca^{2+} permeable ion channels, embedded within the plasma and endoplasmic reticulum membranes [1, 2]. Ion channels are classified according to their mode of activation; examples are the voltage-gated and ligand-gated Ca^{2+} channels, which are activated by membrane depolarisation and specific ligand binding, respectively [1, 2]. Shown in Figure 1-1 are the two discrete pathways, Ca^{2+} influx and Ca^{2+} store release, in which ion channels achieve $[Ca^{2+}]_{CYT}$ increases.

1.1.2.1 Calcium influx

Ca^{2+} influx is Ca^{2+} entry directly from the extracellular medium into the cytoplasm through Ca^{2+}-permeable ion channels in the plasma membrane. Voltage-gated Ca^{2+} channels are sub-divided into L-, N-, P-, Q-, R- and T-type, and are different in their Ca^{2+} conductivity [8]. The α1 channel subunit that mediates L-type channel currents is depicted in Figure 1-1 [8]. Calcium influx is the principal route of Ca^{2+} entry in excitable cells, supporting processes like synaptic transmission — where ion channels open in response to membrane depolarisation, switch on Ca^{2+} influx and encode events like neurotransmitter release [8, 22].

1.1.2.2 Calcium store release

In contrast to the direct nature of Ca^{2+} influx, Ca^{2+} store release involves the redistribution of Ca^{2+} sequestered inside the endoplasmic reticulum into the cytoplasm via the recruitment of an intracellular protein, phospholipase C (PLC) [1, 2]. Ca^{2+} store release is shown schematically in Figure 1-1. This pathway relies on activation of plasma membrane receptors, such as G-protein coupled receptors (GPCRs), which are coupled to the PLC signal transduction pathway [1, 2]. As a consequence of PLC activation, the minor membrane phospholipid, phosphatidylinositol 4,5-bisphosphate (PIP_2) is hydrolysed into inositol (1,4,5) triphosphate (IP_3) [23]. IP_3 engages the Ca^{2+}-permeable ion channel inositol triphosphate receptor (IP_3R), positioned on the endoplasmic reticulum membrane. IP_3R activation releases Ca^{2+} stores and rapidly increases $[Ca^{2+}]_{CYT}$ up to sub-µM levels [24]. The example in Figure 1-1 is agonist activation of muscarinic receptors, where the endogenous agonist acetylcholine binds to the muscarinic receptor, activates the PLC signal transduction pathway, and increases $[Ca^{2+}]_{CYT}$ [9]. This $[Ca^{2+}]_{CYT}$ increase is then decoded into an event like smooth muscle contraction [9].

While most GPCR receptors are reversibly activated by agonists, the subfamily of GPCRs known as proteinase activated receptors (PARs) are irreversibly activated by proteolytic cleavage [10, 11]. Figure 1-1 depicts trypsin (a protease)-mediated cleavage of PAR, which exposes an N-terminal domain that activates this receptor, via intramolecular binding to produce a cell response [10, 11].

1.1.2.3 Calcium efflux

Ca^{2+} efflux mechanisms, in addition to the maintenance of low cytoplasmic Ca^{2+} levels, also participate in terminating Ca^{2+} transients, and therefore shape calcium signals, particularly the decay phase [1, 2]. Equipped with a combination of Ca^{2+} pumps and exchangers, the cell meets the requirements for Ca^{2+} efflux against unfavourable electrochemical gradients [1, 2]. Figure 1-1 highlights the Ca^{2+} efflux mechanisms, sodium (Na^+)-Ca^{2+} exchanger (NCX), the sarcoplasmic-endoplasmic reticulum Ca^{2+} ATPase (SERCA) and the plasma membrane Ca^{2+} ATPase (PMCA) pump [1, 2].

1.1.2.4 Sodium-calcium exchanger (NCX)

Located at the plasma membrane, the sodium-calcium exchanger (NCX) transports Na^+ ions into the cell along its electrochemical gradient in exchange for Ca^{2+} ions, which are removed from the cytoplasm against the electrochemical gradient [12]. The direction of the NCX is reversible under conditions of high intracellular Na^+ levels [12]. Low intracellular Na^+ levels, however, almost always favour Ca^{2+} efflux [12]. NCX1 is illustrated in Figure 1-1 and is the most extensively studied NCX isoform. NCX1 has an affinity for Ca^{2+} in the low µM range, extruding Ca^{2+} most effectively from a stimulated cell, when the magnitude of $[Ca^{2+}]_{CYT}$ is well above resting levels [12].

1.1.2.5 Sarcoplasmic-endoplasmic reticulum calcium ATPase (SERCA)

Positioned on the ER membrane (Figure 1-1), the SERCA pump facilitates Ca^{2+} transport from the cytoplasm into the ER lumen, which terminates $[Ca^{2+}]_{CYT}$ transients and refills the endoplasmic reticulum Ca^{2+} store [12]. SERCA contains a catalytic domain that hydrolyses adenosine-5'-triphosphate (ATP) into adenosine diphosphate (ADP) [25], providing the energy necessary to actively transport Ca^{2+} into the ER [1, 2]. The SERCA pump is a high affinity, low capacity Ca^{2+} transporter, therefore transporting Ca^{2+} in the absence or presence of a Ca^{2+} mobilising stimulus, maintaining basal $[Ca^{2+}]_{CYT}$ and terminating Ca^{2+} signals [1, 2].

1.1.2.6 Plasma membrane calcium ATPase (PMCA)

PMCA calcium pumps share some structural similarities with the SERCA pump [26]. This includes the presence of an intracellular catalytic domain that supports active Ca^{2+} transport through ATP hydrolyses [1, 2, 27]. Similar to the NCX, PMCA pumps are also situated on the plasma membrane (Figure 1-1), and extrude cytoplasmic Ca^{2+} from the cell [1, 2]. Endogenous activators of the PMCA pump include the Ca^{2+}-sensing protein, calmodulin and acidic phospholipids [13, 28]. Both activate PMCA by increasing the maximum velocity of the pump, and reducing its affinity for Ca^{2+} from 10-20 µM to 1 µM [13, 28].

1.1.3 Endoplasmic reticulum calcium levels ($[Ca^{2+}]_{ER}$)

For many Ca^{2+} signals, including those coupled to IP_3 signal transduction (section 1.1.2.2, page 5), the endoplasmic reticulum (ER) is the most important intracellular Ca^{2+} store released in the presence of a stimulus [1, 2]. Redistribution of Ca^{2+} from the ER to the cytoplasm, not only fuels a $[Ca^{2+}]_{CYT}$ increases, but simultaneously depletes ER Ca^{2+} levels ($[Ca^{2+}]_{ER}$). This depletion activates a phase of Ca^{2+} entry that restores high magnitude $[Ca^{2+}]_{ER}$ concentrations. Maintaining $[Ca^{2+}]_{ER}$ up to 1 mM [5] is required for future Ca^{2+} signalling events, but also supports organelle specific functions such as vesicle trafficking, regulation of cholesterol metabolism and protein folding/processing [29]. Figure 1-2 shows the changes in $[Ca^{2+}]_{ER}$ expected during IP_3-mediated calcium signals. The ER Ca^{2+} content is refilled by a mechanism initially proposed by James Putney in 1986 and known as store-operated Ca^{2+} entry (SOCE) [14].

1.1.3.1 Store operated calcium entry

Triggered by ER store depletion, store operated calcium entry (SOCE) activates ion channels at the plasma membrane, resulting in Ca^{2+} entry from the extracellular medium into the ER [14]. Reviewed by Varnai *et al*. [20], the specific proteins mediating SOCE were recently identified as stromal interaction molecule (STIM) and Orai channels. Briefly, at high $[Ca^{2+}]_{ER}$ concentrations STIM1 binds to Ca^{2+} inside the ER lumen [15, 16]. At low $[Ca^{2+}]_{ER}$ concentrations, however, when the intracellular store is depleted during a Ca^{2+} signalling event, STIM1 dissociates from Ca^{2+} and binds to another STIM1 monomer [15, 16]. The resulting STIM1 oligomers, translocate to the plasma membrane in domains adjacent the ER [15, 17, 18], activate Ca^{2+} entry though Orai channels, and replenish intracellular ER Ca^{2+} stores [19]. The Orai1 subunit, depicted in Figure 1-1, is functional as a heteromeric channel consisting of four Orai subunits [20].

1.1.4 Mitochondrial calcium levels ($[Ca^{2+}]_{MIT}$)

In 1992 a mitochondrial-targeted aequorin construct enabled research laboratories to directly monitor mitochondria Ca^{2+} levels ($[Ca^{2+}]_{MIT}$) using luminescence [30]. This technique confirmed that mitochondria are not spectators of calcium signals, but they can rapidly accumulate Ca^{2+} and experience $[Ca^{2+}]_{MIT}$ increases in parallel with $[Ca^{2+}]_{CYT}$ increases [30, 31]. Figure 1-2 illustrates a typical Ca^{2+} signal that mitochondria experience in a stimulated cell.

Mitochondria Ca^{2+} uptake occurs through the low affinity, high capacity mitochondrial uniporter [32, 33], which is thermodynamically driven by an electrochemical gradient generated by oxidative metabolism [34]. Using the mitochondrial-targeted aequorin construct, $[Ca^{2+}]_{MIT}$ levels are reported to be up to concentrations of 5 µM or even 500 µM in some cell types [30, 35]. These values, which can exceed the magnitude of $[Ca^{2+}]_{CYT}$ signals, are surprising because experiments in isolated mitochondria report that MCU has a low Ca^{2+} affinity [34]. This anomaly was resolved by the microdomain hypothesis and the molecular identification of the components responsible for flux of Ca^{2+} ions across mitochondrial membranes as described below.

1.1.4.1 The microdomain hypothesis

The microdomain hypothesis acknowledges the ability for a cell to unevenly distribute Ca^{2+} throughout the cytoplasm, where the Ca^{2+} level in a microdomain can greatly exceed the level of $[Ca^{2+}]_{CYT}$ measured in the bulk cytoplasm [36]. Strategic placement of mitochondria in close proximity to the ER directly exposes the MCU to IP_3R Ca^{2+} release sites [37]. Consequently, despite a low Ca^{2+} affinity, during cell stimulation the mitochondrial calcium uniporter rapidly transports Ca^{2+} into the mitochondria matrix at magnitudes [38] that can surpass $[Ca^{2+}]_{CYT}$ levels.

1.1.4.2 The Mitochondrial Calcium Uniporter (MCU)

Although mitochondrial Ca^{2+} uptake is known to regulate numerous cell events [39] such as catecholamine secretion [35], apoptosis [40] and oxidative metabolism for ATP synthesis [41], the molecular identity of this calcium transporter remained unknown until 2011. Two research laboratories independently identified the pore-forming subunit of the MCU as CCDC109A [32, 33]. This discovery now allows scientists to assess the significance of mitochondria Ca^{2+} uptake by techniques including the genetic manipulation of MCU [42].

(a) Cytoplasmic Ca^{2+}

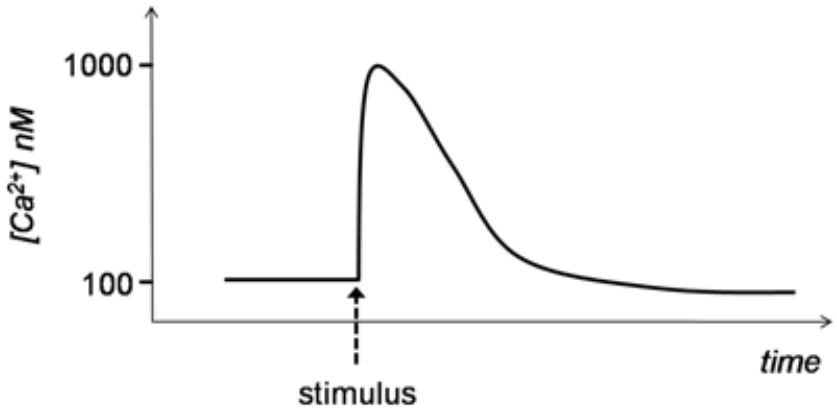

(b) Endoplasmic reticulum Ca^{2+}

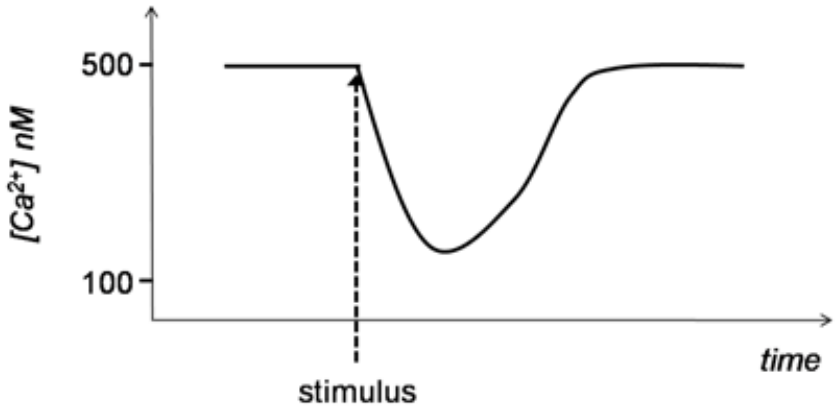

(c) Mitochondrial Ca^{2+}

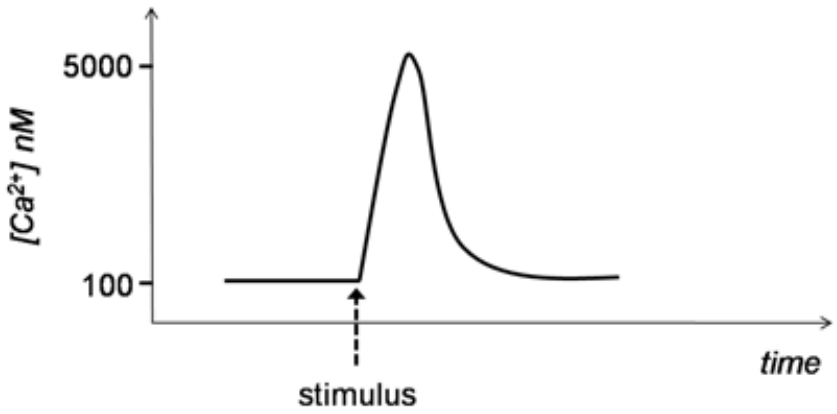

Figure 1-2: Example Ca^{2+} signals expected in different cell compartments in a stimulated cell.

In the presence of a stimulus, intracellular Ca^{2+} is unevenly distributed throughout the various cell compartments [1, 43]: **(A)** the cytoplasm experiences a transient increase in Ca^{2+} [1, 43] **(B)** the ER Ca^{2+} content rapidly decreases due to store release of Ca^{2+} [1, 5, 43] and **(C)** a subpopulation of mitochondria accumulate Ca^{2+} to levels well above that detected in the cytoplasm [30, 31].

1.1.5 Summary

A wide-variety of Ca^{2+} transport proteins, including ion-channels and pumps work in concert to process Ca^{2+} into unique signals, which is then decoded into specific cell events. One calcium transporter, PMCA contributes to calcium homeostasis via Ca^{2+} efflux. As discussed in the next section, PMCA is a very large family of proteins that are extremely diverse in their structure, and regulation at the molecular level. This advocates that PMCA calcium pumps, beyond simple Ca^{2+} efflux pumps actually contribute to many diverse physiological functions.

1.2 The Plasma Membrane Calcium ATPase (PMCA)

1.2.1 Introduction

Originally discovered in 1966 by Schatzmann [44], Plasma Membrane Calcium ATPase (PMCA) pumps consist of four isoforms (PMCA1-4), encoded by separate genes (ATP2B1-4) [45-48] that are subject to alternative splicing, which yields over thirty splice variants [49]. With so many variants, PMCAs are predicted to accomplish many unique tasks throughout the body. This prediction is the natural consequence of PMCA diversity at the molecular level, which will now be discussed.

1.2.2 Molecular structure

PMCA pumps are members of the P-Type ATPase family, which actively pump cations across cell membranes [50]. The SERCA pump (introduced in section 1.1.2.5, page 6) is also a member of the P-Type ATPase family that actively transports Ca^{2+} [27]. The crystal structure of the SERCA pump [25] provides the basis for the structure and mechanism of ATP driven transport [27]. Four domains are conserved amongst the P-Type ATPases, they are a phosphorylation domain (P-domain), a nucleotide binding domain (N-domain), an actuator domain (A-domain) and a membrane domain (M-domain) [27]. Figure 1-3 highlights these domains within the structure of PMCA. The P-domain is the catalytic core that contains the signature motif DKTGILT [27], which harbours the characteristic aspartyl phosphate residue [25]. The N-domain, divides the P-domain and contains a lysine (K) residue important for the binding of the nucleotide, ATP [25, 27]. The discontinuous A-domain contains the TGE sequence [25] that interacts with the aspartyl phosphate residue during pump activity [27]. The M-domain is composed of ten hydrophobic transmembrane regions and is the least conserved region amongst the P-type ATPase family [27]. A comprehensive review of P-type ATPase structure and mechanism is given elsewhere [27]. In addition to features common to P-type ATPases, PMCA also contains two alternative splice sites and a very long intracellular carboxy-terminal region, containing motifs essential for the biochemical regulation of the pump within an intact cell [50]. The section below will discuss these extra features, which are responsible for pump diversity at the molecular level.

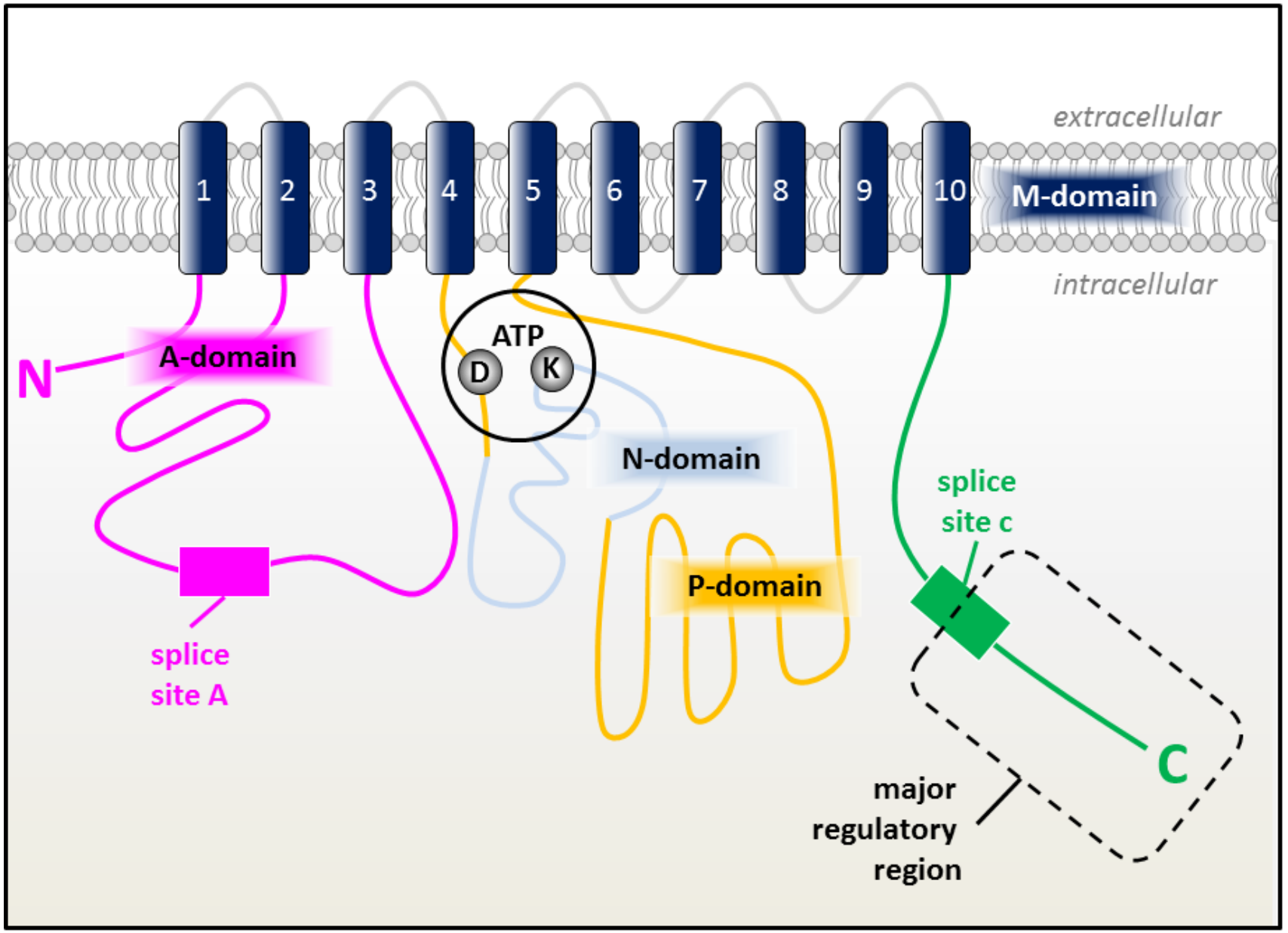
extracellular
1
2
3
4
5
6
7
8
9
10
M-domain
intracellular
N
A-domain
ATP
D
K
N-domain
P-domain
splice
site c
splice
site A
C
major
regulatory
region

Figure 1-3: Predicted membrane topology for the PMCA pump.

PMCA is a P-Type ATPase pump, responsible for the efflux of cytoplasmic Ca^{2+} from the cell [50]. PMCA shares structural features with the SERCA pump [26]. There are four domains, indicated by different colours, that are predicted by the crystal structure of the SERCA pump [25] and the circle depicts the ATP binding site [51]. The P-domain (orange) is the catalytic core and contains the characteristic phosphoryl-aspartate, D [25]. The N-domain (light blue) contains the signature, lysine (K) residue, which is important for the binding of ATP [25, 27]. Alternative splicing increases the molecular diversity amongst the PMCA pumps [49]. The A-domain (pink) contains the alternative splicing site A [49]. The cytoplasmic, C-terminus (green) contains the alternative splicing site C, which overlaps with the major regulatory region of the pump [49, 52] The M-domain (navy blue) is indicated by the hydrophobic transmembrane spanning regions numbered 1-10 [27]. Figure adapted from a review article [50].

1.2.3 Alternative splicing

Alternative RNA splicing describes the process whereby an mRNA precursor is spliced more than one way during mRNA maturation, producing many different proteins encoded by the same gene [53]. Alternative splicing and its regulation have been reviewed by Black *et al* [53]. All PMCA isoforms contain two sites that undergo alternative RNA splicing (Figure 1-3), these splice sites are known as splice site A and splice site C [49, 52, 54]. Because the variable insertion of exons at splice site A and C produces different primary structures, each PMCA splice variant is predicted to adopt a distinct overall three-dimensional conformation, with unique regulatory properties [49, 55]. This phenomenon has led to the discovery of over thirty human PMCA variants, which contribute to Ca^{2+} homeostasis throughout the body [49].

1.2.3.1 Splice site A

Splice site A is positioned within the A-domain of PMCA, and involves the variable insertion of up to three exons to produce the w, x and z variants [49]. Very little is known about the functional role of alternative splicing at site A. Studies of the w variant demonstrate that targeting of PMCA2w to the apical membrane of cells, independent of the configuration at splice site C [56]. This was initially demonstrated using confocal fluorescence microscopy in polarised Madin-Darby canine kidney cells overexpressing PMCA2w [56]. Consistent with this finding, another study reported that endogenous PMCA2w is targeted to hair bundles in rat hair cells [57]. The apical nature of the PMCA2w variant was also confirmed by Reinhardt *et al*. in mouse mammary gland epithelial cells [58, 59]. Endogenous PMCA2bw, the splice variant upregulated during lactation, is targeted to the apical membrane for a key role Ca^{2+} secretion, where large transcellular Ca^{2+} fluxes are required for milk production [58, 59].

1.2.3.2 Splice site C

Splice site C is located at the C-terminus of PMCA and involves either the exclusion or inclusion of one exon [52]. The exclusion of the exon results in the full length PMCAb variants, whereas including the exon shifts the translational reading frame, producing the truncated PMCAa variants [52]. The C splice site overlaps with a key regulatory region positioned in the C-terminus of the pump, containing the calmodulin binding domain [60], which mediates calmodulin-induced pump activation [61]. Alternative splicing at site C, which alters the regulatory region, significantly increases PMCA pump diversity [49, 55].

1.2.4 Biochemical regulation of PMCAs

Biochemical regulation controls the trafficking, functional and degradation properties of proteins [62]. This involves interactions with intracellular proteins through direct protein-protein binding or by chemical modification of amino acids within specific motifs [62]. Primary structure analysis of PMCA reveals several key motifs, concentrated within the C-terminal end of the pump and responsible for its biochemical regulation [50]. The sequence alignment between the C-terminus of the PMCA isoforms and splice variants, shown in Figure 1-4, reinforces sequence diversity amongst the pumps in this region.

1.2.4.1 Auto-inhibition

Auto-inhibition describes the conformation that PMCA adopts in the resting cell, which involves the intra-molecular binding of internal 'receptors sites' [63-65]. These receptor sites are positioned within the C-terminal tail [63], the catalytic domain [64] and the A-domain [65] of the pump. This conformation excludes substrates, like ATP from accessing catalytic sites and restricts pump activity in the resting cell, and $[Ca^{2+}]_{CYT}$ is low [63-65]. During cell stimulation, when $[Ca^{2+}]_{CYT}$ is transiently elevated, calmodulin binds to PMCA within the calmodulin binding domain, displaces auto-inhibition and activates the pump [63-65]. The calmodulin binding domain, highlighted in Figure 1-4, is located in the C-terminus of PMCA [60]. The basal activity and affinity for calmodulin are widely varied amongst the PMCA isoforms and their splice variants [50]. PMCA2 has higher basal activity and is more sensitive to calmodulin compared with other PMCA isoforms [66], independent of the configuration at splice site C [67]. However, sequence variation from alternative splicing at site C in PMCA4 [68, 69] results in the short variant, PMCA4a having a higher basal activity and a reduced affinity for calmodulin in comparison to the full length, PMCA4b variant [70, 71].

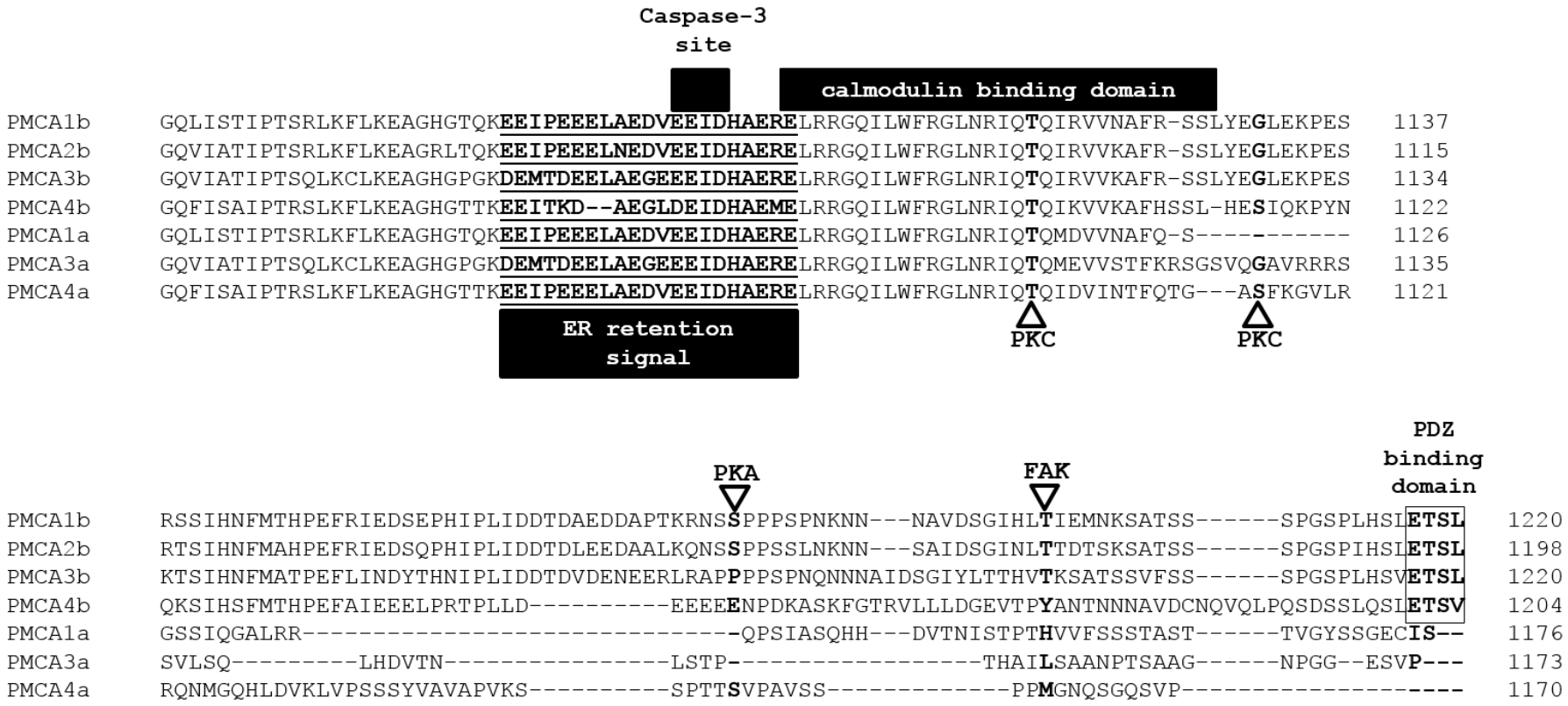
Caspase-3 site
calmodulin binding domain
ER retention signal
PKC
PKC
PKA
FAK
PDZ binding domain
PMCA1b GQLISTIPTSRLKFLKEAGHGTQKEEIPEEELAEDVEEIDHAERELRRGQILWFRGLNRIQTQIRVVNAFR-SSLYEGLEKPES 1137
PMCA2b GQVIATIPTSRLKFLKEAGRLTQKEEIPEEELNEDVEEIDHAERELRRGQILWFRGLNRIQTQIRVVKAFR-SSLYEGLEKPES 1115
PMCA3b GQVIATIPTSQLKCLKEAGHGPGKDEMTDEELAEGEEEIDHAERELRRGQILWFRGLNRIQTQIRVVKAFR-SSLYEGLEKPES 1134
PMCA4b GQFISAIPTRSLKFLKEAGHGTTKEEITKD--AEGLDEIDHAEMELRRGQILWFRGLNRIQTQIKVVKAFHSSL-HESIQKPYN 1122
PMCA1a GQLISTIPTSRLKFLKEAGHGTQKEEIPEEELAEDVEEIDHAERELRRGQILWFRGLNRIQTQMDVVNAFQ-S----------- 1126
PMCA3a GQVIATIPTSQLKCLKEAGHGPGKDEMTDEELAEGEEEIDHAERELRRGQILWFRGLNRIQTQMEVVSTFKRSGSVQGAVRRRS 1135
PMCA4a GQFISAIPTRSLKFLKEAGHGTTKEEIPEEELAEDVEEIDHAERELRRGQILWFRGLNRIQTQIDVINTFQTG---ASFKGVLR 1121
RSSIHNFMTHPEFRIEDSEPHIPLIDDTDAEDDAPTKRNSSPPPSPNKNN---NAVDSGIHLTIEMNKSATSS------SPGSPLHSLETSL 1220
RTSIHNFMAHPEFRIEDSQPHIPLIDDTDLEEDAALKQNSSPPSSLNKNN---SAIDSGINLTTDTSKSATSS------SPGSPIHSLETSL 1198
KTSIHNFMATPEFLINDYTHNIPLIDDTDVDENEERLRAPPPPSPNQNNNAIDSGIYLTTHVTKSATSSVFSS------SPGSPLHSVETSL 1220
QKSIHSFMTHPEFAIEEELPRTPLLD----------EEEEENPDKASKFGTRVLLLDGEVTPYANTNNNAVDCNQVQLPQSDSSLQSLETSV 1204
GSSIQGALRR----------QPSIASQHH---DVTNISTPTHVVFSSSTAST------TVGYSSGECIS-- 1176
SVLSQ---------LHDVTN----------LSTP----------THAILSAANPTSAAG------NPGG--ESVP--- 1173
RQNMGQHLDVKLVPSSSYVAVAPVKS----------SPTTSVPAVSS----------PPMGNQSGQSVP---------- 1170

Figure 1-4: Sequence alignment of the cytoplasmic C-terminal end of some PMCA variants.

The linear amino acid sequences for human PMCA variants were obtained from the National Centre for Biotechnology Information (NCBI) protein database. The cytoplasmic C-terminal portion of PMCA variants were aligned using the ClustalW2 algorithm. Several sequence motifs are concentrated within this region of the pump and are responsible for its biochemical regulation [50]; they are highlighted in the sequence alignment. The calmodulin binding domain mediates calmodulin-induced pump activation [13, 28]. The consensus site for caspase-3 cleavage regulates pump activity during apoptosis [72-76]. Residues phosphorylated by PKA [77, 78], PKC [79, 80] and FAK [81] are illustrated (triangles). A potential ER retention signal has been reported upstream of the calmodulin binding domain [82], which could be important regulatory property of the pump during apoptosis [76]. A PDZ binding domain is only found in the full length PMCA variants [83].

1.2.4.2 Phosphorylation of PMCAs

Phosphorylation is a chemical modification, involving the covalent addition of a phosphate group to a single amino acid residue within a specific motif [62]. Phosphorylation alters protein function through a conformational change or by facilitating interactions with other intracellular proteins, driving the formation of larger protein complexes [62]. Protein kinases catalyse the phosphorylation reaction and include protein kinase A (PKA), protein kinase C (PKC) and focal adhesion kinase (FAK). Figure 1-4 highlights the PKA, PKC and FAK phosphorylation sites reported within the C-terminus of some PMCA pumps. However, not all PMCA pumps contain these sites; therefore, PMCA variants exhibit differences in PKA, PKC and FAK-mediated regulation.

PKA-mediated phosphorylation of the serine (S) residue, downstream of the calmodulin binding domain, within the motif KRNSS, is only reported for PMCA1, and activates this pump isoform [77, 78]. Within the calmodulin binding domain of PMCA, both S and threonine (T) residues are subject to PKC-mediated phosphorylation [79, 80, 84]; and this modification can activate [85] or inhibit PMCA4b [80], modestly inhibit PMCA2a or PMCA3a [86], while PMCA4a is unaffected [87, 88]. FAK-mediated phosphorylation of a tyrosine (Y) residue, within the motif EVTPY is downstream of the calmodulin binding domain and inhibits PMCA4b activity [81, 89]. The functional consequence of this chemical modification, triggered by thrombin has been examined in platelets [90]. Inhibition of PMCA4b-mediated Ca^{2+}efflux increases intracellular Ca^{2+} levels, and activates platelet aggregation [90]. Inhibition of PMCA-mediated Ca^{2+} efflux by FAK, augments intracellular Ca^{2+}, and is associated with hyperactive platelets detected in patients with hypertension [91] and type 2 diabetes [92].

1.2.4.3 PDZ binding domain of PMCAs

PDZ domains were initially discovered in three proteins; post synaptic density protein (PSD95), Drosophila disc large tumor suppressor (DlgA), and zonula occludens-1 protein (zo-1), which is reflected in the acronym PDZ [93]. The longer PMCAb splice variants, but not the shorter PMCAa variants, contain a conserved PDZ binding domain ETS(L/V) at the C-terminal end [83]. The sequence alignment in Figure 1-4 highlights the PDZ binding domain in the full length pump variants. The PDZ binding domain allows some PMCA variants to bind partner proteins with a PDZ domain, which can drive the formation of multiprotein scaffolds and support local signal transduction at the plasma membrane [93]. Kim *et al* were the first to demonstrate the binding of PMCA4 to members of the membrane-associated guanylate kinase (MAGUK) protein family through PDZ domains [83]. Since this first account, PMCA4b has been shown to interact with the important mediator, neuronal nitric oxide synthase-1 (nNOS-1) through its PDZ domain [94]. nNOS-1 is a calmodulin regulated protein that converts L-arginine into nitric oxide (NO) in the presence of Ca^{2+} [95]. PMCA and nNOS are both targeted to sub-cellular domains within cavaolae [95, 96] and associate via the PDZ domain of nNOS [94] to form a scaffold for local signal transduction. PMCA4b negatively regulates nNOS by reducing the local Ca^{2+} concentration, inhibiting NO production. The physiological consequence of this PDZ-mediated interaction was explored in transgenic mice overexpressing PMCA4b, reducing heart contractility [97] and increasing vascular tone [98].

1.2.4.4 Proteolytic cleavage of PMCAs

Another layer of protein regulation is proteolysis, whereby proteases act like molecular scissors by cutting proteins irreversibly within specific consensus sites to fragment proteins to alter their activity and/or location [62]. Calpain and caspases are two families of proteases that cleave PMCA, within or in close proximity to the calmodulin binding domain [50]. Cleavage of PMCA truncates the pump and removes downstream regulatory sequences, affecting the calmodulin binding domain, the receptor site required for auto-inhibition, the phosphorylation sites and the PDZ binding-domain [50].

1.2.4.4.1 *Calpains*

There are two isoforms of calpains, μ and m that are activated by micromolar and millimolar concentrations of Ca^{2+}, respectively [99]. PMCA is cleaved and truncated by calpain to irreversibly activate the pump in isolated membrane preparations [100, 101]. This provides another mechanism for pump activation, in addition to calmodulin and acidic phospholipids [13, 28]. PMCA is likely to be regulated by calpains in a variety of cell signalling pathways because calpain activity is controlled by the ubiquitous second messenger, Ca^{2+} [99]. The precise role of these proteases, although unclear, have been implicated in the cell death pathways, including apoptosis and necrosis [99]

1.2.4.4.2 *Caspases*

Caspases are proteases employed during apoptosis to dismantle cell components for subsequent elimination [72]. They are subdivided into 'initiator' and 'effector' caspases to distinguish those that initiate (caspase-8, -9, -10) and execute (caspase-3,-6,-7) apoptosis [72]. The initiator caspases are activated by homodimerisation on specialised platforms, formed when a cell receives an apoptotic signal [72, 102]. Initiator caspases, once stimulated recruit, cleave and activate the executioner caspases [72]. Active executioner caspases cleave target substrates at the preferred consensus motif DEV(D/G) [72]. This motif in the C-terminus of the PMCA isoforms is highlighted in Figure 1-4. A review by Earnshaw *et al.* provides further details on caspase structure, activation, substrates and function during apoptosis [72]. Patzy *et al.* provided the first report that PMCA4b is cleaved by caspase-3 in cells undergoing staurosporine-induced apoptosis, at the consensus site DEID, upstream of the calmodulin binding domain [75]. This provides a potential link between PMCAs and apoptosis, which is explored in this dissertation.

1.2.5 Tissue distribution of PMCAs

The tissue distribution of PMCA isoforms has been demonstrated at the level of messenger ribonucleic acid (mRNA) [49] and protein [103]. PMCA1 and PMCA4 are expressed ubiquitously throughout the body, while PMCA2 and PMCA3 show a restricted tissue distribution within excitable tissues [49]. PMCA1 is concentrated in the brain, lung and intestine [104], whereas PMCA4 is the predominate isoform expressed in erythrocytes [103] and spermatozoa [105]. PMCA2 is abundantly detected within the cerebellum and cerebral cortex [103] and in the hair cells of the inner ear [106]; while a large quantity of PMCA3 is detected in the choroid plexus [103]. Specific PMCA isoforms can also be transiently expressed in tissues to perform specialised functions. An example of this is upregulation of PMCA2 in the lactating mammary gland [58, 107, 108]. Reinhardt *et al.* have shown that PMCA2 upregulation, parallels increased milk production and is the predominate isoform in the lactating mammary gland [58, 108]. Conversely, when lactation ends and milk production is no longer required, PMCA2 is abruptly downregulated during mammary gland involution [107].

1.2.6 Physiological roles of PMCAs

The contribution of individual PMCA isoforms to Ca^{2+} homeostasis and cell function is not well understood due to the lack of specific PMCA inhibitors. However, the development of PMCA knockout animals [109], and the identification of PMCA genetic mutations [110] has provided insight towards understanding the isoform specific functions of different PMCA isoforms. No genetic mutations have been reported for PMCA1, and mice null for the PMCA1 gene do not survive [111]. This is consistent with the housekeeping function if this isoform, where PMCA1-mediated Ca^{2+} efflux is essential in maintaining the low intracellular Ca^{2+} levels required for Ca^{2+} homeostasis [111]. PMCA4 null mice are viable and, except for male infertility appear healthy [112]. Male infertility, in this context, is the consequence of impaired sperm motility upon the deletion of PMCA4 [105]. Genetic mutations and knockout animals have been described for PMCA2. PMCA2 null mice survive, but have compromised vestibular and auditory systems that manifests as deafness and difficulties in maintaining balance [113]. The deafwaddler mouse encodes a mutant PMCA2 gene that reduces pump activity by 70% [114, 115]. These mice are deaf and display vestibular/motor imbalance [114, 115]. The Wriggle Mouse Sagami is another example of a genetic PMCA2 mutation, and is associated with hereditary hearing loss [116]. Reinhardt *et al.* used a PMCA2 null mouse model to study PMCA2 in lactating rodents. Consistent with PMCA2 upregulation in the lactating mammary gland [58, 108], PMCA2-null mice produce milk with significantly reduced Ca^{2+} concentration [59]. Although PMCA3 null mice have not been reported, genetic defects in PMCA3 have been

documented and affect neural pathologies, and is associated with the developmental delay, hypotonia, cerebellar ataxia [110].

1.2.7 Regulation of calcium homeostasis by PMCAs

The question still remains: how do the PMCA isoforms differentially modulate Ca^{2+} homeostasis and determine cell function? The answer is influenced by the different structural and regulatory properties amongst the pump isoforms. However, the majority of studies on PMCA use the purified pump or isolated membrane preparations, lacking the physiological regulators that determine pump activity *in vivo*. A study by Brini *et al.* is important because intact Chinese hamster ovary (CHO) cells, which overexpress the full length pump variants (PMCA1-4b) were used to investigate the impact of PMCA isoforms on Ca^{2+} homeostasis [117]. In cells overexpressing specific PMCA isoforms, the $[Ca^{2+}]_{CYT}$ and $[Ca^{2+}]_{MIT}$ was significantly reduced upon ATP-induced release of the IP_3-sensitve Ca^{2+} stores, detected as reduced amplitude and shorter duration of the Ca^{2+} signal [117]. The authors attributed this observation to a reduced basal $[Ca^{2+}]_{ER}$; where a small change in $[Ca^{2+}]_{ER}$ significantly reduced the level of Ca^{2+} redistributed into the cytoplasm or mitochondria upon Ca^{2+} store release [117]. This effect was more pronounced for the non-ubiquitous pump isoforms, PMCA2 and PMCA3 and is consistent with their abnormally high affinity for Ca^{2+} determined in isolated membrane preparations [66]. These results are also consistent with the restricted tissue distribution of PMCA2 and PMCA3, which are highly expressed in excitable cells that frequently experience large Ca^{2+} fluxes and require a highly efficient Ca^{2+} efflux system [117].

1.2.8 Summary

PMCA isoforms have unique tissue distribution patterns and are subject to intense regulation at the level of expression, RNA processing, post-translational modification and interactions with intracellular proteins. Although the structure and biochemical properties of PMCA isoforms are well studied, the specific physiological functions of PMCA isoforms in intact cells are not as well defined. Cell death is one pathway where the shape and location of Ca^{2+} may be particularly important. Because Ca^{2+} efflux via PMCA calcium pumps can influence the shape and location of Ca^{2+} signals, the relationship between cell death, Ca^{2+} and PMCA will be reviewed in more detail in the following section.

1.3 Cell Death

1.3.1 Introduction

Cells are eliminated from the body by different cell death pathways, including apoptosis and necrosis [118]. Necrosis proceeds as uncontrolled cell death, involving tissue damage and is observed in the pathological setting of ischemic reperfusion injury, epilepsy, Alzheimer's disease and other inflammatory injuries [118]. Apoptosis is the contrast to necrosis, and proceeds as programmed cell death that physiologically regulates cell populations during embryologic development, metamorphosis and for regulation of tissue size [118]. Deregulation of the apoptotic program is characteristic of diseases such as cancer; where the tumour cell acquires resistance to apoptotic signals that would normally eliminate the cell [119]. This section will outline the morphological and biochemical hallmarks of apoptosis before delineating Ca^{2+} regulation of this signalling pathway.

1.3.2 Morphological features

Kerr *et al.* first documented apoptosis using an electron microscope in 1972 [120]. Morphologically apoptosis is visualised as the formation of apoptotic bodies that are observed as well-preserved, membrane bound compartments that originate from the whole cell [120]. The formation of apoptotic bodies is accompanied by the marked condensation of the cell involving chromatin condensation [121], membrane blebbing [122] and deoxyribonucleic acid (DNA) fragmentation [123]. During the late phase of apoptosis the newly formed apoptotic bodies are engulfed by neighbouring cells, followed by their intracellular degradation [120]. Apoptosis eliminates cells discretely, avoiding the release of intracellular contents into the extracellular medium, which would evoke widespread injury to the neighbouring cells [120].

1.3.3 Biochemical hallmarks

Since its first documentation [120], apoptosis has been under intense investigation. It is now widely accepted that underlying mechanisms include an elevation in ATP, activation of caspases and exposure of phosphatidylserine at the extracellular face of the plasma membrane [124]. Apoptosis is an active event, therefore increased ATP provides the energy to drive the process to completion [125, 126]. Caspases, introduced in section 1.2.4.4.2, page 21, are the proteases that execute apoptosis [72]. Phosphatidyserine is an acidic phospholipid that is found within the inner leaflet of the plasma membrane and redistributes to the outer leaflet during apoptosis, serving as a recognition molecule for phagocytosis [127]. The signalling cascades that activate these biochemical changes to effect apoptosis are divided into intrinsic and extrinsic pathways [128]. Figure 1-5 illustrates these two discrete signalling cascades that result in apoptosis.

1.3.3.1 Intrinsic apoptosis

Apoptosis is the result of death signals like DNA damage, chemotherapeutic agents, serum starvation and UV radiation, and can be intrinsically controlled by the cell's mitochondria [129]. The family of B-cell lymphoma 2 (Bcl-2) proteins receive and then deliver death inputs to the mitochondria [130]. Bcl-2 proteins are sub-divided into three groups and share sequence homology within four Bcl-2 homology (BH) domains (BH1-BH4) [131]. The first group includes Bcl-2, which have an anti-apoptotic function and contain up to four BH domains [131]. The second group are the pro-apoptotic members, BH3-only proteins that initiate the intrinsic cascade [129, 131]. The final group are also anti-apoptotic in nature but they contain multiple BH domains [131]. Bcl-2 proteins are reviewed by Thomadaki *et al.* [131]. Bak and Bax are members of the multiple BH domains subgroup and are activated by the upstream, BH3 proteins which register the death input [129]. When activated, Bax and Bak adopt a new conformation, undergo homo-oligomerisation and relay the death message to the mitochondria [132]. This commits a cell to apoptosis by inducing the formation of the outer mitochondrial membrane pore [132, 133]. While the molecular nature of the outer mitochondrial membrane pore is not fully understood, it functions as a non-specific protein channel that facilitates the egress of apoptotic effectors that reside within the inner mitochondrial space [132]. Cytochrome C is a hallmark apoptotic effector, harboured inside the inner mitochondrial space, which is released though the outer mitochondrial membrane pore [134, 135]. Cytosolic cytochome C is then available to form a caspase-activating scaffold, with apoptotic protease activating factor 1 (Apaf1) in a dATP-dependant manner [136]. Caspase-9 is recruited and activated to this caspase-activating scaffold, which is known as an 'apoptosome' and subsequently activates downstream caspases such as caspase-

3; which execute apoptosis by dismantling the cell [137]. An overall schematic of intrinsic apoptosis is shown in Figure 1-5.

1.3.3.2 Extrinsic apoptosis

Extrinsic apoptosis is a receptor mediated pathway of programmed cell death involving ligand activation of the death receptors, DR4 and DR5, expressed in the plasma membrane [138]. The tumour necrosis factor (TNF) superfamily are death receptor ligands, including the TNF-related apoptosis-inducing ligand (TRAIL). TRAIL binds to either death receptor, DR4 or DR5 on the extracellular face of the plasma membrane and induces death receptor trimerisation [139]. This facilitates clustering of their intracellular death domains and yields a death inducing signalling complex (DISC) [139]. Fas-associated death domain (FADD) is an adapter protein that binds to the DISC signalling complex and the resultant protein scaffold recruits and activates caspase-8 [139]. Active caspase-8 subsequently stimulates downstream caspases to execute apoptosis [140]. Alternatively, caspase-8 can recruit the intrinsic apoptotic pathway by cleaving Bid [141, 142]. Caspase-8 cleaves the BH3-only protein, Bid into its active fragment, tBid to unleash its pro-apoptotic properties [141, 142]. Redistribution of tBid to the mitochondrial membrane induces formation of the outer mitochondrial membrane pore in a Bax and Bak-dependant mechanism [143]. Figure 1-5 depicts extrinsic apoptosis schematically, showing recruitment of the intrinsic pathway through tBid.

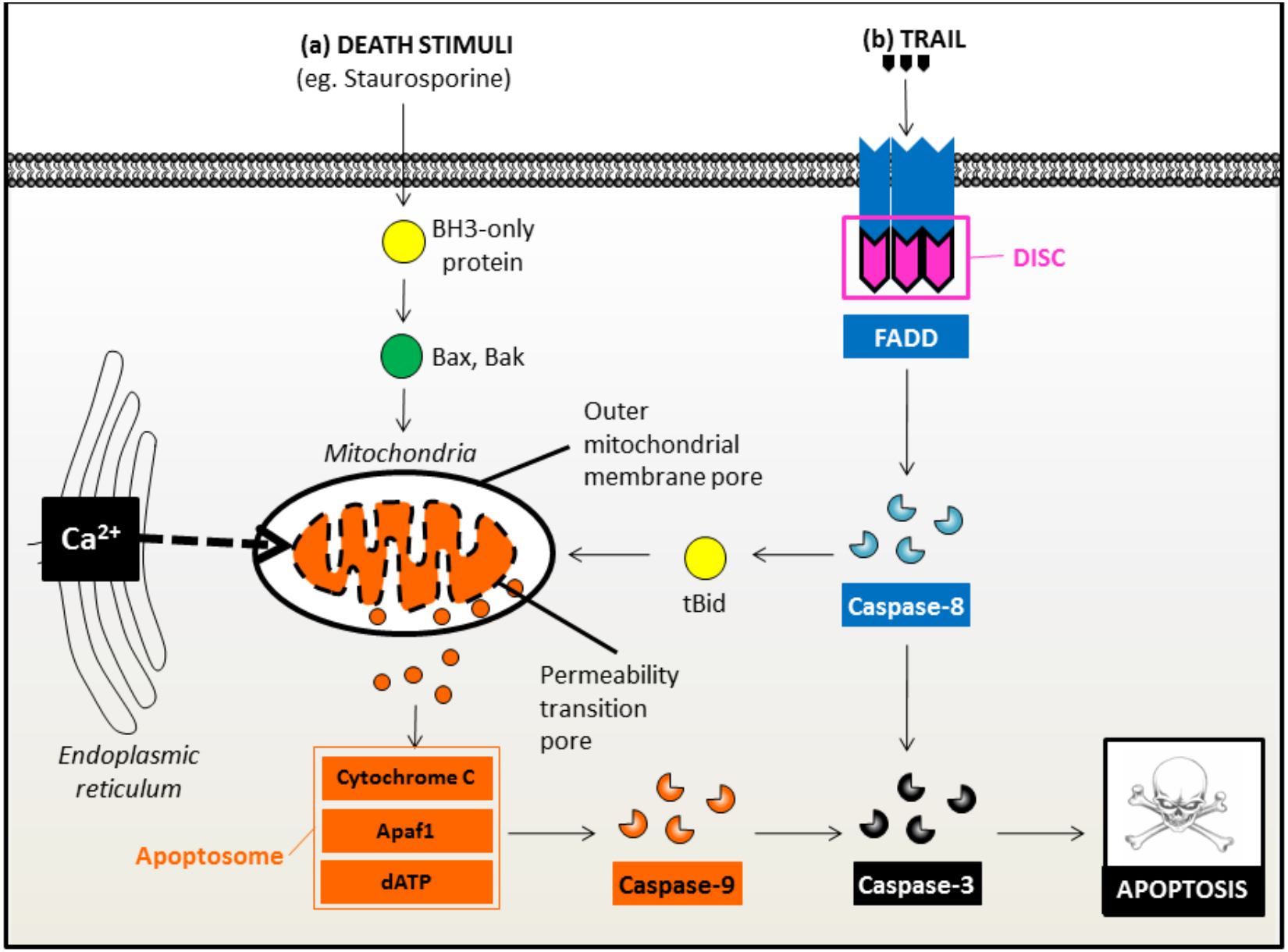
(a) DEATH STIMULI
(eg. Staurosporine)
(b) TRAIL
BH3-only protein
Bax, Bak
DISC
FADD
Mitochondria
Outer mitochondrial membrane pore
Ca2+
tBid
Caspase-8
Permeability transition pore
Endoplasmic reticulum
Cytochrome C
Apaf1
dATP
Apoptosome
Caspase-9
Caspase-3
APOPTOSIS

Figure 1-5: Apoptosis signalling pathways.

Intrinsic and extrinsic apoptosis are the two key pathways that mediate programmed cell death [128]. (a) The intrinsic pathway is coordinated by the cell's mitochondria [129]. For example, a death signal like staurosporine is sensed by the BH3-only proteins (yellow circle), which activate Bax and Bak (green circle) [144, 145]. Bax and Bak are proapoptotic, Bcl-2 proteins that relay this death message to the mitochondria by opening the outer mitochondrial membrane pore, which facilitates the release of cytochrome C (orange circle) from the mitochondria into the cell's cytoplasm [129]. Cytosolic cytochrome C forms a caspase-activating scaffold with Apaf1 and dATP, known as an apoptosome [136]. Caspase-9 is activated upon this apoptosome and subsequently activates caspase-3, which executes apoptosis [137]. (b) The extrinsic pathway involves activation of death receptors (blue) at the plasma membrane by ligands including TRAIL [139]. Ligand-binding prompts receptor trimerisation through their death domains (pink) and recruitment of the adaptor protein, FADD [139]. The resulting caspase-activating scaffold recruits and activates caspase-8 [139]. The initiator caspase-8 can activate caspase-3 to execute apoptosis [140]. Alternatively, caspase-8 cleaves the BH3-only protein, Bid into tBid (yellow circle) [141, 142]. tBid recruits the intrinsic apoptotic pathway by opening the outer mitochondrial membrane pore to evoke downstream events like cytochrome C release [143]. Ca^{2+} accumulation within the mitochondria, which is largely dependent on the local transfer of Ca^{2+} from the ER, can lead to the opening of the mitochondrial PTP on the inner mitochondrial membrane [146-148]. The Ca^{2+}-induced mitochondria PTP is a potent stimulant for the opening of the outer mitochondrial membrane pore and consequently Ca^{2+} is a key modulator of programmed cell death [149-151]

1.3.4 The apoptosis-calcium link

An increase in intracellular Ca^{2+} accompanies many apoptotic insults including ceramide [152] and staurosporine [144, 145]. These death inputs activate intrinsic apoptosis [144, 145, 152], detailed in section 1.3.3.1, page 25 (Figure 1-5). Mechanistically, intrinsic apoptosis is coordinated by the cell's mitochondria and involves cytochrome C release through the outer mitochondrial membrane pore. Mitochondrial Ca^{2+} signals can induce the formation of another pore, the permeability transition pore (PTP), located on the inner mitochondrial membrane, which results in the loss of ion gradients and dissipation of the mitochondrial membrane potential [153]. $[Ca^{2+}]_{MIT}$ increases, can therefore trigger apoptosis by prompting the PTP, which can then trigger the opening of the outer mitochondrial membrane pore [144, 145, 154] and commit a cell to undergo apoptosis [132, 133].

1.3.4.1 Calcium and the mitochondrial PTP

The opening of the mitochondrial PTP is regulated by Ca^{2+} and influenced by the parameters of the Ca^{2+} signal experienced by mitochondria, including the amplitude, frequency [147] and duration [146, 148]. A subpopulation of mitochondria positioned in close proximity to the ER experience $[Ca^{2+}]_{MIT}$ signals ranging from 5 µM up to concentrations of 500 µM [30, 35]. These are concentrations sufficient to induce the permeability transition pore [144, 145, 154]. As discussed in section 1.1.4.1 (page 8), the transfer of Ca^{2+} between the ER and mitochondria depends on IP_3-mediated Ca^{2+} store release [155, 156]. Therefore, the link between Ca^{2+} and apoptosis has been examined with agonists such as ATP, because these agents generate IP_3-mediated Ca^{2+} store release [144, 145, 151, 152]. Figure 1-5 shows Ca^{2+} accumulation in mitochondria, via the local transfer of Ca^{2+} from the ER, can induce the mitochondrial PTP and this can trigger intrinsic apoptosis.

1.3.4.2 Apoptosis and IP_3-store release of calcium

Elevations in $[Ca^{2+}]_{MIT}$ can be decoded by the mitochondria to paradoxically, promote both cell survival and cell death [4]. Hajnoczky *et al.* evaluated IP_3-mediated Ca^{2+} store release during apoptosis in whole cells, exposed to ATP in the absence and presence of the death initiators staurosporine or ceramide [149-151]. Cells exposed to ATP alone experienced a small mitochondrial membrane depolarisation, which does not activate the apoptotic program, but instead elevates ATP synthesis to energise and support cell survival [149-151]. This finding is consistent with the previous literature, where $[Ca^{2+}]_{MIT}$ in the range of 0.1 µM to 3 µM [157], is a positive regulator of dehydrogenases [158] and elevates ATP synthesis for cell survival [159]. In contrast, cells exposed to ATP and either staurosporine or ceramide experienced mitochondrial membrane depolarisation that released cytochrome C release and triggered apoptosis [149-151]. This has led to the hypothesis that the co-incident detection of Ca^{2+} and an apoptotic agent by the mitochondria is efficient to initiate apoptosis [149-151]. In this model, regulating $[Ca^{2+}]_{MIT}$ would be expected to alter the sensitivity of cells to apoptosis initiated by a death stimulus, whose mechanism involves the mitochondria.

1.3.4.3 Anti-apoptotic Bcl-2 proteins

The founding member of the Bcl-2 protein family, Bcl-2 is localised to the ER and mitochondrial membrane and this observation provided the first clue that Ca^{2+} may modulate apoptosis [160]. Indeed, the anti-apoptotic effect of Bcl-2 works in part, by reducing the $[Ca^{2+}]_{ER}$ and decreasing Ca^{2+} uptake into the mitochondria when the IP_3-senstitive Ca^{2+} store is released [161, 162]. This protects cells from apoptosis by preventing activation of the mitochondrial PTP. Pinton *et al.* confirmed the significance of $[Ca^{2+}]_{ER}$ during apoptosis by manipulating $[Ca^{2+}]_{ER}$ levels. HeLa cells exposed to thapsigarin or genetically manipulated to overexpress PMCA, mimicked the effects of Bcl-2 by reducing $[Ca^{2+}]_{ER}$ [117, 163]. Under these conditions, where $[Ca^{2+}]_{ER}$ was reduced, HeLa cells were protected from ceramide-induced apoptosis [152]. Conversely, high $[Ca^{2+}]_{ER}$ levels achieved by overexpressing the SERCA pump [163] sensitised cells to ceramide-induced apoptosis [152].

1.3.5 PMCAs and apoptosis

Initial studies of PMCA-mediated regulation of apoptosis was explored by two independent laboratories using gain-of-function models, where PMCA4b was overexpressed in a panel of cell lines [73-76, 164]. These studies identified a caspase-3 consensus site in the primary sequence of PMCA4b, DEID, located upstream of the calmodulin binding domain (Figure 1-4) [75, 76]. Preventing caspase-3 mediated cleavage of PMCA4b significantly delayed apoptosis [75, 76]. However, the consequence of caspase-3 cleavage on PMCA4b pump activity and localisation have been conflicting [73-76]. Some studies indicate that caspase-mediated cleavage fully activates PMCA4 [73-75], and other studies suggest that caspase-mediated cleavage can inactivate this calcium pump isoform [76].

1.3.6 Summary

Gain-of-function studies have been instrumental in demonstrating that PMCA upregulation can delay and protect cells from undergoing apoptosis. Aberrant PMCA overexpression identified in various cancers including those of the breast, could consequentially promote the cancer phenotype by enabling them to escape cell death. Some studies have examined the potential roles of PMCA isoforms in apoptosis in breast cancer cells, but as described below, at the time the experiments for this thesis were performed, these were overexpression studies.

1.4 Breast Cancer

1.4.1 Introduction

The most common cancer in female Australians is breast cancer. A recent publication – Breast cancer in Australia: an overview – provides the latest information and national statistics on breast cancer in Australia [165]. Not only has the number of women diagnosed with this disease per year doubled since1982, but records show that in 2007 breast cancer (after lung cancer) was the second most common cause of cancer-related deaths in females [165]. Despite improved diagnosis and availability of breast cancer management regimes, the incidence of breast cancer is steadily increasing. Future projections indicate that there will be 14,610 new cases in 2012, compared with 17,210 new cases in 2020 [165]. Moreover, the burden of breast cancer in Australia exceeds that of all other female cancers, and is associated with significant premature mortality [165]. These statistics highlight that continued research is essential to improve breast cancer management.

1.4.2 Molecular classification of breast cancers

In 2000, Peru *et al.* proposed that heterogeneous diversity amongst breast tumours is accompanied by differential gene expression patterns that could be captured from their gene expression profile [166]. This original study used cDNA microarray profiling of forty human breast tumours, grouped on the basis of similarities and differences in their gene expression [166]. Of the five breast cancer subtypes defined, the most striking difference was detected between the luminal-like and basal-like subtypes [166, 167]. Luminal-like tumours are the largest cluster and express the oestrogen receptor, along with many other genes expressed by non-malignant luminal breast cells [166, 167]. Whereas, basal-like tumours are oestrogen receptor negative and express many genes characteristic of non-malignant basal breast epithelial cells [166, 167]. The Erb-B2 tumour subtype is also oestrogen receptor negative, but overexpresses the Erb-B2 oncogene [166, 167].

Such molecular diversity amongst human breast cancers, validated by subsequent studies [168, 169], is significant because it correlates with marked differences in their prognosis and response to chemotherapy [167, 170]. In order to improve the outcome for women diagnosed breast cancer, new tumour suppressing drugs that target the pathways deregulated in these breast cancer subtypes are needed. This approach is particularly urgent for the more aggressive basal-like breast cancers, which owing to their usual lack of HER2, oestrogen receptor and progesterone receptor expression respond poorly to the available therapies including tamoxifen (ER antagonist) and Herceptin (HER2 antagonist) [167, 170].

1.4.3 Calcium and cancer

Proliferation, angiogenesis, replicative immortality, evasion to growth suppressors, resistance to cell death and metastasis are all features of cancer cells [119, 171]. Ca^{2+} transporters, because they regulate many of these pathways deregulated in cancer, are anticipated targets for future anti-cancer drug development [21].

The significance of the Ca^{2+} permeable ion channel TrpM8 and its upregulation reported in prostate cancer has been assessed [172]. In the human LNCap prostate cancer cell line, siRNA-mediated silencing of TrpM8 attenuates cell proliferation, whereas the TrpM8 agonist menthol triggers apoptosis [173]. Altered expression of another Ca^{2+} permeable ion channel, Orai1 is documented in breast cancer cell lines compared with the non-tumourgenic controls [174]. Orai1 plays a key role in store operated Ca^{2+} entry, activated by the depletion of Ca^{2+} within the endoplasmic reticulum. The consequence of Orai1 silencing has been examined in MDA-MB-231 breast cancer cells, and attenuates cell migration and invasion [175]. These studies of TrpM8 and Orai1 support the view that Ca^{2+} transport proteins are plausible anti-cancer drug targets [21]

1.4.4 Breast cancer and PMCAs

Another calcium transporter potentially important in terms of cancer is the calcium pump PMCA. Reports of either PMCA up or downregulation in various cancers [176-180] indicates that remodeling of PMCA-mediated Ca^{2+} efflux may regulate cancer-relevant pathways such as proliferation and/or the resistance to apoptosis. Altered PMCA expression was initially reported in SV40-transformed skin and lung fibroblasts [181]. PMCA1 and PMCA4 were significantly downregulated in SV40-transformed cells compared with the non-transformed cells [181]. The relevance of PMCA4 downregulation, which is also a feature of colon cancers, has been examined by silencing or overexpressing this PMCA isoform in the HT-29 colon cancer cell line [180]. PMCA4 downregulation augments HT-29 cell proliferation and provides a growth advantage, without exerting effects on cell viability [180].

PMCA expression has also been examined in breast cancers. However, unlike colon cancer where PMCA4 downregulation is detected, PMCA upregulation is typical of some breast cancer cell lines [178, 179] that are different in their oestrogen and HER2 receptor status [178, 179]. In some of these breast cancer cell lines, PMCA2 is markedly upregulated from undetectable levels up to 100-fold; whereas PMCA1 is only modestly upregulated, and PMCA4 modestly downregulated [178, 179]. PMCA expression in breast cancer, is to some degree, similar to the changes observed in the lactating mammary gland. Significant PMCA2 upregulation in lactating mammary epithelial cells, increases

their Ca^{2+} efflux capacity, and this is critical for Ca^{2+} secretion into milk, along with the promotion of cell survival and maintenance of low intracellular Ca^{2+} levels [58, 59, 107, 108]. In the pathological setting, aberrant PMCA2 upregulation in breast cancer cells is predicted to reduce intracellular Ca^{2+} levels, and may promote cancer-relevant pathways such as resistance to cell death and/or disrupt cell cycle progression. Indeed, recombinant PMCA2 expression protects against T47D breast cancer cell death following treatment with either docetaxel or ionomycin [182]. Since PMCA2 upregulation in breast cancer cells protects against cell death; PMCA2 inhibition, via elevations of intracellular Ca^{2+} is proposed to promote breast cancer cell death. Very recent PMCA2 studies report that the silencing of this PMCA isoform attenuates MDA-MB-231 breast cancer cell proliferation [183], and promotes SKBr3 breast cancer cell death initiated with the Ca^{2+} ionophore ionomycin [182, 184]. However, the consequence of isoform specific PMCA knockdown on cell death in a basal-like breast cancer cell line has not reported, and the consequence of silencing of specific PMCA isoforms in the promotion of cell death initiated through different mechanisms is still not well understood.

1.4.5 Summary

PMCA-mediated regulation of breast cancer cell death has been reported, but the majority of these studies have involved PMCA overexpression. To assess whether specific PMCA isoforms may serve as therapeutic targets for future breast cancer therapy, PMCA inhibition and/or silencing studies are required. Pharmacological assessment of PMCA isoforms is restricted by the lack of available isoform-specific inhibitors. Some studies have examined the consequences of PMCA silencing in breast cancer. These studies, however have only examined PMCA2 and did not assess isoform-specific PMCA silencing in a basal-like breast cancer cell line that overlaps with triple negative breast cancers, which are generally more aggressive than other breast cancer subtypes. In this thesis, the consequence of isoform-specific PMCA silencing in the basal-like MDA-MB-231 breast cancer cell line and the effects of this silencing on Ca^{2+} signals and on different cell death mechanisms will be examined.

1.5 Hypotheses and Aims

Work undertaken in this thesis was designed to delineate the role of specific PMCA isoforms in the regulation of cytoplasmic Ca^{2+} signals and on different mechanisms of cell death in the MDA-MB-231 breast cancer cell line. Experiments were performed in the MDA-MB-231 breast cancer cell line because these cells express many of the genes characteristic of aggressive, basal-like breast cancer subtypes that urgently require new therapeutic options. This cell line was also selected because MDA-MB-231 cells, along with the PMCA isoforms PMCA1, PMCA4 and PMCA2, express the protease caspase-3 that is essential for the execution of many apoptotic pathways [137].

This thesis research is divided into three chapters. Chapter 2 discusses the development of a high-throughput cell death assay, and details the impact of silencing PMCA1 or PMCA4 on $[Ca^{2+}]_{CYT}$ signals and on cell death mechanisms. Chapter 3 extends these studies to PMCA2. Chapter 4 examines the potential for PMCA-silencing to exert effects on cell death via mitochondrial calcium levels indirectly by evaluating MCU silencing-mediated effects on $[Ca^{2+}]_{CYT}$ and on cell death mechanisms. Chapter-specific aims and hypothesis are listed at the beginning of each chapter. Listed below are the overall hypotheses relevant to this thesis as a whole.

1.5.1 Hypothesis 1

Silencing of specific PMCA isoforms differentially regulates the sensitivity of MDA-MB-231 breast cancer cells to agents that initiate cell death via different mechanisms

1.5.2 Hypothesis 2

Silencing of specific PMCA isoforms distinctly regulate global cytoplasmic Ca^{2+} signals in MDA-MB-231 breast cancer cells and this relates to their effects on cell death

1.5.3 Hypothesis 3

PMCA silencing-mediated effects on cell death could involve changes in mitochondrial calcium levels

2.1 Preface

Plasma membrane calcium (Ca^{2+}) ATPase (PMCA) isoforms, although important for healthy mammary gland development, may also play a role in mammary gland pathophysiology. PMCA-mediated Ca^{2+} efflux, by way of reducing intracellular Ca^{2+} levels, may promote cancer hallmarks including proliferation and the resistance to cell death. Supporting this view, initial reports demonstrated that PMCA isoform expression is altered in breast cancer cell lines compared with non-tumorigenic breast cancer cell lines [178] and antisense-mediated inhibition of PMCA expression attenuates MCF-7 breast cancer cell proliferation [185]. These studies established a link between PMCA and cancer, however, the differential impact of individual PMCA isoforms on cancer-relevant pathways in breast cancer is not clear and very few functional studies have been performed in basal-like breast cancer cell lines.

To evaluate whether individual PMCA isoforms can distinctly influence aspects of cancer biology, this chapter compared the functional effects of silencing either PMCA1 (siPMCA1) or PMCA4 (siPMCA4) expression on cytoplasmic calcium signals ($[Ca^{2+}]_{CYT}$), cell viability and transcription factor activity in MDA-MB-231 breast cancer cells. PMCA1 and PMCA4 were selected for these experiments because of their potential functional differences in the same cell, despite a significant overlap in their expression profile throughout the body [49, 103], has not been thoroughly investigated.

This research was originally published in the Journal of Biological Chemistry. Curry MC, Luk NA, Kenny PA, Roberts-Thomson SJ, Monteith GR. Distinct regulation of cytoplasmic calcium signals and cell death pathways by different plasma membrane calcium ATPase isoforms in MDA-MB-231 breast cancer cells. This publication is incorporated into this thesis chapter, with the original format of the manuscript adjusted to comply with the University of Queensland thesis formatting guidelines.

The manuscript presents novel research findings that were predominantly designed and performed by myself under the supervision of Gregory R Monteith and Sarah J Roberts-Thomson. Additional data, performed by Nicole A Luk and Dr. Paraic A Kenny, was included in the manuscript and has been incorporated into this thesis chapter. During her PhD, Nicole A Luk performed the NFκB translocation studies shown in Figure 2-8A and B. Dr. Paraic A Kenny, an international collaborator, contributed the microarray data illustrated in Figure 2-9.

2.2 Chapter Hypotheses

- Global [Ca^{2+}] are distinctly altered by isoform-specific PMCA1 or PMCA4 knockdown.
- ABT-263 and ionomycin trigger cell death pathways that are differentially dependent on caspase activity.
- Isoform-specific PMCA1 or PMCA4 knockdown distinctly modulate cell death, in the absence and presence of cell death activators.
- Isoform-specific PMCA1 or PMCA4 knockdown distinctly regulates nuclear translocation of nuclear factor κB (NFκB), which may represent a novel mechanism where by some PMCA isoforms regulate cell death.

2.3 Chapter Aims

- To reduce PMCA1 or PMCA4 expression using targeted siRNAs in the MDA-MB-231 breast cancer cells.
- To monitor $[Ca^{2+}]_{CYT}$ increases generated with CPA, ionomycin, ATP and trypsin in siRNA-transfected (PMCA1 siRNA (siPMCA1) or PMCA4 siRNA (siPMCA4) or NT siRNA (siNT)) MDA-MB-231 cells by high-throughput imaging of relative $[Ca^{2+}]_{CYT}$ using a fluorescence imaging plate reader ($FLIPR^{TETRA}$).
- To use the high content imaging assay developed to assess the consequence of PMCA1 and PMCA4 knockdown on MDA-MB-231 cell death in the absence and presence of the cell death activators, ABT-263, ionomycin, ceramide and staurosporine.
- To determine effects of PMCA1 or PMCA4 knockdown on the nuclear translocation of nuclear factor kappa B (NFκB).
- To ascertain the consequences of pharmacological inhibition of NFκB on caspase-dependent ABT-263-induced cell death.

2.4 Capsule

- **Background:** The roles of different PMCA isoforms are not fully understood particularly in cell death.
- **Results:** PMCA4 and PMCA1 silencing has differential effects on Ca^{2+} signalling and caspase dependent and independent cell death in MDAMB-231 cells.
- **Conclusion:** PMCA isoforms have distinct roles in the control of cell death pathways.
- **Significance:** Inhibition of PMCA4 may increase the effectiveness of some cancer therapies.

2.5 Summary

PMCAs actively extrude Ca^{2+} from the cell and are essential components in maintaining intracellular Ca^{2+} homeostasis. There are four PMCA isoforms (PMCA 1-4) and alternative splicing of the PMCA genes creates a suite of calcium efflux pumps. The role of these different PMCA isoforms in the control of calcium-regulated cell death pathways and the significance of the expression of multiple isoforms of PMCA in the same cell type are not well understood. In these studies, we assessed the impact of PMCA1 and PMCA4 silencing on cytoplasmic free Ca^{2+} signals and cell viability in MDA-MB-231 breast cancer cells. The PMCA1 isoform was the predominant regulator of global Ca^{2+} signals in MDA-MB-231 cells. PMCA4 played only a minor role in the regulation of bulk cytosolic Ca^{2+}, which was more evident at higher Ca^{2+} loads. Although PMCA1 or PMCA4 knockdown alone had no effect on MDA-MB-231 cell viability, silencing of these isoforms had distinct consequences on caspase-independent (ionomycin) and dependent (ABT-263) cell death. PMCA1 knockdown augmented necrosis mediated by the Ca^{2+} ionophore ionomycin, whereas apoptosis mediated by the Bcl-2 inhibitor ABT-263 was enhanced by PMCA4 silencing.

PMCA4 silencing was also associated with an inhibition of NFκB nuclear translocation and an NFκB inhibitor phenocopied the effects of PMCA4 silencing in promoting ABT-263 induced cell death. This study demonstrates distinct roles for PMCA1 and PMCA4 in the regulation of calcium signalling and cell death pathways despite the widespread distribution of these two isoforms. The targeting of some PMCA isoforms may enhance the effectiveness of therapies that act through the promotion of cell death pathways in cancer cells.

2.6 Introduction

Studies have started to identify some of the potential mechanisms that may underpin the functions predicted for specific PMCA isoforms. One such example is the differential association of PMCA1, PMCA2 and PMCA4 with calcineurin in MCF-7 cells [186]. The functional significance of this interaction has not been investigated in MCF-7 cells, however, in cardiac cells PMCA4 regulates nuclear factor of activated T-cells (NFAT), a calcineurin regulated transcription factor, and cardiac hypertrophy [187].

One process where the relative contribution of specific PMCA isoforms may be particularly important, but has not been fully addressed is cell death, where the duration and amplitude of increases in $[Ca^{2+}]_{CYT}$ are critical [4, 188]. Initiators of cell death include Ca^{2+} ionophores that produce sustained (µM) increases in $[Ca^{2+}]_{CYT}$ that can induce necrotic cell death [6] and inhibitors of B cell lymphoma-2 protein (Bcl-2) [189-191]. Bcl-2 inhibitors promote apoptosis by blocking the prosurvival activity of Bcl-2 proteins [189-191] and are undergoing clinical trial assessment for the treatment of specific types of lymphomas and solid lung cancers [192].

A few studies have assessed the consequences of PMCA expression on cell death. In HeLa cells, PMCA overexpression protects from ceramide induced cell death [152]. The authors attributed this to alterations in intracellular Ca^{2+} stores, given that PMCA overexpression in CHO cells reduces Ca^{2+} levels within the endoplasmic reticulum and mitochondria [163]. In the context of breast cancer, where cells acquire the ability to evade cell death [171], assessment of PMCA has been restricted to overexpression studies in T47D breast cancer cells [182]. Recombinant PMCA2 expression attenuates increases in $[Ca^{2+}]_{CYT}$, associated with ionomycin induced cell death [182].

Although PMCA2 knockdown has been assessed in spinal cord neurons [193] and SH-SY5Y neuroblastoma cells [194], and PMCA4 knockdown evaluated in HT-29 colon cancer cells [180], isoform-specific PMCA knockdown has not yet been studied in breast cancer cells. In addition, the differential role of PMCA isoforms in the regulation of distinct cell death mechanisms, within the same cell type has not been evaluated. In the present study we compared siRNA-mediated knockdown effects of PMCA1 and PMCA4 in the regulation of global Ca^{2+} signals and assessed the effects on the viability of MDA-MB-231 breast cancer cells, in the absence and presence of the cell death initiators, ionomycin (Ca^{2+} ionophore) and ABT-263 (Bcl-2 inhibitor). The basal breast cancer molecular subtype is associated with a particularly poor prognosis, therefore MDA-MB-231 breast cancer cells were selected for these studies since they are a widely used model of the basal-like phenotype.

2.7 Experimental Procedures

2.7.1 Cell culture

The human breast cancer cell line MDA-MB-231 (American Type Culture Collection) was cultured in high glucose DMEM (Sigma Aldrich) supplemented with 10% FBS and 4 mM L-glutamine (Gibco) at 37°C/5% CO_2 in a humidified air incubator. All cultures were periodically screened for mycoplasma infection.

2.7.2 siRNA-mediated knockdown of PMCA4 and PMCA1 gene expression

MDA-MB-231 cells were seeded into 96-well plates and allowed to adhere overnight. DharmaFECT 4 (0.1-0.2 µL/well, Dharmacon) was used to transfect cells with Dharmacon ON-TARGET*plus*™ SMARTpool siRNA, which consists of four pooled siRNA sequences rationally designed to minimise off target effects [195, 196]. Transfection media was prepared according to the manufacturer's protocol and contained 8% FBS. The siRNAs used in this study included those for PMCA4 (siPMCA4, L-006118-00), PMCA1 (siPMCA1, L-006115-00) and the non-targeting control siRNA (siNT, D-001810-10). All experiments had mRNA knockdown >70% at 24 h or 48 h post-siRNA

2.7.3 Real time RT-PCR

Cells were plated at 5.0×10^3 cells per well into 96-well plates and siRNA-transfected. Total RNA was isolated (RNeasy Plus Mini Kit; Qiagen) 24 h, 48 h or 120 h post-transfection and then reverse transcribed using the Omniscript RT kit (Qiagen) according to the manufacturer's protocol. Target cDNA were amplified using the TaqMan Fast Universal PCR Master Mix (Applied Biosystems) and TaqMan Gene Expression assays (PMCA4, Hs00608066_m1; PMCA1, Hs00155949_m1) and standard cycling conditions with a StepOnePlus Real Time PCR system (Applied Biosystems). PMCA4 and PMCA1 mRNA levels were quantified by the comparative *Ct* method as previously described [197], normalising to 18S rRNA (4319413E) and presented relative to the siNT control.

2.7.4 Cytoplasmic free calcium measurements

MDA-MB-231 cells were plated at 7.5×10^3 cells per well into 96-well plates and siRNA transfected. Transfection media was removed 72 h post-siRNA treatment and cells were loaded with culture medium containing Fluo-4 AM (4 µM; Molecular Probes) or Fluo-4FF AM (4 µM; Molecular Probes) and incubated at 37°C for 30 min in a 5% CO_2 humidified air incubator. Loading solution was replaced with physiological salt solution (PSS; 5.9 mM KCl, 1.4 mM $MgCl_2$, 10 mM HEPES, 1.2 mM NaH_2PO_4, 5 mM $NaHCO_3$, 140 mM NaCl, 11.5 mM Glucose, 1.8 mM $CaCl_2$), cells were equilibrated to room temperature and then washed twice with PSS containing bovine serum albumin (BSA, 0.3%). $[Ca^{2+}]_{CYT}$ was measured in Ca^{2+} probe loaded cells using a fluorescence imaging plate reader [198] (FLIPR^{TETRA}, Molecular Devices Corporation) using an excitation intensity of 470-495 nm and a 515-575 nm emission filter. Fluorescence was normalised to baseline values to assess relative $[Ca^{2+}]_{CYT}$.

2.7.5 Immunoblotting

Cells were plated at 5.0×10^3 cells per well into 96-well plates and siRNA transfected. Cell extracts were harvested 72 h post transfection in protein lysis buffer supplemented with protease inhibitor cocktail (Roche Applied Science) as previously described [180]. Proteins were separated using gel electrophoresis and transferred onto a polyvinylidene fluoride membrane as previously described [199].

Membranes were probed with monoclonal antiPMCA4 antibody (1:1000, JA9, Pierce Antibodies), monoclonal anti-PMCA antibody (1:2000, 5F10, Pierce Antibodies) and monoclonal anti-β-actin antibody (1:10,000, Sigma Aldrich). Anti-mouse horseradish peroxidase-conjugated secondary antibody (1:10000, BioRad) was used to visualise protein bands by chemiluminescence using Super-Signal West Dura (Pierce). All antibodies were diluted in PBST (0.1% Tween-20 in PBS) with skim milk powder (2.5%). Images were acquired and analysed by densitometry using a VersaDoc instrument and Quantity One Analysis software (Bio-Rad), respectively. All data were normalised to the β-actin loading control and are presented relative to siNT.

2.7.6 Assessment of cell viability

MDA-MB-231 cells were plated at 5.0×10^3 cells per well into 96-well plates and siRNA-transfected. At 72 h post-transfection media was removed and cells were treated with ABT-263 (Selleckchem), ionomycin (Enzo Life Sciences), Z-VAD-FMK (Enzo Life Sciences), IMD-0354 (Sigma-Aldrich) or DMSO (up to 1%) for 48 h in phenol-red free DMEM containing FBS (8%). Live cells were stained

at 37°C for 15 min with Hoechst 33342 (10 µg/mL, Invitrogen) and propidium iodide (1 µg/mL, Invitrogen). Images were acquired using an ImageXpress micro automated epifluorescence microscope (Molecular Devices Corporation) with a 10X objective, a system previously used for cell death assays [200-202]. Four images were automatically acquired per well in the DAPI and Cy3 channel for Hoechst 33342 and propidium iodide respectively. The multi-wavelength cell scoring application module (MetaXpress v3.1.0.83; Molecular Devices Corporation) was used to segment cell nuclei to calculate the average Hoechst 33342 integrated intensity and the average propidium iodide intensity emitted per cell. Criteria for viable, apoptotic and necrotic (and secondary apoptosis) are shown graphically in figures and validated using the caspase inhibitor Z-VAD-FMK.

2.7.7 Assessment of NFκB nuclear translocation

MDA-MB-231 cells were plated at 3.5×10^3 cells per well into 96-well plates and transfected with siRNA. Post-siRNA transfection (48 h), media was removed and cells were serum reduced (2% FBS) for 12 h, prior to the addition of phorbol 12- myristate 13-acetate (PMA, 50 nM, Sigma) or DMSO (0.05%) for 1 h in DMEM (10% FBS) [203]. Cells were fixed (4% paraformaldehyde in PBS), blocked (PBS, 5% normal goat serum and 0.3% Triton X-100) and then stained with the polyclonal anti-NFκB p65 antibody (Cell Signaling Technologies) diluted 1:100 in PBS containing BSA (1%) and Triton X-100 (0.3%). NFkB was visualised using anti-rabbit IgG (H+L), $F(ab')_2$ Fragment Alexa Fluor® 555 Conjugate Secondary antibody (1:500, Cell Signaling Technologies). Cell nuclei were stained with DAPI (40 nM, Invitrogen) and images acquired using an ImageXpress micro automated epifluorescence microscope (Molecular Devices Corporation) with a 10X objective as described above. The ImageXpress platform has been utilised in translocation studies previously [204] and the basis of the translocation assay has been reviewed [205]. NFκB translocation was assessed using the translocation package (MetaXpress v3.1.0.83; Molecular Devices Corporation).

2.7.8 Analysis of PMCA1 and PMCA4 levels in published datasets

Gene expression data for breast cancer cell lines in 3D culture [206] or for breast tumors [207] were obtained from online repositories (ArrayExpress no. E-TABM-244 (cell lines) and NCBI GEO no. GSE2034 (tumors)). Affymetrix probes for PMCA1 (215716_s_at) and PMCA4 (212136_at) were shared between these datasets. Samples were stratified based on their reported annotations (basal *versus* luminal for cell lines, and ER- *versus* ER+ for tumors). Normalised gene expression levels (log_2) were plotted and median levels of each gene were compared between groups (Mann-Whitney test). For relapse free survival analysis, tumors were stratified into groups corresponding to the upper and lower quartiles and the interquartile range for Kaplan-Meier analysis.

2.7.9 Statistical Analysis

All statistical tests were performed as described in the figure legends using GraphPad Prism (version 5.04) for Windows. For cell death, given the batch to batch variability of ionomycin, for all studies controls and experimental treatments were matched and performed simultaneously for each passage replicate.

2.8 Results

2.8.1 siRNA-mediated knockdown of specific PMCA isoforms in MDA-MB-231 breast cancer cells

There was a significant ($P < 0.05$) reduction in PMCA4 (Figure 2-1A) and PMCA1 (Figure 2-1B) mRNA levels in cells transfected with PMCA4 siRNA or PMCA1 siRNA, respectively, compared to the siNT control. PMCA4 protein expression was also significantly ($P < 0.05$) reduced by PMCA4 siRNA (Figure 2-1C and D), but was not associated with significant changes in total PMCA protein expression (Figure 2-1C and E). Consistent with high levels of PMCA1, total PMCA protein levels were reduced by PMCA1 siRNA (Figure 2-1C and E; $P < 0.05$). This was not associated with changes in PMCA4 expression (Figure 2-1C and D).

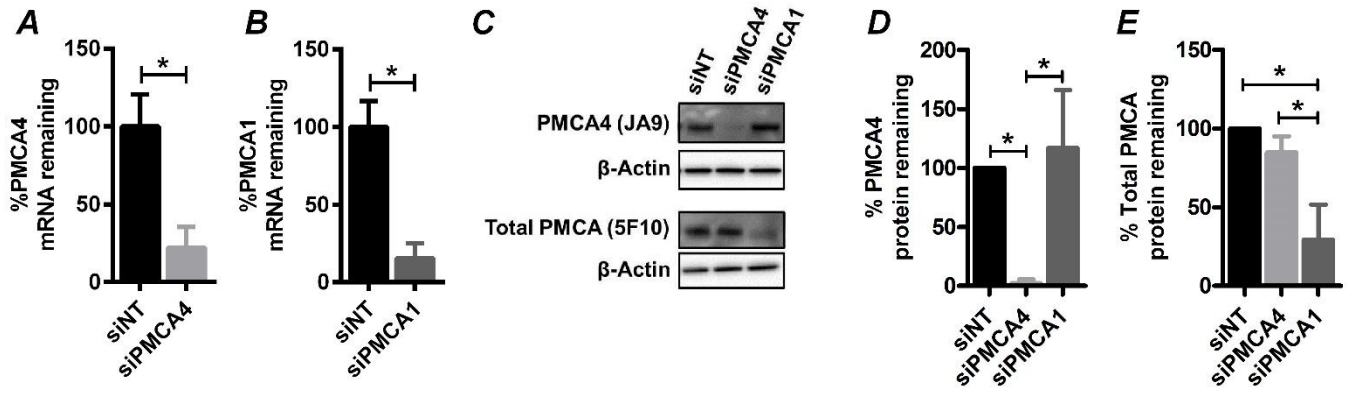

Figure 2-1: Silencing of PMCA4 and PMCA1 in MDA-MB-231 cells.

Quantification of **(A)** PMCA4 mRNA and **(B)** PMCA1 mRNA levels, 48 h post-siRNA transfection with siPMCA4, siPMCA1 or siNT. Real time RT-PCR data were pooled from three independent experiments performed in triplicate, $*P < 0.05$, one-tailed student's *t* test. **(C)** Immunoblots of PMCA4 and total PMCA protein expression, 72 h post-siRNA transfection. **(D)** PMCA4 and **(E)** total PMCA protein expression from densitometic analysis normalised to the β-actin loading control, from three independent experiments. $*P < 0.05$, one-way ANOVA, Bonferroni post-hoc analysis. All data shown are mean ± S.D.

2.8.2 Consequences of PMCA1 or PMCA4 knockdown on cytoplasmic free calcium in MDA-MB-231 breast cancer cells

In the absence of extracellular Ca^{2+}, increases in $[Ca^{2+}]_{CYT}$ elicited by the sarcoplasmic-endoplasmic reticulum Ca^{2+}-ATPase inhibitor cyclopiazonic acid (CPA, 10 µM) were markedly altered with siRNA-mediated knockdown of PMCA1, but not by PMCA4 knockdown (Figure 2-2A-D). PMCA1 silencing significantly ($P < 0.05$) delayed the time to reach the maximal Ca^{2+} response (Figure 2-2B), increased the half-peak decay time (Figure 2-2C) and increased the area under the curve (Figure 2-2*D*) compared to siNT. The effect was isoform-specific, as PMCA4 knockdown did not alter the nature of the CPA-induced Ca^{2+} response when compared with siNT (Figure 2-2A-D).

The purinergic receptor agonist ATP (100 µM) induced a rapid rise in $[Ca^{2+}]_{CYT}$ (Figure 2-2E), with no significant difference in the peak maximum between siRNA treatments (mean ± SD; siPMCA1, 2.56 ± 0.23; siPMCA4, 2.68 ± 0.31; siNT, 2.99 ± 0.39). However, PMCA1 knockdown significantly altered the recovery of $[Ca^{2+}]_{CYT}$ after ATP stimulation (Figure 2-2F-H) in comparison to siNT, resulting in a slower rate of $[Ca^{2+}]_{CYT}$ decay in the absence of extracellular Ca^{2+} (Figure 2-2F), a delay in half peak decay time (Figure 2-2G) and an increase in the area under the curve (Figure 2-2H). These effects were isoform-specific as similar changes were not seen with PMCA4 silencing (Figure 2-2E-H). To assess the consequences of isoform-specific PMCA knockdown with $[Ca^{2+}]_{CYT}$ increases of a greater magnitude, we compared the effects of PMCA4 or PMCA1 siRNA on $[Ca^{2+}]_{CYT}$ changes mediated by the Ca^{2+} ionophore ionomycin in the presence of extracellular Ca^{2+} (1.8 mM).

Increases in $[Ca^{2+}]_{CYT}$ mediated by ionomycin (3 µM) were significantly ($P < 0.05$) increased with PMCA1 or PMCA4 knockdown compared to siNT (Figure 2-3A and B). These effects were more pronounced ($P < 0.05$) with PMCA1 knockdown compared to PMCA4 knockdown (Figure 2-3A and B). Silencing of PMCA1 or PMCA4 also augmented increases in $[Ca^{2+}]_{CYT}$ mediated by 10 µM ionomycin, however, in contrast to 3 µM ionomycin there were no differences in effect between the two isoforms (Figure 2-3C and D).

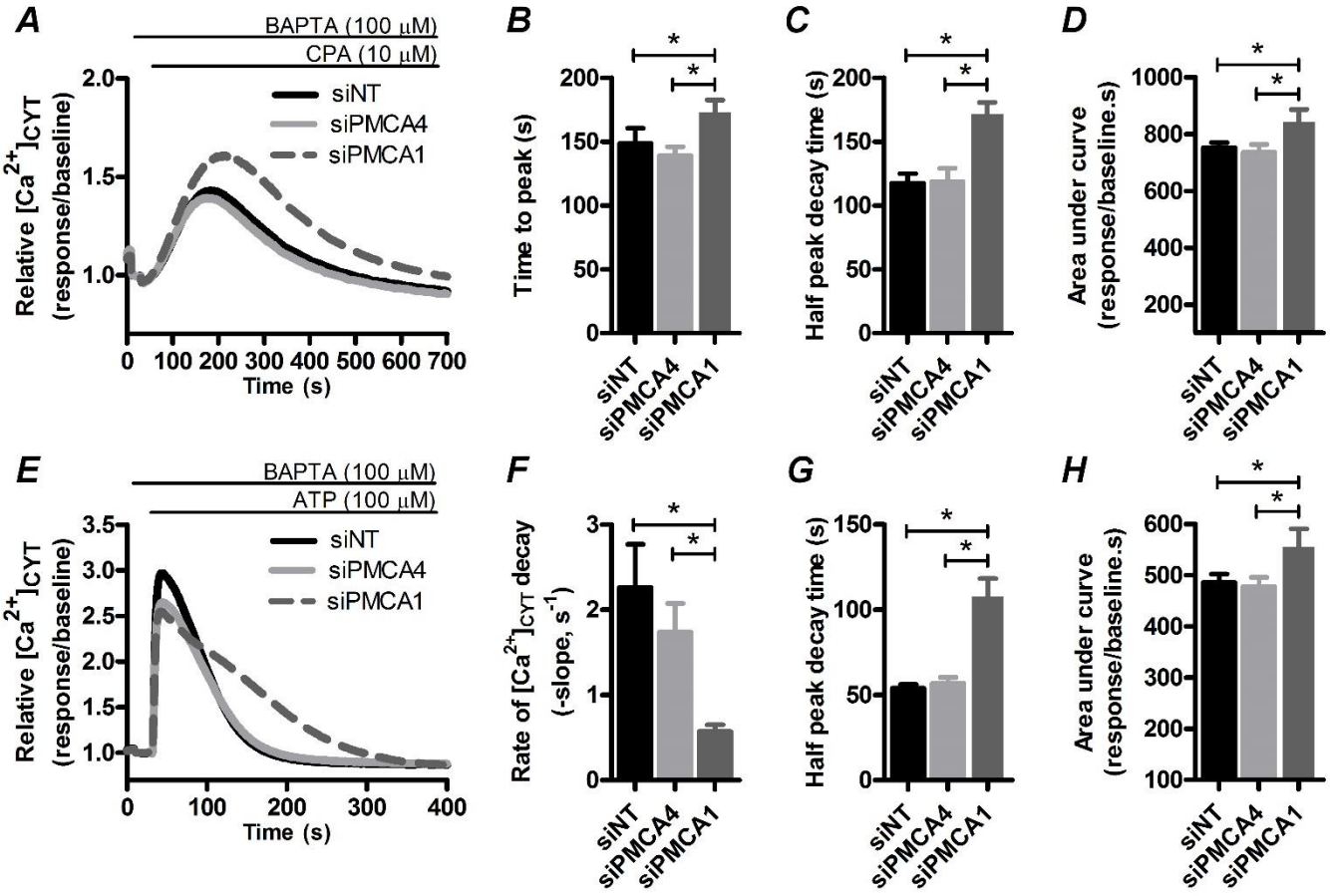

Figure 2-2: Effect of PMCA1 and PMCA4 silencing on CPA and ATP evoked $[Ca^{2+}]_{CYT}$ increases in MDA-MB-231 breast cancer cells.

(A) CPA (10 µM)-mediated and **(E)** ATP (100 µM)-mediated $[Ca^{2+}]_{CYT}$ after transfection with siPMCA1, siPMCA4 or siNT in the presence of extracellular BAPTA (100 µM). Ca^{2+} traces represent relative mean fluorescence. **(B and F)** Time to peak $[Ca^{2+}]_{CYT}$ and rate of $[Ca^{2+}]_{CYT}$ decay after CPA and ATP responses, respectively. **(C and G)** Half peak decay time for CPA and ATP responses, respectively. **(D and H)** Area under the curve for CPA and ATP responses, respectively. Bar graphs are mean ± SD for Ca^{2+} transient parameters. All data were pooled from nine individual wells, from three independent experiments performed in triplicate. $*P < 0.05$, one-way ANOVA, Bonferroni post-hoc analysis. BAPTA, 1,2-bis(o-aminophenoxylethane)-N,N,N',N'-tetraacetic acid.

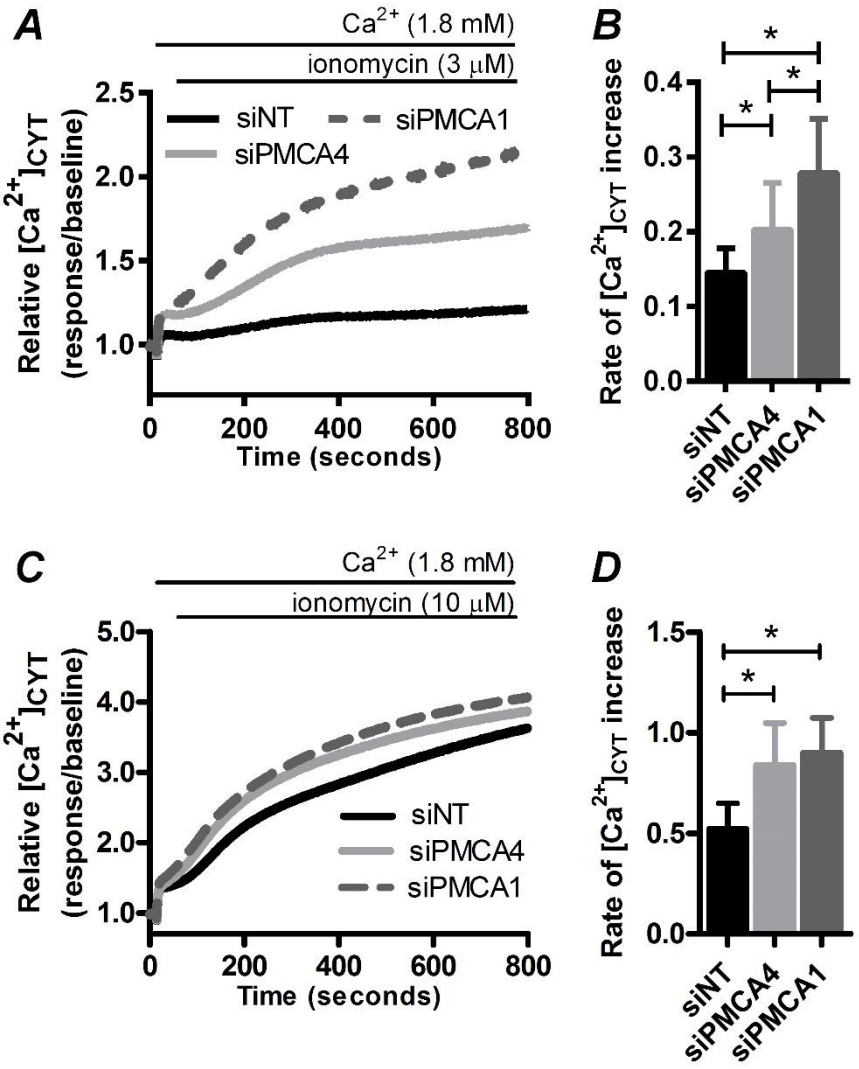

Figure 2-3: Ionomycin-evoked $[Ca^{2+}]_{CYT}$ signals in the presence of PMCA1 and PMCA4 silencing.

MDA-MB-231 breast cancer cells were transfected with siPMCA1, siPMCA4 or siNT and changes in $[Ca^{2+}]_{CYT}$ were assessed after the addition of ionomycin (**(A)** 3 μM or **(C)** 10 μM. Ca^{2+} traces represent relative mean fluorescence. **(B and D)** Rate of $[Ca^{2+}]_{CYT}$ increase for 3 μM and 10 μM ionomycin Ca^{2+} responses, respectively. Bar graphs are mean ± S.D for Ca^{2+} transient parameters. All data were pooled from nine individual wells, from three independent experiments performed in triplicate. *$P < 0.05$, one-way ANOVA, Bonferroni post-hoc analysis.

2.8.3 Assessment of PMCA1 or PMCA4 knockdown on cell viability in MDA-MB-231 breast cancer cells

No effect on cell viability was detected with knockdown of PMCA4 (Figure 2-4A, B and D) or PMCA1 (Figure 2-4A, C and D) compared to siNT. PMCA1 and PMCA4 were effectively silenced at the time of the assessment of cell viability (Figure 2-4E and F). Reduced Ca^{2+}-efflux mediated by either PMCA1 or PMCA4 silencing was therefore insufficient for the activation of cell death pathways in MDA-MB-231 cells.

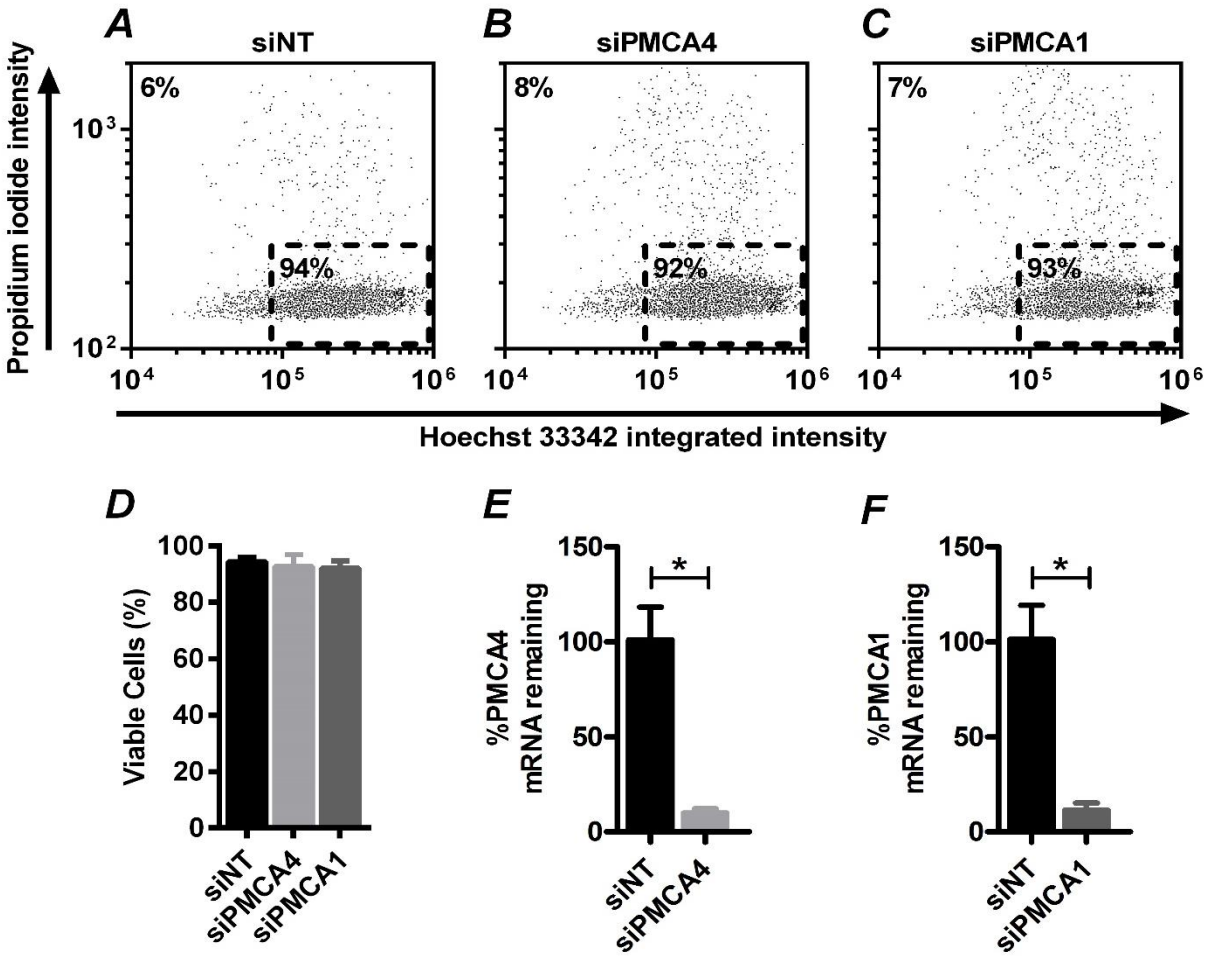

Figure 2-4: Cell viability in the presence of siRNA-mediated silencing of PMCA1 and PMCA4 gene expression.

MDA-MB-231 breast cancer cells were transfected with siPMCA4, siPMCA1 or siNT, incubated for a further 48 h and then assessed for cell viability. Cell viability for **(A)** siNT, **(B)** siPMCA4 and **(C)** siPMCA1 presented as dot plots of Hoechst 33342 and propidium iodide fluorescence. Each dot plot shows an equal cell number (10,000 cells) randomly selected from three independent experiments performed in triplicate wells. **(D)** Bar graph showing the mean ± SD of the proportion of viable cells 120 h post-siRNA transfection from 3 independent experiments performed in triplicate wells, **P* < 0.05, one-way ANOVA, Bonferroni post-hoc analysis. **(E)** PMCA4 mRNA and **(F)** PMCA1 mRNA levels, 120 h post-siRNA transfection with siPMCA4, siPMCA1, or siNT. Real time RT-PCR data were pooled from six individual wells, from three independent experiments performed in duplicate. * *P* < 0.05, one-tailed Student's *t* test.

2.8.4 Mechanism of ionomycin and ABT-263 activated cell death in MDA-MB-231 cells

To assess whether reduced PMCA1 or PMCA4 expression could alter the responsiveness of breast cancer cells to different cell death mechanisms, we first characterised cell death in MDA-MB-231 cells initiated by the Ca^{2+} ionophore ionomycin (Figure 2-5A and C) and the Bcl-2 inhibitor, ABT-263 (Figure 2-5A and E). Ionomycin (10 µM) and ABT-263 (10 µM) both initiated significant ($P < 0.05$) increases in cell death compared to control (Figure 2-5G and H). The nature of the initiated cell death was probed using the pan-caspase inhibitor, Z-VAD-FMK (50 µM). Consistent with a necrotic mechanism (13) ionomycin (10 µM)-induced cell death was not affected by Z-VAD-FMK (Figure 2-5C, D and G) whereas cell death initiated by ABT-263 was almost entirely prevented by caspase inhibition (Figure 2-5E, F and H) indicating an apoptotic pathway [208].

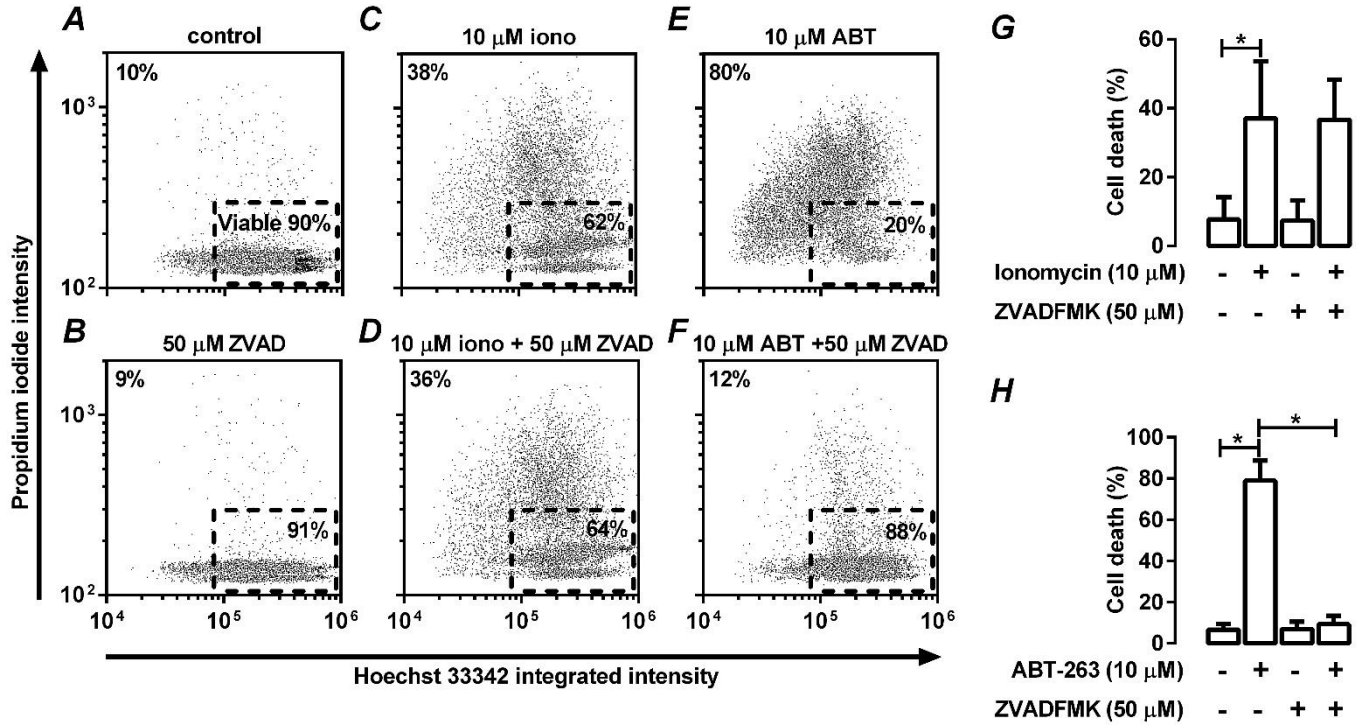

Figure 2-5: Effects of the caspase inhibitor Z-VAD-FMK on ionomycin and ABT-263 mediated cell death in MDA-MB-231 breast cancer cells.

(A-F) Dot plots for control, ionomycin or ABT-263 in either in the absence or presence of Z-VAD-FMK. Each dot plot represents an equal number of total cells (10,000 cells) selected at random from three independent experiments. **(G and H)** The pooled data for the effect of Z-VAD-FMK on the proportion of dead cells induced by ionomycin or ABT-263 (mean ± S.D), from three independent experiments. **P* < 0.05, repeated measures two-way ANOVA, Bonferroni post-hoc analysis

2.8.5 Consequences of PMCA1 or PMCA4 silencing on ionomycin-induced necrosis in MDA-MB-231 breast cancer cells

Necrosis mediated by submaximal ionomycin (3 µM) was not significantly affected by PMCA4 knockdown (Figure 2-6A, B and G), however, it was significantly ($P < 0.05$) augmented with PMCA1 silencing (Figure 2-6A, C and G).

For the higher ionomycin concentration (10 µM) knockdown of both PMCA4 (Figure 2-6D, E and G) and PMCA1 (Figure 2-6D, F and G) significantly ($P < 0.05$) elevated the proportion of necrotic cells compared to siNT. However, similar to their effects on $[Ca^{2+}]_{CYT}$, the isoform-specific differences seen with submaximal ionomycin concentration (3 µM) were not detected at higher Ca^{2+} loads associated with 10 µM ionomycin (Figure 2-6G).

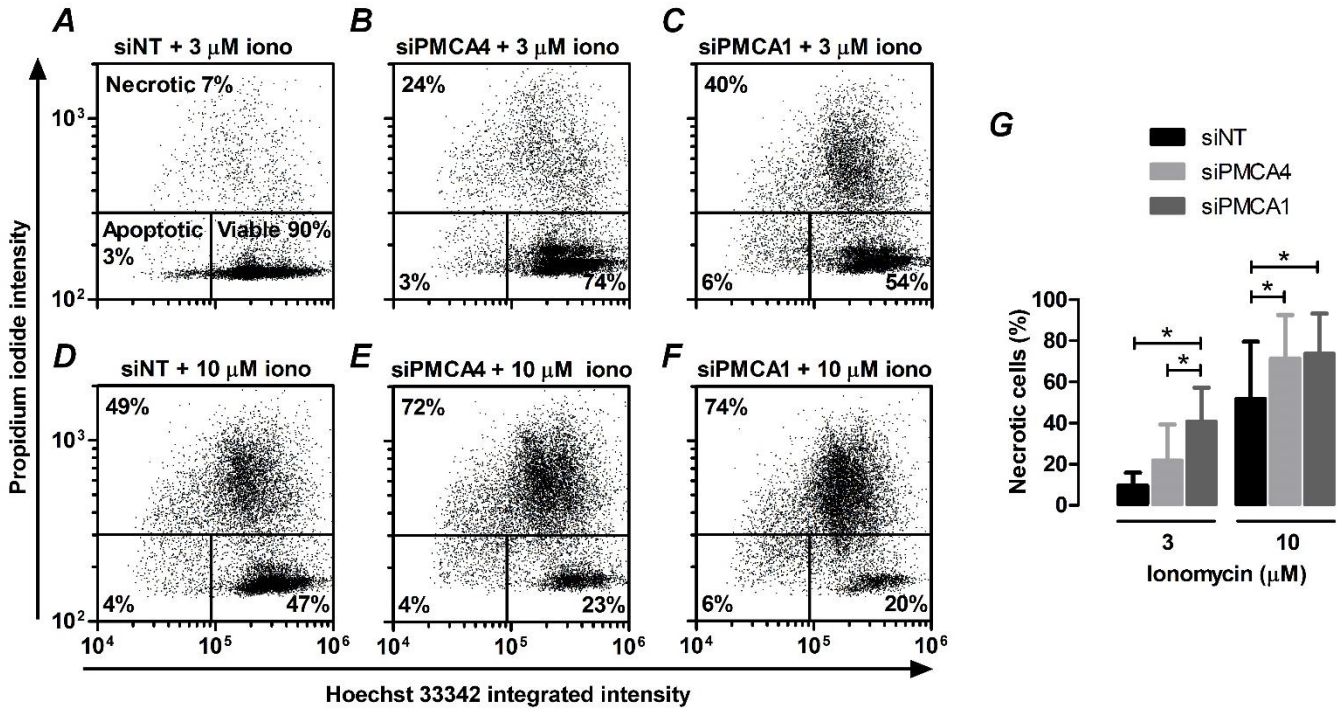

Figure 2-6: PMCA1 and PMCA4 silencing effects in promoting ionomycin-mediated cell death in MDAMB-231 breast cancer cells.

Dot plots of Hoechst 33342 and propidium iodide fluorescence in cells transfected with **(A and D)** siNT, **(B and E)** siPMCA4, or **(C and F)** siPMCA1 following treatment with 3 μM or 10 μM ionomycin (iono). Each dot plot represents an equal number of total cells (10,000 cells) selected at random from three independent experiments. **(G)** The proportion of necrotic cells pooled from three independent experiments (mean ± S.D). *P < 0.05, repeated measures two-way ANOVA, Bonferroni post-hoc analysis.

2.8.6 Consequences of PMCA1 or PMCA4 silencing on ABT-263-induced apoptosis in MDA-MB-231 breast cancer cells

Submaximal ABT-263 (3 µM) induced-apoptosis was significantly ($P < 0.05$) augmented by PMCA4 siRNA compared to siNT (Figure 2-7A, B and G). This effect was isoform-specific, as PMCA1 knockdown did not alter apoptosis compared to siNT (Figure 2-7A, C and G). In contrast, ABT-263 (10 µM)-mediated cell death was not modulated by either PMCA4 siRNA or PMCA1 siRNA compared to siNT (Figure 2-7D-G).

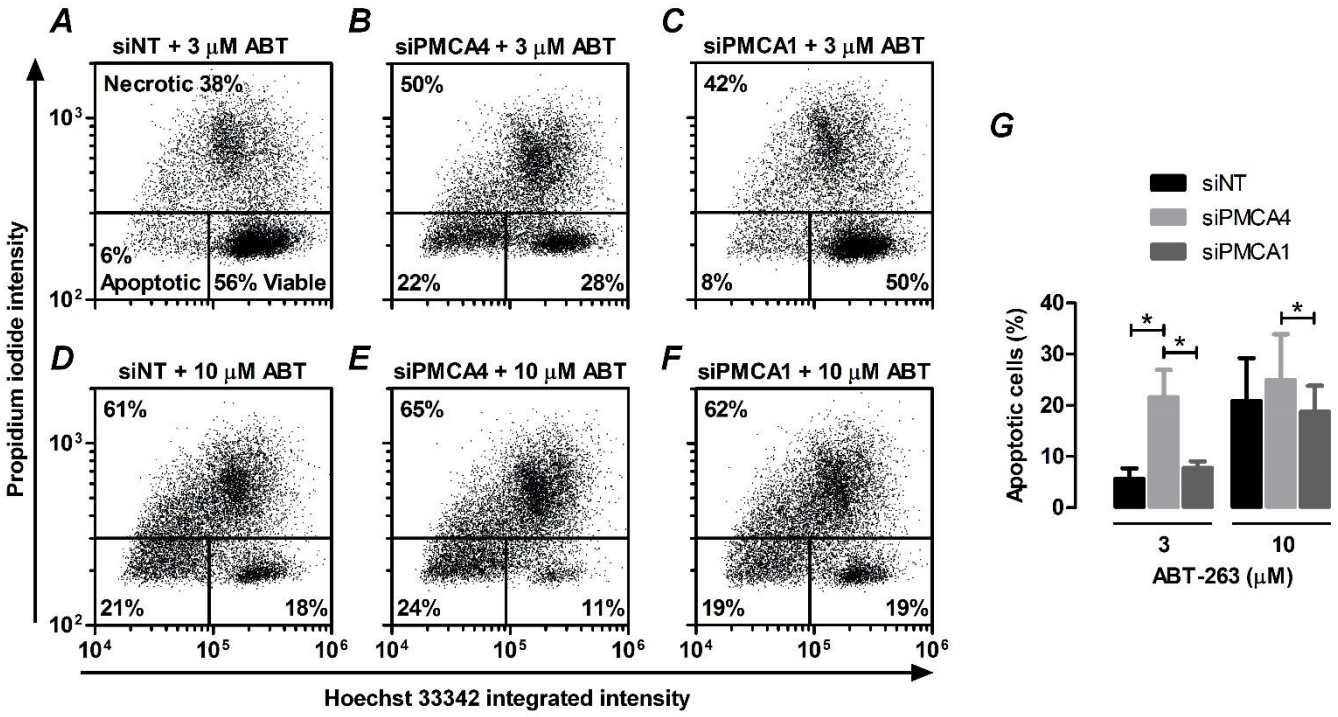

Figure 2-7: PMCA1 and PMCA4 silencing effects in promoting ABT-263-mediated cell death in MDAMB-231 breast cancer cells.

Dot plots of Hoechst 33342 and propidium iodide florescence in cells transfected with **(A and D)** siNT, **(B and E)** siPMCA4, or **(C and F)** siPMCA1 following treatment with ABT-263 (ABT). Each dot plot represents an equal number of total cells (10,000 cells) selected at random from three independent experiments. **(G)** The proportion of apoptotic cells pooled from three independent experiments (mean ± S.D). **P* < 0.05, repeated measures two-way ANOVA, Bonferroni post-hoc analysis.

2.8.7 PMCA4 but not PMCA1 knockdown inhibits NFκB translocation in MDA-MB-231 breast cancer cells

Nuclear factor-κB (NFκB) is a Ca^{2+} dependent transcription factor [209-211], which is implicated in breast cancer progression [212] and the resistance to cancer therapies [213, 214]. PMCA4 is linked to the regulation of Ca^{2+} dependent transcription factors such as NFAT, independent of bulk $[Ca^{2+}]_{CYT}$ changes [187]. We assessed the effects of PMCA4 and PMCA1 silencing on nuclear translocation of NFκB induced by PMA (50 nM) [203]. PMA-induced NFκB nuclear translocation (Figure 2-8A and B) was not affected by PMCA1 silencing but was significantly ($P < 0.05$) reduced by PMCA4 siRNA relative to siNT.

2.8.8 Effects of NFκB inhibition on ABT-263- induced MDA-MB-231 cell death

To further explore the possible link between PMCA4 and NFκB on MDA-MB-231 cell death, we assessed whether NFκB inhibition could mimic PMCA4 siRNA by augmenting cell death induced by ABT-263 (3 μM). The NFκB inhibitor IMD-0354 (10 μM) [215] did not induce cell death alone (Figure 2-8C and F), however, it did significantly ($P < 0.05$) augment ABT-263-mediated apoptosis (Figure 2-8C-I) suggesting that IMD-0354 phenocopies the effect of PMCA4 siRNA on ABT-263-mediated cell death.

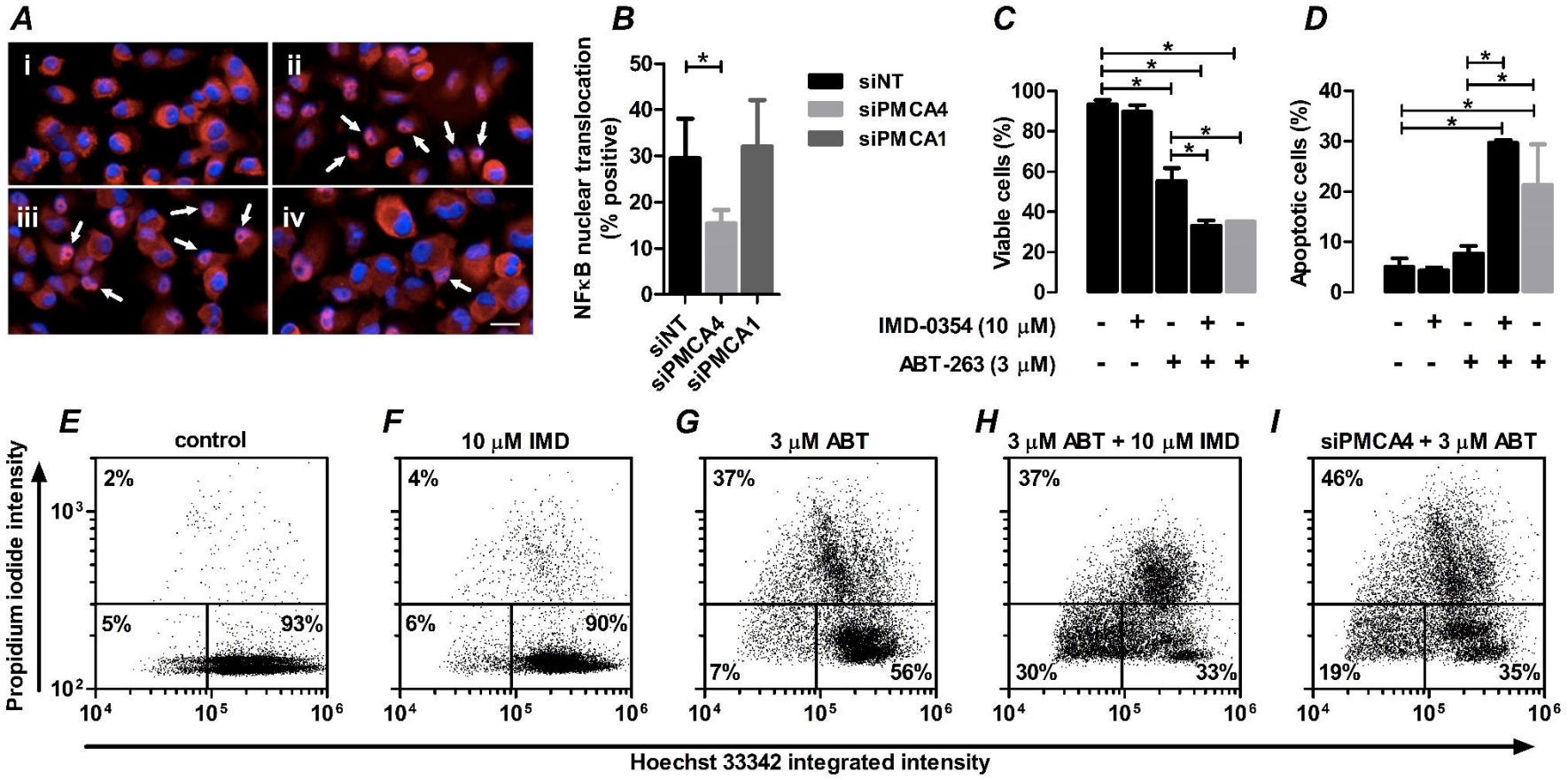
A
i
ii
iii
iv
B
NFκB nuclear translocation (% positive)
siNT
siPMCA4
siPMCA1
C
Viable cells (%)
IMD-0354 (10 μM)
ABT-263 (3 μM)
D
Apoptotic cells (%)
E
control
F
10 μM IMD
G
3 μM ABT
H
3 μM ABT + 10 μM IMD
I
siPMCA4 + 3 μM ABT
2%
5%
93%
4%
6%
90%
37%
7%
56%
37%
30%
33%
46%
19%
35%
Propidium iodide intensity
Hoechst 33342 integrated intensity

Figure 2-8: NFκB activity in the presence of PMCA1 and PMCA4 siRNA and the effect of pharmacological inhibition of NFκB on ABT-263-mediated cell death.

(A) MDA-MB-231 breast cancer cells stained for NFκB (orange) with DAPI (nuclei, blue) and with white arrows depicting translocation of NFκB to the nucleus in the **(i)** absence of PMA (50 nM), **(ii)** presence of PMA (50 nM), **(iii)** presence of siPMCA1 and PMA (50 nM) and **(iv)** presence of siPMCA4 and PMA (50 nM). **(B)** Percentage of cells with NFκB nuclear translocation in siRNA transfected cells following the addition of PMA (50 nM) normalised to the dimethyl sulfoxide (DMSO) control. **(C)** The proportion of viable cells following IMD-0354 (IMD) and/or ABT-263 (ABT) treatment. **(D)** The proportion of apoptotic cells following IMD-0354 and/or ABT-263 treatment. **(E-I)** Dot plots of Hoechst 33342 and propidium iodide fluorescence in cells transfected with siNT or with siPMCA4 in the presence of IMD-0354 and/or ABT-263. Each dot plot represents an equal number of total cells (10,000 cells) selected at random from three independent experiments. All data were from three independent experiments and are presented as mean ± SD where relevant. $*P < 0.05$, repeated measures two-way ANOVA, Bonferroni post-hoc analysis. Scale bar = 25 µm.

2.8.9 PMCA1 and PMCA4 in clinical breast cancers

To determine the distribution of PMCA1 and PMCA4 in breast cancer, we first examined their expression in a panel of breast cancer cell lines grown in 3D culture [206]. Expression varied widely between cell lines, with variation between the highest and lowest measurements being 18.9- fold and 12.8-fold for PMCA1 and PMCA4, respectively (Figure 2-9A and B). PMCA1 expression measurements were found throughout this range in both luminal and basal cell lines (Figure 2-9A), however, PMCA4 was most highly expressed in the basal cell lines (Figure 2-9B, $P = 0.007$). We next evaluated the level of these genes in a cohort of 286 node-negative breast cancer patients described by Wang and co-workers [207]. Consistent with the non-significant trend suggested in the cell line data (Figure 2-9A), PMCA1 was expressed at higher levels in the ER-positive tumors (Figure 2-9C, $P = 0.007$). Median PMCA4 levels were higher in the ER-negative tumors (Figure 2-9D, $P = 0.028$). No differences were observed in patient outcomes when tumors were stratified by PMCA1 (Figure 2-9E, $P = 0.92$) or PMCA4 (Figure 2-9F, $P = 0.76$) levels.

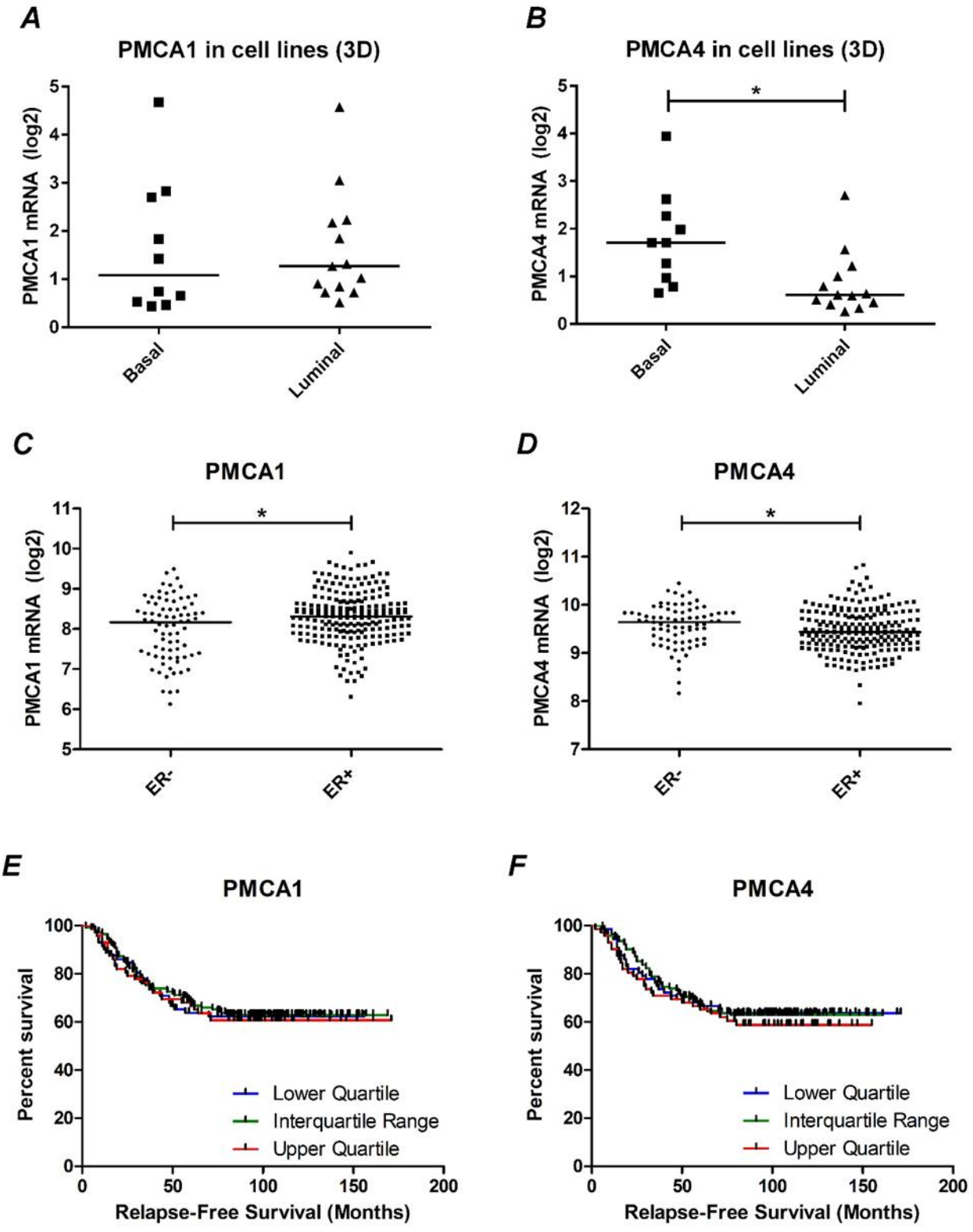
A
PMCA1 in cell lines (3D)
PMCA1 mRNA (log2)
Basal
Luminal
B
PMCA4 in cell lines (3D)
PMCA4 mRNA (log2)
*
Basal
Luminal
C
PMCA1
PMCA1 mRNA (log2)
*
ER-
ER+
D
PMCA4
PMCA4 mRNA (log2)
*
ER-
ER+
E
PMCA1
Percent survival
Lower Quartile
Interquartile Range
Upper Quartile
Relapse-Free Survival (Months)
F
PMCA4
Percent survival
Lower Quartile
Interquartile Range
Upper Quartile
Relapse-Free Survival (Months)

Figure 2-9: The expression of PMCA1 and PMCA4 in breast cancer cell lines and clinical samples.

(A) The relative expression level (log_2) of PMCA1 was assessed in a microarray data set consisting of luminal (n = 13) and basal (n = 10) breast cancer cell lines grown in three-dimensional culture. **(B)** Relative PMCA4 expression levels in these breast cancer cell lines. **(C)** The relative expression level of PMCA1 was assessed in a microarray data set consisting of oestrogen receptor-negative (n = 77) and -positive (n = 209) breast tumors. **(D)** The relative expression level of PMCA4 was assessed in the same breast tumor data set. A bar indicates the median, and significance was evaluated using the Mann-Whitney test. *P > 0.05. **(E)** Kaplan-Meier analysis of relapse-free survival of the breast cancer patients stratified by their tumor levels of PMCA1. **(F)** Relapse-free survival of breast cancer patients stratified by their tumor levels of PMCA4. 3D, three-dimensional.

2.9 Discussion

Despite the proposed differential contributions of PMCA isoforms in Ca^{2+} dependent cellular processes few studies have evaluated the specific roles of different PMCA isoforms in shaping intracellular Ca^{2+} signals and cellular responses in the same cell types. PMCA1 and PMCA4 have a broad tissue distribution and frequently co-express within the same cell [103]. We compared the consequences of knockdown of these two PMCA isoforms on $[Ca^{2+}]_{CYT}$ signals generated by various Ca^{2+} mobilising agents. Pronounced effects with PMCA1 knockdown but not with PMCA4 knockdown were seen on the nature of CPA- and ATP-induced $[Ca^{2+}]_{CYT}$ transients. PMCA1 siRNA reduced the rate of $[Ca^{2+}]_{CYT}$ decay and prolonged the ATP Ca^{2+} response. Previous studies overexpressing PMCA isoforms in CHO cells found that some variants not only alter Ca^{2+} homeostasis within the cytoplasm but also within sub-cellular compartments such as the endoplasmic reticulum [117]. Increases in $[Ca^{2+}]_{CYT}$ mediated by sarcoplasmic endoplasmic reticulum Ca^{2+}-ATPase inhibitors have been reported to correlate with the calcium content of the ER [216]. Hence, increases in the CPA-mediated $[Ca^{2+}]_{CYT}$ transient upon PMCA1 silencing, in addition to being a consequence of reduced Ca^{2+} efflux, may also involve increases in endoplasmic reticulum Ca^{2+} levels.

Our study suggests that in MDA-MB-231 breast cancer cells, the PMCA1 isoform is the major regulator of global $[Ca^{2+}]_{CYT}$ increases, such as those generated by IP3-mediated Ca^{2+} release after G-protein coupled receptor activation. The significance of PMCA4 in MDA-MB-231 cells may become apparent during very high Ca^{2+} loads. Indeed, during the high magnitude increases in $[Ca^{2+}]_{CYT}$ initiated by 3 µM ionomycin, a contribution for PMCA4 was identified. However, this PMCA4 siRNA-mediated effect was not as pronounced as seen with PMCA1 knockdown. This finding is also consistent with a predominant role for PMCA1 in the regulation of global $[Ca^{2+}]_{CYT}$ signals in this cell type and is consistent with previous studies, demonstrating distinct phenotypes in PMCA1 and PMCA4 knockout animals [105, 111, 112]. PMCA1 ablation is lethal during embryogenesis, indicative of its vital role in the maintenance of $[Ca^{2+}]_{CYT}$ homeostasis in an array of cell types [111]. Although PMCA4 has a broad tissue distribution, PMCA4 null mice reach adulthood and exhibit tissue specific phenotypes such as male infertility [105, 111, 112]. These differences suggest that PMCA1 adopts a vital housekeeping function by regulating global Ca^{2+} homeostasis and supports the involvement of PMCA4 in Ca^{2+}-dependent signal transduction and cell processes by shaping of Ca^{2+} signals within sub-cellular domains [105, 111, 112].

We extended our study to examine the consequences of PMCA4 and PMCA1 siRNA on cell death in the presence of cell death stimuli. Initial studies, in the absence of any stimuli, showed that the viability of MDA-MB-231 breast cancer cells was not affected by PMCA1 or PMCA4 knockdown.

In contrast, PMCA2 knockdown produces spinal cord neuronal cell death [193, 217] in the absence of external stimuli. Assessment of PMCA1 and PMCA4 knockdown on cell death initiated by ionomycin or ABT-263 demonstrated distinct roles for PMCA1 and PMCA4 in the regulation of caspase-independent and dependent cell death pathways, respectively. Consistent with the effects seen with ionomycin induced $[Ca^{2+}]_{CYT}$ transients, PMCA1 knockdown had a more pronounced effect on ionomycin induced cellular necrosis than PMCA4 knockdown. This result further underscores the more subtle nature of the change in calcium handling in the cell with PMCA4 knockdown. Previous results examining PMCA4 as a sensitiser of cell death in HT-29 colon cancer cells showed that PMCA4 silencing does not alter the sensitivity of HT-29 cells to TRAIL or CCCP-induced cell death [180]. Reduced expression of another PMCA isoform, PMCA2, augments ionomycin-mediated cell death in SH-SY5Y neuroblastoma cells [194]. Whereas its overexpression in T47D breast cancer cells bestows resistance to ionomycin-mediated cell death through the attenuation of $[Ca^{2+}]_{CYT}$ responses [182].The potential significance of this survival advantage is reflected in the poorer prognosis of breast cancer patients with elevated expression of PMCA2 [182]. Our silencing studies suggest that modulators of PMCA isoforms involved in global $[Ca^{2+}]_{CYT}$ may sensitise cells to cell death stimuli.

The Bcl-2 inhibitor (ABT-263) used in this study to induce apoptotic cell death in MDA-MB- 231 breast cancer cells is progressing through clinical trials [192]. A structurally related analogue (ABT-737) sensitises Bcl-2−expressing breast cancers to chemotherapies [218], highlighting the potential for Bcl-2 inhibitors as a therapeutic option for breast cancer. ABT-263-induced cell death was not affected by PMCA1 knockdown, but instead was augmented upon reduced expression of PMCA4. These distinct differences in the consequences of isoform-specific PMCA knockdown on ionomycin and ABT-263 initiated cell death is not totally unexpected, considering these agents activate cell death by distinct mechanisms and have markedly different effects on Ca^{2+} signals. Ionomycin produces sustained global increases in $[Ca^{2+}]_{CYT}$, augmented by PMCA1 siRNA, resulting in Ca^{2+} overload and cell necrosis. Bcl-2 inhibitors such as ABT-263 initiate caspase-dependent apoptosis by binding to and blocking the pro-survival activity of BH3 domains present within Bcl-2 proteins [189-191]. Increases in intracellular Ca^{2+} signals, particularly within subcellular compartments, such as the endoplasmic reticulum and mitochondria can modulate Bcl-2- mediated survival pathways [152, 219, 220]. Our identification of PMCA4 as a modulator of ABT- 263 mediated cell death may be analogous to the characterised role of PMCA4 in cardiac cells, where altered PMCA4 expression appears to play little role in shaping global $[Ca^{2+}]_{CYT}$ increases [187, 221] yet is an important regulator of the Ca^{2+}- dependent transcription factor NFAT influencing outcomes such as cardiac hypertrophy [186, 187]. Ca^{2+}- dependent gene transcription critically depends on localisation of Ca^{2+} signals as

well as Ca^{2+} oscillation frequency and amplitude [209, 210]. Hence PMCA4-mediated regulation of transcription may be mediated through the fine-tuning of Ca^{2+} signals within localised sub-cellular domains or through alterations in oscillation frequency. Context dependent modulation of apoptosis by PMCAs is reflected in PMCA4 knockout mice studies. Smooth muscle cells from the portal veins of PMCA4 knockout mice on a mixed 129/SvJ and Black Swiss background display features of apoptosis during in vitro contraction studies [112].

Our study identified PMCA4 siRNA-mediated inhibition of NFκB nuclear translocation. Pharmacological inhibition of NFκB phenocopied the augmentation of ABT-263-mediated apoptosis produced by PMCA4 silencing, suggesting that PMCA4 siRNA-augmentation of apoptosis may be due to modulation of NFκB. The ability of PMCA4 silencing to inhibit NFκB is significant. The activity of NFκB is governed by the nature of Ca^{2+} signals [209-211]and Ca^{2+} influx mediated by the calcium channel TRPC1 can inhibit NFκB activity in an intestinal epithelial cell line [222]. Breast cancers with a poor prognosis are associated with elevated constitutive activity of NFκB [213, 214]. Agents that inhibit NFκB are themselves promising anti-tumour modulators for the treatment of breast cancers [223, 224] and can enhance the effects of Bcl-2 inhibitors [225]. Our studies comparing PMCA1 and PMCA4 in clinical samples suggest that although inhibition of PMCA4 in basal breast cancer may be an effective way to augment responsiveness to Bcl-2 inhibitors in breast cancer therapy, increases in PMCA4 (or PMCA1) expression are not a cause of general apoptotic resistance in breast cancer, as there was no association between PMCA4 (or PMCA1) levels and prognosis.

In summary, we show that PMCA1 is a major regulator of global Ca^{2+} homeostasis in MDA-MB-231 breast cancer cells and this is associated with an ability of PMCA1 silencing to augment necrotic cell death generated by high Ca^{2+} loads. Although, PMCA4 is not a key regulator of global changes in $[Ca^{2+}]_{CYT}$ associated with many stimuli, our study demonstrates a novel relationship between PMCA4 and NFκB. Our study highlights isoform diversity between the two almost ubiquitously expressed PMCA isoforms (PMCA1 and PMCA4) and identifies PMCA4 as a potential anti-tumor modulator. Inhibitors of PMCA4 [226] may be novel therapeutics to sensitise some cancer cells to apoptotic stimuli.

2.10 Acknowledgements

This work was supported by the National Health and Medical Research Council (631347) and Susan G. Komen for the Cure (KG100888).

2.11 Additional experiments and data not included in the published manuscript, but relevant to this chapter

2.11.1 Introduction

The published manuscript achieved PMCA1 and PMCA4 silencing and assessed the consequence of this on MDA-MB-231 cell death using ABT-263 and ionomycin to initiate caspase-independent and -dependent cell death mechanisms, respectively [227]. Additional experiments presented here, describe in more detail the methods and optimisation of the high-throughput cell death assay, and the effects of PMCA1 or PMCA4 silencing on the death triggered by ceramide and staurosporine in MDA-MB-231 cells. Also examined in more detail are the effects of PMCA-silencing on GPCR-induced Ca^{2+} signals initiated by ATP and trypsin, and on store-operated Ca^{2+} entry upon CPA-mediated store depletion.

2.11.2 Materials and methods

2.11.2.1 Cell culture

MDA-MB-231 breast cancer cells were cultured as described in section 2.7.1, page 41.

2.11.2.2 Silencing of PMCA4 and PMCA1 gene expression

PMCA4 and PMCA1 knockdown in MDA-MB-231 breast cancer cells was achieved according to the method in section 2.7.2, page 41.

2.11.2.3 Real time RT-PCR

Knockdown of PMCA4 and PMCA1 was confirmed by the real time RT-PCR protocol in section 2.7.3, page 41.

2.11.2.4 Cytosolic free calcium measurements

Cytoplasmic free calcium was measured according to the method 2.7.4, page 42.

2.11.2.5 *Assessment of cell viability (in more detail)*

2.11.2.5.1 *Treatment of MDA-MB-231 breast cancer cells with staurosporine and ceramide*

MDA-MB-231 cells were plated (5 x 10^3 cells per well) into a 96-well imaging plate, and incubated for 24 h. The following day, MDA-MB-231 cells were siRNA transfected as previously described (section 2.7.2, page 41) or the culture medium was refreshed. Cells were incubated for a further 72 hours, and then cell death was initiated by adding staurosporine (Sigma-Aldrich) or ceramide (Sigma-Aldrich) to confluent cell cultures.

Staurosporine (at concentrations up to 3 µM) was prepared in phenol red-free media, supplemented with 10% FBS from a stock solution of 1 mM in DMSO stored at -22ºC. Ceramide (at concentrations up to 300 µM) was also prepared in phenol red-free media, supplemented with 10% FBS, from a 30 mM stock solution in DMSO stored at -22ºC.

Figure 2-10 illustrates a typical experiment timeline performed routinely, which incorporates multiple techniques including the addition of cell death stimuli along with other methods such as siRNA transfection, mRNA isolation, protein isolation, $[Ca^{2+}]_{CYT}$ assessment and cell death analysis.

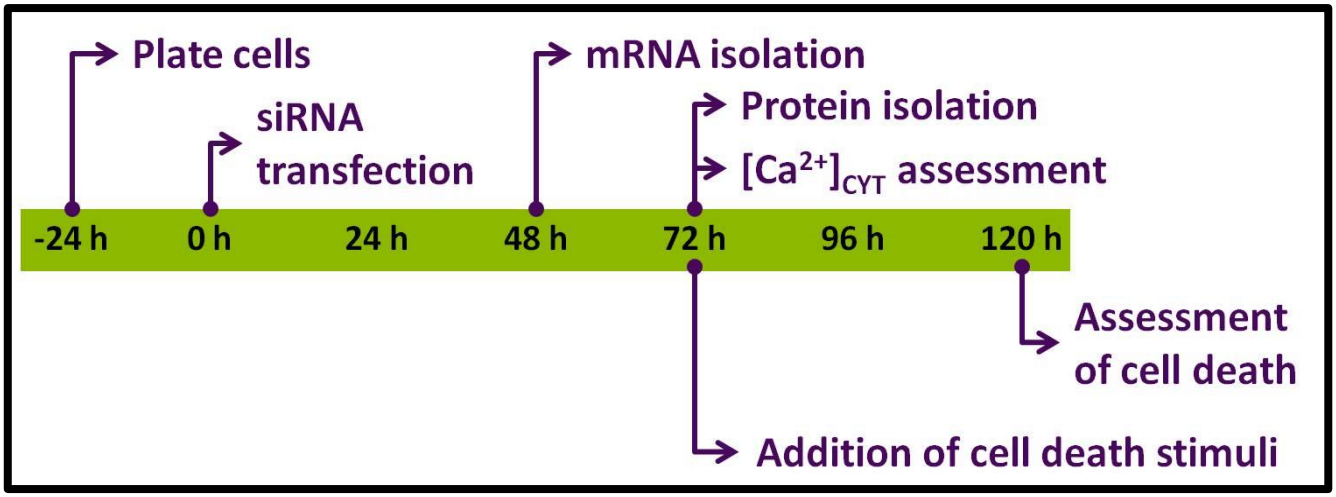

Figure 2-10: A typical timeline, showing multiple endpoint experiments.

2.11.2.5.2 *Live cell staining with Hoechst 33342 and propidium iodide*

Live cell imaging was performed by a high-throughput approach to assess cell death based on the morphological changes, and changes in plasma membrane integrity [208, 228]. The fluorescent dye Hoechst 33442 was used to stain cell nuclei and assess changes in nuclear morphology associated

with apoptotic cells, which arises from a combination of nuclear condensation, DNA fragmentation and subsequent DNA loss [208, 228]. For the assessment of cell death, Hoechst 33342 was added to the individual wells of a 96-well imaging plate at a final concentration of 10.0 µg/mL in phenol red-free media, prepared from a stock solution of 10 mg/mL in water (stored at 4ºC).

Cells were simultaneously stained with propidium iodide, a fluorescent dye that stains DNA. Unlike Hoechst 33442, propidium iodide is cell impermeable and is excluded from apoptotic cells that maintain plasma membrane integrity [208, 228]. Therefore, cells positive for propidium iodide at this time point are distinguished as necrotic cells, where the plasma membrane has fragmented [208, 228]. At extended time points *in vitro*, apoptotic cells eventually lose their plasma membrane integrity and uptake propidium iodide (secondary necrosis) [208, 228]. For the assessesment of cell death, propidium iodide was added to the individual wells of a 96-well imaging plate at a final concentration of 1.0 µg/mL cells in phenol red-free media supplemented with 10% FBS, prepared from a stock solution of 1.0 mg/mL in water (stored at 4ºC).

2.11.2.5.3 *High-content imaging of MDA-MB-231 breast cancer cell death*

For image acquisition, fluorescence was measured using an inverted automated epifluorescent microscope. With a 10X objective, four images were automatically acquired per well in the DAPI channel for Hoechst 33342 and, in the Cy3 channel for propidium iodide. The multi-wavelength cell scoring application module (MetaXpress v3.1.0.83; Molecular Devices Corporation) was used to segment cell nuclei, calculate the average Hoechst 33342 integrated intensity and the average propidium iodide intensity emitted per cell. Parameters to detect nuclei fluorescence for the DAPI channel are shown in Figure 2-11. The same configure settings were applied to the Cy3 channel to detect propidium iodide uptake. Exposure times were automated to a maximum 3000 relative fluorescence units per image. Example images and nuclear segmentation for non-treated and staurosporine (3 µM) treated MDA-MB-231 breast cancer cells are illustrated in Figure 2-12 and Figure 2-13. Fluorescence per cell was exported into Microsoft Office Excel from the multi-wavelength cell scoring application module (MetaXpress, version 3.1.0.83; Molecular Devices Corporation). Viable, apoptotic and necrotic cell populations were identified according to the same criteria outlined in Section 2.7.6, page 42.

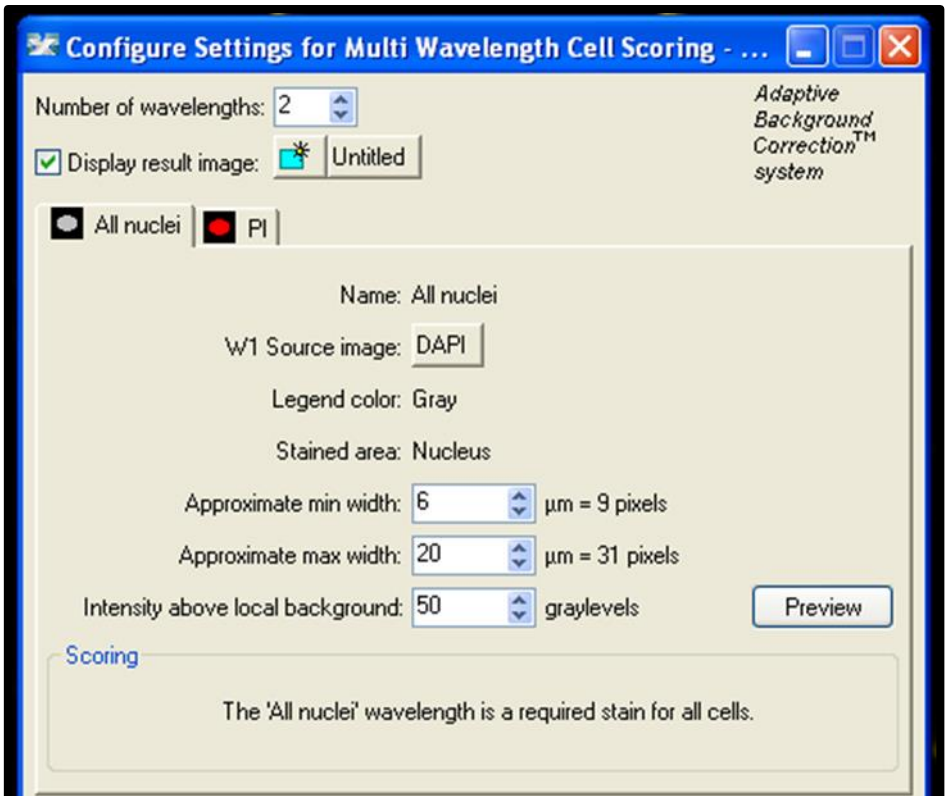

Figure 2-11: Configure Settings to detect cell nuclei using the multi-wavelength cell scoring application module (MetaXpress v3.1.0.83) in the DAPI channel.

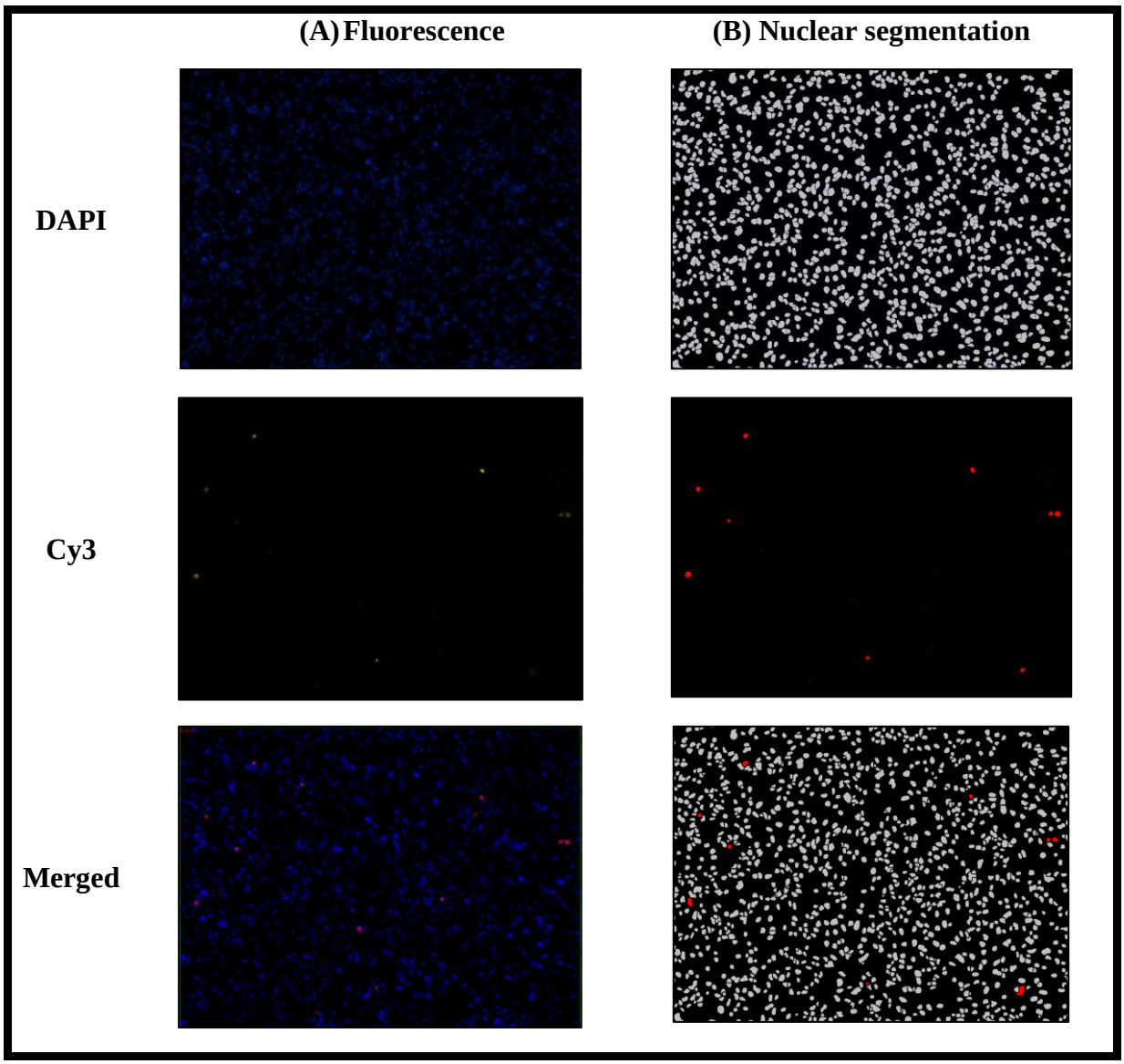

Figure 2-12: Example fluorescent images and nuclear segmentation in non-treated MDA-MB-231 cells using the ImageXpress micro automated epifluorescence microscope.

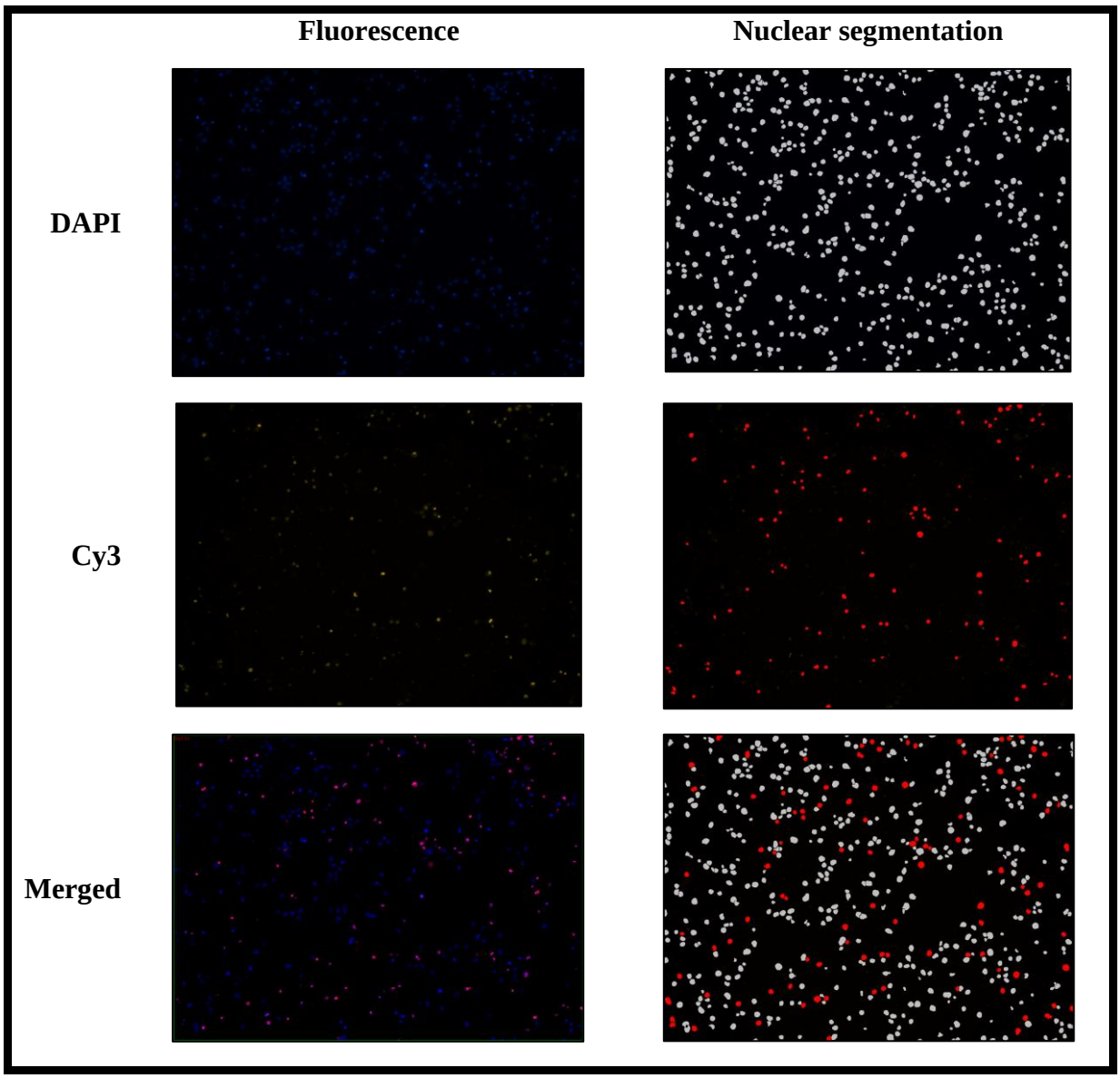

Figure 2-13: Example fluorescent images and nuclear segmentation in staurosporine (3 µM)-treated MDA-MB-231 cells using the ImageXpress micro automated epifluorescence microscope.

2.11.2.6 Statistical analysis

All statistical tests were performed as described in the figure legends using GraphPad Prism, version 6.04 or 7.00 for Windows, GraphPad Software, San Diego California USA, www.graphpad.com.

2.11.3 Results

2.11.3.1 Assessment of cell death at two time points

An initial experiment was performed to assess cell death following 16 h or 48 h incubation with staurosporine (STS). The results are presented as dot plots in Figure 2-14A-D. Compared with the other treatment protocols (Figure 2-14A-C), MDA-MB-231 cells treated for 48 h with 3 µM STS clearly show three cell populations (Figure 2-14D). The third cell population, positioned in the bottom left hand side of the dot plot (Figure 2-14D) are propidium iodide negative (intact plasma membranes), and have reduced Hoechst 33342 integrated intensity suggesting cells undergoing apoptosis [208, 228]. The apoptotic nature of these cells was also evident in Hoechst 33342 intensity frequency histograms (Figure 2-14E-F), where a sub-G1 peak was detected in MDA-MB-231 cells treated for 48 h with 3 µM STS (Figure 2-14F). The presence of a sub-G1 population is an accepted marker of apoptotic cell death [208, 228]. Cell death throughout this thesis, was assessed in MDA-MB-231 cells after 48 h incubation with various cell death stimuli, because at this time point viable, apoptotic and necrotic cells can be detected.

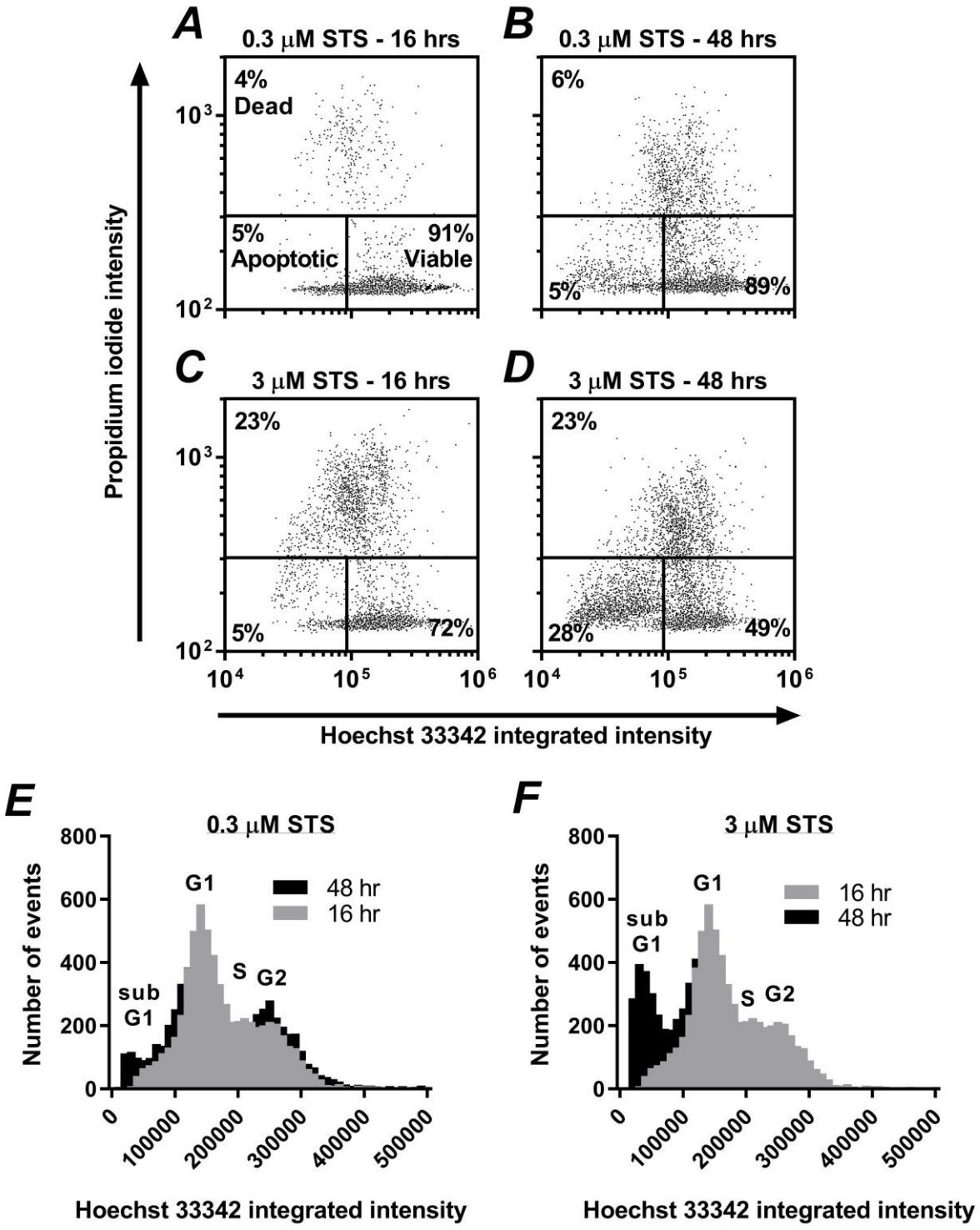
A
0.3 μM STS - 16 hrs
4%
Dead
5%
Apoptotic
91%
Viable
B
0.3 μM STS - 48 hrs
6%
5%
89%
C
3 μM STS - 16 hrs
23%
5%
72%
D
3 μM STS - 48 hrs
23%
28%
49%
Propidium iodide intensity
Hoechst 33342 integrated intensity
E
0.3 μM STS
Number of events
sub G1
G1
S
G2
48 hr
16 hr
Hoechst 33342 integrated intensity
F
3 μM STS
Number of events
sub G1
G1
S
G2
16 hr
48 hr
Hoechst 33342 integrated intensity

Figure 2-14: MDA-MB-231 breast cancer cell viability after 16 h and 48 h exposure to staurosporine.

MDA-MB-231 cells were plated (5 x 10^3 cells per well), and after 96 h incubation, staurosporine (3 µM or 0.3 µM, STS) was added to initiate cell death in confluent MDA-MB-231 cells. Cell death was assessed following 16 h or 48 h exposure to STS as described in section 2.11.2.5. Dot plots show Hoechst 33342 and propidium iodide florescence per cell after treatment with **(A and B)** 0.3 µM STS or **(C and D)** 3 µM STS for either **(A and C)** 16 h or **(B and D)** 48 h. Each dot plot represents an equal number of total cells (6,434 cells) from a single optimisation experiment performed in triplicate wells. Hoechst 33342 intensity frequency histograms for cells exposed to **(E)** 0.3 µM STS or **(F)** 3 µM STS for 16 h or 48 h.

2.11.3.2 Effects of PMCA1 or PMCA4 knockdown on MDA-MB-231 breast cancer cell death triggered by ceramide and staurosporine

Using the high throughput cell death assay aforementioned (section 2.11.3.1, page 74), the ability of PMCA1 or PMCA4 silencing in the regulation of MDA-MB-231 cell death was examined. Ceramide (C2) and staurosporine (STS) were selected to initiate cell death, because these agents have previously been used in studies of PMCA.

Only a few reports have examined PMCA-mediated regulation of cell death initiated by either ceramide or staurosporine. Pinton *et al* used recombinant PMCA4 expression in HeLa cells to reduce $[Ca^{2+}]_{ER}$, and this protected this cell line against ceramide-induced cell death [152]. Another study overexpressed PMCA4 mutants in CHO cells, which were designed not to be cleaved by caspases [76]. Expression of these mutant constructs delayed STS-induced apoptosis and was associated with altered global $[Ca^{2+}]_{CYT}$ signals [76].

In this thesis study, MDA-MB-231 cell death triggered by ceramide at sub-maximum (30 µM) and maximum (300 µM) concentrations were not ($P > 0.05$) altered by either siPMCA1 or siPMCA4 (Figure 2-15) at the time point assessed.

Modest, but statistically significant ($P < 0.05$) effects on cell death were detected when MDA-MB-231 cells were exposed to STS (Figure 2-16). siPMCA1 protected against STS (0.3 µM) by increasing the number of viable cells (Figure 2-16G) and reducing those with necrotic characteristics (Figure 2-16I). On the other hand, at the maximal STS concentration (3 µM), siPMCA4 increased the number of cells undergoing apoptosis (Figure 2-16H). Given the subtle nature of these effects on cell death, compared with the data obtained when ABT-263 and ionomycin were used to initiate cell death, these results were not the subject of further detailed investigation and were not included in the published manuscript [227].

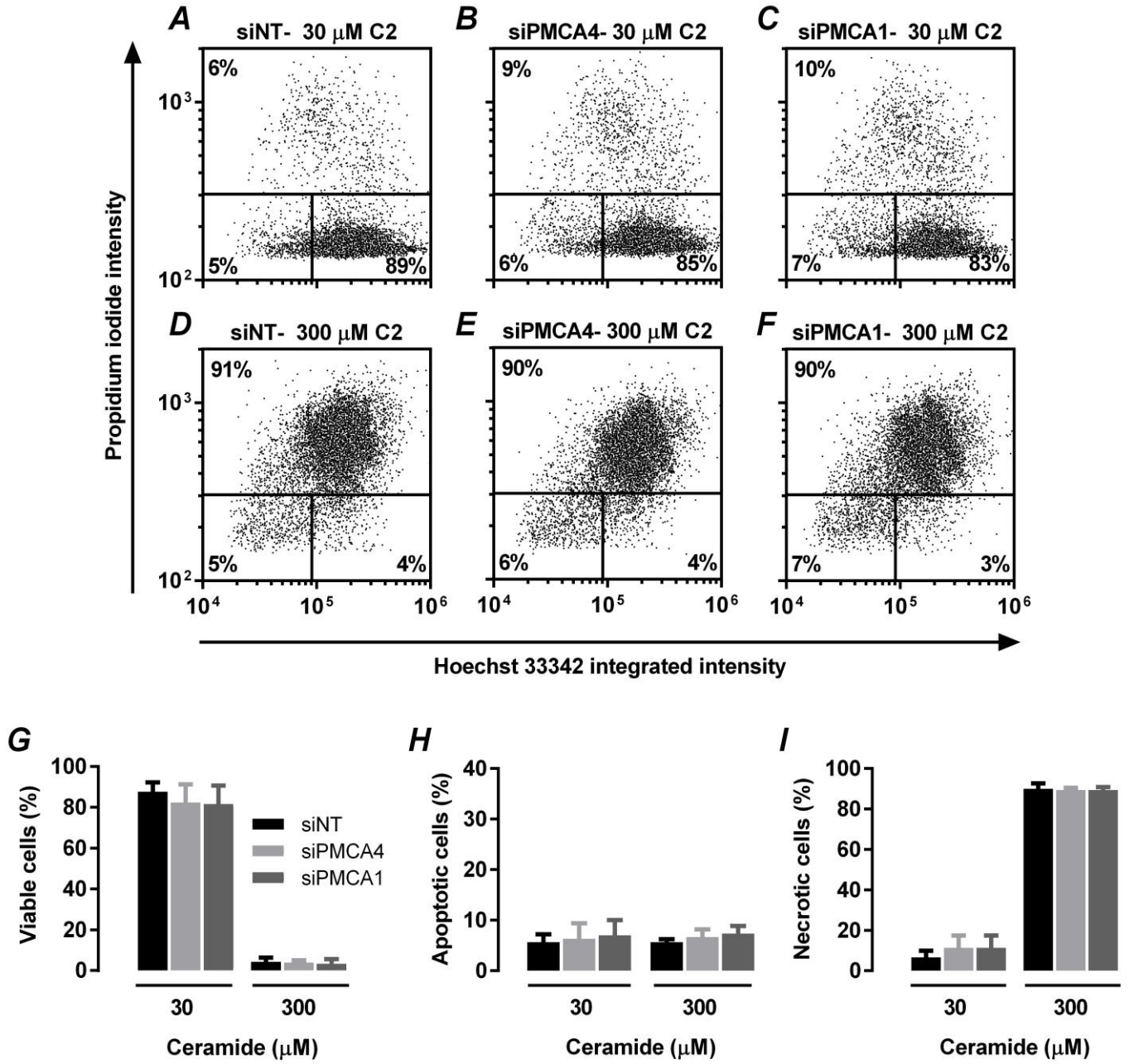
A
siNT- 30 μM C2
6%
5%
89%
B
siPMCA4- 30 μM C2
9%
6%
85%
C
siPMCA1- 30 μM C2
10%
7%
83%
D
siNT- 300 μM C2
91%
5%
4%
E
siPMCA4- 300 μM C2
90%
6%
4%
F
siPMCA1- 300 μM C2
90%
7%
3%
Propidium iodide intensity
Hoechst 33342 integrated intensity
G
Viable cells (%)
siNT
siPMCA4
siPMCA1
Ceramide (μM)
H
Apoptotic cells (%)
Ceramide (μM)
I
Necrotic cells (%)
Ceramide (μM)

Figure 2-15: PMCA1 and PMCA4 silencing-mediated effects on cell death in MDA-MB-231 cells exposed to ceramide.

Dot plots of Hoechst 33342 and propidium iodide florescence in cells transfected with **(A and D)** siNT, **(B and E)** siPMCA4, or **(C and F)** siPMCA1 following 48 h exposure to **(A-C)** 30 µM or **(D-F)** 300 µM ceramide (C2). Dot plots represent an equal number of total cells (10,000 cells) selected at random from three independent experiments. The percentage of **(G)** viable, **(H)** apoptotic and **(I)** necrotic cells pooled from three independent experiments. Bar graphs are (mean ± SD). *$P < 0.05$, repeated measures two-way ANOVA, Bonferroni post-hoc analysis.

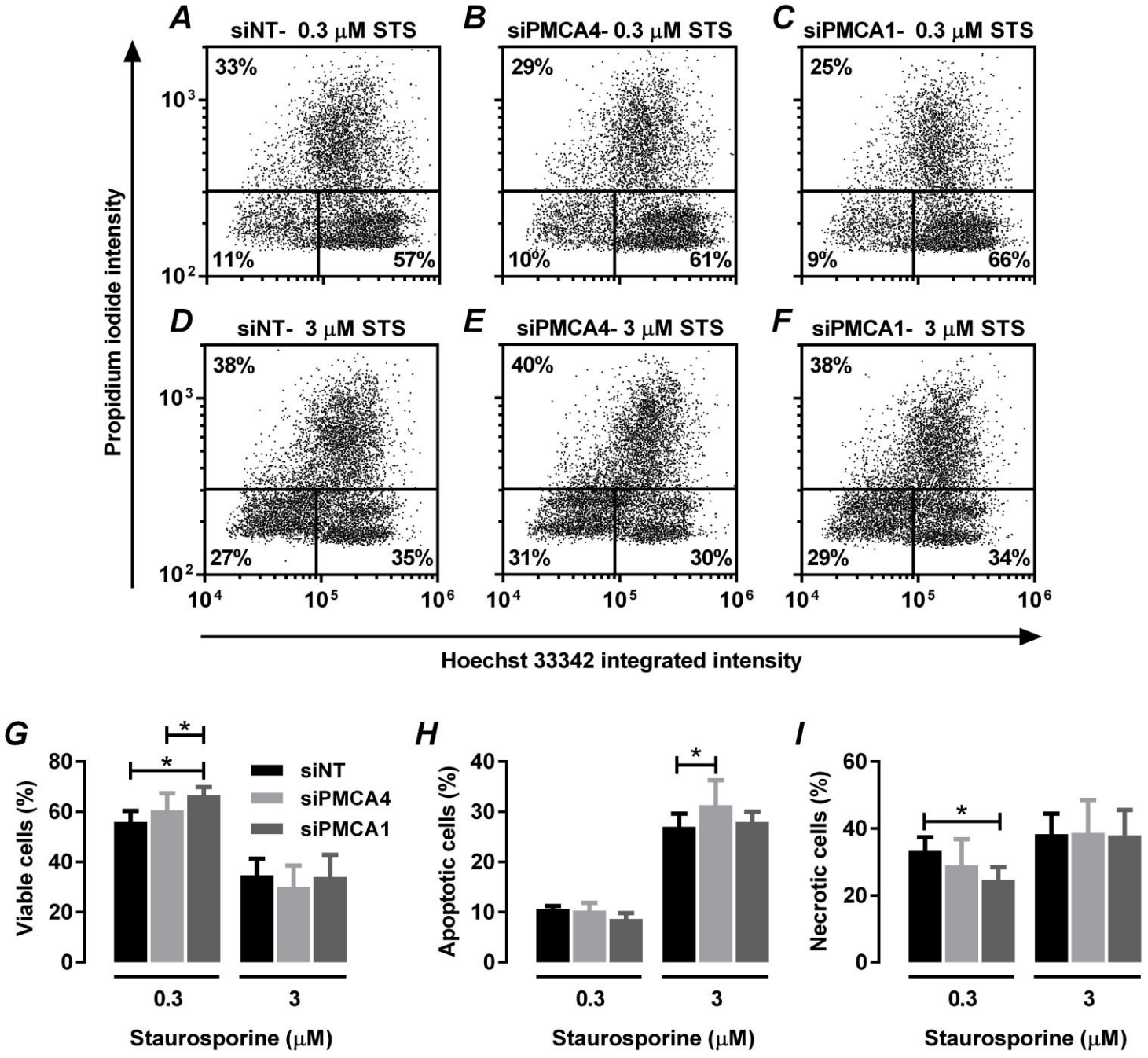
A
siNT- 0.3 μM STS
33%
11%
57%
B
siPMCA4- 0.3 μM STS
29%
10%
61%
C
siPMCA1- 0.3 μM STS
25%
9%
66%
D
siNT- 3 μM STS
38%
27%
35%
E
siPMCA4- 3 μM STS
40%
31%
30%
F
siPMCA1- 3 μM STS
38%
29%
34%
Propidium iodide intensity
Hoechst 33342 integrated intensity
G
Viable cells (%)
siNT
siPMCA4
siPMCA1
Staurosporine (μM)
H
Apoptotic cells (%)
Staurosporine (μM)
I
Necrotic cells (%)
Staurosporine (μM)

Figure 2-16: PMCA1 and PMCA4 silencing-mediated effects on cell death in MDA-MB-231 cells exposed to staurosporine.

Dot plots of Hoechst 33342 and propidium iodide florescence in cells transfected with **(A and D)** siNT, **(B and E)** siPMCA4, or **(C and F)** siPMCA1 following 48 exposure to **(A-C)** 0.3 µM or **(D-F)** 3 µM STS. Dot plots represent an equal number of total cells (10,000 cells) selected at random from three independent experiments. The percentage of **(G)** viable, **(H)** apoptotic and **(I)** necrotic cells pooled from three independent experiments. Bar graphs are (mean ± SD). *$P < 0.05$, repeated measures two-way ANOVA, Bonferroni post-hoc analysis.

2.11.3.3 Consequences of PMCA1 or PMCA4 knockdown on cytoplasmic free calcium increases associated with the PAR activator trypsin in MDA-MB-231 breast cancer cells

The ability of PMCA1 or PMCA4 silencing in shaping ATP Ca^{2+} signals is presented in section 2.8.2, page 47 (published manuscript) [227]. PMCA1 silencing, but not siPMCA4 increased the half peak decay time and prolonged the duration of the ATP Ca^{2+} transient. Extending these studies, the ability of siPMCA1 or siPMCA4 in shaping trypsin-induced Ca^{2+}signals was assessed here. Both ATP and trypsin, elicit $[Ca^{2+}]_{CYT}$ increases via IP_3 signal transduction, however, they do so by activating different GPCRs located at the cell surface. ATP activates P2Y [229], whereas trypsin activates PARs (protease activated receptors) [230].

Effects of siPMCA1 or siPMCA4 on trypsin Ca^{2+} signals were determined by assessment of the Ca^{2+} transient parameters peak amplitude (Figure 2-17B), area under the curve (Figure 2-17C), rate of $[Ca^{2+}]_{CYT}$ decay (Figure 2-17D) and half peak decay time (Figure 2-17E). PMCA4 knockdown had no effect ($P > 0.05$) on the trypsin Ca^{2+} transient (Figure 2-17A), which is consistent with the conclusion that in some cells PMCA4 can exert effects acting through local Ca^{2+} signals, rather than bulk $[Ca^{2+}]_{CYT}$ [187].

Although PMCA1 knockdown produced no effect ($P > 0.05$) on either the peak amplitude (Figure 2-17B) or area under the curve (Figure 2-17C), silencing of this PMCA isoform significantly ($P < 0.05$) reduced the rate of $[Ca^{2+}]_{CYT}$ decay (Figure 2-17D) and delayed the half peak decay time (Figure 2-17E) of the trypsin Ca^{2+} signal relative to the siNT control.

The effect of siPMCA1 on the half peak decay time was also compared between the two GPCR activators, ATP *versus* trypsin (Figure 2-17F). This analysis demonstrated that siPMCA1-mediated regulation of the trypsin Ca^{2+} signal is fairly modest ($P > 0.05$), when compared to the pronounced effect ($P < 0.05$) that siPMCA exerts on the ATP-induced Ca^{2+} signal.

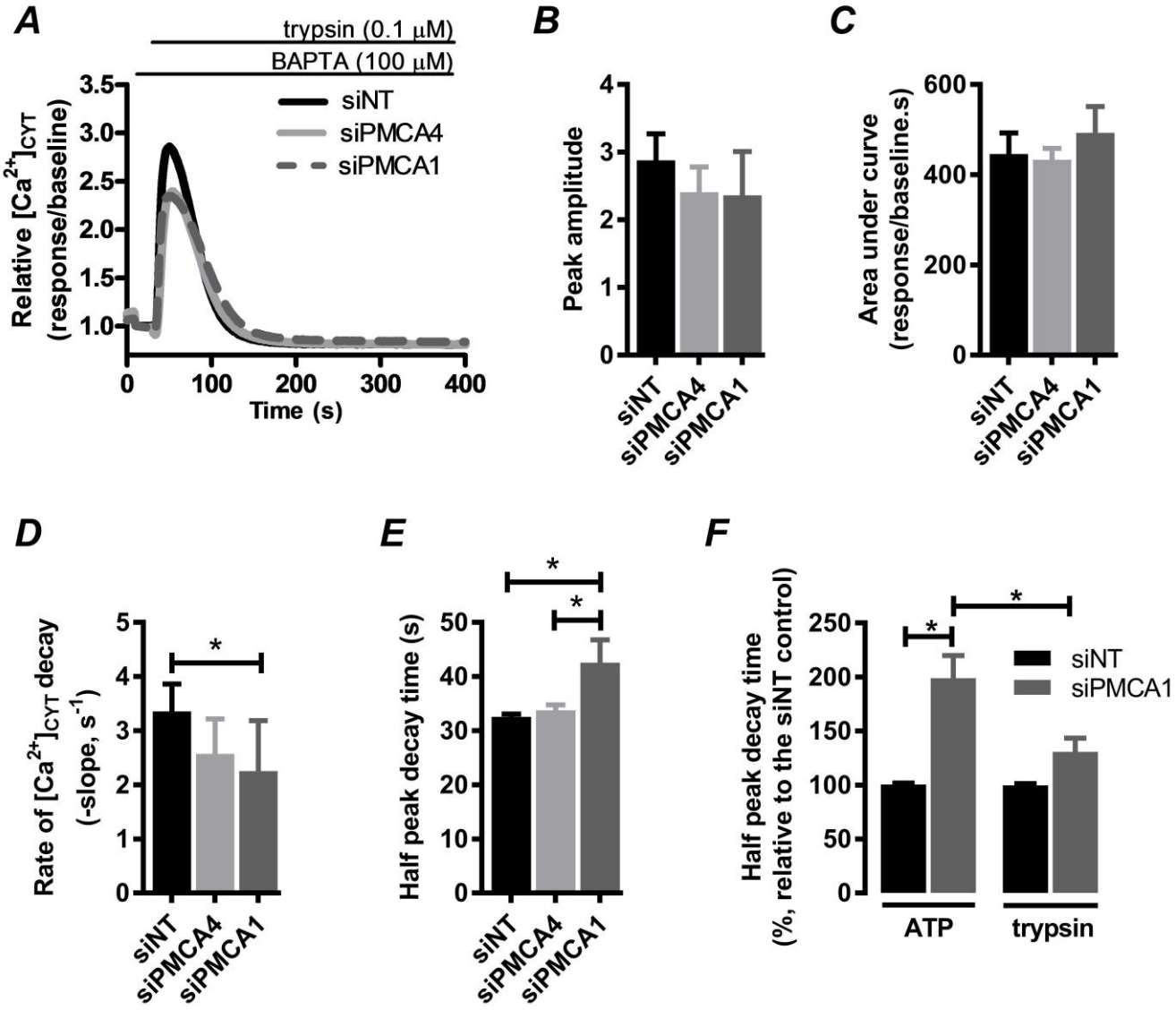
A
trypsin (0.1 μM)
BAPTA (100 μM)
siNT
siPMCA4
siPMCA1
Relative [Ca2+]CYT (response/baseline)
Time (s)
B
Peak amplitude
C
Area under curve (response/baseline.s)
D
Rate of [Ca2+]CYT decay (-slope, s-1)
E
Half peak decay time (s)
F
Half peak decay time (%, relative to the siNT control)
ATP
trypsin

Figure 2-17: Effect of PMCA1 and PMCA4 silencing on trypsin-induced $[Ca^{2+}]_{CYT}$ increases in MDA-MB-231 breast cancer cells.

(A) Trypsin (0.1 µM)-mediated $[Ca^{2+}]_{CYT}$ signals after transfection with siPMCA1, siPMCA4 or siNT in the presence of extracellular BAPTA (100 µM) in nominal Ca^{2+} free medium. Ca^{2+} traces represent relative mean fluorescence. Assessment of the Ca^{2+} transient parameters **(B)** peak amplitude **(C)** area under the curve **(D)** rate of $[Ca^{2+}]_{CYT}$ decay and **(E)** half peak decay time. **(F)** Half peak decay time, ATP compared with trypsin-induced Ca^{2+} responses. All data were pooled from three independent experiments performed in triplicate. Bar graphs are mean ± SD, and $*P < 0.05$. **(B-E)** One-way ANOVA, Bonferroni post-hoc analysis, and **(F)** Two-way ANOVA, Bonferroni post-hoc analysis.

2.11.3.4 *Effect of CPA on PMCA1 or PMCA4 knockdown during GPCR-linked cytoplasmic free calcium increases associated trypsin in MDA-MB-231 breast cancer cells*

SERCA is another Ca^{2+} pump that contributes to $[Ca^{2+}]_{CYT}$ clearance (section 1.1.2.5, page 6). Calcium efflux via SERCA may be a compensatory mechanism for PMCA1 or PMCA4 silencing, during trypsin and ATP-induced Ca^{2+} signals. This possibility was examined using the reversible inhibitor CPA to pharmacologically block SERCA activity [231, 232].

Trypsin-induced Ca^{2+} signals were recorded in the absence and presence of CPA in siRNA-transfected MDA-MB-231 cells (Figure 2-18) and the Ca^{2+} transient parameters peak amplitude (Figure 2-18C) and half peak decay time (Figure 2-18D) were quantified. The peak amplitudes were not significantly ($P > 0.05$) different between siRNA treatments, and were independent of CPA (Figure 2-18C). However, when PMCA1 was downregulated, the addition of CPA significantly ($P < 0.05$) delayed the half peak decay time compared with the other treatment combinations (Figure 2-18B and D). This suggests that SERCA activity may compensate for impaired PMCA1 Ca^{2+} efflux (siPMCA1) during PAR-induced Ca^{2+} signals.

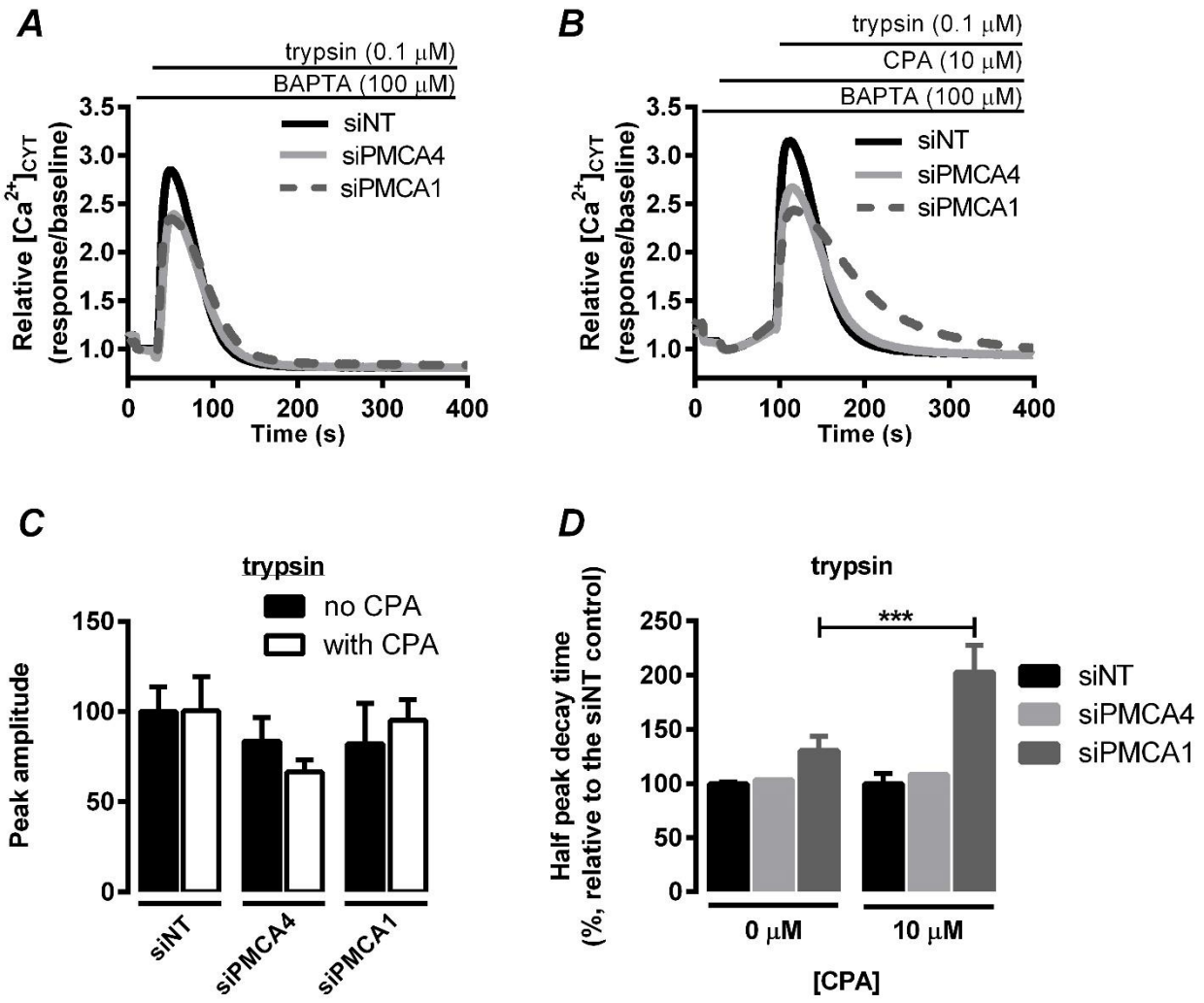

Figure 2-18: Effects of SERCA inhibition on trypsin-induced Ca^{2+} signals when PMCA1 or PMCA4 are silenced in MDA-MB-231 breast cancer cells.

Trypsin-mediated cytosolic [Ca^{2+}] transients were recorded using the Ca^{2+} indicator Fluo-4AM in siRNA-transfected MDA-MB-231 cells (siNT, siPMCA1 or siPMCA4) with extracellular BAPTA (100 μM) in nominal Ca^{2+}-free medium. Effects of PMCA1 or PMCA4 silencing on $[Ca^{2+}]_{CYT}$ increases in the **(A)** absence and **(B)** presence of the SERCA inhibitor CPA (10 μM). Bar graphs show the mean ± S.D for the **(C)** peak amplitude and **(D)** half peak decay time calculated in the absence or presence of CPA. Ca^{2+} traces represent relative mean fluorescence. All data were obtained from three independent experiments ($n = 3$) performed in triplicate. ***$P < 0.001$, two-way ANOVA, Bonferroni post-hoc analysis.

2.11.3.5 *Effect of CPA on PMCA1 or PMCA4 knockdown during GPCR-linked cytoplasmic free calcium increases associated with ATP in MDA-MB-231 breast cancer cells*

The potential for SERCA activity to compensate for PMCA1 or PMCA4 silencing was examined for ATP-induced Ca^{2+} signals (Figure 2-19). In the absence and presence of CPA, ATP-induced Ca^{2+} signals were recorded in siRNA-transfected MDA-MB-231 cells and the Ca^{2+} transient parameters peak amplitude (Figure 2-19C) and half peak decay time (Figure 2-19D) were quantified. ATP initiated a Ca^{2+} signal where the peak amplitude was not affected ($P > 0.05$) by the siRNA treatment or by the addition of CPA (Figure 2-19C). When PMCA1 was downregulated, the addition of CPA significantly ($P < 0.05$) delayed the half peak decay time compared with the treatment of siPMCA1 alone (Figure 2-19D). However, the magnitude of the effect by siPMCA1 was most pronounced ($P < 0.0001$) in the absence of CPA (Figure 2-19D). These results suggest, although SERCA contributes to $[Ca^{2+}]_{CYT}$ clearance, PMCA1 is the critical determinant of $[Ca^{2+}]_{CYT}$ clearance associated with ATP-mediated Ca^{2+} signals.

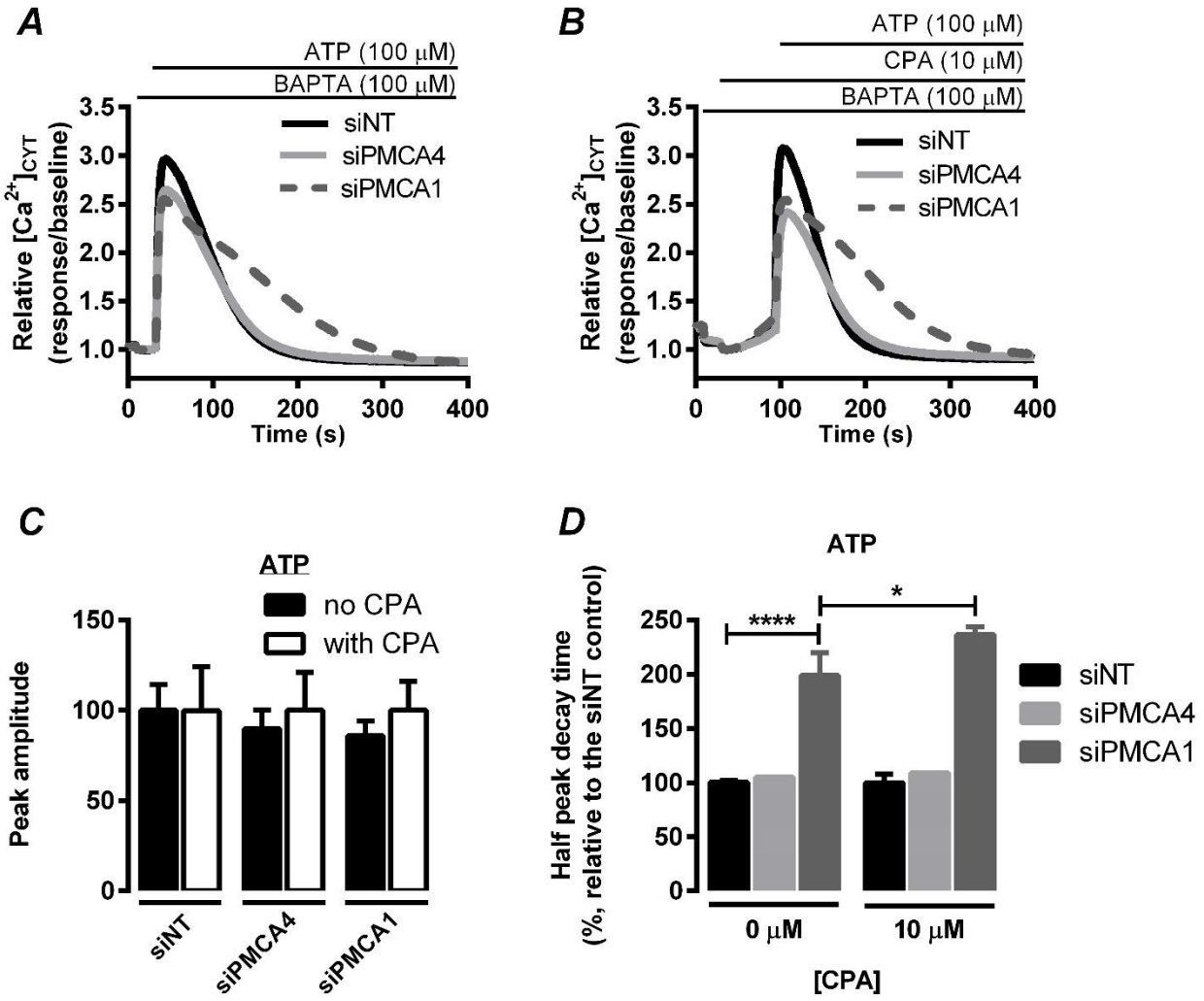

Figure 2-19: Effects of SERCA inhibition on ATP-induced Ca^{2+} signals when PMCA1 or PMCA4 are silenced in MDA-MB-231 breast cancer cells.

ATP-mediated cytosolic [Ca^{2+}] transients were recorded using the Ca^{2+} indicator Fluo-4AM in siRNA-transfected MDA-MB-231 cells (siNT, siPMCA1 or siPMCA4) with extracellular BAPTA (100 μM) in nominal Ca^{2+}-free medium. Effect of PMCA1 or PMCA4 silencing on $[Ca^{2+}]_{CYT}$ increases in the **(A)** absence and **(B)** presence of the SERCA inhibitor CPA (10 μM). Bar graphs show the mean ± S.D for the **(C)** peak amplitude and **(D)** half peak decay time calculated in the absence or presence of CPA. Ca^{2+} traces represent relative mean fluorescence. All data were obtained from three independent experiments (n = 3) performed in triplicate. *P < 0.05, **** P < 0.0001, two-way ANOVA, Bonferroni post-hoc analysis. BAPTA,

Data from sections 2.11.3.3 - 2.11.3.5 were collectively assessed using the three-way ANOVA analysis presented in Figure 2-20, which provides a statistical test for experiments with three factors. For these sets of experiments, the factors are siRNA treatment (siNT or siPMCA1), the presence of CPA and the GPCR activator (ATP or trypsin). Interpretation of this statistical test is outlined in dot points below for the reader's convenience.

- siPMCA1 significantly delayed the half peak decay time of the ATP Ca^{2+} response compared with the siNT control, indicating that Ca^{2+} efflux via PMCA1 is critical for ATP-induced $[Ca^{2+}]_{CYT}$ clearance.
- siPMCA1 did not have a significant effect on the half peak decay time of the trypsin Ca^{2+} response compared with the siNT control, suggesting that Ca^{2+} efflux via PMCA1 is not critical for trypsin-induced $[Ca^{2+}]_{CYT}$ clearance.
- When PMCA1 is silenced, CPA had a significant effect on the half peak decay time of the trypsin Ca^{2+} response compared with the control treatment siPMCA1 without CPA, suggesting that SERCA-mediated Ca^{2+} efflux compensates for PMCA1 silencing during PAR activation.
- When PMCA1 is silenced, CPA had no effect on the half peak decay time of the ATP Ca^{2+} response compared with the control treatment siPMCA1 without CPA. This data supports the view that SERCA-mediated Ca^{2+} efflux does not compensate for PMCA1 silencing during P2Y receptor activation.
- When PMCA1 is silenced, the effect of CPA on the half peak decay time was not significant between the GPCR activators, ATP and trypsin.

In summary, the data presented in sections 2.11.3.3 - 2.11.3.5 supports the hypothesis that the different GPCRs, PAR and P2Y can recruit specific Ca^{2+} clearance mechanisms to shape intracellular Ca^{2+} signals in MDA-MB-231 breast cancer cells. Mechanistically, this could involve second messenger pathways that couple differentially to P2Y *versus* PAR upon their activation with ATP and trypsin, respectively. The recruitment of PMCA pumps by GPCR signal transduction has been reported in neurons. ATP and bradykinin activate GPCR receptors and accelerate PMCA-mediated Ca^{2+} efflux by a PKC-dependent mechanism [87].

The ability of SERCA to compensate for PAR-induced, but not P2Y Ca^{2+} signals could involve spatial constraints, possibly via the PDZ binding domain of PMCA1. One report has demonstrated that PMCA1, but not PMCA4, rapidly translocates to the plasma membrane in HT-29 cells following muscarinic receptor activation [233]. PMCA1 translocation following activation of this GPCR depends on the PDZ-containing protein Na^+/H^+ exchanger regulatory factor 2 (NHERF), and

regulates the rate of Ca^{2+} efflux [233]. Perhaps a similar relationship between P2Y receptors and PMCA1 exists in MDA-MB-231 cells, and is functionally significant in regulating the rate of Ca^{2+} efflux associated with the ATP Ca^{2+} signal. Differential regulation of PMCA1-mediated Ca^{2+} efflux by different GPCR activators in MDA-MB-231 breast cancer cells requires further examination, in particular potential mechanisms (e.g. differential kinase mediated regulation of Ca^{2+}-ATPases and changes in plasma membrane PMCA1 expression).

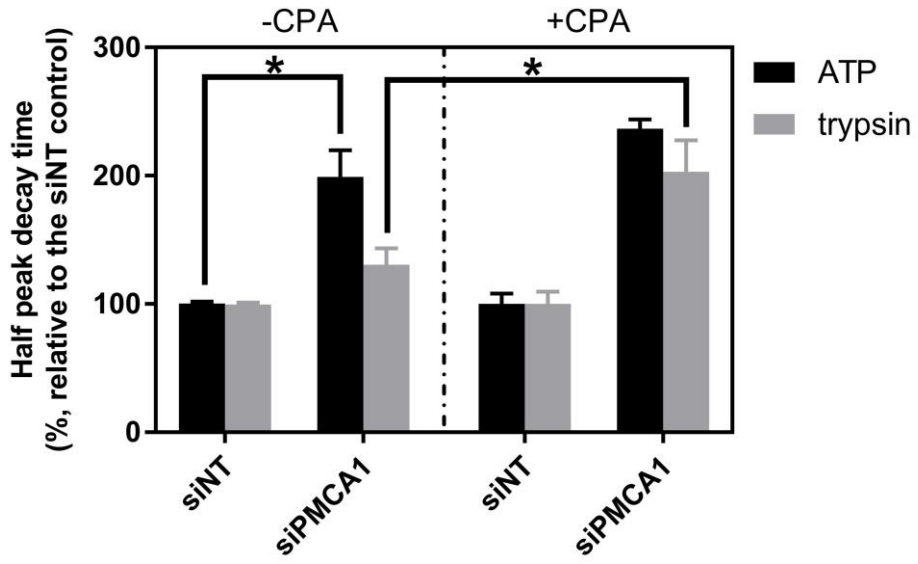

Figure 2-20: Effects of CPA-mediated SERCA inhibition on trypsin and ATP-induced Ca^{2+} signals in MDA-MB-231 breast cancer cells transfected with siNT or siPMCA1.

Bar graphs show the mean ± S.D for the half peak decay time All data were obtained from three independent experiments ($n = 3$) performed in triplicate. *$P < 0.05$, three-way ANOVA, Bonferroni post-hoc analysis.

2.11.3.6 Consequences of PMCA1 or PMCA4 knockdown on Ca^{2+} influx via receptor operated calcium entry evoked by ATP, trypsin in MDA-MB-231 breast cancer cells

The consequence of PMCA1 silencing on receptor operated calcium entry (ROCE) was assessed using the physiologically relevant GPCR activators trypsin (PAR-2) and ATP (P2Y) (Figure 2-21). This assay involved the re-addition of Ca^{2+} to delineate ROCE as described in other studies [174, 234]. Following the addition of ATP (Figure 2-21A) or trypsin (Figure 2-21D), the re-addition of extracellular Ca^{2+} stimulated a second phase of Ca^{2+} entry, and the effect of siPMCA1 or siPMCA4 on this second phase of Ca^{2+} entry was determined by assessment of the peak ratio derived by the calculation peak two amplitude divided by peak one amplitude [174, 234]. PMCA4 silencing was included in these sets of experiments, but had no effect ($P > 0.05$) on global $[Ca^{2+}]_{CYT}$ associated with either receptor-operated (section 2.11.3.6) or store-operated calcium entry (section 2.11.3.7); therefore the discussion of these results will focus on the PMCA1 isoform.

PMCA1 silencing, despite an increase ($P < 0.05$) in the area under the curve (Figure 2-21B), produced no significant effect ($P > 0.05$) on the peak ratio (Figure 2-21C) associated with ATP-induced ROCE. When trypsin was used to stimulate cells, PMCA1 silencing had no effect ($P < 0.05$) on the area under the curve (Figure 2-21E), yet significantly ($P < 0.05$) reduced the peak ratio (Figure 2-21F).

The meaning of these results are unclear, however, this data may be consistent with evidence presented in this thesis, where increased Ca^{2+} efflux via SERCA may compensate for PMCA1 silencing during trypsin-induced Ca^{2+} signals (section 2.11.3.4, page 85). In this context, the proposed increase in SERCA activity, analogous to SERCA overexpression in CHO cells [163], would be expected to increase $[Ca^{2+}]_{ER}$ levels. This increase in $[Ca^{2+}]_{ER}$ levels could be a crucial factor that alters the magnitude of ROCE during trypsin-mediated Ca^{2+} signals when PMCA1 is silenced (Figure 2-21D). Consistent with this idea, CPA-mediated inhibition of SERCA had no effect ($P > 0.05$) on ATP-induced Ca^{2+} signals when PMCA1 was silenced (section 2.11.3.5, page 87) and silencing the PMCA1 isoform produced no effect ($P > 0.05$) on ATP-mediated ROCE (Figure 2-21B). Future experiments, including those that directly monitor $[Ca^{2+}]_{ER}$ [235] are required to further investigate this hypothesis.

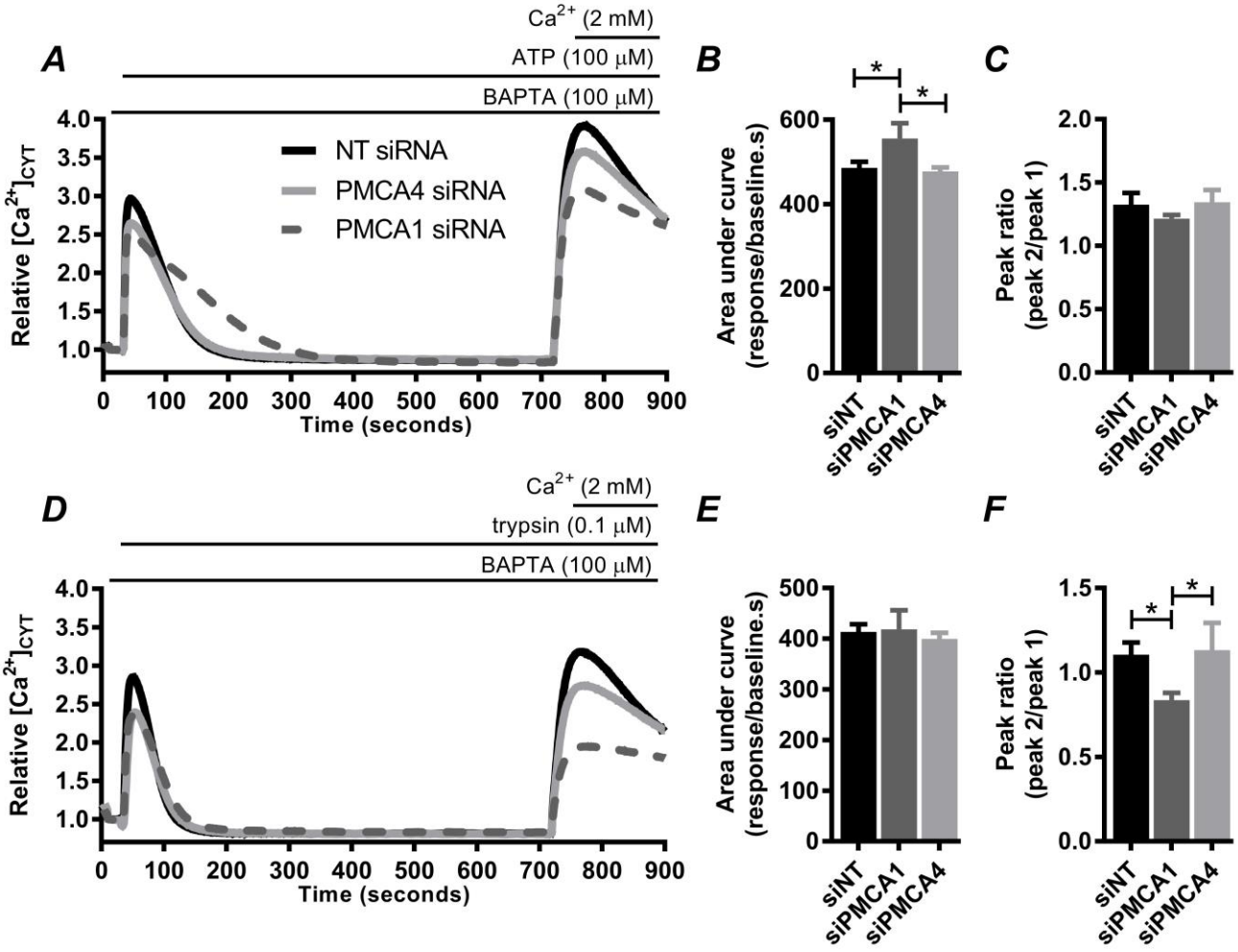

Figure 2-21: Effects of PMCA1 or PMCA4 silencing on receptor-operated Ca^{2+} entry in MDA-MB-231 breast cancer cells

(A) ATP and **(D)** trypsin-induced $[Ca^{2+}]_{CYT}$ signals were recorded in siRNA-transfected MDA-MB-231 cells (siNT, siPMCA1 or siPMCA4) using the Ca^{2+} indicator Fluo-4AM in nominal Ca^{2+}-free media in the presence of extracellular BAPTA (100 μM). After the initial $[Ca^{2+}]_{CYT}$ transients returned to baseline, the re-addition of Ca^{2+} stimulated a second phase of Ca^{2+} entry. Ca^{2+} traces represent relative mean fluorescence. Bar graphs show the mean ± S.D for the calcium transient parameters **(B and E)** peak 1 area under the curve, and the **(C and F)** peak ratio, derived from peak 2 amplitude divided by peak 1 amplitude for the Ca^{2+} signals stimulated by **(A-C)** 100 μM ATP, or **(D-E)** 0.1 μM trypsin. All data were obtained from three independent experiments (n = 3) performed in triplicate, *P < 0.05, repeated measures, one-way ANOVA, Bonferroni post-hoc analysis.

2.11.3.7 *Consequences of PMCA1 or PMCA4 knockdown on Ca^{2+} influx via store operated calcium entry in MDA-MB-231 breast cancer cells*

The consequence of siPMCA1 on CPA-mediated store-operated calcium entry (SOCE) was also assessed (Figure 2-22). As previously reported (section 2.8.2, page 47) siPMCA1 amplified the initial CPA-induced Ca^{2+} signal (Figure 2-22B). PMCA1 silencing, however, significantly ($P < 0.05$) attenuated the peak ratio associated with CPA-mediated SOCE (Figure 2-22C). This finding could be the consequence of the combination, SERCA inhibition *plus* impaired PMCA1-mediated Ca^{2+} efflux *plus* a sustained $[Ca^{2+}]_{CYT}$ increase, all of which could reduce SOCE via a negative feedback mechanism to prevent intracellular Ca^{2+} toxicity. A functional interaction between PMCAs and SOCE has been reported in primary human aortic myocytes [236]. Orai1 silencing downregulated the Ca^{2+} efflux mechanisms, PMCA1 and NCX1, and this increased the initial CPA-mediated Ca^{2+} signal, but attenuated SOCE mediated by CPA [236].

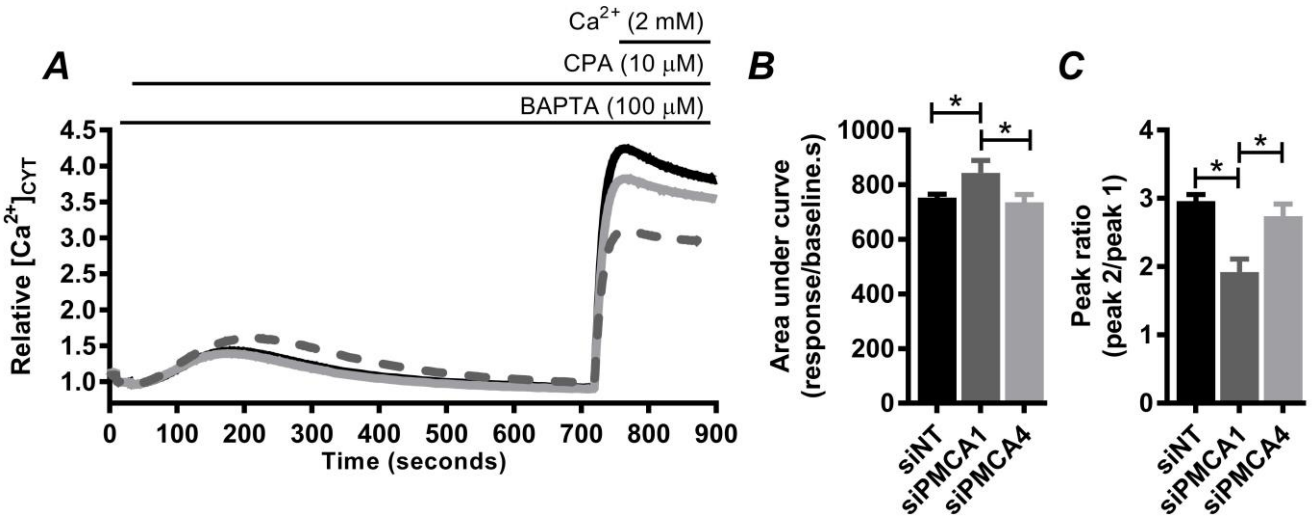

Figure 2-22: Effects of PMCA1 or PMCA4 silencing on store-operated Ca^{2+} entry in MDA-MB-231 breast cancer cells

(A) Average CPA-induced $[Ca^{2+}]_{CYT}$ signals were recorded in siRNA-transfected MDA-MB-231 cells (siNT, siPMCA1 or siPMCA4) using the Ca^{2+} indicator Fluo-4AM in nominal Ca^{2+}-free media in the presence of extracellular BAPTA (100 μM). After the initial $[Ca^{2+}]_{CYT}$ transients returned to baseline, the re-addition of Ca^{2+} stimulated a second phase of Ca^{2+} entry. Bar graphs show the mean ± S.D for the calcium transient parameters **(B)** peak 1 area under the curve, and the **(C)** peak ratio derived from peak 2 amplitude divided by peak 1 amplitude. All data were obtained from three independent experiments (n = 3) performed in triplicate, *P < 0.05, repeated measures, one-way ANOVA, Bonferroni post-hoc analysis.

2.12 Chapter Summary

The work presented in this chapter demonstrates in the MDA-MB-231 breast cancer cell line, that as a consequence of isoform-specific knockdown, PMCA1 and PMCA4 have distinct roles in the regulation of global calcium signals and in the regulation of caspase-dependent and independent cell death. The data presented supports a major role for PMCA1 in the regulation of global calcium signals and in the promotion of caspase-independent (necrotic) cell death evoked by the calcium ionophore ionomycin, with no effect detected on the sensitivity of caspase-dependent (apoptosis) cell death induced by ABT-263. In contrast, this study indicates that PMCA4 is not a key regulator of global calcium signals, with modest effects in the augmentation of ionomycin-induced cell death detected when compared to PMCA1. However, PMCA4 promoted caspase-dependent (apoptosis) cell death mediated by ABT-263. In addition, a novel interaction between NFκB and PMCA4 was identified that may underpin the effects of PMCA4 siRNA-mediated promotion in ABT-263-induced cell death. The supplementary data reports the consequence of PMCA1 or PMCA4 silencing in the regulation of ceramide and staurosporine-induced cell death. Although statistically significant effects upon isoform-specific knockdown of PMCA1 and PMCA4 were detected, these effects were modest at the time point examined. Work in the supplementary section of this chapter has also begun to explore a potential complex activator and isoform dependent regulation of PMCAs in MDA-MB-231 breast cancer cells that should be the focus of future studies. In conclusion, this study supports a major "housekeeping: role for PMCA1 in global calcium signals and a role for PMCA4 in the regulation of calcium-dependent signal transduction pathways, highlighting the anti-tumour potential of PMCA4 silencing and/or pharmacological inhibition. The following chapter will investigate the significance of another PMCA isoform expressed in the MDA-MB-231 breast cancer cell line, PMCA2.

3.1 Preface

The previous chapter demonstrated that PMCA isoforms have distinct effects on cell death pathways in breast cancer cells. PMCA4 silencing, but not PMCA1 silencing, promoted caspase-dependent cell death initiated by Bcl-2 inhibition using ABT-263 (Navitoclax). Continuing along this theme, the current chapter evaluates the effect of another calcium pump isoform, PMCA2 on breast cancer cell death.

Despite aberrant PMCA2 overexpression in human breast cancer cell lines and in clinical breast cancer samples [178, 183, 184], the functional consequence of PMCA2 silencing on ABT-263-mediated cell death is not known. Although very recent silencing studies in breast cancer cell lines find that PMCA2 reduces proliferation [183], PMCA2 silencing-mediated effects on cell death have focused on the Ca^{2+} ionophore ionomycin [182, 184]. The ability of PMCA2 silencing to augment other death stimuli, of more therapeutic relevance such as Bcl-2 inhibitors has not been examined [237, 238]. In this chapter, PMCA2 silencing-mediated effects on global [Ca^{2+}] and on cell death initiated with numerous agents including ABT-263 was assessed.

A manuscript, entitled 'PMCA2 silencing potentiates MDA-MB-231 breast cancer cell death initiated with the Bcl-2 inhibitor ABT-263' was prepared and submitted to the Journal Biochemical and Biophysical Research Communications. The manuscript presents novel research findings that were predominantly designed and performed by myself under the supervision of Gregory R Monteith and Sarah J Roberts-Thomson and is incorporated into this thesis chapter. Adjustments have been made to the format of this draft manuscript to comply with The University of Queensland thesis formatting guidelines.

3.2 Chapter Hypothesis

- PMCA2 silencing sensitises MDA-MB-231 breast cancer cells to cell death responses by processing calcium signals

3.3 Chapter Aims

- To investigate the functional significance of PMCA2 upregulation in the context of basal breast cancer using the MDA-MB-231 breast cancer cell line
- To inhibit PMCA2 using specific siRNAs to silence expression of the ATB2B gene
- To study the consequence of PMCA2 silencing on cell death initiated with ionomycin and other agents (ABT-263, ceramide and staurosporine)
- To assess PMCA2 silencing-mediated effects in shaping bulk $[Ca^{2+}]_{CYT}$ increases evoked by ATP, trypsin, ionomycin, and CPA

3.4 Highlights

- PMCA2 silencing can augment ionomycin-mediated cell death
- Global cytoplasmic calcium signals were not markedly altered by PMCA2 silencing
- PMCA2 silencing sensitised cells to apoptotic cell death initiated with ABT-263
- PMCA2 inhibitors may potentiate anti-cancer drugs that block Bcl-2 activity

3.5 Abstract

PMCA2 overexpression in some breast cancers suggests that this calcium pump isoform may play a role in breast pathophysiology. To investigate PMCA2 as a potential drug target for breast cancer therapy, we assessed the functional consequence of PMCA2 silencing on cell death pathways and calcium signals in the basal-like MDA-MB-231 breast cancer cell line. Silencing PMCA2 expression alone has no effect on MDA-MB-231 cell viability, however, PMCA2 silencing promotes calcium-induced cell death initiated with the calcium ionophore ionomycin. Assessment of cytoplasmic calcium responses generated with various agents including ionomycin demonstrates that in MDA-MB-231 cells, PMCA2 does not play a major role in shaping global calcium signals. We also examined the ability of PMCA2 silencing to modulate caspase-dependent cell death triggered by a Bcl-2 inhibitor that is in clinical development for the treatment of various cancers, ABT-263 (Navitoclax). Despite the lack of effect on global calcium responses, PMCA2 silencing augmented Bcl-2 inhibitor (ABT-263)-mediated MDA-MB-231 breast cancer cell death. These studies provide evidence that PMCA2 inhibitors could sensitise PMCA2-positive breast cancers to cell death initiators that work through mechanisms involving the Bcl-2 survival pathway.

3.6 Introduction

The calcium efflux pump, plasma membrane calcium ATPase (PMCA) isoform 2 has been proposed as potential target for the treatment of some breast cancers [239]. Aberrant overexpression of PMCA2 in some breast cancer cell lines [178] and the positive correlation between PMCA2 protein expression and tumor characteristics including tumor grade and HER2 status in clinical breast cancer cases [182] suggests that PMCA2 could facilitate disease progression [182]. More recently, PMCA2 mRNA levels were assessed in breast cancers grouped by molecular subtype [183]. PMCA2 mRNA was higher in basal breast cancers compared to HER2, luminal A and luminal B subtypes [183]. Although a feature of some breast cancers, only a few studies have evaluated the functional significance of PMCA2 upregulation in the context of cell death in breast cancer; and detailed assessment of PMCA2 through overexpression or silencing techniques has been limited to luminal-like breast cancer cell lines that express at least one hormone receptor (oestrogen or progesterone receptors) or those with HER2 amplification [182, 184]. Heterologous PMCA2 expression in T47D cells attenuates global cytosolic free Ca^{2+} levels ($[Ca^{2+}]_{CYT}$) and protects T47D cells from calcium-induced cell death initiated with ionomycin [182]. Assessment of PMCA2 silencing in the context of HER2 positive breast cancers has been examined in the SKBR3 and BT474 breast cancer cell lines [184], both of which are positive for HER2 amplification [240]. PMCA2 knockdown in SKBR3 promotes ionomycin cell death and downregulates HER2 signaling [184].

Until recently the consequence of PMCA2 silencing in a basal-like breast cancer cell line had not been evaluated. One cell line widely used as a model for basal breast cancer subtypes, which overlaps with breast cancers that are negative for hormone receptor expression and HER2 amplification is the MDA-MB-231 breast cancer cell line [240]. Studies in this cell line demonstrate PMCA2 silencing attenuates proliferation and potentiates the anti-proliferative action of low concentrations of the cytotoxic doxorubicin [183]. Since neither PMCA1 nor PMCA4 silencing produced effects on cell proliferation, PMCA-mediated regulation of MDA-MB-231 cell growth appears to be PMCA2 specific in this breast cancer cell line. This and other studies emphasize that PMCA isoforms are functionally distinct, even when expressed in the same cell type.

PMCA2 silencing-mediated effects on breast cancer cell death have focused on ionomycin [184], which can trigger cell death through sustained $[Ca^{2+}]_{CYT}$ increases of high magnitude [6, 184, 227]. The consequence of PMCA2 knockdown on B-cell lymphoma-2 (Bcl-2) inhibitor-mediated apoptosis has not been assessed. Bcl-2 is a pro-survival oncogene overexpressed in 75% of breast cancers [237]. ABT-263 (Navitoclax) is a Bcl-2 inhibitor undergoing clinical trial assessment for various cancer indications including lymphoma, prostate and colon cancer [238]. Studies of PMCA knockdown-

mediated effects on Bcl-2 inhibitor (ABT-263)-induced apoptosis have only so far been examined for PMCA1 and PMCA4 isoforms [227]. PMCA1 regulates global $[Ca^{2+}]_{CYT}$ signals, however, PMCA1 knockdown had no effect on Bcl-2 inhibitor-mediated cell death [227]. Whereas, PMCA4 silencing promoted apoptosis in MDA-MB-231 cells initiated with the Bcl-2 inhibitor ABT-263, without significant effects on global calcium signals [227]. Isoform-specific PMCA knockdown in MDA-MB-231 cells produces very different outcomes on $[Ca^{2+}]_{CYT}$, and on the cancer-relevant pathways proliferation and apoptosis. However, the consequence of PMCA2 silencing on Bcl-2 inhibitor-mediated cell death has not been evaluated.

In this current study, we examined the effects of PMCA2 silencing in MDA-MB-231 breast cancer cells on global calcium signals and in the modulation of cell death initiated with ionomycin and the Bcl-2 inhibitor ABT-263. Our findings suggest that PMCA2 inhibitors, in combination with anti-cancer agents that work through the Bcl-2 pathway, could be effective for the treatment of PMCA2-positive breast cancers; including breast cancer cases that are typically unresponsive to targeted therapies such as those targeting HER2 (e.g. trastuzumab) and the oestrogen receptor (e.g. tamoxifen) [167, 170].

3.7 Material and Methods

3.7.1 Cell culture

Human MDA-MB- 231 breast cancer cells (American Type Culture Collection, Rockville, MD, USA) were maintained in high glucose DMEM (D6546, Sigma Aldrich, St Louis, MO, USA) containing 10% fetal bovine serum and 4 mM L-glutamine (25030081, Invitrogen, Carlsbad, CA, USA) at 37°C/5% CO_2 in a humidified air incubator. All cultures were periodically screened for mycoplasma infection.

3.7.2 RNA interference

PMCA2 levels were downregulated in MDA-MB-231 cells according to methods previously described [183, 227] using ON-TARGET*plus*™ Human SMARTpool siRNAs (Thermo Scientific, Waltham, MA, USA). These siRNAs consist of four pooled sequences rationally designed to minimise off-target effects [195, 196, 241]. The ON-TARGET*plus*™ Human SMARTpool siRNA sequences used were PMCA2 (siPMCA2, L-006116-00) and the non-targeting control siRNA (siNT, D-001810-10). For all experiments knockdown of PMCA2 (>70%) was confirmed by real time RT-PCR at 120 h post-siRNA transfection.

3.7.3 Real time RT-PCR

At 48 h or 120 h post-siRNA transfection quantitative real time RT-PCR was performed as previously reported [227]. Total RNA was isolated (74134, RNeasy Plus mini kit; Qiagen, Hilden, Germany) and then reverse transcribed (205111, Omniscript RT kit; Qiagen). The target cDNAs were amplified using the TaqMan Fast Universal PCR Master Mix (4352043, Applied Biosystems, Carlsbad, CA, USA) and TaqMan Gene Expression assays (PMCA2, Hs00155975_m1 and 18S rRNA, 4319413E; Applied Biosystems) under universal cycling conditions with a StepOnePlus real time PCR system (Applied Biosystems). Target mRNA levels were quantified by the comparative C*t* method as described previously [197], normalising to 18S rRNA.

3.7.4 Cytoplasmic free calcium measurements

At 120 h post-siRNA transfection, media was removed from MDA-MB-231 cells and replaced with culture medium containing Fluo-4 AM (4 μM; Molecular Probes, Eugene, OR, USA) or Fluo-4FF AM (4 μM; Molecular Probes). Using these Ca^{2+} indicators changes in $[Ca^{2+}]_{CYT}$ were recorded using a fluorescence imaging plate reader [198] ($FLIPR^{TETRA}$, Molecular Devices, Sunnyvale, CA, USA) as previously described [227]. To assess relative $[Ca^{2+}]_{CYT}$, fluorescence values were normalised to initial baseline values.

3.7.5 Assessment of cell viability

MDA-MB-231 cells were siRNA-transfected for 72 h, and then treated for an additional 48 h with ionomycin (Enzo Life Sciences, Farmingdale, NY, USA), ABT-263 (S1001, Selleckchem, Houston, TX, USA), or dimethyl sulfoxide (up to 0.33%). Cells were then stained with Hoechst 33342 (10 μg/mL; H3570, Invitrogen) and propidium iodide (1 μg/mL; P3566, Invitrogen) at 37°C for 15 min and cell death assessed using an ImageXpress micro automated epifluorescence microscope (Molecular Devices Corporation) and the multi-wavelength cell scoring application module (MetaXpress v3.1.0.83; Molecular Devices) as previously described [227]. Cell viability was determined by combining propidium iodide positive cells and those identified as apoptotic to calculate the total number of dead cells [227].

3.7.6 Statistical analysis

All statistical tests were performed as described in the figure legends using GraphPad Prism (version 6.07) for Windows (GraphPad Software, Inc., La Jolla, CA, USA).

3.8 Results

3.8.1 PMCA2 silencing and consequences on MDA-MB-231 breast cancer cell viability in the absence and presence of the calcium ionophore ionomycin

To explore the functional significance of PMCA2 in a basal like breast cancer cell line, we silenced PMCA2 gene expression in MDA-MB-231 cells. Non-targeting (siNT) and PMCA2 (siPMCA2) siRNAs were transfected into MDA-MB-231 cells and PMCA2 silencing was confirmed by mRNA analysis. Cells transfected with siPMCA2 showed a significant ($P < 0.05$) downregulation in PMCA2 mRNA, at both time points 48 h and 120 h post-transfection, compared with siNT controls (Figure 3-1A).

Using this model, we assessed siPMCA2-mediated regulation of cell viability. With no stimulus, PMCA2 silencing had no effect on MDA-MB-231 cell viability compared with the siNT control (Figure 3-1B and C). However, in the presence of sub-maximum (3 μM) ionomycin, siPMCA2 significantly ($P < 0.05$) reduced cell viability compared to the siNT control (Figure 3-1C). No measurable effect ($P > 0.05$) on cell viability was detected at the maximum (10 μM) ionomycin concentration, comparing siPMCA2 with the siNT control (Figure 3-1C). These findings suggest that PMCA2 silencing without a stimulus does not trigger cell death, although, siPMCA2 can modestly promote Ca^{2+}-induced MDA-MB-231 cell death initiated by sub-maximal concentrations of ionomycin.

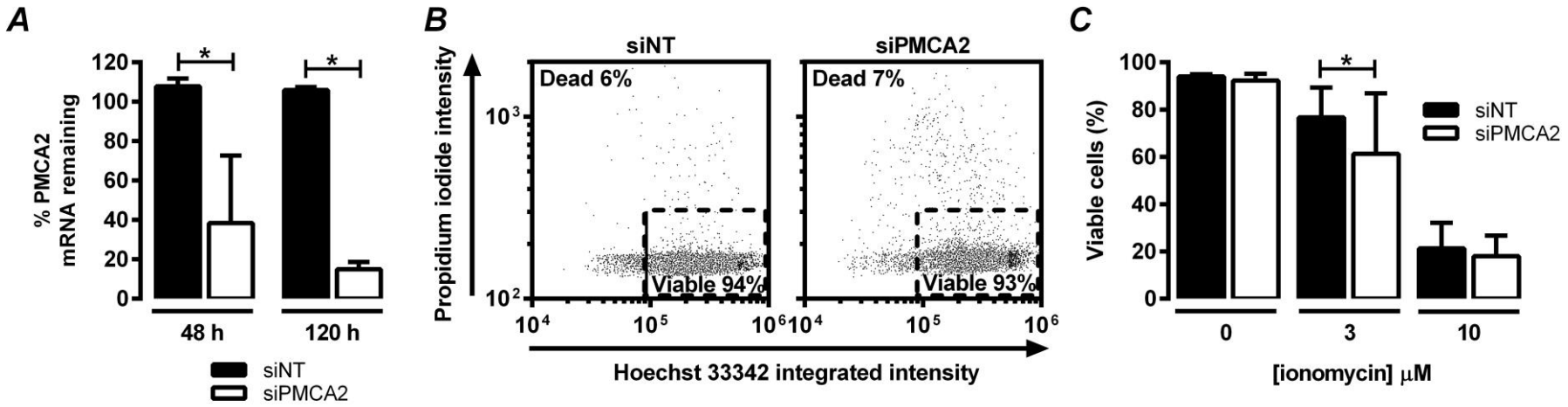

Figure 3-1 PMCA2 silencing in MDA-MB-231 breast cancer cells and the consequence of silencing on cell viability and ionomycin-induced cell death.

PMCA2 silencing in MDA-MB-231 breast cancer cells and the consequence of silencing on cell viability and ionomycin-induced cell death. PMCA2 expression was silenced using siRNA and then cell viability assessed in the absence and presence of the calcium ionophore ionomycin, comparing siPMCA2 with the siNT control. **(A)** PMCA2 mRNA levels 48 h and 120 h post-siRNA, **P* < 0.05, two-way ANOVA, Bonferroni post hoc analysis. **(B)** Representative dot plots show cell viability with siNT and siPMCA2. Dot plots are Hoechst 33342 and propidium iodide fluorescence measured in random cells (10 000 cells/dot plot) selected from three experiments (*n* = 3). **(C)** Cell viability following siNT and siPMCA2 transfection, either in the absence (0 μM) or presence of ionomycin (3 μM or 10 μM). **P* < 0.05, repeated-measures, two-way ANOVA, Bonferroni post hoc analysis. All bar graphs show mean ± S.D obtained from three independent experiments (*n* = 3), performed in duplicate or triplicate wells.

3.8.2 Effects of PMCA2 silencing on ionomycin-induced cytoplasmic calcium signals in MDA-MB-231 cells

To further evaluate the relationship between PMCA2 and ionomycin, high magnitude $[Ca^{2+}]_{CYT}$ signals generated using ionomycin were measured in siRNA-transfected MDA-MB-231 cells using the low affinity Ca^{2+} indicator Fluo-4FF AM, in the presence of extracellular calcium. As reflected by assessment of the calcium transient parameter, area under the curve (Figure 3-2B and D), calcium signals at sub-maximum (3 μM; Figure 3-2A and B) and maximum (10 μM; Figure 3-2C and D) ionomycin concentrations were not significantly ($P > 0.05$) altered by PMCA2 silencing, compared with the siNT controls. These data indicate that siPMCA2 does not elicit profound effects on $[Ca^{2+}]_{CYT}$ signals generated with ionomycin in MDA-MB-231 breast cancer cells.

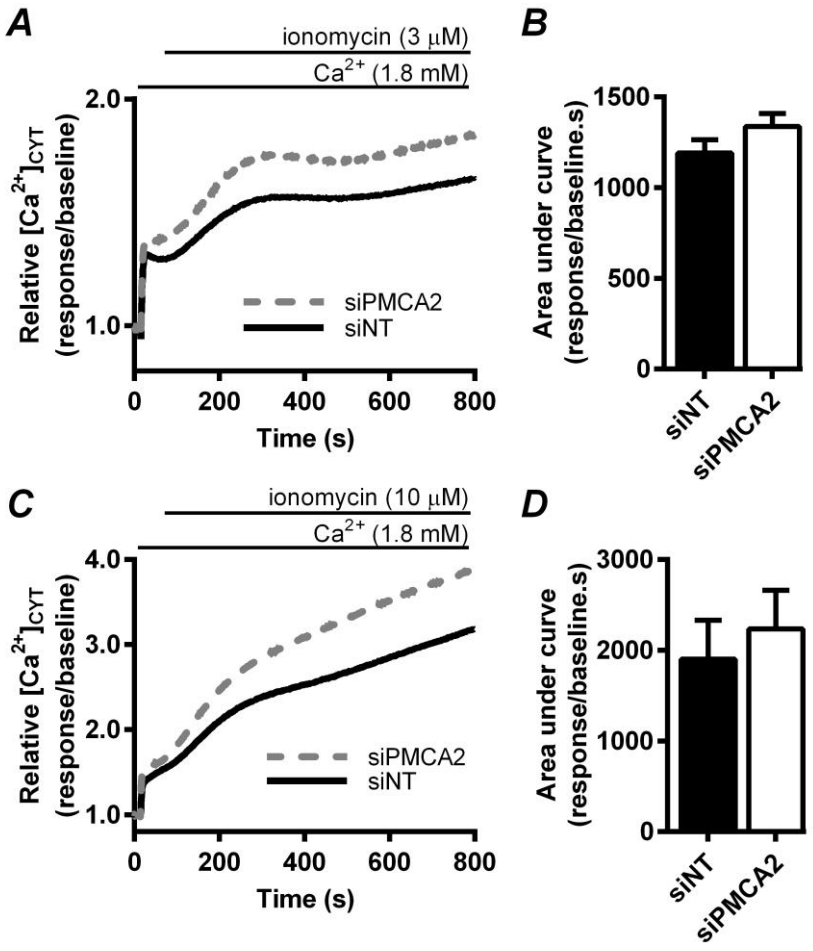

Figure 3-2. Effect of PMCA2 silencing on ionomycin-induced calcium signals in MDA-MB-231 breast cancer cells.

$[Ca^{2+}]_{CYT}$ signals generated with the calcium ionophore ionomycin at **(A)** 3 μM and **(C)** 10 μM were recorded in cells transfected with siPMCA2 or siNT. Calcium traces depict mean relative $[Ca^{2+}]_{CYT}$ fluorescence. Area under the curve for the **(B)** 3 μM and **(D)** 10 μM ionomycin Ca^{2+} signals. Bar graphs are mean ± S.D, unpaired two-tailed student's *t* test. All data were pooled from three independent experiments (n = 3), performed in triplicate wells.

3.8.3 Consequences of PMCA2 silencing on CPA, ATP and trypsin induced calcium signals in MDA-MB-231 breast cancer cells

The potential of PMCA2 to shape bulk $[Ca^{2+}]_{CYT}$ increases of more moderate magnitudes was also examined using the high affinity Ca^{2+} indicator Fluo-4 AM. In siRNA-transfected MDA-MB-231 cells, $[Ca^{2+}]_{CYT}$ signals were monitored in the presence of the Ca^{2+} chelator BAPTA (100 μM) in nominal free Ca^{2+} physiological salt solution, following the addition of the sarco/endoplasmic reticulum Ca^{2+} ATPase (SERCA) inhibitor cyclopiazonic acid (CPA, 10 μM, Figure 3-3A), the purinergic receptor agonist ATP (100 μM, Figure 3-3D) or the protease activated receptor activator trypsin (0.1 μM, Figure 3-3G). Assessment of the calcium transient parameters, half peak decay time (Figure 3-3B, E and H) and area under the curve (Figure 3-3C, F and I) demonstrated that compared with the siNT control, PMCA2 silencing did not significantly ($P > 0.05$) shape Ca^{2+} responses associated with either CPA (Figure 3-3B and C), ATP (Figure 3-3E and F), or trypsin (Figure 3-3H and I). These data support the conclusion that PMCA2 in MDA-MB-231 cells is not a key regulator of bulk $[Ca^{2+}]_{CYT}$ signals.

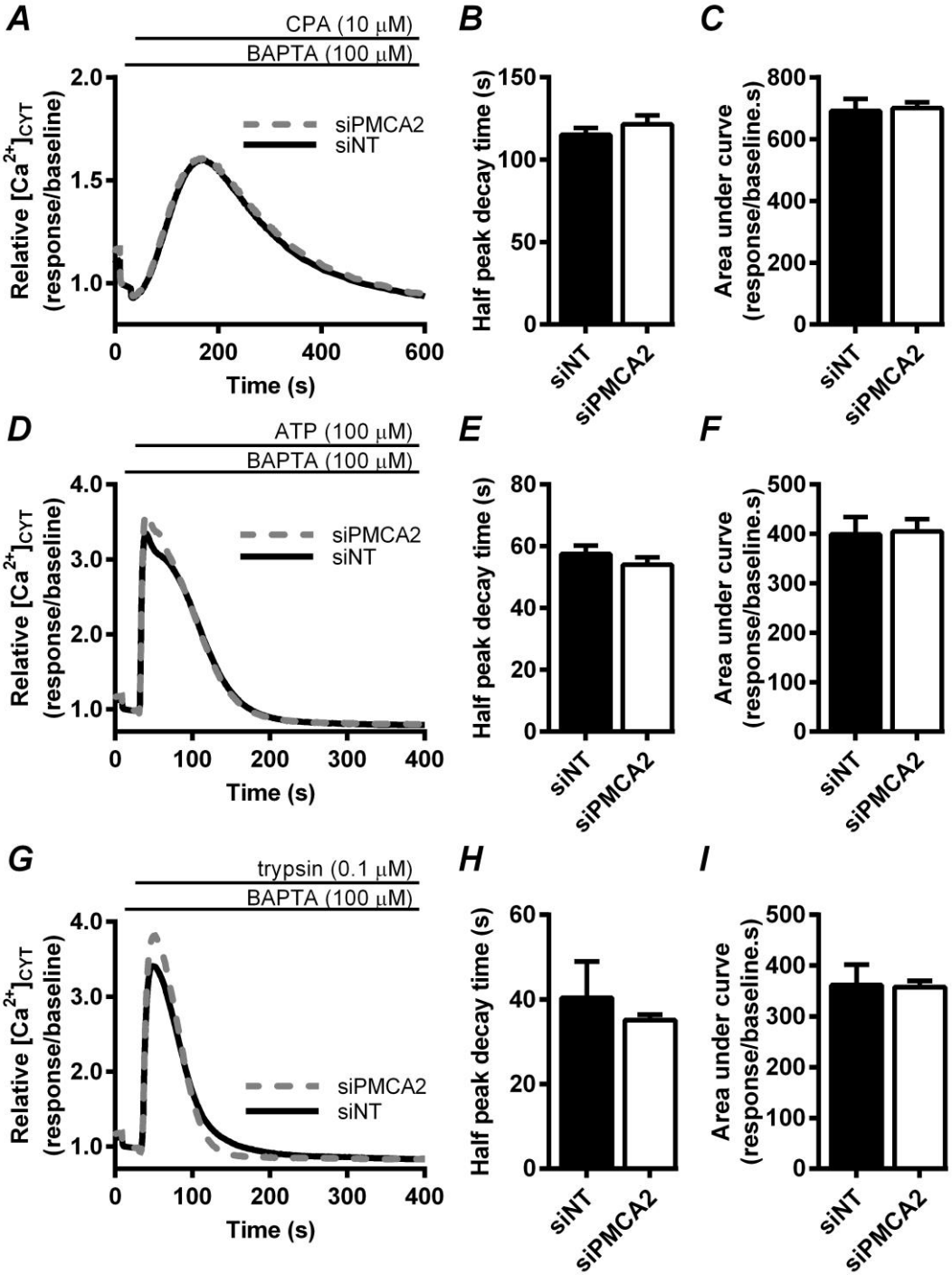
A
CPA (10 μM)
BAPTA (100 μM)
siPMCA2
siNT
Relative [Ca2+]CYT (response/baseline)
Time (s)
B
Half peak decay time (s)
siNT
siPMCA2
C
Area under curve (response/baseline.s)
siNT
siPMCA2
D
ATP (100 μM)
BAPTA (100 μM)
siPMCA2
siNT
Relative [Ca2+]CYT (response/baseline)
Time (s)
E
Half peak decay time (s)
siNT
siPMCA2
F
Area under curve (response/baseline.s)
siNT
siPMCA2
G
trypsin (0.1 μM)
BAPTA (100 μM)
siPMCA2
siNT
Relative [Ca2+]CYT (response/baseline)
Time (s)
H
Half peak decay time (s)
siNT
siPMCA2
I
Area under curve (response/baseline.s)
siNT
siPMCA2

Figure 3-3: Effect of PMCA2 silencing on various agents that increase global cytoplasmic free calcium.

siRNA-transfected MDA-MB-231 breast cancer cells were treated with the calcium mobilising agents **(A)** CPA (10 μM), **(D)** ATP (100 μM), and **(G)** trypsin (0.1 μM) in the presence of extracellular BAPTA (100 μM) in nominal free Ca^{2+}. Calcium traces depict mean relative $[Ca^{2+}]_{CYT}$. Half peak decay time calculated for the **(B)** CPA, **(E)** ATP and **(H)** trypsin Ca^{2+} responses. Area under the curve calculated for the **(C)** CPA, **(F)** ATP and **(I)** trypsin responses. Bar graphs quantitate calcium transient parameters as mean ± S.D. **P* < 0.05, unpaired two-tailed student's *t* test. All data were pooled from three independent experiments (*n* = 3), performed in triplicate wells.

3.8.4 Regulation of ABT-263-mediated cell death by PMCA2 silencing in MDA-MB-231 cells

PMCA4 potentiates caspase-dependent cell death, initiated with the Bcl-2 inhibitor ABT-263 in MDA-MB-231 cells [227]. We therefore investigated whether PMCA2 silencing modulates ABT-263-mediated death responses. At 1 µM, ABT-263-mediated cell death was almost doubled by knocking down PMCA2 (mean ± S.D.; 36 ± 11% for the siNT control *versus* 68 ± 5% for siPMCA2; Figure 3-4A and B). To characterise this effect, cell viability was measured in siRNA-transfected MDA-MB-231 cells, treated at increasing concentrations of the Bcl-2 inhibitor ABT-263 (0.1 – 10 µM; Figure 3-4C). Compared to the siNT control, siPMCA2 significantly ($P < 0.05$) reduced cell viability in the presence of ABT-263. This was evidenced by a 4.5-fold leftward shift in the half maximal inhibitory concentration (IC_{50}), from 2.2 µM for siNT *versus* 0.48 µM for siPMCA2. These data show that PMCA2 silencing sensitises the MDA-MB-231 cell line to caspase-dependent ABT-263-mediated cell apoptosis.

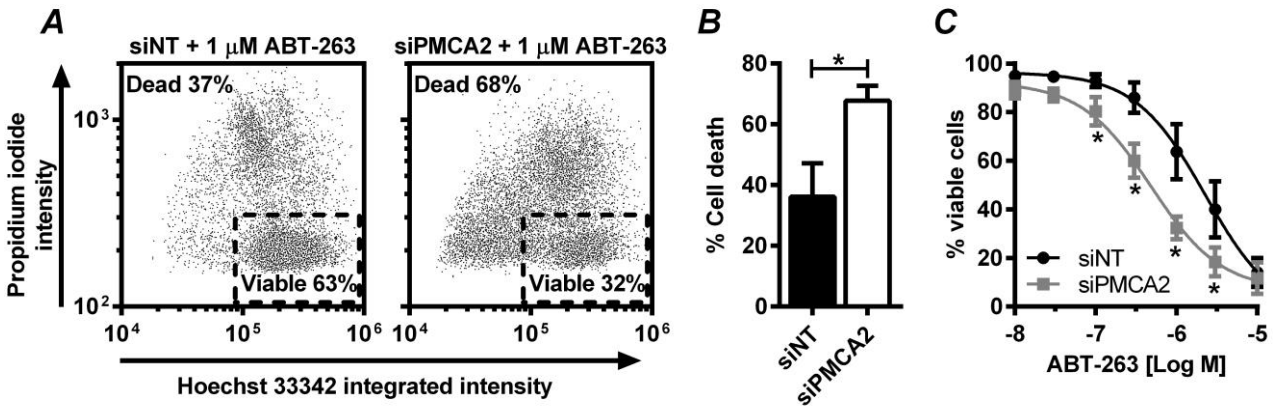

Figure 3-4: Effects of PMCA2 silencing of MDA-MB-231 breast cancer cell death initiated by the Bcl-2 inhibitor ABT-263.

(A) Representative dot plots are Hoechst 33342 and propidium iodide fluorescence detected in cells transfected with siNT or siPMCA2 and treated with 1 μM ABT-263. Dot plots show an equal cell number (10,000 cells/dot plot), randomly selected from three independent experiments (n = 3). **(B)** Effect of siPMCA2 and siNT on cell death at 1 μM ABT-263. Bar graph shows mean ± S.D, *P < 0.05, paired two-tailed student's t test **(C)** Concentration-response curves show the effect of siNT and siPMCA2 on cell death initiated at various ABT-263 concentrations (0.01 – 10 μM). Values plotted are mean ± S.D, *P < 0.05, siNT compared to siPMCA2 at the indicated ABT-263 concentration, repeated measures, two-way ANOVA, Bonferroni post hoc test. Data were obtained from three independent experiments (n = 3), performed in triplicate wells.

3.9 Discussion

This report extends previous studies of PMCA1 and PMCA4 in MDA-MB-231 breast cancer cells [227], and evaluated PMCA2-mediated effects on cell death and calcium signaling in this cell line using targeted siRNAs to silence PMCA2 gene expression. Initial experiments showed that PMCA2 silencing alone does not alter MDA-MB-231 cell viability. Since PMCA isoforms are known regulators of calcium-induced cell death [182, 184, 227], we assessed the consequence of PMCA2 silencing on ionomycin death responses. Our results indicated that PMCA2 silencing modestly promoted ionomycin MDA-MB-231 cell death at submaximal concentrations. This is consistent with other studies that demonstrate through overexpression or downregulation systems, that PMCA2 modulates ionomycin cell death in the T47D and SK-Br-3 breast cancer cell lines [182, 184].

We found that PMCA2 is not a key regulator of global $[Ca^{2+}]_{CYT}$ signals generated with ionomycin, or those associated with physiologically relevant mediators ATP and trypsin, which increase $[Ca^{2+}]_{CYT}$ via G protein-coupled receptor activation. This result may be surprising, however, not entirely unexpected because PMCA2 expression is relatively low in MDA-MB-231 cells compared with other isoforms [183]. PMCA1, which is the predominate isoform expressed in MDA-MB-231 cells, when knocked down has a pronounced effect on the shape of global $[Ca^{2+}]_{CYT}$ signals generated with many stimuli [183, 227].

Although reported for PMCA1 and PMCA4 [227], PMCA2-mediated regulation of Bcl-2 inhibitor-mediated cell death has not been previously examined. Our data demonstrated that despite no significant effects on global calcium signaling, PMCA2 silencing augmented ABT-263-mediated MDA-MB-231 cell death. This finding is analogous to PMCA4, where knocking down PMCA4 sensitised MDA-MB-231 cells to ABT-263 initiated cell death, independent of global calcium [227]. While PMCA4 and PMCA2 distinctly regulate cell proliferation [183], these isoforms appear to have related effects on the Bcl-2 survival pathway.

Growing evidence indicates that PMCA isoforms regulate calcium-dependent signal transduction through protein-protein interactions, and fine-tuning of localised calcium signals [183, 187, 221, 227, 242]. The ability for PMCA2 silencing to promote ABT-263-mediated cell death, is likely the result of disrupting pro-survival protein-protein interactions through processing localised calcium signals. PMCA2 interacts with the calcium-dependent signaling molecule calcineurin, and this interaction can regulate cell death [186, 243]. Preventing the interaction between PMCA2 and calciuneurin, upregulates pro-apoptotic protein expression via the nuclear factor of activated T cell (NFAT) transcriptional pathway [243]. This intervention reduces cell viability across a panel of breast cancer

cell lines, and enhances paclitaxel-induced cytotoxicity in MCF-7 and ZR-75-1 breast cancer cells [243]. PMCA2-mediated regulation of the Bcl-2 survival pathway may also involve another calcium-dependent transcription factor nuclear factor-kappa B (NFκB). We previously demonstrated that PMCA4 silencing inhibits NFκB nuclear translocation, and that pharmacological inhibition of NFκB phenocopies the promotion of ABT-263-mediated cell death produced by PMCA4 silencing [227]. Mechanistic studies are now required to clarify the importance of the calcineurin/NFAT and/or NFκB transcription factor pathways in the promotion of Bcl-2 inhibitor cell death produced by PMCA2 silencing in MDA-MB-231 breast cancer cells.

In conclusion, this study provides further evidence supporting the view that PMCA2 inhibitors may be a novel treatment for PMCA2-positive breast cancers. This approach may be most effective in basal-like subtypes of breast cancers when delivered in combination with agents that initiate cell death via effects on the Bcl-2 cell survival pathway.

3.10 Acknowledgements

The research was supported by the National Health and Medical Research Council (NHMRC; project grant 631347). G.R.M is supported by the Mater Foundation. The Translational Research Institute is supported by a grant from the Australian Government.

3.11 Additional experiments relevant to chapter three, but not included in the manuscript

3.11.1 Introduction

The data submitted for publication in the journal of Biochemical and Biophysical Research Communications illustrate that in MDA-MB-231 breast cancer cells, PMCA2 is not a major regulator of global $[Ca^{2+}]_{CYT}$ and PMCA2 silencing promotes cell death associated with ionomycin and via the inhibition of Bcl-2. Additional experiments presented here, examine in more detail PMCA2 mRNA expression in MDA-MB-231 cells, and assessed the consequence of PMCA2 silencing on other death stimuli, cell number, and on calcium influx associated with CPA-induced Ca^{2+} store depletion, and via GPCR activation using ATP and trypsin.

3.11.2 Materials and methods

3.11.2.1 Cell culture

MDA-MB-231 breast cancer cells were cultured as described in the prepared manuscript, section 3.7.1, page 102.

3.11.2.2 RNA interference

Specific knockdown of PMCA isoform 2 was performed as described in the manuscript, section 3.7.2, page 102.

3.11.2.3 Real time RT-PCR

PMCA1, PMCA2 and PMCA4 mRNA levels were measured as described in the manuscript, section 3.7.3, page 102. Additional TaqMan Gene Expression assays were used to quantify PMCA4 (Hs00608066_m1, Applied Biosystems) and PMCA1 (Hs00155949_m1, Applied Biosystems).

3.11.2.4 Cell enumeration

At 120 h post-siRNA transfection, media was removed and MDA-MB-231 cells were assessed for cell death as detailed in section 3.7.5, page 103. Cells were enumerated in siNT and siPMCA2 treated cells, not exposed to a death stimulus. Cell number was measured using the multi-wavelength cell scoring application module, counting the number of nuclei stained with Hoechst 33342 (MetaXpress v3.1.0.83; Molecular Devices).

3.11.2.5 Cytosolic free calcium measurements

Cytoplasmic free calcium was measured according to the method in section 3.7.4, page 103.

3.11.2.6 Statistical analysis

All statistical tests were performed as described in the figure legends using GraphPad Prism (version 6.0) for Windows (GraphPad Software, Inc., La Jolla, CA, USA).

3.11.3 Results and discussion

3.11.3.1 Relative PMCA2 expression in MDA-MB-231 breast cancer cells

PMCA2 mRNA levels in MDA-MB-231 cells were assessed using real time RT-PCR. PMCA2 mRNA increased significantly ($P < 0.05$) with increasing cell confluence (Figure 3-5A). This result suggests that PMCA2 is upregulated with increasing cell density, which may relate to elevated PMCA2 levels detected in more advanced breast cancer cases that are characteristically larger, and higher grade [182]. Despite this increase in PMCA2 mRNA, analysis of relative PMCA isoform expression in confluent cultures indicated that PMCA1 is the primary transcript expressed in this cell line (Figure 3-5B).

PMCA2 upregulation in the lactating mammary gland exceeds the expression levels of other PMCA isoforms [58, 108]. This difference of expression in the lactating mammary gland *versus* breast cancer, may reflect the different function of PMCA2 in the physiological *versus* pathological setting. PMCA2 in the lactating mammary gland is critical for Ca^{2+} secretion and milk production [58, 59, 107, 108]. Whereas, PMCA2 expression in breast cancer, where the goal is not milk production, appears to confer the resistance to death stimuli [182-184, 243]. Detailed assessment of PMCA2 silencing on other cancer-relevant pathways such as proliferation and/or metastasis are required to fully understand the role of PMCA2 in breast cancer.

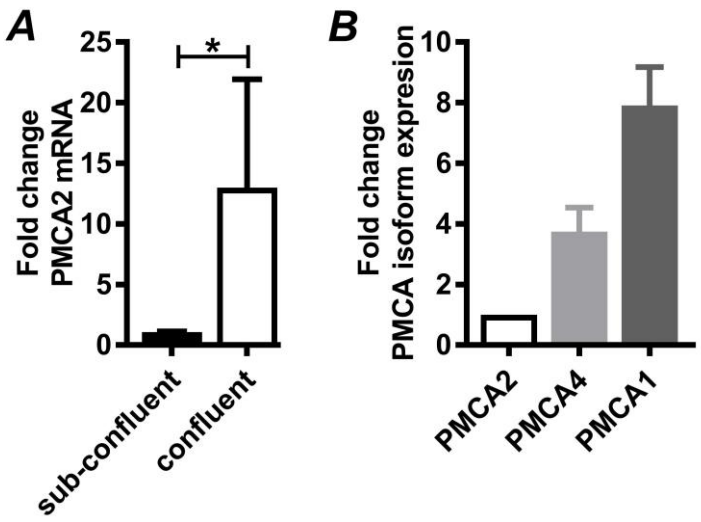

Figure 3-5: Relative PMCA2 expression in MDA-MB-231 breast cancer cells.

Assessment of PMCA2 mRNA levels in MDA-MB-231 cells transfected for 120 h with ON-TARGET*plus* siRNA. **(A)** Changes in PMCA2 mRNA expression in sub-confluent and confluent cell cultures. **(B)** Expression of PMCA2, PMCA4 and PMCA1 mRNA presented relative to PMCA2 mRNA levels in confluent cultures. Bar graphs show mean ± S.D, and were pooled from three independent experiments (n = 3) performed in duplicate or triplicate wells, *P < 0.05, two-tailed student's t-test.

3.11.3.2 PMCA2 silencing-mediated effects on cell enumeration in MDA-MB-231 breast cancer cells

PMCA2 upregulation in the pathological setting of breast cancer could be tailored to promote another cancer hallmark, increased cell proliferation [119, 171]. Therefore, the siPMCA2-mediated regulation of cell number was examined. Knocking down PMCA2 significantly ($P < 0.05$) reduced MDA-MB-231 cell numbers compared with the siNT control (Figure 3-6A). This result is consistent with a recent study, which I co-authored that showed PMCA2 downregulation, but not PMCA1 or PMCA4 silencing, attenuates MDA-MB-231 cell proliferation [183]. Hence, PMCA2 may be the responsible isoform that when inhibited attenuates MCF-7 breast cancer cell proliferation via the non-selective inhibition of all PMCA isoforms via antisense [185]. PMCA2 inhibitors, along with the promotion of cell apoptosis, could therefore also exert anti-cancer properties via anti-proliferative actions.

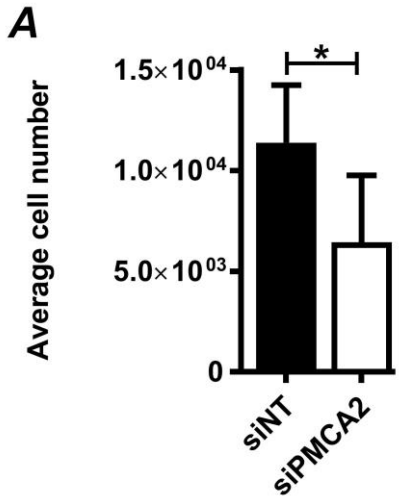

Figure 3-6: PMCA2 silencing-mediated effects on MDA-MB-231 breast cancer cell number.

(A) Bar graph of average cell number shows reduced MDA-MB-231 cell number with siRNA-transfection, compared with the siNT control. Data are obtained from three independent experiments ($n = 3$). *$P < 0.05$, paired two-tailed student's *t*-test.

3.11.3.3 Consequences of PMCA2 silencing on Ca^{2+} entry following intracellular store depletion associated with CPA, ATP and trypsin in MDA-MB-231 breast cancer cells

The consequence of PMCA2 silencing on Ca^{2+} entry following intracellular store depletion associated with the GPCR activators ATP (100 μM) and trypsin (0.1 μM) and with the SERCA inhibitor CPA (10 μM) was examined in siRNA-transfected MDA-MB-231 cells in nominal free Ca^{2+} physiological salt solution, containing BAPTA (100 μM, Figure 3-7). After the initial $[Ca^{2+}]_{CYT}$ Ca^{2+} transients returned to baseline, a second phase of $[Ca^{2+}]_{CYT}$ increase was monitored following the re-addition of external Ca^{2+} (Figure 3-7A, C and E). Assessment of the peak ratio calculated by dividing the second peak amplitude with the first peak amplitude [29, 234] was used to determine PMCA2-silencing mediated effects on ROCE (Figure 3-7B and D) and on SOCE (Figure 3-7F).

PMCA2 knockdown produced no significant ($P > 0.05$) effect on the peak ratio associated with the Ca^{2+} signals generated using ATP (Figure 3-7B) or trypsin (Figure 3-7D) or CPA (Figure 3-7F). Therefore, PMCA2 is not a major regulator of bulk $[Ca^{2+}]_{CYT}$ increases associated with SOCE induced by CPA or ROCE associated with either trypsin or ATP-induced Ca^{2+} signals.

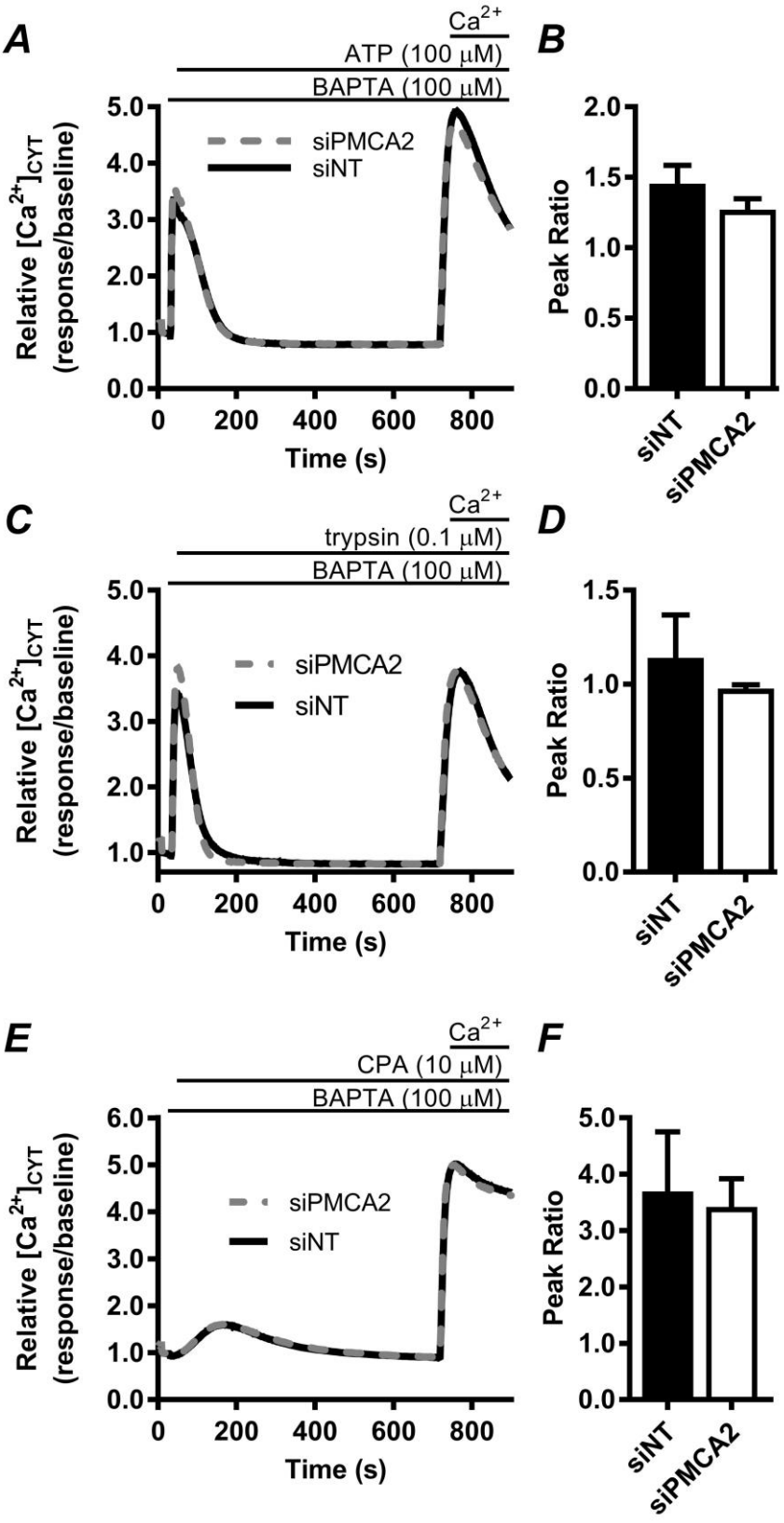
A
Ca2+
ATP (100 μM)
BAPTA (100 μM)
siPMCA2
siNT
Relative [Ca2+]CYT (response/baseline)
Time (s)
B
Peak Ratio
siNT
siPMCA2
C
Ca2+
trypsin (0.1 μM)
BAPTA (100 μM)
siPMCA2
siNT
Relative [Ca2+]CYT (response/baseline)
Time (s)
D
Peak Ratio
siNT
siPMCA2
E
Ca2+
CPA (10 μM)
BAPTA (100 μM)
siPMCA2
siNT
Relative [Ca2+]CYT (response/baseline)
Time (s)
F
Peak Ratio
siNT
siPMCA2

Figure 3-7: Effects of PMCA2 silencing on receptor-operated and store-operated Ca^{2+} entry in MDA-MB-231 breast cancer cells

(A) ATP, **(C)** trypsin and **(E)** CPA-induced $[Ca^{2+}]_{CYT}$ signals were recorded in siRNA-transfected MDA-MB-231 cells (siNT or siPMCA2) using the Ca^{2+} indicator Fluo-4AM in nominal Ca^{2+}-free media in the presence of extracellular BAPTA (100 μM). After the initial $[Ca^{2+}]_{CYT}$ transients returned to baseline, the re-addition of Ca^{2+} stimulated a second phase of Ca^{2+} entry. Ca^{2+} traces represent relative mean fluorescence. Bar graphs show the mean ± S.D for the peak ratio calculated for the Ca^{2+} signals generated with **(B)** 100 μM ATP, **(D)** 0.1 μM trypsin, and **(F)** 10 μM CPA. All data were obtained from three independent experiments ($n = 3$) performed in triplicate, $^*P < 0.05$, paired two-tailed *t* test.

3.11.4 Chapter summary

PMCA2 is proposed as a drug target for breast cancer therapies [183, 184, 239, 244]. Supporting this view, PMCA2 expression has a restricted tissue distribution, with high amounts in the central nervous system [103], and appears to be differentially expressed in the mammary gland [58, 108]. Although undetected or at very low levels in normal, non-lactating mammary glands, PMCA2 is overexpressed in a significant amount of human breast cancers cases [182, 183]. The utility of PMCA2 inhibitors for therapeutic agent development, however, requires validation studies. To address this, the functional significance of PMCA2 silencing on calcium signals and on the cancer-relevant pathways cell death and proliferation was examined in MDA-MB-231 breast cancer cells.

The bulk of the research findings were submitted for publication in the journal BBRC, and focused on PMCA2 silencing-mediated regulation of cell death. PMCA2 silencing sensitised MDA-MB-231 breast cancer cells to ionomycin toxicity and Bcl-2 inhibitor-mediated apoptosis. The ability of PMCA2 silencing to promote Bcl-2 inhibitor (ABT-263)-mediated cell death is significant. Bcl-2 is an oncogene that inhibits cell death and protects cells against a broad range of cytotoxic agents including anti-cancer drugs [238]. The Bcl-2 inhibitors ABT-737, ABT-199, along with the inhibitor used in these thesis studies ABT-263, are in clinical trial assessment for various cancer indications [238]. Approximately 75% of breast cancers express Bcl-2, and preclinical assessment of Bcl-2 inhibitors showed efficacy in breast cancer [237, 238].

Antisense-mediated inhibition of PMCA isoforms attenuates MCF-7 breast cancer cell proliferation [185]. PMCA2 silencing reduced MDA-MB-231 cell number. A recent study co-authored by me, in the same cell line, also detected the anti-proliferative effect of PMCA2 and demonstrated that knockdown of other PMCA isoforms (PMCA1/4) has no effect on proliferation [183]. Although these results need confirmation studies in other breast cancer cells, and in the presence of agents that either promote or inhibit proliferation, therapeutic targeting of PMCA2 in PMCA2-positive breast cancers could combat this disease through the promotion of cell death and suppressing cell proliferation.

In contrast with MDA-MB-231 breast cancer cells, where PMCA2 was expressed at relatively low levels compared with PMCA1 and PMCA4; PMCA2 expression in lactation supersedes that of other PMCA isoforms (PMCA1/4). These differences in expression may reflect the different functional roles of PMCA2 in the lactating mammary gland *versus* breast cancer. Mammary secretory cells in lactation transport Ca^{2+} from the blood to milk, and studies in rodents demonstrate PMCA2 is critical for the secretion of Ca^{2+} into milk, protects against calcium toxicity, and prevents early involution and milk stasis [58, 59, 107, 108]. Rather than fulfilling the physiological demands associated with

lactation and milk production, aberrant PMCA2 in MDA-MB-231 cells appears to protect against death stimuli and promote cell proliferation [182-184]. PMCA2-mediated regulation of Bcl-2 survival pathways and cell proliferation, may therefore be relevant even when PMCA2 is not the predominant isoform expressed.

Overall, this chapter demonstrates that PMCA2 inhibitors could represent a therapeutic option for the clinical treatment of PMCA2-positive breast cancers.

4.1 Preface

Chapters two and three demonstrated that isoform-specific silencing of PMCAs effects cell death independently of global $[Ca^{2+}]_{CYT}$. Although there is precedent for PMCA pumps to influence cell events via localised calcium signals within cytoplasmic micro-domains, overexpression studies show that PMCA isoforms can also modulate calcium signals within sub-cellular compartments. Because mitochondria orchestrate cell death, PMCA-mediated effects on mitochondrial calcium levels could determine the sensitivity of MDA-MB-231 cells to death stimuli. This chapter, therefore evaluated the potential role of proteins that regulate mitochondrial calcium levels on ionomycin and ABT-263 cell death responses in MDA-MB-231 breast cancer cells.

Mitochondrial calcium uptake was attenuated by silencing mitochondria calcium uniporter (MCU) expression. Then the consequence of MCU silencing on MDA-MB-231 breast cancer cells death and global $[Ca^{2+}]_{CYT}$ was assessed. It was predicted that knocking down MCU expression would reduce mitochondrial calcium levels, independently of global $[Ca^{2+}]_{CYT}$ and hence protect MDA-MB-231 cells against death insults.

This chapter consists of a manuscript published in the journal Biochemical and Biophysical Research Communications, entitled 'Mitochondrial calcium uniporter silencing potentiates caspase-independent cell death in MDA-MB-231 breast cancer cells' [245]. Minor adjustments have been made to the original format of the published manuscript to adhere to The University of Queensland thesis formatting guidelines.

The paper presents novel research findings that were predominantly designed and performed by myself, Merril C Curry under the supervision of Gregory R Monteith and Sarah J Roberts-Thomson. Additional experiments and data performed by Dr. Amelia Peters and Dr. Paraic Kenny were also included in the manuscript and have been incorporated into this thesis chapter. Dr. Amelia Peters, a fellow laboratory member performed the proliferation studies (Figure 4-2C and D). Dr. Paraic Kenny, an international collaborator contributed the microarray data presented in Figure 4-1.

4.2 Chapter Hypothesis

- Altered mitochondrial calcium uniporter (MCU) mRNA levels is a feature of specific breast cancer molecular subtypes
- Silencing of the mitochondrial calcium uniporter modulates cell death responses and shapes cytoplasmic calcium signals in breast cancer cells

4.3 Chapter Aims

- To determine MCU expression levels in clinical breast cancer samples grouped by oestrogen receptor status or molecular subtype
- To assess the function significance of MCU in the context of basal breast cancer using the MDA-MB-231 breast cancer cell line
- To inhibit MCU with specific siRNAs to silence expression of this target gene
- To study the consequence of MCU silencing on cell death initiated with different stimuli
- To assess MCU silencing-mediated effects in shaping bulk cytoplasmic calcium signals generated using different agents

4.4 Highlights

- Some clinical breast cancers are associated with MCU overexpression
- MCU silencing did not alter cell death initiated with the Bcl-2 inhibitor ABT-263
- MCU silencing potentiated caspase-independent cell death initiated by ionomycin
- MCU silencing promoted ionomycin-mediated cell death without changes in bulk calcium

4.5 Abstract

The mitochondrial calcium uniporter (MCU) transports free ionic Ca^{2+} into the mitochondrial matrix. We assessed MCU expression in clinical breast cancer samples using microarray analysis and the consequences of MCU silencing in a breast cancer cell line. Our results indicate that oestrogen receptor negative and basal-like breast cancers are characterised by elevated levels of MCU. Silencing of MCU expression in the basal-like MDA-MB-231 breast cancer cell line produced no change in proliferation or cell viability. However, distinct consequences of MCU silencing were seen on cell death pathways. Caspase-dependent cell death initiated by the Bcl-2 inhibitor ABT-263 was not altered by MCU silencing; whereas caspase-independent cell death induced by the calcium ionophore ionomycin was potentiated by MCU silencing. Measurement of cytosolic Ca^{2+} levels showed that the promotion of ionomycin-induced cell death by MCU silencing occurs independently of changes in bulk cytosolic Ca^{2+} levels. This study demonstrates that MCU overexpression is a feature of some breast cancers and that MCU overexpression may offer a survival advantage against some cell death pathways. MCU inhibitors may be a strategy to increase the effectiveness of therapies that act through the induction of caspase-independent cell death pathways in oestrogen receptor negative and basal-like breast cancers.

4.6 Introduction

Mitochondria regulate numerous cellular processes and are vital for both sustaining cell survival and the initiation of cell death [4, 246]. The uptake of Ca^{2+} by mitochondria can buffer increases in cytosolic free Ca^{2+} ($[Ca^{2+}]_{CYT}$) and stimulate specific mitochondrial functions such as ATP synthesis [4, 246]. Mitochondrial Ca^{2+} levels may also influence sensitivity to cell death activators [40, 152]. In malignant transformation, remodeling of Ca^{2+} homeostasis and reprogramming of mitochondrial functions could confer cancer cells with a survival advantage and an ability to evade cell death [21, 247]. Calcium transporters including the voltage-dependent anion-selective channel (VDAC) and the mitochondrial Ca^{2+} uniporter (MCU) [246] participate in mitochondrial Ca^{2+} uptake and have been proposed as potential regulators of cell death [248, 249].

Since the molecular identification of MCU [32, 33], several studies have investigated the significance of mitochondrial Ca^{2+} uptake on specific cellular processes through the modulation of MCU expression levels. In cardiomyocytes MCU silencing amplifies bulk $[Ca^{2+}]_{CYT}$ and is associated with increased contractile responses [250]. In breast cancer cells sustained increases of bulk $[Ca^{2+}]_{CYT}$ are associated with the promotion of cell death responses [227]. In the context of breast cancer, a recent study in a panel of breast cancer cells lines, including MDA-MB-231 cells, demonstrated that mitochondrial-Ca^{2+} uptake via MCU is critical for tumour growth and metastasis [251]. In this thesis, the impact of MCU silencing on cell death was examined in the MDA-MB-231 breast cancer cell line.

MCU has been studied in other cancer types. One recent study identified MCU downregulation as a characteristic feature of some human colon and prostate cancer cells [252]. Down-regulation of MCU in colon and prostate-derived cancers promotes increased proliferation and bestows resistance to cell death stimuli through diminished mitochondrial Ca^{2+} levels [252]. At the time of these studies there had been no published assessment of MCU in the context of breast cancer.

In this study we assessed MCU expression in clinical breast cancers and evaluated the functional significance of MCU silencing on proliferation, cell death pathways and on bulk $[Ca^{2+}]_{CYT}$ in MDA-MB-231 breast cancer cells. Our results suggest that MCU inhibition may sensitise some breast cancers to some inducers of cell death.

4.7 Materials and Methods

4.7.1 Analysis of MCU levels in human breast cancer cases

Gene expression data for 180 human breast cancer cases [253] were obtained from NCBI-GEO (Accession GSE3165) and imported into Partek Genomics Suite (version 6.6). MCU (annotated on these microarrays as C10orf42) expression was analysed in samples grouped by both oestrogen receptors status and PAM50 molecular subtype [254].

4.7.2 Cell culture

Human MDA-MB-231 breast cancer cells (American Type Culture Collection) were grown in high glucose DMEM (Sigma Aldrich) supplemented with 10% FBS and 4 mM Lglutamine (Invitrogen) at 37 °C/5% CO_2 in a humidified air incubator.

4.7.3 Silencing of MCU expression

MDA-MB-231 cells were transfected as previously described [227] with ON-TARGET*plus*™ SMARTpool siRNAs (Dharmacon), consisting of four pooled siRNA sequences rationally designed to minimise off-target effects [195, 196]. The specific siRNAs used in this study were MCU siRNA (siMCU, L-015519-02) and the non-targeting control siRNA (siNT, D-001810- 10). For all experiments MCU mRNA silencing (>70%) was confirmed at 48 h post-siRNA.

4.7.4 Quantitative real time RT-PCR

Quantitative real time RT-PCR was performed as described previously [227]. Briefly, at 48 or 120 h post siRNA-transfection total RNA was isolated (RNeasy Plus mini kit; Qiagen), and then reverse transcribed (Omniscript RT kit; Qiagen). The cDNA of interest were amplified using the TaqMan Fast Universal PCR Master Mix (Applied Biosystems) and TaqMan Gene Expression assays (MCU, Hs00293548_m1; 18 S rRNA, 4319413E; Applied Biosystems) under universal cycling conditions with a StepOnePlus real time PCR system (Applied Biosystems). MCU mRNA levels were quantified by the comparative C*t* method as described [197] normalised to 18 S rRNA and presented relative to the siNT control.

4.7.5 Cell enumeration and S-phase analysis

MDA-MB-231 cells were transfected with siRNA for 120 h and then cell enumeration and S-phase analysis were performed as previously described [255]. Briefly, cells with newly synthesised DNA were stained, according to the manufacturer's instructions using the ClickiT® EdU cell proliferation assay (Alexa Fluor 555; Invitrogen). DAPI-stained cell nuclei (400 nM; 90 min) and EdU-positive cells were imaged with a 10× objective using an ImageXpress Micro automated epifluorescence microscope (Molecular Devices Corporation) [199]. Cell number and percentage of EdU positive cells were calculated using the multiwavelength cell scoring application module (MetaXpress v3.1.0.83; Molecular Devices).

4.7.6 Assessment of cell viability

At 72 h post siRNA-transfection MDA-MB-231 cells were treated with the cell death activators ABT-263 (Selleckchem), ionomycin (Enzo Life Sciences), or with dimethyl sulfoxide (up to 0.33%) and incubated for an additional 48 h. Cell viability was then assessed in non-fixed cells as previously reported by evaluating Hoechst 33342 (10 μg/mL; Invitrogen) and propidium iodide (1 μg/mL; Invitrogen) staining [227]. Imaging was performed using an ImageXpress Micro automated epifluorescence microscope (Molecular Devices Corporation). Criteria for viable and propidium iodide positive cells (PI+) were defined as previously described [227].

4.7.7 Cytosolic free calcium measurements

At 72 h post siRNA-transfection MDA-MB-231 breast cancer cells were loaded with either a high Ca^{2+} affinity (Fluo-4AM (4 μM; Molecular Probes)) or a low Ca^{2+} affinity (Fluo-4FF (4 μM; Molecular Probes)) Ca^{2+} indicator according to published methods [227]. $[Ca^{2+}]_{CYT}$ was then monitored using a fluorescence imaging plate reader [198] (Molecular Devices Corporation) as previously described [227]. To assess relative $[Ca^{2+}]_{CYT}$ fluorescence was normalised to base-line values.

4.7.8 Statistical analysis

Statistical tests were performed as described in the figure legends using GraphPad Prism version 5.04 for Windows.

4.8 Results

4.8.1 MCU mRNA levels in clinical breast cancer samples

Assessment of MCU mRNA levels in a cohort of 180 breast cancer cases [253] showed a significantly ($P < 0.05$; Figure 4-1A) higher level of MCU in oestrogen receptor-negative breast cancers. When breast cancers were stratified by molecular subtype the highest levels of MCU were seen in basal-like breast cancers ($P < 0.05$; basal-like *versus* luminal A and B subtypes; Figure 1B), while other subtypes expressed intermediated MCU levels (Figure 4-1B). Oestrogen receptor-negative and basal-like breast cancers are associated with a particularly poor prognosis [167, 170].

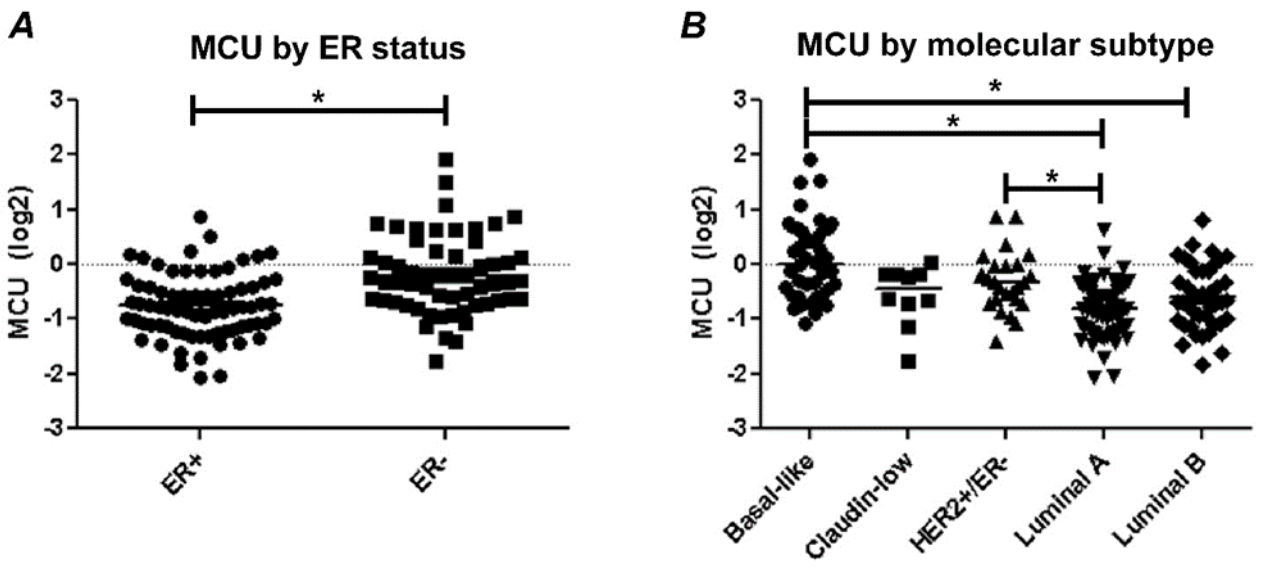

Figure 4-1**:** MCU expression in clinical breast cancers is associated with oestrogen receptor status and molecular subtype.

Relative MCU levels were analysed in human breast cancer cases (n = 180) stratified by **(A)** oestrogen receptor (ER) status and **(B)** molecular subtype. MCU levels were highest in oestrogen receptor-negative tumors ($P < 0.05$, Mann-Whitney test) and showed the strongest enrichment in the basal-like subtype ($P < 0.05$; basal-like *versus* Luminal A and B, Kruskall-Wallis test with Dunn's post-test for multiple comparisons).

4.8.2 Effects of MCU silencing on proliferation and cell viability in MDA-MB-231 breast cancer cells

To assess the possible role of MCU overexpression in breast cancer, we used specific siRNAs to silence MCU expression in basal-like MDA-MB-231 breast cancer cells [240]. Compared to the siNT control, cells transfected with siMCU showed a significant ($P < 0.05$) decrease in MCU mRNA levels at 48 h (Figure 4-2A) and 120 h (Figure 4-2B) post-siRNA. Using this model, we assessed the effects of MCU knockdown on proliferation and cell viability.

Effects of MCU silencing on cell proliferation were evaluated by cell enumeration and S-phase analysis (EdU staining). MCU silencing did not significantly alter cell number (Figure 4-2C), or the percentage of cells in S-phase (EdU positive; Figure 4-2D) compared to the siNT control. Cell viability was also quantified; MCU silencing had no significant effect on the percentage of viable cells compared to the siNT control (Figure 4-2E-G).

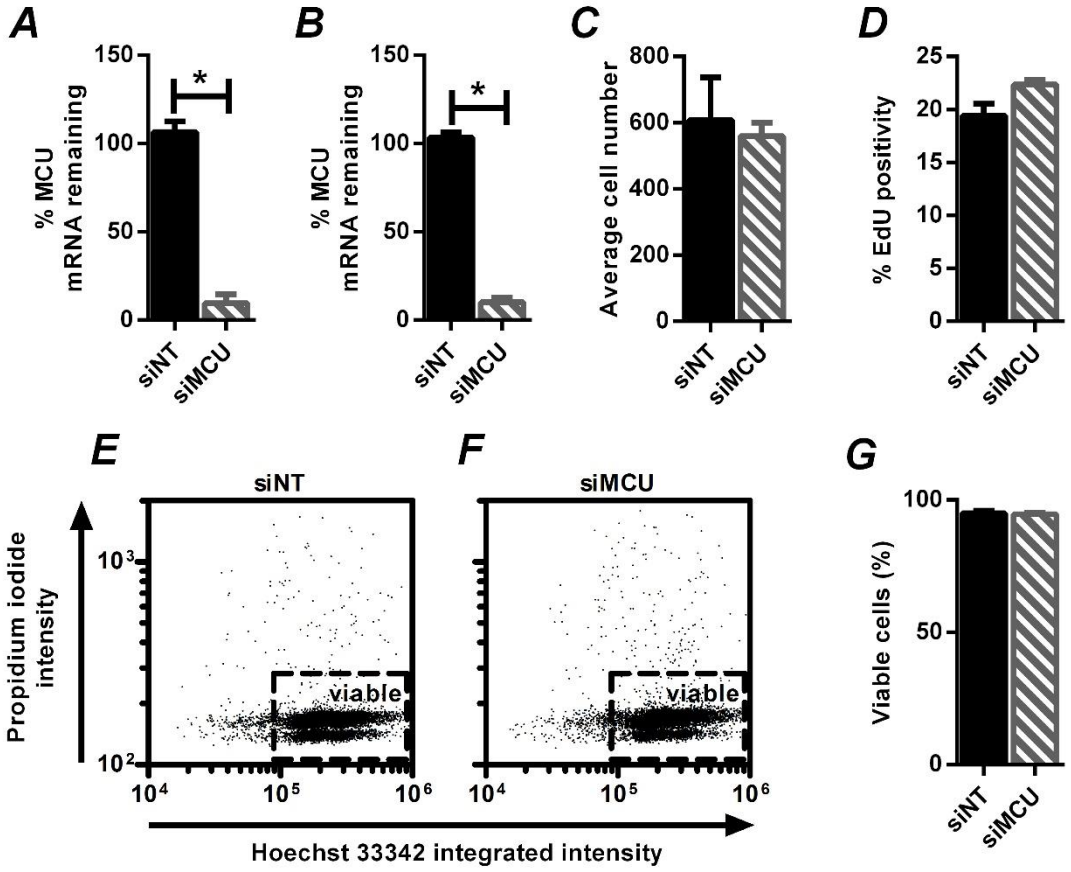

Figure 4-2: MCU silencing in MDA-MB-231 cells and the effects of silencing on proliferation and cell viability.

MCU was silenced in MDA-MB-231 cells using siRNA and the effects on cell number, S-phase and cell viability were compared to the siNT control. Relative MCU mRNA levels at **(A)** 48 h and **(B)** 120 h post-transfection with siMCU or siNT. Effects of MCU knockdown on **(C)** average cell number, **(D)** percentage S-phase (EdU-positive cells) and **(G)** percentage viable cells. Bar graphs show the mean ± S.D obtained from three independent experiments ($n = 3$) performed in triplicate. Dot plots show changes in cell viability with either **(E)** siNT or **(F)** siMCU for 10,000 cells randomly selected from three independent experiments ($n = 3$) performed in triplicate wells. *$P < 0.05$, paired two-tailed t test.

4.8.3 MCU silencing sensitises MDA-MB-231 breast cancer cells to ionomycin-mediated cell death

To analyse whether MCU silencing regulates breast cancer cell responses to death activators, siRNA-transfected MDA-MB-231 cells were treated with the Ca^{2+} ionophore ionomycin to initiate caspase-independent cell death [227]. Compared to the siNT control MCU silencing potentiated sub-maximal ionomycin (3 μM)-mediated cell death, with a significant ($P < 0.05$) reduction in cell viability and a marked ($P < 0.05$) increase in the proportion of propidium iodide positive cells (Figure 4-3A). Silencing of MCU did not alter cell viability at a higher ionomycin concentration (10 μM) compared to the siNT control (Figure 4-3B). These data suggest MCU silencing sensitises MDA-MB-231 cells to caspase-independent cell death initiated with ionomycin.

4.8.4 MCU silencing does not modulate ABT-263-mediated MDA-MB-231 breast cancer cell death

The Bcl-2 inhibitor ABT-263 was used to address the consequence of MCU silencing on caspase-dependent cell death in the MDA-MB-231 breast cancer cell line [227]. Compared with //the siNT control, MCU silencing exerted no effect on cell death initiated at either the sub-maximal (3 μM; Figure 4-3C) or high (10 μM; Figure 4-3D) ABT-263 concentrations. This suggests that MCU knockdown does not sensitise MDA-MB-231 cells to caspase-dependent cell death initiated by ABT-263.

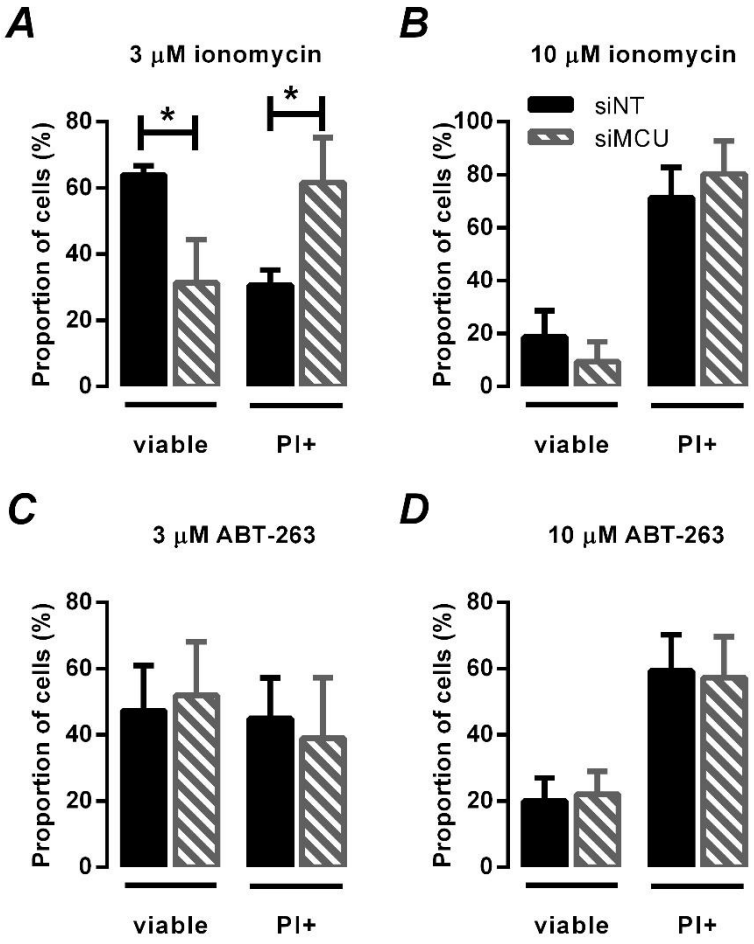

Figure 4-3**:** Consequences of MCU silencing on ionomycin- and ABT-263-initiated cell death in MDA-MB-231 cells.

MCU was silenced in MDA-MB-231 cells using siRNA and then cells were treated with **(A)** 3 μM ionomycin, **(B)** 10 μM ionomycin, **(C)** 3 μM ABT-263 or with **(D)** 10 μM ABT-263 for 48 h prior to cell death assessment. Bar graphs show mean ± S.D of the proportion of viable and propidium iodide positive (PI+) cells in siMCU and siNT transfected cells. Data were obtained from three independent experiments ($n = 3$) performed in triplicate. *$P < 0.05$, repeated measures two-way ANOVA, Bonferroni post-hoc analysis.

4.8.5 Effects of MCU silencing on increases in bulk cytosolic calcium

To assess whether MCU silencing modified the nature of bulk $[Ca^{2+}]_{CYT}$ increases, we challenged siRNA-transfected MDA-MB-231 breast cancer cells with different initiators of $[Ca^{2+}]_{CYT}$ increases. Moderate increases in bulk $[Ca^{2+}]_{CYT}$ were induced with the sarcoendoplasmic reticulum Ca^{2+}-ATPase (SERCA) inhibitor cyclopiazonic acid (CPA; 10 μM) or the protease activated receptor activator trypsin (0.1 μM) under Ca^{2+}-free conditions. Compared with the siNT control, silencing of MCU did not alter either CPA (Figure 4-4A) or trypsin (Figure 4-4C) Ca^{2+} responses, with no significant difference detected for area under the curve (Figure 4-4B and D) or other Ca^{2+} transient parameters such as peak $[Ca^{2+}]_{CYT}$ and half peak decay time (*data not shown*).

A role for MCU in shaping Ca^{2+} signals of higher magnitude was evaluated in the presence of extracellular Ca^{2+} (2 mM) using the Ca^{2+} ionophore ionomycin. Assessment of $[Ca^{2+}]_{CYT}$ with the low affinity Ca^{2+} indicator Fluo-4FF, showed that MCU silencing compared to the siNT control had no major effects on bulk $[Ca^{2+}]_{CYT}$ increases, at either sub-maximal (3 μM; Figure 4-4E-F) or high (10 μM; Figure 4-4G-H) ionomycin concentrations. Collectively, these findings demonstrate that MCU does not have a major role in the regulation of bulk $[Ca^{2+}]_{CYT}$ in MDA-MB-231 breast cancer cells.

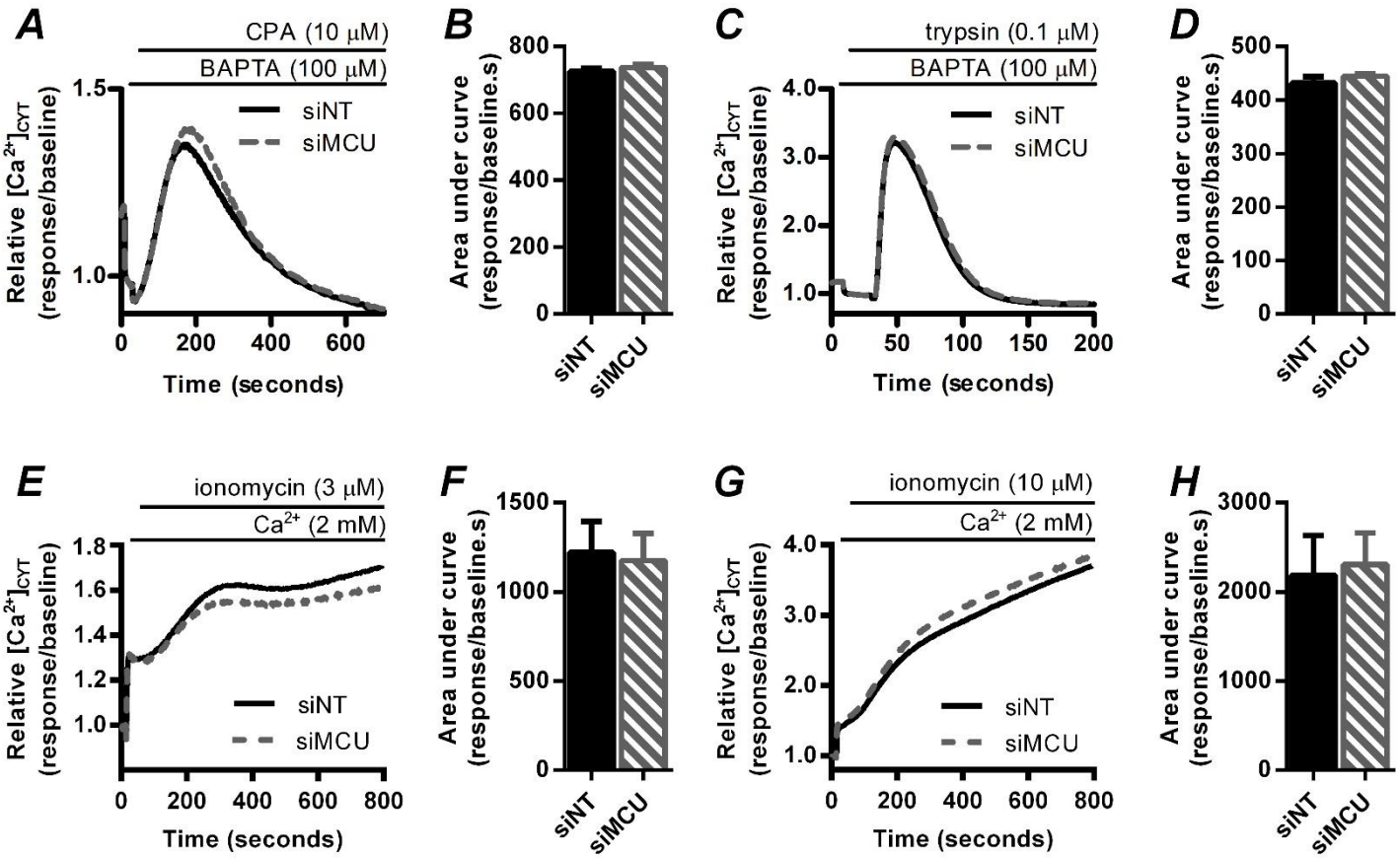
A
CPA (10 μM)
BAPTA (100 μM)
siNT
siMCU
Relative [Ca2+]CYT (response/baseline)
Time (seconds)
B
Area under curve (response/baseline.s)
C
trypsin (0.1 μM)
BAPTA (100 μM)
D
E
ionomycin (3 μM)
Ca2+ (2 mM)
F
G
ionomycin (10 μM)
Ca2+ (2 mM)
H

Figure 4-4: Effect of MCU silencing on bulk $[Ca^{2+}]_{CYT}$ increases stimulated by various initiators of $[Ca^{2+}]_{CYT}$ increases.

(A) CPA (10 μM)-mediated and **(C)** trypsin (0.1 μM)-induced $[Ca^{2+}]_{CYT}$ transients measured with the Ca^{2+} indicator Fluo-4AM after transfection with siMCU or siNT in the presence of extracellular BAPTA (100 μM). **(E)** 3 μM ionomycin and **(G)** 10 μM ionomycin $[Ca^{2+}]_{CYT}$ transients recorded using the Ca^{2+} indicator Fluo-4FF in cells transfected with siNT or siMCU. Bar graphs show the mean ± S.D for the area under the curve calculated for the **(B)** 10 μM CPA, **(D)** 0.1 μM trypsin, **(F)** 3 μM ionomycin and **(H)** 10 μM ionomycin $[Ca^{2+}]_{CYT}$ increases. Ca^{2+} traces represent relative mean fluorescence. All data were obtained from three independent experiments (n = 3) performed in triplicate. *P < 0.05, paired two-tailed t test.

4.9 Discussion

A previous study identified MCU downregulation in prostate and colon-derived cancers [252], here we present data showing that MCU is upregulated in some clinical breast cancer subtypes. MCU was most highly expressed in oestrogen receptor-negative and basal-like breast cancers both of which are associated with a poor prognosis [167, 170]. To understand the implication of MCU overexpression in breast cancer, we assessed the functional consequences of MCU silencing on proliferation, cell death and bulk $[Ca^{2+}]_{CYT}$ in the basal-like MDA-MB-231 breast cancer cell line.

Our silencing studies in MDA-MB-231 cells showed MCU knockdown had no effect on proliferation or cell viability. However, assessment of MCU knockdown on cell death initiated by ABT-263 and ionomycin defined a distinct role for MCU in the regulation of caspase-independent and -dependent cell death pathways, respectively. MCU silencing did not affect ABT-263-mediated cell death, but acted as a sensitiser of cell death initiated with ionomycin. MCU silencing attenuates mitochondrial Ca^{2+} uptake [32, 33] and reduced mitochondrial Ca^{2+} levels act to suppress cell death in a variety of malignant cell lines, including those derived from the cervix [152] central nervous system [256], head and neck [257] and lymph [258] tissues. We therefore hypothesised that MCU knockdown in MDA-MB-231 breast cancer cells would also protect from death insults. However, MCU knockdown did not protect against ABT-263-induced cell death, and potentiated ionomycin-initiated cell death.

Alterations in bulk $[Ca^{2+}]_{CYT}$ signals were examined as a potential mechanism of MCU silencing-mediated promotion of ionomycin-initiated cell death. In cardiomyocytes MCU silencing amplifies cytosolic Ca^{2+} signals [250] and we have recently shown sustained increases of bulk $[Ca^{2+}]_{CYT}$ are associated with the promotion of ionomycin-mediated MDA-MB-231 cell death [227]. However, our assessment of bulk $[Ca^{2+}]_{CYT}$ showed no major changes upon MCU knockdown on Ca^{2+} signals stimulated with CPA, trypsin or ionomycin. These data suggest that MCU does not significantly contribute in buffering global cytosolic free Ca^{2+}; therefore increases in bulk $[Ca^{2+}]_{CYT}$ are unlikely to explain the promotion of ionomycin-initiated cell death upon MCU silencing.

The ability of MCU silencing to sensitise MDA-MB-231 cells to ionomycin-mediated cell death could be due to diminished mitochondrial Ca^{2+} uptake and alterations in the autophagy survival pathway, as the specific MCU inhibitor Ru360 regulates autophagy in HEK293 and DT40 cells [259]. Another mechanism may involve alterations in localised Ca^{2+} signals within specialised signaling domains at the endoplasmic reticulum-mitochondrial interface, known as mitochondrial-associated-membranes (MAMs) [260]. A recent study investigated reduced mitochondrial Ca^{2+} uptake through knockdown of the MAM-enriched calcium transporter, VDAC1 [261]. VDAC1 silencing potentiates

the response of human-derived HeLa cervical cancer cells to death activators without affecting bulk $[Ca^{2+}]_{CYT}$, this sensitisation was not dependent on diminished mitochondrial Ca^{2+} levels [261]. Localised Ca^{2+} signals possibly within MAM domains may represent another regulatory site for Ca^{2+}-dependent death signals in breast cancer cells and along with MCU-mediated regulation of autophagy requires further investigation.

In this report, we have identified MCU overexpression in some clinical breast cancers, in particular those subtypes associated with a poor prognosis (oestrogen receptor negative and basal-like). MCU silencing in the basal-like MDA-MB-231 breast cancer cell line promoted ionomycin-initiated but not ABT-263-mediated cell death. MCU inhibitors may therefore represent novel therapies for some breast cancers by potentiating some caspase-independent cell death mechanisms.

4.10 Acknowledgements

National Health and Medical Research Council Grant 631347 and Susan G. Komen for the Cure (KG100888).

4.11 Additional experiments relevant to chapter four, but not included in the manuscript

4.11.1 Introduction

Extending upon the studies published in the Journal of Biochemical and Biophysical Research Communications [245], the consequence of MCU silencing on ATP calcium responses and on store-operated calcium entry, along with MCU-mediated effects on ceramide cell death was also assessed.

4.11.2 Materials and methods

4.11.2.1 Cell culture

Human MDA-MB-231 breast cancer cells were cultured as described in section 4.7.2, page 130.

4.11.2.2 Silencing of MCU expression

MCU expression was silenced by the methods detailed in section 4.7.3, page 130.

4.11.2.3 Quantitative real time RT-PCR

MCU mRNA silencing (>70%) was confirmed for all experiments, as detailed in section 4.7.4, page 130 using quantitative real time RT-PCR.

4.11.2.4 Assessment of cell viability

At 72 h post siRNA-transfected MDA-MB-231 cells were treated with ceramide (Sigma Aldrich), or with dimethyl sulfoxide (up to 0.33%) and incubated for 48 h. Assessment was then performed according to the method in section 4.7.6, page 131.

4.11.2.5 Cytosolic free calcium measurements

$[Ca^{2+}]_{CYT}$ was assessed as described in section 4.7.7, page 131.

4.11.2.6 Statistical analysis

Statistical tests were performed as described in the figure legends using GraphPad Prism version 6.0 for Windows.

4.11.3 Results and discussion

4.11.3.1 MCU silencing-mediated regulation of MDA-MB-231 breast cancer cell death initiated with ceramide

MCU silencing-mediated effects on ceramide cell death were examined. In MDA-MB-231 breast cancer cells, ceramide induced cell death at sub-maximum (30 μM; Figure 4-5A) and maximum (10 μM; Figure 4-5B) concentrations, both of which were not altered ($P > 0.05$) upon MCU silencing compared to the siNT control.

In these thesis studies, the lack of effect detected by MCU silencing on ceramide (Figure 4-5) and ABT-263 (section 4.8.4, page 136) cell death responses is consistent with other reports. Hall *et al.* [262] report by silencing and overexpression techniques, although a regulator of mitochondrial calcium levels, MCU-mediated Ca^{2+} uptake does not modulate MDA-MB-231 cell death initiated by various stress protocols and the lipid mediator ceramide [262]. Another study in multiple breast cancer cells lines including MDA-MB-468, BT-549 and MDA-MB-231 cells, demonstrates that mitochondrial-Ca^{2+} uptake via MCU, although not crucial for cell death, is instrumental for other cancer-relevant pathways such as tumour growth and metastasis [251].

In this thesis work, MUC silencing had no effect on ABT-263 cell death, however, cell death initiated with ionomycin was augmented by MCU silencing. The mechanism associated with siMCU-mediated sensitisation of ionomycin-induced cell death is unclear (section 4.8.3, page 136), however, this effect may involve changes in local Ca^{2+} signals within cytoplasmic domains or even changes in $[Ca^{2+}]_{ER}$, which are probably undetected in the measurements of bulk $[Ca^{2+}]_{CYT}$ [151, 261]. Future assessment of Ca^{2+} signals in the mitochondria and in the endoplasmic reticulum would provide a better understanding of siMCU-mediated regulation of ionomycin cell death in MDA-MB-231 cells.

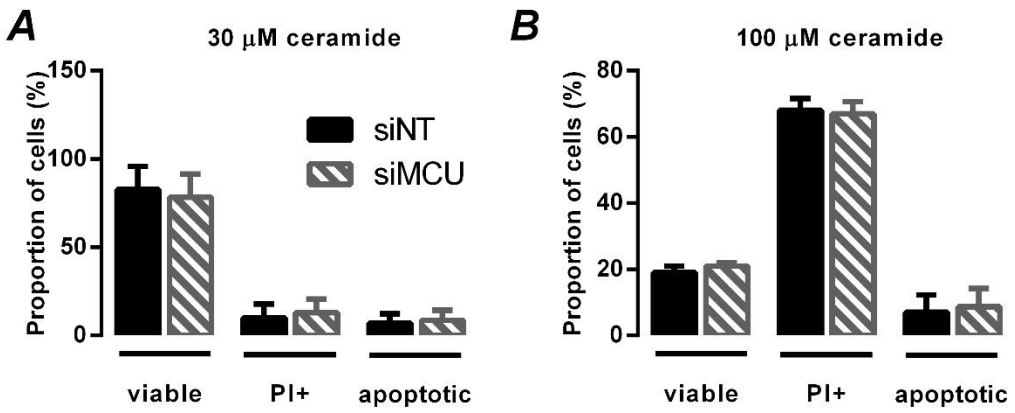

Figure 4-5**:** Consequences of MCU silencing on ceramide-initiated cell death in MDA-MB-231 cells.

MCU was silenced in MDA-MB-231 cells using specific siRNAs, and then cells were treated with either **(A)** 30 μM ceramide, or **(B)** 100 μM ceramide for 48 h prior to cell death assessment. Bar graphs are mean ± S.D, and show the proportion of viable, propidium iodide positive (PI+) and apoptotic cells in siMCU and siNT transfected cells. Data were obtained from three independent experiments (n = 3) performed in triplicate. *$P < 0.05$, repeated measures two-way ANOVA, Bonferroni post-hoc analysis.

4.11.3.2 Effects of MCU silencing on cytoplasmic free calcium signals associated with ATP

The ability of MCU silencing to modify purinergic receptor agonist ATP calcium signals was tested. siRNA-transfected MDA-MB-231 breast cancer cells were treated with ATP (100 μM) in nominal free Ca^{2+} physiological salt solution containing BAPTA (100 μM). Compared with the siNT control, silencing MCU produced very subtle, but statistically significant ($P < 0.05$) effects on the calcium transient parameters area under the curve (Figure 4-6B) and half peak decay time (Figure 4-6C). Although siMCU had no effect ($P > 0.05$) on peak amplitude (Figure 4-6D), the ability for siMCU to modestly increase the area under the curve and delay the half peak time highlights the potential for MCU-mediated Ca^{2+} influx to fine-tune cytoplasmic Ca^{2+} signals. Future studies could assess the functional significance on such fine tuning (e.g. gene transcription).

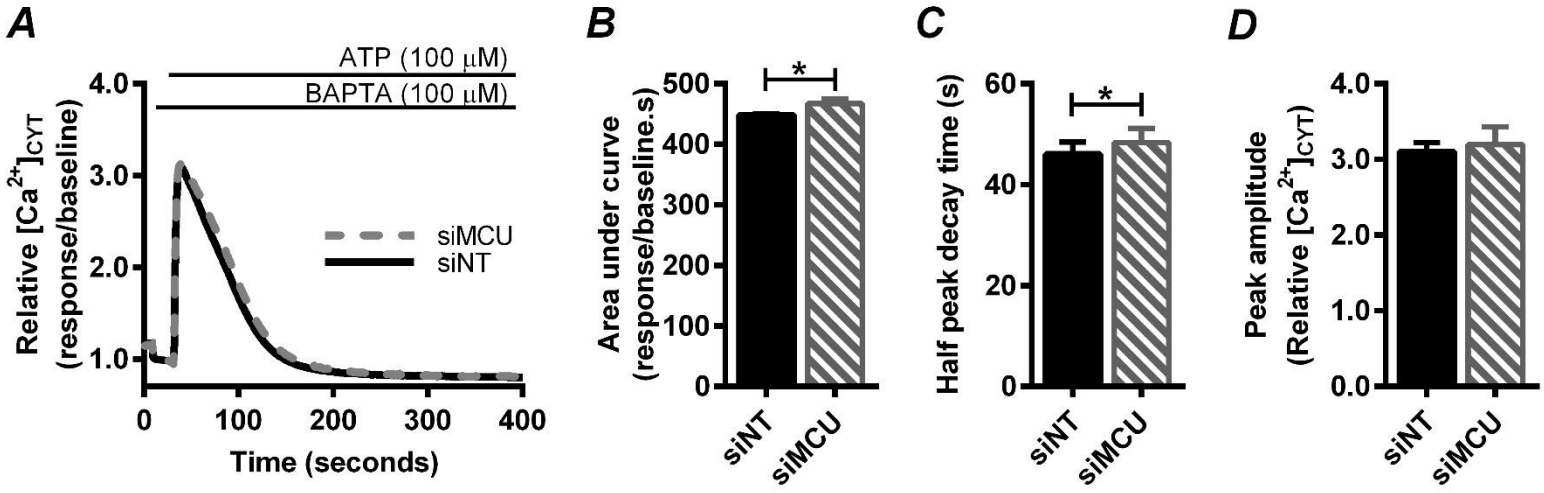

Figure 4-6: Effect of MCU silencing on ATP-mediated $[Ca^{2+}]_{CYT}$ increases in MDA-MB-231 breast cancer cells.

Cells transfected with siMCU or siNT were challenged with **(A)** ATP (100 μM) and $[Ca^{2+}]_{CYT}$ were measured in the presence of extracellular BAPTA (100 μM) in nominal free Ca^{2+}. Bar graphs show the mean ± S.D for the calcium transient parameters **(B)** area under the curve **(C)** half peak decay time and **(D)** peak amplitude associated with the ATP calcium responses. Ca^{2+} traces represent relative mean fluorescence. All data were obtained from three independent experiments (n = 3) performed in triplicate. *P < 0.05, paired two-tailed t test.

4.11.3.3 Effects of MCU silencing on receptor operated and store operated calcium entry in MDA-MB-231 breast cancer cells

The ability for mitochondria Ca^{2+}-uptake to buffer cytoplasmic Ca^{2+} signals including Ca^{2+} influx via store operated calcium entry (SOCE) is reported [246, 263]. Mitochondrial Ca^{2+} uptake, in addition to regulating mitochondria function, can therefore shape bulk $[Ca^{2+}]_{CYT}$ signals [4, 246]. In this thesis, to examine whether MCU silencing modified bulk $[Ca^{2+}]_{CYT}$ increases associated with ROCE and SOCE, siRNA-transfected MDA-MB-231 cells were treated with either CPA (10 μM), trypsin (0.1 μM) or ATP (100 μM), in nominal free Ca^{2+} physiological salt solution containing BAPTA (100 μM) (Figure 4-7). After the initial $[Ca^{2+}]_{CYT}$ increases returned to baseline, a second phase of $[Ca^{2+}]_{CYT}$ increase was monitored following the re-addition of external Ca^{2+} (Figure 4-7A, C and E). MCU silencing-mediated effects on ROCE (Figure 4-7D and E) and on SOCE (Figure 4-7B) were determined by assessment of peak ratio derived by dividing the second peak amplitude with the first peak amplitude [29, 234].

MCU knockdown had no effect on the peak ratio associated with CPA (Figure 4-7B) or trypsin (Figure 4-7D). However, siMCU produced a subtle, but statistically significant ($P < 0.05$) increase in the peak ratio (Figure 4-7F) associated with the purinergic receptor agonist ATP. Although MCU is not a major regulator of bulk $[Ca^{2+}]_{CYT}$ these data identify that MCU can fine-tune cytoplasmic calcium signals for some stimuli. Future investigations are required to ascertain the ability of MCU silencing to shape those Ca^{2+} signals associated with SOCE within localised regions of MDA-MB-231 breast cancer cells.

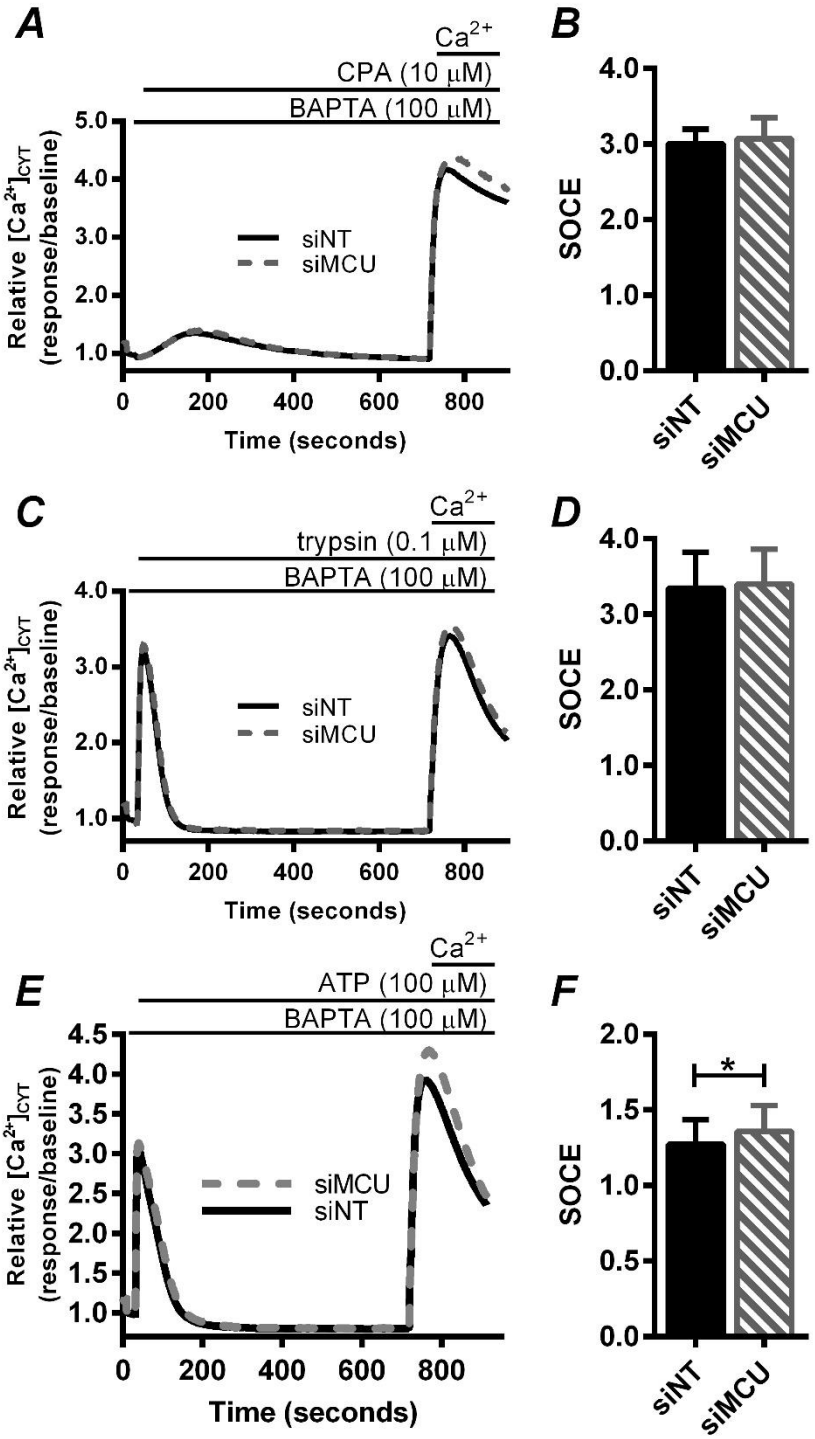
A
Ca2+
CPA (10 μM)
BAPTA (100 μM)
Relative [Ca2+]CYT (response/baseline)
siNT
siMCU
Time (seconds)
B
SOCE
siNT
siMCU
C
Ca2+
trypsin (0.1 μM)
BAPTA (100 μM)
Relative [Ca2+]CYT (response/baseline)
siNT
siMCU
Time (seconds)
D
SOCE
siNT
siMCU
E
Ca2+
ATP (100 μM)
BAPTA (100 μM)
Relative [Ca2+]CYT (response/baseline)
siMCU
siNT
Time (seconds)
F
SOCE
*
siNT
siMCU

Figure 4-7: Consequence of MCU silencing on store-operated, ATP and trypsin stimulated calcium entry in MDA-MB-231 breast cancer cells

In the presence of external BAPTA (100 μM) and under nominal free Ca^{2+} conditions, $[Ca^{2+}]_{CYT}$ increases were measured in MDA-MB-231 cells transfected with siMCU or siNT and challenged with **(A)** CPA (100 μM), **(C)** trypsin (0.1 μM) or **(E)** ATP (100 μM). After the initial phase of Ca^{2+} influx returned to baseline, cells were treated with external Ca^{2+} to stimulate a second phase of Ca^{2+} influx. **(B, D and F)** Bar graphs show the mean ± S.D for the calcium transient parameter peak ratio associated with **(B)** CPA, **(D)** trypsin and **(F)** ATP Ca^{2+} signals. Ca^{2+} traces are relative mean fluorescence. All data were obtained from three independent experiments ($n = 3$) performed in triplicate. $*P < 0.05$, paired two-tailed *t* test.

4.12 Chapter Summary

Forming the main content of this chapter was the manuscript published in the Journal of Biochemical Research Communications. High MCU mRNA levels were detected in oestrogen receptor-negative and basal-like breast cancer subtypes. The functional significance of MCU expression on cell death was examined by assessing the consequence of MCU silencing on global calcium signals and on cell death responses in the basal-like MDA-MB-231 breast cancer cell line.

No measurable effect on cell proliferation or viability was detected with MCU knockdown. Therefore, MCU silencing-mediated effects on cell death initiated with the Bcl-2 inhibitor (ABT-263), ionomycin and ceramide were examined. MCU silencing had no effect on cell death triggered by either the Bcl-2 inhibitor ABT-263 or the lipid mediator ceramide. These data show that MCU-calcium uptake may not be a critical factor that determines MDA-MB-231 cell responsiveness to some death stimuli.

Surprisingly, ionomycin initiated caspase-independent cell death was augmented by MCU silencing. Reduced calcium uptake via MCU may therefore, indirectly promote cell death through effects on global $[Ca^{2+}]_{CYT}$. Assessment of bulk $[Ca^{2+}]_{CYT}$ increases generated with different agents, illustrated that MCU-silencing is not a predominant regulator of bulk $[Ca^{2+}]_{CYT}$ in MDA-MB-231 breast cancer cells. Only modest effects on the calcium transient parameters associated with ATP calcium signals were detected.

Although unclear, MCU silencing-mediated promotion of ionomycin cell death could depend on fine-tuning localised Ca^{2+} signals within $[Ca^{2+}]$ micro-domains. Since the calcium assays in this thesis were designed to monitor bulk $[Ca^{2+}]_{CYT}$, the effect of MCU silencing on local calcium signals were probably overlooked. Assessment of MCU silencing effects on local calcium signals, and on other events such as NFκB transcription factor activity, which are influenced by calcium signal oscillation frequency [263], requires further investigation in MDA-MB-231 cells.

These initial studies provide evidence that in aggressive subtypes of breast cancer, only some cell death responses (e.g. ionomycin-induced cell death) are promoted by MCU silencing, and this promotion is most likely to involve effects on localised Ca^{2+} signals within subcellular-domains, rather than bulk $[Ca^{2+}]_{CYT}$.

PMCA calcium pumps are widely distributed throughout the body, and based on their molecular features are predicted to regulate innumerable processes in different cell types. The work in this thesis describes the role of PMCA isoforms in the regulation of cell death in the human MDA-MB-231 breast cancer cell line. In addition to cell death, the ability of PMCA isoforms in shaping Ca^{2+} signals generated using a panel of Ca^{2+} mobilising agents was characterised in this thesis.

Chapter Two demonstrated that PMCA1 and PMCA4 distinctly shape Ca^{2+} signals and differentially regulate cell death. PMCA1 was identified as a major regulator of global $[Ca^{2+}]_{CYT}$. PMCA1 silencing promoted ionomycin-initiated cell death and was associated $[Ca^{2+}]_{CYT}$ increases. The consequences of PMCA1 silencing, were in contrast to those effects identified with PMCA4 silencing. PMCA4 did not significantly regulate global $[Ca^{2+}]_{CYT}$ signals and PMCA4 silencing did not promote ionomycin-initiated cell death. Silencing of PMCA4, did however promote Bcl-2 inhibitor-initiated apoptosis.

The ability of PMCA4 silencing to regulate Bcl-2 inhibitor-mediated cell death was the subject of further investigation. Effects of PMCA1 or PMCA4 silencing on NFκB nuclear translocation was examined and the effect of NFκB inhibition was also assessed in MDA-MB-231 cells. NFκB nuclear translocation, although unaffected by PMCA1 silencing, was attenuated by PMCA4 silencing. In addition, the ability for the NFκB-inhibitor IMD-0354 to mimic the effect of PMCA4 silencing in the promotion of Bcl-2 inhibitor cell apoptosis was identified. These results indicate that PMCA4-mediated modulation of breast cancer cell death, rather than acting through global $[Ca^{2+}]_{CYT}$ increases, could involve the regulation of NFκB transcription factor activity via changes in local calcium signals.

Additional Ca^{2+} studies examined in more depth, the consequence of PMCA1 silencing on GPCR-linked Ca^{2+} signals when SERCA activity was pharmacologically blocked with CPA. These set of experiments identify a critical role for PMCA1-mediated Ca^{2+} efflux during P2Y receptor activation. The ability of SERCA activity to compensate for impaired PMCA1 efflux during PAR receptor activation became apparent through assessment of ROCE associated with trypsin-mediated Ca^{2+} signalling. PMCA1 silencing reduced ROCE stimulated with trypsin, and this could be the consequence of increased $[Ca^{2+}]_{ER}$ via increased SERCA activity. However, future assessment of $[Ca^{2+}]_{ER}$ under these same experimental conditions are required to examine this possibility.

Chapter three extended these thesis studies to PMCA2, and assessed the potential of PMCA2-silencing to activate MDA-MB-231 cell death and augment intracellular Ca^{2+} signals. Previous

reports indicate that PMCA2-mediated regulation of breast cancer cell death involves changes in global Ca^{2+} signals. However, in thesis studies, PMCA2 was shown to be expressed at relatively low levels in MDA-MB-231 breast cancer cells, and although not a major regulator of global $[Ca^{2+}]_{CYT}$, PMCA2-mediated silencing promoted Bcl-2 inhibitor apoptosis. Analogous to PMCA4 silencing in this cell line, PMCA2 silencing is probably promoting Bcl-2 inhibitior apoptosis via local calcium signals, and likely associated with effects on the Ca^{2+} dependent transcription factor NFκB, although this requires direct assessment in future studies.

Mitochondrial Ca^{2+} signals can determine cellular sensitivity to death stimuli. Because $[Ca^{2+}]_{MIT}$ could be regulated by PMCA isoforms, PMCA-mediated regulation of cell death identified in thesis chapters two and three could involve changes in $[Ca^{2+}]_{MIT}$. Therefore, in chapter four of this thesis I examined the ability of MCU silencing to protect against ABT-263 or ionomycin MDA-MB-231 cell death. Surprisingly, MCU silencing had no effect on Bcl-2 inhibitor apoptosis, yet promoted ionomycin-mediated cell death. Although future studies are required to confirm the role of $[Ca^{2+}]_{MIT}$ levels under these experimental conditions, these initial studies indicate that MCU-mediated calcium uptake into the mitochondria does not modulate MDA-MB-231 cell death initiated via Bcl-2 inhibition. Therefore, the promotion of Bcl-2 inhibition-initiated apoptosis in this breast cancer cell line by PMCA4 and PMCA2 silencing may be independent of $[Ca^{2+}]_{MIT}$.

In summary, these studies provide evidence that PMCA isoforms expressed in the same cell can carry out very different functions. Even though PMCA1 appears to be the so-called “housekeeping” isoform in MDA-MB-231 cells, this isoform can still exert very specific effects on GPCR-linked calcium signals. Therefore, PMCA1 is equipped with the capacity to do more than simply efflux Ca^{2+}, PMCA1 may be able to make specific contributions to cellular signalling. To fully understand the translational impact of these silencing studies in the context of breast cancer, however, future studies with PMCA specific inhibitors are essential. Until recently, the lack of specific PMCA inhibitors has been a limitation in the field of PMCA research. The identification of a potent PMCA4 inhibitor aurintricarboxylic [264] and the ability of this drug-like molecule to inhibit and reverse cardiac hypertrophy in mice [265] provides clear evidence that PMCAs are emerging drug targets [266].

In MDA-MB-231 cells, PMCA4 and PMCA2 are both expressed at lower levels compared with the PMCA1 isoform. However, these isoforms should not be considered redundant just because they do not significantly shape global calcium signals in this cell line. Instead, PMCA4 and PMCA2 in this cell line appear to play an important role in regulating cell death via more subtle effects on local calcium signals or other mechanisms independent of global $[Ca^{2+}]_{CYT}$ levels. As indicated by the work in this thesis, PMCA2 or PMCA4 inhibitors may represent a strategy to sensitise some breast

cancer subtypes to anti-cancer therapies that work via the inhibition of Bcl-2. This approach may be especially relevant in the context of basal-like subtypes of cancer that overlap with triple negative breast cancers, which urgently require new targeted therapies.

[1] M.J. Berridge, M.D. Bootman, H.L. Roderick, Calcium signalling: dynamics, homeostasis and remodelling, Nat Rev Mol Cell Biol, 4 (2003) 517-529.

[2] M.J. Berridge, P. Lipp, M.D. Bootman, The versatility and universality of calcium signalling, Nat Rev Mol Cell Biol, 1 (2000) 11-21.

[3] M.J. Berridge, Neuronal calcium signaling, Neuron, 21 (1998) 13-26.

[4] M.J. Berridge, M.D. Bootman, P. Lipp, Calcium--a life and death signal, Nature, 395 (1998) 645-648.

[5] V.A. Golovina, L.L. Bambrick, P.J. Yarowsky, B.K. Krueger, M.P. Blaustein, Modulation of two functionally distinct Ca2+ stores in astrocytes: role of the plasmalemmal Na/Ca exchanger, Glia, 16 (1996) 296-305.

[6] B.J. Gwag, L.M. Canzoniero, S.L. Sensi, J.A. Demaro, J.Y. Koh, M.P. Goldberg, M. Jacquin, D.W. Choi, Calcium ionophores can induce either apoptosis or necrosis in cultured cortical neurons, Neuroscience, 90 (1999) 1339-1348.

[7] G.R. Monteith, F.M. Davis, S.J. Roberts-Thomson, Calcium channels and pumps in cancer: changes and consequences, J Biol Chem, 287 (2012) 31666-31673.

[8] W.A. Catterall, Structure and regulation of voltage-gated Ca2+ channels, Annu Rev Cell Dev Biol, 16 (2000) 521-555.

[9] M.P. Caulfield, N.J. Birdsall, International Union of Pharmacology. XVII. Classification of muscarinic acetylcholine receptors, Pharmacol Rev, 50 (1998) 279-290.

[10] R. Kaufmann, M.D. Hollenberg, Proteinase-activated receptors (PARs) and calcium signaling in cancer, Adv Exp Med Biol, 740 (2012) 979-1000.

[11] M.D. Hollenberg, S.J. Compton, International Union of Pharmacology. XXVIII. Proteinase-activated receptors, Pharmacol Rev, 54 (2002) 203-217.

[12] J. Lytton, Na+/Ca2+ exchangers: three mammalian gene families control Ca2+ transport, Biochem J, 406 (2007) 365-382.

[13] V. Niggli, E.S. Adunyah, E. Carafoli, Acidic phospholipids, unsaturated fatty acids, and limited proteolysis mimic the effect of calmodulin on the purified erythrocyte Ca2+ - ATPase, J Biol Chem, 256 (1981) 8588-8592.

[14] J.W. Putney, Jr., A model for receptor-regulated calcium entry, Cell Calcium, 7 (1986) 1-12.

[15] J. Liou, M. Fivaz, T. Inoue, T. Meyer, Live-cell imaging reveals sequential oligomerization and local plasma membrane targeting of stromal interaction molecule 1 after Ca2+ store depletion, Proc Natl Acad Sci U S A, 104 (2007) 9301-9306.

[16] P.B. Stathopulos, G.Y. Li, M.J. Plevin, J.B. Ames, M. Ikura, Stored Ca2+ depletion-induced oligomerization of stromal interaction molecule 1 (STIM1) via the EF-SAM region: An initiation mechanism for capacitive Ca2+ entry, J Biol Chem, 281 (2006) 35855-35862.

[17] Y. Baba, K. Hayashi, Y. Fujii, A. Mizushima, H. Watarai, M. Wakamori, T. Numaga, Y. Mori, M. Iino, M. Hikida, T. Kurosaki, Coupling of STIM1 to store-operated Ca2+ entry through its constitutive and inducible movement in the endoplasmic reticulum, Proc Natl Acad Sci U S A, 103 (2006) 16704-16709.

[18] M.M. Wu, J. Buchanan, R.M. Luik, R.S. Lewis, Ca2+ store depletion causes STIM1 to accumulate in ER regions closely associated with the plasma membrane, J Cell Biol, 174 (2006) 803-813.

[19] M. Prakriya, S. Feske, Y. Gwack, S. Srikanth, A. Rao, P.G. Hogan, Orai1 is an essential pore subunit of the CRAC channel, Nature, 443 (2006) 230-233.

[20] P. Varnai, L. Hunyady, T. Balla, STIM and Orai: the long-awaited constituents of store-operated calcium entry, Trends Pharmacol Sci, 30 (2009) 118-128.

[21] G.R. Monteith, D. McAndrew, H.M. Faddy, S.J. Roberts-Thomson, Calcium and cancer: targeting Ca2+ transport, Nat Rev Cancer, 7 (2007) 519-530.

[22] T.C. Sudhof, The synaptic vesicle cycle, Annu Rev Neurosci, 27 (2004) 509-547.

[23] M.J. Berridge, R.F. Irvine, Inositol trisphosphate, a novel second messenger in cellular signal transduction, Nature, 312 (1984) 315-321.

[24] S.K. Joseph, A.P. Thomas, R.J. Williams, R.F. Irvine, J.R. Williamson, myo-Inositol 1,4,5-trisphosphate. A second messenger for the hormonal mobilization of intracellular Ca2+ in liver, J Biol Chem, 259 (1984) 3077-3081.

[25] C. Toyoshima, M. Nakasako, H. Nomura, H. Ogawa, Crystal structure of the calcium pump of sarcoplasmic reticulum at 2.6 A resolution, Nature, 405 (2000) 647-655.

[26] K.J. Sweadner, C. Donnet, Structural similarities of Na,K-ATPase and SERCA, the Ca(2+)-ATPase of the sarcoplasmic reticulum, Biochem J, 356 (2001) 685-704.

[27] W. Kuhlbrandt, Biology, structure and mechanism of P-type ATPases, Nat Rev Mol Cell Biol, 5 (2004) 282-295.

[28] V. Niggli, E.S. Adunyah, J.T. Penniston, E. Carafoli, Purified (Ca2+-Mg2+)-ATPase of the erythrocyte membrane. Reconstitution and effect of calmodulin and phospholipids, J Biol Chem, 256 (1981) 395-401.

[29] A.B. Parekh, J.W. Putney, Jr., Store-operated calcium channels, Physiol Rev, 85 (2005) 757-810.

[30] R. Rizzuto, A.W. Simpson, M. Brini, T. Pozzan, Rapid changes of mitochondrial Ca2+ revealed by specifically targeted recombinant aequorin, Nature, 358 (1992) 325-327.

[31] R. Rizzuto, C. Bastianutto, M. Brini, M. Murgia, T. Pozzan, Mitochondrial Ca2+ homeostasis in intact cells, J Cell Biol, 126 (1994) 1183-1194.

[32] J.M. Baughman, F. Perocchi, H.S. Girgis, M. Plovanich, C.A. Belcher-Timme, Y. Sancak, X.R. Bao, L. Strittmatter, O. Goldberger, R.L. Bogorad, V. Koteliansky, V.K. Mootha, Integrative genomics identifies MCU as an essential component of the mitochondrial calcium uniporter, Nature, 476 (2011) 341-345.

[33] D. De Stefani, A. Raffaello, E. Teardo, I. Szabo, R. Rizzuto, A forty-kilodalton protein of the inner membrane is the mitochondrial calcium uniporter, Nature, 476 (2011) 336-340.

[34] D. Nicholls, K. Akerman, Mitochondrial calcium transport, Biochim Biophys Acta, 683 (1982) 57-88.

[35] M. Montero, M.T. Alonso, E. Carnicero, I. Cuchillo-Ibanez, A. Albillos, A.G. Garcia, J. Garcia-Sancho, J. Alvarez, Chromaffin-cell stimulation triggers fast millimolar mitochondrial Ca2+ transients that modulate secretion, Nat Cell Biol, 2 (2000) 57-61.

[36] R. Rizzuto, T. Pozzan, Microdomains of intracellular Ca2+: molecular determinants and functional consequences, Physiol Rev, 86 (2006) 369-408.

[37] C. Giorgi, D. De Stefani, A. Bononi, R. Rizzuto, P. Pinton, Structural and functional link between the mitochondrial network and the endoplasmic reticulum, Int J Biochem Cell Biol, 41 (2009) 1817-1827.

[38] T. Pozzan, R. Rizzuto, High tide of calcium in mitochondria, Nat Cell Biol, 2 (2000) E25-27.

[39] T.E. Gunter, S.S. Sheu, Characteristics and possible functions of mitochondrial Ca(2+) transport mechanisms, Biochim Biophys Acta, 1787 (2009) 1291-1308.

[40] P. Pinton, C. Giorgi, R. Siviero, E. Zecchini, R. Rizzuto, Calcium and apoptosis: ER-mitochondria Ca2+ transfer in the control of apoptosis, Oncogene, 27 (2008) 6407-6418.

[41] E.J. Griffiths, G.A. Rutter, Mitochondrial calcium as a key regulator of mitochondrial ATP production in mammalian cells, Biochim Biophys Acta, 1787 (2009) 1324-1333.

[42] C. Mammucari, A. Raffaello, D. Vecellio Reane, R. Rizzuto, Molecular structure and pathophysiological roles of the Mitochondrial Calcium Uniporter, Biochim Biophys Acta, (2016).

[43] M.J. Berridge, The versatility and complexity of calcium signalling, Novartis Found Symp, 239 (2001) 52-64; discussion 64-57, 150-159.

[44] H.J. Schatzmann, ATP-dependent Ca++-extrusion from human red cells, Experientia, 22 (1966) 364-365.

[45] P. Brandt, E. Ibrahim, G.A. Bruns, R.L. Neve, Determination of the nucleotide sequence and chromosomal localization of the ATP2B2 gene encoding human Ca(2+)-pumping ATPase isoform PMCA2, Genomics, 14 (1992) 484-487.

[46] F. Latif, F.M. Duh, J. Gnarra, K. Tory, I. Kuzmin, M. Yao, T. Stackhouse, W. Modi, L. Geil, L. Schmidt, et al., von Hippel-Lindau syndrome: cloning and identification of the plasma membrane Ca(++)-transporting ATPase isoform 2 gene that resides in the von Hippel-Lindau gene region, Cancer Res, 53 (1993) 861-867.

[47] S. Olson, M.G. Wang, E. Carafoli, E.E. Strehler, O.W. McBride, Localization of two genes encoding plasma membrane Ca2(+)-transporting ATPases to human chromosomes 1q25-32 and 12q21-23, Genomics, 9 (1991) 629-641.

[48] M.G. Wang, H. Yi, H. Hilfiker, E. Carafoli, E.E. Strehler, O.W. McBride, Localization of two genes encoding plasma membrane Ca2+ ATPases isoforms 2 (ATP2B2) and 3 (ATP2B3) to human chromosomes 3p26-->p25 and Xq28, respectively, Cytogenet Cell Genet, 67 (1994) 41-45.

[49] E.E. Strehler, D.A. Zacharias, Role of alternative splicing in generating isoform diversity among plasma membrane calcium pumps, Physiol Rev, 81 (2001) 21-50.

[50] F. Di Leva, T. Domi, L. Fedrizzi, D. Lim, E. Carafoli, The plasma membrane Ca2+ ATPase of animal cells: structure, function and regulation, Arch Biochem Biophys, 476 (2008) 65-74.

[51] C. Toyoshima, T. Mizutani, Crystal structure of the calcium pump with a bound ATP analogue, Nature, 430 (2004) 529-535.

[52] T.P. Keeton, S.E. Burk, G.E. Shull, Alternative splicing of exons encoding the calmodulin-binding domains and C termini of plasma membrane Ca(2+)-ATPase isoforms 1, 2, 3, and 4, J Biol Chem, 268 (1993) 2740-2748.

[53] D.L. Black, Mechanisms of alternative pre-messenger RNA splicing, Annu Rev Biochem, 72 (2003) 291-336.

[54] T.P. Stauffer, H. Hilfiker, E. Carafoli, E.E. Strehler, Quantitative analysis of alternative splicing options of human plasma membrane calcium pump genes, J Biol Chem, 268 (1993) 25993-26003.

[55] E.E. Strehler, A.G. Filoteo, J.T. Penniston, A.J. Caride, Plasma-membrane Ca(2+) pumps: structural diversity as the basis for functional versatility, Biochem Soc Trans, 35 (2007) 919-922.

[56] M.C. Chicka, E.E. Strehler, Alternative splicing of the first intracellular loop of plasma membrane Ca2+-ATPase isoform 2 alters its membrane targeting, J Biol Chem, 278 (2003) 18464-18470.

[57] J.K. Hill, D.E. Williams, M. LeMasurier, R.A. Dumont, E.E. Strehler, P.G. Gillespie, Splice-site A choice targets plasma-membrane Ca2+-ATPase isoform 2 to hair bundles, J Neurosci, 26 (2006) 6172-6180.

[58] T.A. Reinhardt, A.G. Filoteo, J.T. Penniston, R.L. Horst, Ca(2+)-ATPase protein expression in mammary tissue, Am J Physiol Cell Physiol, 279 (2000) C1595-1602.

[59] T.A. Reinhardt, J.D. Lippolis, G.E. Shull, R.L. Horst, Null mutation in the gene encoding plasma membrane Ca2+-ATPase isoform 2 impairs calcium transport into milk, J Biol Chem, 279 (2004) 42369-42373.

[60] P. James, M. Maeda, R. Fischer, A.K. Verma, J. Krebs, J.T. Penniston, E. Carafoli, Identification and primary structure of a calmodulin binding domain of the Ca2+ pump of human erythrocytes, J Biol Chem, 263 (1988) 2905-2910.

[61] V. Niggli, P. Ronner, E. Carafoli, J.T. Penniston, Effects of calmodulin on the (Ca2+ + Mg2+)ATPase partially purified from erythrocyte membranes, Arch Biochem Biophys, 198 (1979) 124-130.

[62] J. Boyle, Molecular biology of the cell, 5th edition by B. Alberts, A. Johnson, J. Lewis, M. Raff, K. Roberts, and P. Walter, Biochemistry and Molecular Biology Education, 36 (2008) 317-318.

[63] A. Enyedi, T. Vorherr, P. James, D.J. McCormick, A.G. Filoteo, E. Carafoli, J.T. Penniston, The calmodulin binding domain of the plasma membrane Ca2+ pump interacts both with calmodulin and with another part of the pump, J Biol Chem, 264 (1989) 12313-12321.

[64] R. Falchetto, T. Vorherr, J. Brunner, E. Carafoli, The plasma membrane Ca2+ pump contains a site that interacts with its calmodulin-binding domain, J Biol Chem, 266 (1991) 2930-2936.

[65] R. Falchetto, T. Vorherr, E. Carafoli, The calmodulin-binding site of the plasma membrane Ca2+ pump interacts with the transduction domain of the enzyme, Protein Sci, 1 (1992) 1613-1621.

[66] H. Hilfiker, D. Guerini, E. Carafoli, Cloning and expression of isoform 2 of the human plasma membrane Ca2+ ATPase. Functional properties of the enzyme and its splicing products, J Biol Chem, 269 (1994) 26178-26183.

[67] N.L. Elwess, A.G. Filoteo, A. Enyedi, J.T. Penniston, Plasma membrane Ca2+ pump isoforms 2a and 2b are unusually responsive to calmodulin and Ca2+, J Biol Chem, 272 (1997) 17981-17986.

[68] A.K. Verma, A. Enyedi, A.G. Filoteo, J.T. Penniston, Regulatory region of plasma membrane Ca2+ pump. 28 residues suffice to bind calmodulin but more are needed for full auto-inhibition of the activity, J Biol Chem, 269 (1994) 1687-1691.

[69] A.K. Verma, A. Enyedi, A.G. Filoteo, E.E. Strehler, J.T. Penniston, Plasma membrane calcium pump isoform 4a has a longer calmodulin-binding domain than 4b, J Biol Chem, 271 (1996) 3714-3718.

[70] A. Enyedi, A.K. Verma, R. Heim, H.P. Adamo, A.G. Filoteo, E.E. Strehler, J.T. Penniston, The Ca2+ affinity of the plasma membrane Ca2+ pump is controlled by alternative splicing, J Biol Chem, 269 (1994) 41-43.

[71] B.S. Preiano, D. Guerini, E. Carafoli, Expression and functional characterization of isoforms 4 of the plasma membrane calcium pump, Biochemistry, 35 (1996) 7946-7953.

[72] W.C. Earnshaw, L.M. Martins, S.H. Kaufmann, Mammalian caspases: structure, activation, substrates, and functions during apoptosis, Annu Rev Biochem, 68 (1999) 383-424.

[73] K. Paszty, G. Antalffy, L. Hegedus, R. Padanyi, A.R. Penheiter, A.G. Filoteo, J.T. Penniston, A. Enyedi, Cleavage of the plasma membrane Ca+ATPase during apoptosis, Ann N Y Acad Sci, 1099 (2007) 440-450.

[74] K. Paszty, G. Antalffy, A.R. Penheiter, L. Homolya, R. Padanyi, A. Ilias, A.G. Filoteo, J.T. Penniston, A. Enyedi, The caspase-3 cleavage product of the plasma membrane Ca2+-ATPase 4b is activated and appropriately targeted, Biochem J, 391 (2005) 687-692.

[75] K. Paszty, A.K. Verma, R. Padanyi, A.G. Filoteo, J.T. Penniston, A. Enyedi, Plasma membrane Ca2+ATPase isoform 4b is cleaved and activated by caspase-3 during the early phase of apoptosis, J Biol Chem, 277 (2002) 6822-6829.

[76] B.L. Schwab, D. Guerini, C. Didszun, D. Bano, E. Ferrando-May, E. Fava, J. Tam, D. Xu, S. Xanthoudakis, D.W. Nicholson, E. Carafoli, P. Nicotera, Cleavage of plasma membrane calcium pumps by caspases: a link between apoptosis and necrosis, Cell Death Differ, 9 (2002) 818-831.

[77] P.H. James, M. Pruschy, T.E. Vorherr, J.T. Penniston, E. Carafoli, Primary structure of the cAMP-dependent phosphorylation site of the plasma membrane calcium pump, Biochemistry, 28 (1989) 4253-4258.

[78] J.T. Penniston, A. Enyedi, Modulation of the plasma membrane Ca2+ pump, J Membr Biol, 165 (1998) 101-109.

[79] A.K. Verma, K. Paszty, A.G. Filoteo, J.T. Penniston, A. Enyedi, Protein kinase C phosphorylates plasma membrane Ca2+ pump isoform 4a at its calmodulin binding domain, J Biol Chem, 274 (1999) 527-531.

[80] K.K. Wang, L.C. Wright, C.L. Machan, B.G. Allen, A.D. Conigrave, B.D. Roufogalis, Protein kinase C phosphorylates the carboxyl terminus of the plasma membrane Ca(2+)-ATPase from human erythrocytes, J Biol Chem, 266 (1991) 9078-9085.

[81] T.C. Wan, M. Zabe, W.L. Dean, Plasma membrane Ca2+-ATPase isoform 4b is phosphorylated on tyrosine 1176 in activated human platelets, Thromb Haemost, 89 (2003) 122-131.

[82] E. Zvaritch, F. Vellani, D. Guerini, E. Carafoli, A signal for endoplasmic reticulum retention located at the carboxyl terminus of the plasma membrane Ca(2+)-ATPase isoform 4CI, J Biol Chem, 270 (1995) 2679-2688.

[83] E. Kim, S.J. DeMarco, S.M. Marfatia, A.H. Chishti, M. Sheng, E.E. Strehler, Plasma membrane Ca2+ ATPase isoform 4b binds to membrane-associated guanylate kinase (MAGUK) proteins via their PDZ (PSD-95/Dlg/ZO-1) domains, J Biol Chem, 273 (1998) 1591-1595.

[84] F. Hofmann, J. Anagli, E. Carafoli, T. Vorherr, Phosphorylation of the calmodulin binding domain of the plasma membrane Ca2+ pump by protein kinase C reduces its interaction with calmodulin and with its pump receptor site, J Biol Chem, 269 (1994) 24298-24303.

[85] A. Enyedi, A.K. Verma, A.G. Filoteo, J.T. Penniston, Protein kinase C activates the plasma membrane Ca2+ pump isoform 4b by phosphorylation of an inhibitory region downstream of the calmodulin-binding domain, J Biol Chem, 271 (1996) 32461-32467.

[86] A. Enyedi, N.L. Elwess, A.G. Filoteo, A.K. Verma, K. Paszty, J.T. Penniston, Protein kinase C phosphorylates the "a" forms of plasma membrane Ca2+ pump isoforms 2 and 3 and prevents binding of calmodulin, J Biol Chem, 272 (1997) 27525-27528.

[87] Y.M. Usachev, S.J. DeMarco, C. Campbell, E.E. Strehler, S.A. Thayer, Bradykinin and ATP accelerate Ca(2+) efflux from rat sensory neurons via protein kinase C and the plasma membrane Ca(2+) pump isoform 4, Neuron, 33 (2002) 113-122.

[88] J.J. Peluso, Basic fibroblast growth factor (bFGF) regulation of the plasma membrane calcium ATPase (PMCA) as part of an anti-apoptotic mechanism of action, Biochem Pharmacol, 66 (2003) 1363-1369.

[89] W.L. Dean, D. Chen, P.C. Brandt, T.C. Vanaman, Regulation of platelet plasma membrane Ca2+-ATPase by cAMP-dependent and tyrosine phosphorylation, J Biol Chem, 272 (1997) 15113-15119.

[90] L.D. Bozulic, M.T. Malik, W.L. Dean, Effects of plasma membrane Ca(2+) -ATPase tyrosine phosphorylation on human platelet function, J Thromb Haemost, 5 (2007) 1041-1046.

[91] K.A. Blankenship, C.B. Dawson, G.R. Aronoff, W.L. Dean, Tyrosine phosphorylation of human platelet plasma membrane Ca(2+)-ATPase in hypertension, Hypertension, 35 (2000) 103-107.

[92] J.A. Rosado, F.R. Saavedra, P.C. Redondo, J.M. Hernandez-Cruz, G.M. Salido, J.A. Pariente, Reduced plasma membrane Ca2+-ATPase function in platelets from patients with non-insulin-dependent diabetes mellitus, Haematologica, 89 (2004) 1142-1144.

[93] C.C. Garner, J. Nash, R.L. Huganir, PDZ domains in synapse assembly and signalling, Trends Cell Biol, 10 (2000) 274-280.

[94] K. Schuh, S. Uldrijan, M. Telkamp, N. Rothlein, L. Neyses, The plasmamembrane calmodulin-dependent calcium pump: a major regulator of nitric oxide synthase I, J Cell Biol, 155 (2001) 201-205.

[95] S. Oess, A. Icking, D. Fulton, R. Govers, W. Muller-Esterl, Subcellular targeting and trafficking of nitric oxide synthases, Biochem J, 396 (2006) 401-409.

[96] A. Hammes, S. Oberdorf-Maass, T. Rother, K. Nething, F. Gollnick, K.W. Linz, R. Meyer, K. Hu, H. Han, P. Gaudron, G. Ertl, S. Hoffmann, U. Ganten, R. Vetter, K. Schuh, C. Benkwitz, H.G. Zimmer, L. Neyses, Overexpression of the sarcolemmal calcium pump in the myocardium of transgenic rats, Circ Res, 83 (1998) 877-888.

[97] D. Oceandy, E.J. Cartwright, M. Emerson, S. Prehar, F.M. Baudoin, M. Zi, N. Alatwi, L. Venetucci, K. Schuh, J.C. Williams, A.L. Armesilla, L. Neyses, Neuronal nitric oxide synthase signaling in the heart is regulated by the sarcolemmal calcium pump 4b, Circulation, 115 (2007) 483-492.

[98] R. Gros, T. Afroze, X.M. You, G. Kabir, R. Van Wert, W. Kalair, A.E. Hoque, I.N. Mungrue, M. Husain, Plasma membrane calcium ATPase overexpression in arterial smooth muscle increases vasomotor responsiveness and blood pressure, Circ Res, 93 (2003) 614-621.

[99] D.E. Goll, V.F. Thompson, H. Li, W. Wei, J. Cong, The calpain system, Physiol Rev, 83 (2003) 731-801.

[100] K.K. Wang, B.D. Roufogalis, A. Villalobo, Calpain I activates Ca2+ transport by the reconstituted erythrocyte Ca2+ pump, J Membr Biol, 112 (1989) 233-245.

[101] P. James, T. Vorherr, J. Krebs, A. Morelli, G. Castello, D.J. McCormick, J.T. Penniston, A. De Flora, E. Carafoli, Modulation of erythrocyte Ca2+-ATPase by selective calpain cleavage of the calmodulin-binding domain, J Biol Chem, 264 (1989) 8289-8296.

[102] T.T. Yamin, J.M. Ayala, D.K. Miller, Activation of the native 45-kDa precursor form of interleukin-1-converting enzyme, J Biol Chem, 271 (1996) 13273-13282.

[103] T.P. Stauffer, D. Guerini, E. Carafoli, Tissue distribution of the four gene products of the plasma membrane Ca2+ pump. A study using specific antibodies, J Biol Chem, 270 (1995) 12184-12190.

[104] J. Greeb, G.E. Shull, Molecular cloning of a third isoform of the calmodulin-sensitive plasma membrane Ca2+-transporting ATPase that is expressed predominantly in brain and skeletal muscle, J Biol Chem, 264 (1989) 18569-18576.

[105] K. Schuh, E.J. Cartwright, E. Jankevics, K. Bundschu, J. Liebermann, J.C. Williams, A.L. Armesilla, M. Emerson, D. Oceandy, K.P. Knobeloch, L. Neyses, Plasma membrane Ca2+ ATPase 4 is required for sperm motility and male fertility, J Biol Chem, 279 (2004) 28220-28226.

[106] H. Furuta, L. Luo, K. Hepler, A.F. Ryan, Evidence for differential regulation of calcium by outer versus inner hair cells: plasma membrane Ca-ATPase gene expression, Hear Res, 123 (1998) 10-26.

[107] T.A. Reinhardt, J.D. Lippolis, Mammary gland involution is associated with rapid down regulation of major mammary Ca2+-ATPases, Biochem Biophys Res Commun, 378 (2009) 99-102.

[108] T.A. Reinhardt, R.L. Horst, Ca2+-ATPases and their expression in the mammary gland of pregnant and lactating rats, Am J Physiol, 276 (1999) C796-802.

[109] V. Prasad, G. Okunade, L. Liu, R.J. Paul, G.E. Shull, Distinct phenotypes among plasma membrane Ca2+-ATPase knockout mice, Ann N Y Acad Sci, 1099 (2007) 276-286.

[110] M. Brini, E. Carafoli, T. Cali, The plasma membrane calcium pumps: focus on the role in (neuro)pathology, Biochem Biophys Res Commun, (2016).

[111] V. Prasad, G.W. Okunade, M.L. Miller, G.E. Shull, Phenotypes of SERCA and PMCA knockout mice, Biochem Biophys Res Commun, 322 (2004) 1192-1203.

[112] G.W. Okunade, M.L. Miller, G.J. Pyne, R.L. Sutliff, K.T. O'Connor, J.C. Neumann, A. Andringa, D.A. Miller, V. Prasad, T. Doetschman, R.J. Paul, G.E. Shull, Targeted ablation of plasma membrane Ca2+-ATPase (PMCA) 1 and 4 indicates a major housekeeping function for PMCA1 and a critical role in hyperactivated sperm motility and male fertility for PMCA4, J Biol Chem, 279 (2004) 33742-33750.

[113] P.J. Kozel, R.A. Friedman, L.C. Erway, E.N. Yamoah, L.H. Liu, T. Riddle, J.J. Duffy, T. Doetschman, M.L. Miller, E.L. Cardell, G.E. Shull, Balance and hearing deficits in mice with a null mutation in the gene encoding plasma membrane Ca2+-ATPase isoform 2, J Biol Chem, 273 (1998) 18693-18696.

[114] V.A. Street, J.W. McKee-Johnson, R.C. Fonseca, B.L. Tempel, K. Noben-Trauth, Mutations in a plasma membrane Ca2+-ATPase gene cause deafness in deafwaddler mice, Nat Genet, 19 (1998) 390-394.

[115] A.R. Penheiter, A.G. Filoteo, C.L. Croy, J.T. Penniston, Characterization of the deafwaddler mutant of the rat plasma membrane calcium-ATPase 2, Hear Res, 162 (2001) 19-28.

[116] K. Takahashi, K. Kitamura, A point mutation in a plasma membrane Ca(2+)-ATPase gene causes deafness in Wriggle Mouse Sagami, Biochem Biophys Res Commun, 261 (1999) 773-778.

[117] M. Brini, L. Coletto, N. Pierobon, N. Kraev, D. Guerini, E. Carafoli, A comparative functional analysis of plasma membrane Ca2+ pump isoforms in intact cells, J Biol Chem, 278 (2003) 24500-24508.

[118] N. Festjens, T. Vanden Berghe, P. Vandenabeele, Necrosis, a well-orchestrated form of cell demise: signalling cascades, important mediators and concomitant immune response, Biochim Biophys Acta, 1757 (2006) 1371-1387.

[119] D. Hanahan, R.A. Weinberg, The hallmarks of cancer, Cell, 100 (2000) 57-70.

[120] J.F. Kerr, A.H. Wyllie, A.R. Currie, Apoptosis: a basic biological phenomenon with wide-ranging implications in tissue kinetics, Br J Cancer, 26 (1972) 239-257.

[121] A.H. Wyllie, G.J. Beattie, A.D. Hargreaves, Chromatin changes in apoptosis, Histochem J, 13 (1981) 681-692.

[122] G.C. Godman, A.F. Miranda, A.D. Deitch, S.W. Tanenbaum, Action of cytochalasin D on cells of established lines. III. Zeiosis and movements at the cell surface, J Cell Biol, 64 (1975) 644-667.

[123] A.H. Wyllie, Glucocorticoid-induced thymocyte apoptosis is associated with endogenous endonuclease activation, Nature, 284 (1980) 555-556.

[124] N.N. Danial, S.J. Korsmeyer, Cell death: critical control points, Cell, 116 (2004) 205-219.

[125] M. Leist, B. Single, A.F. Castoldi, S. Kuhnle, P. Nicotera, Intracellular adenosine triphosphate (ATP) concentration: a switch in the decision between apoptosis and necrosis, J Exp Med, 185 (1997) 1481-1486.

[126] Y. Eguchi, S. Shimizu, Y. Tsujimoto, Intracellular ATP levels determine cell death fate by apoptosis or necrosis, Cancer Res, 57 (1997) 1835-1840.

[127] S.J. Martin, C.P. Reutelingsperger, A.J. McGahon, J.A. Rader, R.C. van Schie, D.M. LaFace, D.R. Green, Early redistribution of plasma membrane phosphatidylserine is a general feature of apoptosis regardless of the initiating stimulus: inhibition by overexpression of Bcl-2 and Abl, J Exp Med, 182 (1995) 1545-1556.

[128] M.O. Hengartner, The biochemistry of apoptosis, Nature, 407 (2000) 770-776.

[129] S.N. Willis, J.M. Adams, Life in the balance: how BH3-only proteins induce apoptosis, Curr Opin Cell Biol, 17 (2005) 617-625.

[130] J.E. Chipuk, T. Moldoveanu, F. Llambi, M.J. Parsons, D.R. Green, The BCL-2 family reunion, Mol Cell, 37 (2010) 299-310.

[131] H. Thomadaki, A. Scorilas, BCL2 family of apoptosis-related genes: functions and clinical implications in cancer, Crit Rev Clin Lab Sci, 43 (2006) 1-67.

[132] G. Dewson, R.M. Kluck, Mechanisms by which Bak and Bax permeabilise mitochondria during apoptosis, J Cell Sci, 122 (2009) 2801-2808.

[133] G. Dewson, T. Kratina, P. Czabotar, C.L. Day, J.M. Adams, R.M. Kluck, Bak activation for apoptosis involves oligomerization of dimers via their alpha6 helices, Mol Cell, 36 (2009) 696-703.

[134] X. Liu, C.N. Kim, J. Yang, R. Jemmerson, X. Wang, Induction of apoptotic program in cell-free extracts: requirement for dATP and cytochrome c, Cell, 86 (1996) 147-157.

[135] R.M. Kluck, E. Bossy-Wetzel, D.R. Green, D.D. Newmeyer, The release of cytochrome c from mitochondria: a primary site for Bcl-2 regulation of apoptosis, Science, 275 (1997) 1132-1136.

[136] P. Li, D. Nijhawan, I. Budihardjo, S.M. Srinivasula, M. Ahmad, E.S. Alnemri, X. Wang, Cytochrome c and dATP-dependent formation of Apaf-1/caspase-9 complex initiates an apoptotic protease cascade, Cell, 91 (1997) 479-489.

[137] R.U. Janicke, M.L. Sprengart, M.R. Wati, A.G. Porter, Caspase-3 is required for DNA fragmentation and morphological changes associated with apoptosis, J Biol Chem, 273 (1998) 9357-9360.

[138] A. Thorburn, Death receptor-induced cell killing, Cell Signal, 16 (2004) 139-144.

[139] S. Wang, W.S. El-Deiry, TRAIL and apoptosis induction by TNF-family death receptors, Oncogene, 22 (2003) 8628-8633.

[140] S. Fulda, Caspase-8 in cancer biology and therapy, Cancer Lett, 281 (2009) 128-133.

[141] H. Li, H. Zhu, C.J. Xu, J. Yuan, Cleavage of BID by caspase 8 mediates the mitochondrial damage in the Fas pathway of apoptosis, Cell, 94 (1998) 491-501.

[142] X. Luo, I. Budihardjo, H. Zou, C. Slaughter, X. Wang, Bid, a Bcl2 interacting protein, mediates cytochrome c release from mitochondria in response to activation of cell surface death receptors, Cell, 94 (1998) 481-490.

[143] L.P. Billen, A. Shamas-Din, D.W. Andrews, Bid: a Bax-like BH3 protein, Oncogene, 27 Suppl 1 (2008) S93-104.

[144] Z. Assefa, G. Bultynck, K. Szlufcik, N. Nadif Kasri, E. Vermassen, J. Goris, L. Missiaen, G. Callewaert, J.B. Parys, H. De Smedt, Caspase-3-induced truncation of type 1 inositol trisphosphate receptor accelerates apoptotic cell death and induces inositol trisphosphate-independent calcium release during apoptosis, J Biol Chem, 279 (2004) 43227-43236.

[145] L.K. Nutt, J. Chandra, A. Pataer, B. Fang, J.A. Roth, S.G. Swisher, R.G. O'Neil, D.J. McConkey, Bax-mediated Ca2+ mobilization promotes cytochrome c release during apoptosis, J Biol Chem, 277 (2002) 20301-20308.

[146] G. Csordas, G. Hajnoczky, Plasticity of mitochondrial calcium signaling, J Biol Chem, 278 (2003) 42273-42282.

[147] F. Ichas, L.S. Jouaville, S.S. Sidash, J.P. Mazat, E.L. Holmuhamedov, Mitochondrial calcium spiking: a transduction mechanism based on calcium-induced permeability transition involved in cell calcium signalling, FEBS Lett, 348 (1994) 211-215.

[148] H. Kroner, Ca2+ ions, an allosteric activator of calcium uptake in rat liver mitochondria, Arch Biochem Biophys, 251 (1986) 525-535.

[149] G. Hajnoczky, G. Csordas, M. Madesh, P. Pacher, Control of apoptosis by IP(3) and ryanodine receptor driven calcium signals, Cell Calcium, 28 (2000) 349-363.

[150] S.K. Joseph, G. Hajnoczky, IP3 receptors in cell survival and apoptosis: Ca2+ release and beyond, Apoptosis, 12 (2007) 951-968.

[151] G. Szalai, R. Krishnamurthy, G. Hajnoczky, Apoptosis driven by IP(3)-linked mitochondrial calcium signals, EMBO J, 18 (1999) 6349-6361.

[152] P. Pinton, D. Ferrari, E. Rapizzi, F. Di Virgilio, T. Pozzan, R. Rizzuto, The Ca2+ concentration of the endoplasmic reticulum is a key determinant of ceramide-induced apoptosis: significance for the molecular mechanism of Bcl-2 action, EMBO J, 20 (2001) 2690-2701.

[153] R.A. Haworth, D.R. Hunter, The Ca2+-induced membrane transition in mitochondria. II. Nature of the Ca2+ trigger site, Arch Biochem Biophys, 195 (1979) 460-467.

[154] H.K. Baumgartner, J.V. Gerasimenko, C. Thorne, P. Ferdek, T. Pozzan, A.V. Tepikin, O.H. Petersen, R. Sutton, A.J. Watson, O.V. Gerasimenko, Calcium elevation in mitochondria is the main Ca2+ requirement for mitochondrial permeability transition pore (mPTP) opening, J Biol Chem, 284 (2009) 20796-20803.

[155] G. Csordas, A.P. Thomas, G. Hajnoczky, Quasi-synaptic calcium signal transmission between endoplasmic reticulum and mitochondria, EMBO J, 18 (1999) 96-108.

[156] R. Rizzuto, M. Brini, M. Murgia, T. Pozzan, Microdomains with high Ca2+ close to IP3-sensitive channels that are sensed by neighboring mitochondria, Science, 262 (1993) 744-747.

[157] T.E. Gunter, K.K. Gunter, S.S. Sheu, C.E. Gavin, Mitochondrial calcium transport: physiological and pathological relevance, Am J Physiol, 267 (1994) C313-339.

[158] J.G. McCormack, A.P. Halestrap, R.M. Denton, Role of calcium ions in regulation of mammalian intramitochondrial metabolism, Physiol Rev, 70 (1990) 391-425.

[159] L.S. Jouaville, P. Pinton, C. Bastianutto, G.A. Rutter, R. Rizzuto, Regulation of mitochondrial ATP synthesis by calcium: evidence for a long-term metabolic priming, Proc Natl Acad Sci U S A, 96 (1999) 13807-13812.

[160] S. Krajewski, S. Tanaka, S. Takayama, M.J. Schibler, W. Fenton, J.C. Reed, Investigation of the subcellular distribution of the bcl-2 oncoprotein: residence in the nuclear envelope, endoplasmic reticulum, and outer mitochondrial membranes, Cancer Res, 53 (1993) 4701-4714.

[161] D. Ferrari, P. Pinton, G. Szabadkai, M. Chami, M. Campanella, T. Pozzan, R. Rizzuto, Endoplasmic reticulum, Bcl-2 and Ca2+ handling in apoptosis, Cell Calcium, 32 (2002) 413-420.

[162] M.J. Thomenius, C.W. Distelhorst, Bcl-2 on the endoplasmic reticulum: protecting the mitochondria from a distance, J Cell Sci, 116 (2003) 4493-4499.

[163] M. Brini, D. Bano, S. Manni, R. Rizzuto, E. Carafoli, Effects of PMCA and SERCA pump overexpression on the kinetics of cell Ca(2+) signalling, EMBO J, 19 (2000) 4926-4935.

[164] M. Chami, D. Ferrari, P. Nicotera, P. Paterlini-Brechot, R. Rizzuto, Caspase-dependent alterations of Ca2+ signaling in the induction of apoptosis by hepatitis B virus X protein, J Biol Chem, 278 (2003) 31745-31755.

[165] AIHW, Breast cancer in Australia: an overview, Cancer series no. 71. Cat. no. CAN 67. Canberra: AIHW, (2012).

[166] C.M. Perou, T. Sorlie, M.B. Eisen, M. van de Rijn, S.S. Jeffrey, C.A. Rees, J.R. Pollack, D.T. Ross, H. Johnsen, L.A. Akslen, O. Fluge, A. Pergamenschikov, C. Williams, S.X. Zhu, P.E. Lonning, A.L. Borresen-Dale, P.O. Brown, D. Botstein, Molecular portraits of human breast tumours, Nature, 406 (2000) 747-752.

[167] T. Sorlie, C.M. Perou, R. Tibshirani, T. Aas, S. Geisler, H. Johnsen, T. Hastie, M.B. Eisen, M. van de Rijn, S.S. Jeffrey, T. Thorsen, H. Quist, J.C. Matese, P.O. Brown, D. Botstein, P.E. Lonning, A.L. Borresen-Dale, Gene expression patterns of breast carcinomas distinguish tumor subclasses with clinical implications, Proc Natl Acad Sci U S A, 98 (2001) 10869-10874.

[168] Z. Hu, C. Fan, D.S. Oh, J.S. Marron, X. He, B.F. Qaqish, C. Livasy, L.A. Carey, E. Reynolds, L. Dressler, A. Nobel, J. Parker, M.G. Ewend, L.R. Sawyer, J. Wu, Y. Liu, R. Nanda, M. Tretiakova, A. Ruiz Orrico, D. Dreher, J.P. Palazzo, L. Perreard, E. Nelson, M. Mone, H. Hansen, M. Mullins, J.F. Quackenbush, M.J. Ellis, O.I. Olopade, P.S. Bernard, C.M. Perou, The molecular portraits of breast tumors are conserved across microarray platforms, BMC Genomics, 7 (2006) 96.

[169] T. Sorlie, R. Tibshirani, J. Parker, T. Hastie, J.S. Marron, A. Nobel, S. Deng, H. Johnsen, R. Pesich, S. Geisler, J. Demeter, C.M. Perou, P.E. Lonning, P.O. Brown, A.L. Borresen-Dale, D. Botstein, Repeated observation of breast tumor subtypes in independent gene expression data sets, Proc Natl Acad Sci U S A, 100 (2003) 8418-8423.

[170] T. Sorlie, Y. Wang, C. Xiao, H. Johnsen, B. Naume, R.R. Samaha, A.L. Borresen-Dale, Distinct molecular mechanisms underlying clinically relevant subtypes of breast cancer: gene expression analyses across three different platforms, BMC Genomics, 7 (2006) 127.

[171] D. Hanahan, R.A. Weinberg, Hallmarks of cancer: the next generation, Cell, 144 (2011) 646-674.

[172] L. Tsavaler, M.H. Shapero, S. Morkowski, R. Laus, Trp-p8, a novel prostate-specific gene, is up-regulated in prostate cancer and other malignancies and shares high homology with transient receptor potential calcium channel proteins, Cancer Res, 61 (2001) 3760-3769.

[173] L. Zhang, G.J. Barritt, Evidence that TRPM8 is an androgen-dependent Ca2+ channel required for the survival of prostate cancer cells, Cancer Res, 64 (2004) 8365-8373.

[174] D. McAndrew, D.M. Grice, A.A. Peters, F.M. Davis, T. Stewart, M. Rice, C.E. Smart, M.A. Brown, P.A. Kenny, S.J. Roberts-Thomson, G.R. Monteith, ORAI1-mediated calcium influx in lactation and in breast cancer, Mol Cancer Ther, 10 (2011) 448-460.

[175] S. Yang, J.J. Zhang, X.Y. Huang, Orai1 and STIM1 are critical for breast tumor cell migration and metastasis, Cancer Cell, 15 (2009) 124-134.

[176] Y.M. Usachev, S.L. Toutenhoofd, G.M. Goellner, E.E. Strehler, S.A. Thayer, Differentiation induces up-regulation of plasma membrane Ca(2+)-ATPase and concomitant increase in Ca(2+) efflux in human neuroblastoma cell line IMR-32, J Neurochem, 76 (2001) 1756-1765.

[177] K. Saito, K. Uzawa, Y. Endo, Y. Kato, D. Nakashima, K. Ogawara, M. Shiba, H. Bukawa, H. Yokoe, H. Tanzawa, Plasma membrane Ca2+ ATPase isoform 1 down-regulated in human oral cancer, Oncol Rep, 15 (2006) 49-55.

[178] W.J. Lee, S.J. Roberts-Thomson, G.R. Monteith, Plasma membrane calcium-ATPase 2 and 4 in human breast cancer cell lines, Biochem Biophys Res Commun, 337 (2005) 779-783.

[179] W.J. Lee, S.J. Roberts-Thomson, N.A. Holman, F.J. May, G.M. Lehrbach, G.R. Monteith, Expression of plasma membrane calcium pump isoform mRNAs in breast cancer cell lines, Cell Signal, 14 (2002) 1015-1022.

[180] C.S. Aung, W. Ye, G. Plowman, A.A. Peters, G.R. Monteith, S.J. Roberts-Thomson, Plasma membrane calcium ATPase 4 and the remodeling of calcium homeostasis in human colon cancer cells, Carcinogenesis, 30 (2009) 1962-1969.

[181] P.D. Reisner, P.C. Brandt, T.C. Vanaman, Analysis of plasma membrane Ca(2+)-ATPase expression in control and SV40-transformed human fibroblasts, Cell Calcium, 21 (1997) 53-62.

[182] J. VanHouten, C. Sullivan, C. Bazinet, T. Ryoo, R. Camp, D.L. Rimm, G. Chung, J. Wysolmerski, PMCA2 regulates apoptosis during mammary gland involution and predicts outcome in breast cancer, Proc Natl Acad Sci U S A, 107 (2010) 11405-11410.

[183] A.A. Peters, M.J. Milevskiy, W.C. Lee, M.C. Curry, C.E. Smart, J.M. Saunus, L. Reid, L. da Silva, D.L. Marcial, E. Dray, M.A. Brown, S.R. Lakhani, S.J. Roberts-Thomson, G.R. Monteith, The calcium pump plasma membrane Ca(2+)-ATPase 2 (PMCA2) regulates breast cancer cell proliferation and sensitivity to doxorubicin, Sci Rep, 6 (2016) 25505.

[184] J. Jeong, J.N. VanHouten, P. Dann, W. Kim, C. Sullivan, H. Yu, L. Liotta, V. Espina, D.F. Stern, P.A. Friedman, J.J. Wysolmerski, PMCA2 regulates HER2 protein kinase localization and signaling and promotes HER2-mediated breast cancer, Proc Natl Acad Sci U S A, (2016).

[185] W.J. Lee, J.A. Robinson, N.A. Holman, M.N. McCall, S.J. Roberts-Thomson, G.R. Monteith, Antisense-mediated Inhibition of the plasma membrane calcium-ATPase suppresses proliferation of MCF-7 cells, J Biol Chem, 280 (2005) 27076-27084.

[186] M. Holton, D. Yang, W. Wang, T.M. Mohamed, L. Neyses, A.L. Armesilla, The interaction between endogenous calcineurin and the plasma membrane calcium-dependent ATPase is isoform specific in breast cancer cells, FEBS Lett, 581 (2007) 4115-4119.

[187] X. Wu, B. Chang, N.S. Blair, M. Sargent, A.J. York, J. Robbins, G.E. Shull, J.D. Molkentin, Plasma membrane Ca2+-ATPase isoform 4 antagonizes cardiac hypertrophy in association with calcineurin inhibition in rodents, J Clin Invest, 119 (2009) 976-985.

[188] S. Orrenius, B. Zhivotovsky, P. Nicotera, Regulation of cell death: the calcium-apoptosis link, Nat Rev Mol Cell Biol, 4 (2003) 552-565.

[189] P.N. Kelly, A. Strasser, The role of Bcl-2 and its pro-survival relatives in tumourigenesis and cancer therapy, Cell Death Differ, 18 (2011) 1414-1424.

[190] M. Vogler, D. Dinsdale, M.J. Dyer, G.M. Cohen, Bcl-2 inhibitors: small molecules with a big impact on cancer therapy, Cell Death Differ, 16 (2009) 360-367.

[191] M.R. Warr, G.C. Shore, Small-molecule Bcl-2 antagonists as targeted therapy in oncology, Curr Oncol, 15 (2008) 256-261.

[192] S.K. Tahir, J. Wass, M.K. Joseph, V. Devanarayan, P. Hessler, H. Zhang, S.W. Elmore, P.E. Kroeger, C. Tse, S.H. Rosenberg, M.G. Anderson, Identification of expression signatures predictive of sensitivity to the Bcl-2 family member inhibitor ABT-263 in small cell lung carcinoma and leukemia/lymphoma cell lines, Mol Cancer Ther, 9 (2010) 545-557.

[193] M.P. Kurnellas, H. Li, M.R. Jain, S.N. Giraud, A.B. Nicot, A. Ratnayake, R.F. Heary, S. Elkabes, Reduced expression of plasma membrane calcium ATPase 2 and collapsin response mediator protein 1 promotes death of spinal cord neurons, Cell Death Differ, 17 (2010) 1501-1510.

[194] D. Fernandes, A. Zaidi, J. Bean, D. Hui, M.L. Michaelis, RNA--induced silencing of the plasma membrane Ca2+-ATPase 2 in neuronal cells: effects on Ca2+ homeostasis and cell viability, J Neurochem, 102 (2007) 454-465.

[195] A. Birmingham, E.M. Anderson, A. Reynolds, D. Ilsley-Tyree, D. Leake, Y. Fedorov, S. Baskerville, E. Maksimova, K. Robinson, J. Karpilow, W.S. Marshall, A. Khvorova, 3' UTR seed matches, but not overall identity, are associated with RNAi off-targets, Nat Methods, 3 (2006) 199-204.

[196] A.L. Jackson, J. Burchard, D. Leake, A. Reynolds, J. Schelter, J. Guo, J.M. Johnson, L. Lim, J. Karpilow, K. Nichols, W. Marshall, A. Khvorova, P.S. Linsley, Position-specific chemical modification of siRNAs reduces "off-target" transcript silencing, RNA, 12 (2006) 1197-1205.

[197] K.M. Suchanek, F.J. May, J.A. Robinson, W.J. Lee, N.A. Holman, G.R. Monteith, S.J. Roberts-Thomson, Peroxisome proliferator-activated receptor alpha in the human breast cancer cell lines MCF-7 and MDA-MB-231, Mol Carcinog, 34 (2002) 165-171.

[198] G.R. Monteith, G.S. Bird, Techniques: high-throughput measurement of intracellular Ca(2+) -- back to basics, Trends Pharmacol Sci, 26 (2005) 218-223.

[199] F.M. Davis, P.A. Kenny, E.T. Soo, B.J. van Denderen, E.W. Thompson, P.J. Cabot, M.O. Parat, S.J. Roberts-Thomson, G.R. Monteith, Remodeling of purinergic receptor-mediated Ca2+ signaling as a consequence of EGF-induced epithelial-mesenchymal transition in breast cancer cells, PLoS One, 6 (2011) e23464.

[200] K.Y. Chu, Y. Lin, A. Hendel, J.E. Kulpa, R.W. Brownsey, J.D. Johnson, ATP-citrate lyase reduction mediates palmitate-induced apoptosis in pancreatic beta cells, J Biol Chem, 285 (2010) 32606-32615.

[201] J. Liou, M.L. Kim, W.D. Heo, J.T. Jones, J.W. Myers, J.E. Ferrell, Jr., T. Meyer, STIM is a Ca2+ sensor essential for Ca2+-store-depletion-triggered Ca2+ influx, Curr Biol, 15 (2005) 1235-1241.

[202] K.D. Jeffrey, E.U. Alejandro, D.S. Luciani, T.B. Kalynyak, X. Hu, H. Li, Y. Lin, R.R. Townsend, K.S. Polonsky, J.D. Johnson, Carboxypeptidase E mediates palmitate-induced beta-cell ER stress and apoptosis, Proc Natl Acad Sci U S A, 105 (2008) 8452-8457.

[203] P. Signorelli, C. Luberto, Y.A. Hannun, Ceramide inhibition of NF-kappaB activation involves reverse translocation of classical protein kinase C (PKC) isoenzymes: requirement for kinase activity and carboxyl-terminal phosphorylation of PKC for the ceramide response, FASEB J, 15 (2001) 2401-2414.

[204] R.N. Ghosh, R. DeBiasio, C.C. Hudson, E.R. Ramer, C.L. Cowan, R.H. Oakley, Quantitative cell-based high-content screening for vasopressin receptor agonists using transfluor technology, J Biomol Screen, 10 (2005) 476-484.

[205] P. Gribbon, A. Sewing, Fluorescence readouts in HTS: no gain without pain?, Drug Discov Today, 8 (2003) 1035-1043.

[206] P.A. Kenny, G.Y. Lee, C.A. Myers, R.M. Neve, J.R. Semeiks, P.T. Spellman, K. Lorenz, E.H. Lee, M.H. Barcellos-Hoff, O.W. Petersen, J.W. Gray, M.J. Bissell, The morphologies of breast cancer cell lines in three-dimensional assays correlate with their profiles of gene expression, Mol Oncol, 1 (2007) 84-96.

[207] Y. Wang, J.G. Klijn, Y. Zhang, A.M. Sieuwerts, M.P. Look, F. Yang, D. Talantov, M. Timmermans, M.E. Meijer-van Gelder, J. Yu, T. Jatkoe, E.M. Berns, D. Atkins, J.A. Foekens, Gene-expression profiles to predict distant metastasis of lymph-node-negative primary breast cancer, Lancet, 365 (2005) 671-679.

[208] Z. Darzynkiewicz, S. Bruno, G. Del Bino, W. Gorczyca, M.A. Hotz, P. Lassota, F. Traganos, Features of apoptotic cells measured by flow cytometry, Cytometry, 13 (1992) 795-808.

[209] M.J. Berridge, The AM and FM of calcium signalling, Nature, 386 (1997) 759-760.

[210] R.E. Dolmetsch, K. Xu, R.S. Lewis, Calcium oscillations increase the efficiency and specificity of gene expression, Nature, 392 (1998) 933-936.

[211] D.E. Nelson, A.E. Ihekwaba, M. Elliott, J.R. Johnson, C.A. Gibney, B.E. Foreman, G. Nelson, V. See, C.A. Horton, D.G. Spiller, S.W. Edwards, H.P. McDowell, J.F. Unitt, E. Sullivan, R. Grimley,

N. Benson, D. Broomhead, D.B. Kell, M.R. White, Oscillations in NF-kappaB signaling control the dynamics of gene expression, Science, 306 (2004) 704-708.

[212] H. Nakshatri, P. Bhat-Nakshatri, D.A. Martin, R.J. Goulet, Jr., G.W. Sledge, Jr., Constitutive activation of NF-kappaB during progression of breast cancer to hormone-independent growth, Mol Cell Biol, 17 (1997) 3629-3639.

[213] S. Braunstein, S.C. Formenti, R.J. Schneider, Acquisition of stable inducible up-regulation of nuclear factor-kappaB by tumor necrosis factor exposure confers increased radiation resistance without increased transformation in breast cancer cells, Mol Cancer Res, 6 (2008) 78-88.

[214] C. Montagut, I. Tusquets, B. Ferrer, J.M. Corominas, B. Bellosillo, C. Campas, M. Suarez, X. Fabregat, E. Campo, P. Gascon, S. Serrano, P.L. Fernandez, A. Rovira, J. Albanell, Activation of nuclear factor-kappa B is linked to resistance to neoadjuvant chemotherapy in breast cancer patients, Endocr Relat Cancer, 13 (2006) 607-616.

[215] A. Tanaka, S. Muto, M. Konno, A. Itai, H. Matsuda, A new IkappaB kinase beta inhibitor prevents human breast cancer progression through negative regulation of cell cycle transition, Cancer Res, 66 (2006) 419-426.

[216] O. Thastrup, P.J. Cullen, B.K. Drobak, M.R. Hanley, A.P. Dawson, Thapsigargin, a tumor promoter, discharges intracellular Ca2+ stores by specific inhibition of the endoplasmic reticulum Ca2(+)-ATPase, Proc Natl Acad Sci U S A, 87 (1990) 2466-2470.

[217] M.P. Kurnellas, A. Nicot, G.E. Shull, S. Elkabes, Plasma membrane calcium ATPase deficiency causes neuronal pathology in the spinal cord: a potential mechanism for neurodegeneration in multiple sclerosis and spinal cord injury, FASEB J, 19 (2005) 298-300.

[218] S.R. Oakes, F. Vaillant, E. Lim, L. Lee, K. Breslin, F. Feleppa, S. Deb, M.E. Ritchie, E. Takano, T. Ward, S.B. Fox, D. Generali, G.K. Smyth, A. Strasser, D.C. Huang, J.E. Visvader, G.J. Lindeman, Sensitization of BCL-2-expressing breast tumors to chemotherapy by the BH3 mimetic ABT-737, Proc Natl Acad Sci U S A, 109 (2012) 2766-2771.

[219] C.W. Distelhorst, M.D. Bootman, Bcl-2 interaction with the inositol 1,4,5-trisphosphate receptor: role in Ca(2+) signaling and disease, Cell Calcium, 50 (2011) 234-241.

[220] Y.P. Rong, G. Bultynck, A.S. Aromolaran, F. Zhong, J.B. Parys, H. De Smedt, G.A. Mignery, H.L. Roderick, M.D. Bootman, C.W. Distelhorst, The BH4 domain of Bcl-2 inhibits ER calcium release and apoptosis by binding the regulatory and coupling domain of the IP3 receptor, Proc Natl Acad Sci U S A, 106 (2009) 14397-14402.

[221] T.M. Mohamed, D. Oceandy, M. Zi, S. Prehar, N. Alatwi, Y. Wang, M.A. Shaheen, R. Abou-Leisa, C. Schelcher, Z. Hegab, F. Baudoin, M. Emerson, M. Mamas, G. Di Benedetto, M. Zaccolo, M. Lei, E.J. Cartwright, L. Neyses, Plasma membrane calcium pump (PMCA4)-neuronal nitric-oxide synthase complex regulates cardiac contractility through modulation of a compartmentalized cyclic nucleotide microdomain, J Biol Chem, 286 (2011) 41520-41529.

[222] B.S. Marasa, J.N. Rao, T. Zou, L. Liu, K.M. Keledjian, A.H. Zhang, L. Xiao, J. Chen, D.J. Turner, J.Y. Wang, Induced TRPC1 expression sensitizes intestinal epithelial cells to apoptosis by inhibiting NF-kappaB activation through Ca2+ influx, Biochem J, 397 (2006) 77-87.

[223] C. Van Waes, Nuclear factor-kappaB in development, prevention, and therapy of cancer, Clin Cancer Res, 13 (2007) 1076-1082.

[224] C.M. Schlotter, U. Vogt, H. Allgayer, B. Brandt, Molecular targeted therapies for breast cancer treatment, Breast Cancer Res, 10 (2008) 211.

[225] J.M. Tromp, C.R. Geest, E.C. Breij, J.A. Elias, J. van Laar, D.M. Luijks, A.P. Kater, T. Beaumont, M.H. van Oers, E. Eldering, Tipping the Noxa/Mcl-1 balance overcomes ABT-737 resistance in chronic lymphocytic leukemia, Clin Cancer Res, 18 (2012) 487-498.

[226] J. Pande, M.M. Szewczyk, I. Kuszczak, S. Grover, E. Escher, A.K. Grover, Functional effects of caloxin 1c2, a novel engineered selective inhibitor of plasma membrane Ca(2+)-pump isoform 4, on coronary artery, J Cell Mol Med, 12 (2008) 1049-1060.

[227] M.C. Curry, N.A. Luk, P.A. Kenny, S.J. Roberts-Thomson, G.R. Monteith, Distinct regulation of cytoplasmic calcium signals and cell death pathways by different plasma membrane calcium ATPase isoforms in MDA-MB-231 breast cancer cells, J Biol Chem, 287 (2012) 28598-28608.

[228] R. Sgonc, J. Gruber, Apoptosis detection: an overview, Exp Gerontol, 33 (1998) 525-533.

[229] I. von Kugelgen, Pharmacological profiles of cloned mammalian P2Y-receptor subtypes, Pharmacol Ther, 110 (2006) 415-432.

[230] S.K. Bohm, W. Kong, D. Bromme, S.P. Smeekens, D.C. Anderson, A. Connolly, M. Kahn, N.A. Nelken, S.R. Coughlin, D.G. Payan, N.W. Bunnett, Molecular cloning, expression and potential functions of the human proteinase-activated receptor-2, Biochem J, 314 (Pt 3) (1996) 1009-1016.

[231] K. Moncoq, C.A. Trieber, H.S. Young, The molecular basis for cyclopiazonic acid inhibition of the sarcoplasmic reticulum calcium pump, J Biol Chem, 282 (2007) 9748-9757.

[232] N. Demaurex, D.P. Lew, K.H. Krause, Cyclopiazonic acid depletes intracellular Ca2+ stores and activates an influx pathway for divalent cations in HL-60 cells, J Biol Chem, 267 (1992) 2318-2324.

[233] W.A. Kruger, G.R. Monteith, P. Poronnik, NHERF-1 regulation of EGF and neurotensin signalling in HT-29 epithelial cells, Biochem Biophys Res Commun, 432 (2013) 568-573.

[234] J.C. Mercer, W.I. Dehaven, J.T. Smyth, B. Wedel, R.R. Boyles, G.S. Bird, J.W. Putney, Jr., Large store-operated calcium selective currents due to co-expression of Orai1 or Orai2 with the intracellular calcium sensor, Stim1, J Biol Chem, 281 (2006) 24979-24990.

[235] M. Montero, M. Brini, R. Marsault, J. Alvarez, R. Sitia, T. Pozzan, R. Rizzuto, Monitoring dynamic changes in free Ca2+ concentration in the endoplasmic reticulum of intact cells, EMBO J, 14 (1995) 5467-5475.

[236] S.G. Baryshnikov, M.V. Pulina, A. Zulian, C.I. Linde, V.A. Golovina, Orai1, a critical component of store-operated Ca2+ entry, is functionally associated with Na+/Ca2+ exchanger and plasma membrane Ca2+ pump in proliferating human arterial myocytes, Am J Physiol Cell Physiol, 297 (2009) C1103-1112.

[237] D. Merino, S.W. Lok, J.E. Visvader, G.J. Lindeman, Targeting BCL-2 to enhance vulnerability to therapy in estrogen receptor-positive breast cancer, Oncogene, 35 (2016) 1877-1887.

[238] A.R. Delbridge, S. Grabow, A. Strasser, D.L. Vaux, Thirty years of BCL-2: translating cell death discoveries into novel cancer therapies, Nat Rev Cancer, 16 (2016) 99-109.

[239] M.C. Curry, S.J. Roberts-Thomson, G.R. Monteith, Plasma membrane calcium ATPases and cancer, Biofactors, 37 (2011) 132-138.

[240] R.M. Neve, K. Chin, J. Fridlyand, J. Yeh, F.L. Baehner, T. Fevr, L. Clark, N. Bayani, J.P. Coppe, F. Tong, T. Speed, P.T. Spellman, S. DeVries, A. Lapuk, N.J. Wang, W.L. Kuo, J.L. Stilwell, D. Pinkel, D.G. Albertson, F.M. Waldman, F. McCormick, R.B. Dickson, M.D. Johnson, M. Lippman, S. Ethier, A. Gazdar, J.W. Gray, A collection of breast cancer cell lines for the study of functionally distinct cancer subtypes, Cancer Cell, 10 (2006) 515-527.

[241] E.M. Anderson, A. Birmingham, S. Baskerville, A. Reynolds, E. Maksimova, D. Leake, Y. Fedorov, J. Karpilow, A. Khvorova, Experimental validation of the importance of seed complement frequency to siRNA specificity, RNA, 14 (2008) 853-861.

[242] D. Oceandy, T.M. Mohamed, E.J. Cartwright, L. Neyses, Local signals with global impacts and clinical implications: lessons from the plasma membrane calcium pump (PMCA4), Biochim Biophys Acta, 1813 (2011) 974-978.

[243] R.R. Baggott, T.M. Mohamed, D. Oceandy, M. Holton, M.C. Blanc, S.C. Roux-Soro, S. Brown, J.E. Brown, E.J. Cartwright, W. Wang, L. Neyses, A.L. Armesilla, Disruption of the interaction between PMCA2 and calcineurin triggers apoptosis and enhances paclitaxel-induced cytotoxicity in breast cancer cells, Carcinogenesis, 33 (2012) 2362-2368.

[244] S.J. Roberts-Thomson, M.C. Curry, G.R. Monteith, Plasma membrane calcium pumps and their emerging roles in cancer, World J Biol Chem, 1 (2010) 248-253.

[245] M.C. Curry, A.A. Peters, P.A. Kenny, S.J. Roberts-Thomson, G.R. Monteith, Mitochondrial calcium uniporter silencing potentiates caspase-independent cell death in MDA-MB-231 breast cancer cells, Biochem Biophys Res Commun, 434 (2013) 695-700.

[246] R. Rizzuto, D. De Stefani, A. Raffaello, C. Mammucari, Mitochondria as sensors and regulators of calcium signalling, Nat Rev Mol Cell Biol, 13 (2012) 566-578.

[247] D.C. Wallace, Mitochondria and cancer, Nat Rev Cancer, 12 (2012) 685-698.

[248] V. Shoshan-Barmatz, V. De Pinto, M. Zweckstetter, Z. Raviv, N. Keinan, N. Arbel, VDAC, a multi-functional mitochondrial protein regulating cell life and death, Mol Aspects Med, 31 (2010) 227-285.

[249] M. Patron, A. Raffaello, V. Granatiero, A. Tosatto, G. Merli, D. De Stefani, L. Wright, G. Pallafacchina, A. Terrin, C. Mammucari, R. Rizzuto, The mitochondrial calcium uniporter (MCU): molecular identity and physiological roles, J Biol Chem, 288 (2013) 10750-10758.

[250] I. Drago, D. De Stefani, R. Rizzuto, T. Pozzan, Mitochondrial Ca2+ uptake contributes to buffering cytoplasmic Ca2+ peaks in cardiomyocytes, Proc Natl Acad Sci U S A, 109 (2012) 12986-12991.

[251] A. Tosatto, R. Sommaggio, C. Kummerow, R.B. Bentham, T.S. Blacker, T. Berecz, M.R. Duchen, A. Rosato, I. Bogeski, G. Szabadkai, R. Rizzuto, C. Mammucari, The mitochondrial calcium uniporter regulates breast cancer progression via HIF-1alpha, EMBO Mol Med, 8 (2016) 569-585.

[252] S. Marchi, L. Lupini, S. Patergnani, A. Rimessi, S. Missiroli, M. Bonora, A. Bononi, F. Corra, C. Giorgi, E. De Marchi, F. Poletti, R. Gafa, G. Lanza, M. Negrini, R. Rizzuto, P. Pinton,

Downregulation of the mitochondrial calcium uniporter by cancer-related miR-25, Curr Biol, 23 (2013) 58-63.

[253] J.I. Herschkowitz, K. Simin, V.J. Weigman, I. Mikaelian, J. Usary, Z. Hu, K.E. Rasmussen, L.P. Jones, S. Assefnia, S. Chandrasekharan, M.G. Backlund, Y. Yin, A.I. Khramtsov, R. Bastein, J. Quackenbush, R.I. Glazer, P.H. Brown, J.E. Green, L. Kopelovich, P.A. Furth, J.P. Palazzo, O.I. Olopade, P.S. Bernard, G.A. Churchill, T. Van Dyke, C.M. Perou, Identification of conserved gene expression features between murine mammary carcinoma models and human breast tumors, Genome Biol, 8 (2007) R76.

[254] J.S. Parker, M. Mullins, M.C. Cheang, S. Leung, D. Voduc, T. Vickery, S. Davies, C. Fauron, X. He, Z. Hu, J.F. Quackenbush, I.J. Stijleman, J. Palazzo, J.S. Marron, A.B. Nobel, E. Mardis, T.O. Nielsen, M.J. Ellis, C.M. Perou, P.S. Bernard, Supervised risk predictor of breast cancer based on intrinsic subtypes, J Clin Oncol, 27 (2009) 1160-1167.

[255] A.A. Peters, P.T. Simpson, J.J. Bassett, J.M. Lee, L. Da Silva, L.E. Reid, S. Song, M.O. Parat, S.R. Lakhani, P.A. Kenny, S.J. Roberts-Thomson, G.R. Monteith, Calcium channel TRPV6 as a potential therapeutic target in estrogen receptor-negative breast cancer, Mol Cancer Ther, 11 (2012) 2158-2168.

[256] Kruman, II, M.P. Mattson, Pivotal role of mitochondrial calcium uptake in neural cell apoptosis and necrosis, J Neurochem, 72 (1999) 529-540.

[257] H.I. Hung, J.M. Schwartz, E.N. Maldonado, J.J. Lemasters, A.L. Nieminen, Mitoferrin-2-dependent mitochondrial iron uptake sensitizes human head and neck squamous carcinoma cells to photodynamic therapy, J Biol Chem, 288 (2013) 677-686.

[258] H. Zaid, S. Abu-Hamad, A. Israelson, I. Nathan, V. Shoshan-Barmatz, The voltage-dependent anion channel-1 modulates apoptotic cell death, Cell Death Differ, 12 (2005) 751-760.

[259] C. Cardenas, R.A. Miller, I. Smith, T. Bui, J. Molgo, M. Muller, H. Vais, K.H. Cheung, J. Yang, I. Parker, C.B. Thompson, M.J. Birnbaum, K.R. Hallows, J.K. Foskett, Essential regulation of cell bioenergetics by constitutive InsP3 receptor Ca2+ transfer to mitochondria, Cell, 142 (2010) 270-283.

[260] S. Patergnani, J.M. Suski, C. Agnoletto, A. Bononi, M. Bonora, E. De Marchi, C. Giorgi, S. Marchi, S. Missiroli, F. Poletti, A. Rimessi, J. Duszynski, M.R. Wieckowski, P. Pinton, Calcium signaling around Mitochondria Associated Membranes (MAMs), Cell Commun Signal, 9 (2011) 19.

[261] D. De Stefani, A. Bononi, A. Romagnoli, A. Messina, V. De Pinto, P. Pinton, R. Rizzuto, VDAC1 selectively transfers apoptotic Ca2+ signals to mitochondria, Cell Death Differ, 19 (2012) 267-273.

[262] D.D. Hall, Y. Wu, F.E. Domann, D.R. Spitz, M.E. Anderson, Mitochondrial calcium uniporter activity is dispensable for MDA-MB-231 breast carcinoma cell survival, PLoS One, 9 (2014) e96866.

[263] K. Samanta, S. Douglas, A.B. Parekh, Mitochondrial calcium uniporter MCU supports cytoplasmic Ca2+ oscillations, store-operated Ca2+ entry and Ca2+-dependent gene expression in response to receptor stimulation, PLoS One, 9 (2014) e101188.

[264] T.M. Mohamed, R. Abou-Leisa, F. Baudoin, N. Stafford, L. Neyses, E.J. Cartwright, D. Oceandy, Development and characterization of a novel fluorescent indicator protein PMCA4-GCaMP2 in cardiomyocytes, J Mol Cell Cardiol, 63 (2013) 57-68.

[265] T.M. Mohamed, R. Abou-Leisa, N. Stafford, A. Maqsood, M. Zi, S. Prehar, F. Baudoin-Stanley, X. Wang, L. Neyses, E.J. Cartwright, D. Oceandy, The plasma membrane calcium ATPase 4 signalling in cardiac fibroblasts mediates cardiomyocyte hypertrophy, Nat Commun, 7 (2016) 11074.

[266] E.E. Strehler, Plasma membrane calcium ATPases as novel candidates for therapeutic agent development, J Pharm Pharm Sci, 16 (2013) 190-206.